Effect of High Shearing on the Rheological / Structural Properties of Highly Concentrated W/O Emulsions

by

HAMAT ABDERRAHMANE YAKHOUB

Thesis submitted in accordance with the requirements for the Degree of

MASTER TECHNOLOGIAE: CHEMICAL ENGINEERING

in the

Faculty of Engineering

CAPE PENINSULA UNIVERSITY OF TECHNOLOGY

EFFECT OF HIGH SHEARING ON THE RHEOLOGICAL / STRUCTURAL PROPERTIES OF HIGHLY CONCENTRATED W/O EMULSIONS

by

HAMAT ABDERRAHMANE YAKHOUB

Thesis submitted in accordance with the requirements
for the Degree
of

MAGISTER TECHNOLOGIAE:
CHEMICAL ENGINEERING
in the
FACULTY OF ENGINEERING

CAPE PENINSULA UNIVERSITY OF TECHNOLOGY

Supervisor:	Professor Irina Masalova
Co-Supervisor:	Professor Rainer Haldenwang

ABSTRACT

Emulsion explosives are classified as highly concentrated water-in-oil emulsions with high droplet volume fraction that exceeding the close packing limit of spherical droplets. These emulsions are commonly used as re-pumpable materials. Thus, the shearing action resulting from the transportation process of these materials has a tremendous impact on their structures and functionality and might reduce the shelf-life and performance of the products. Therefore the main goal of this research was to investigate the stability of highly concentrated water-in-oil emulsion under shearing using a newly designed piston-pumping instrument.

The results of measurement included the droplet size distribution, microscopic observation, flow and viscoelastic properties of the materials. Neither crystallisation nor other destabilisation phenomena such as coalescence, partial coalescence, or phase inversion occurred during the shearing process of these emulsions, regardless of their formulation content. It was found that the high shearing action within this research experimental window induced droplet refinement. The changes in droplet size distribution were achieved by multi-pass flow through a small orifice set as outlet of the piston-chamber pumping instrument, and intensive shearing provided the shift of the droplet sizes to the smaller-size side of the distribution. Their distributions were wider and of Gaussian type. Two models were proposed and used to fit the refinement evolution and the width of distributions respectively. An engineering illustration of the work done on the emulsion during shear was derived in terms of energy density, through which the power law equation describing the energy characterisation for refinement efficiency was achieved. The droplet size versus number of pumping was expressed by the fitting parameters (θ_D, θ_ω, $D_{crit.}$, $\omega_{critical}$ and C) which, in turn, gave a clear estimation of factors that influence refinement during shearing. These factors involved surfactant type and surfactant concentration, where higher surfactant concentration induced higher efficiency with regard to droplet disruption. The central result of the investigation is however the experimental proof that the shear modulus versus droplet size is expressed not obligatory by a linear reciprocal dependence, but by an exponent approximately equal to 2. It was shown that the stability of highly concentrated emulsions in shearing is determined by some critical value of deformation with reference to the yielding conditions. This value on average equalled 0.07 for all samples under investigation.

When the ammonium nitrated concentration was lowered from >80% to 65% by mass of dispersed phase, the same trend in terms of stability with shearing followed: refinement of droplets, narrowing of the width of distribution, increase in rehological properties and the mechanism associated them. However, the pressure drop during pumping of fresh emulsion materials as predicted using the computerized numerical integration of the Rabinowitsch-Weissenberg equation, increased significantly with decreased of droplet size.

DECLARATION

I, **Hamat Abderrahmane YAKHOUB**, hereby declare that the contents of this dissertation/thesis represent my own unaided work, and that the dissertation/thesis has not previously been submitted for academic examination towards any qualification. Furthermore, it represents my own opinions and not necessarily those of the CAPE PENINSULA UNIVERSITY OF TECHNOLOGY.

Hamat Abderrahmane YAKHOUB

April 2009

DEDICATION

I would like to thanks first of all "AL - RAHIM" of guiding me, through my whole life, my entire undergraduate studies till the completion of my Bachelor degree, and now my Master thesis.

I dedicate this thesis to my dear Mom, ZAHRA HAMAT who loved me, missed me and never stop thinking of me. Thanks Mom for everything, without you, your support, your love, your education, your patience; I wouldn't reach this level and achieved this thesis.

Same dedication goes to my unique, unforgettable and talented Dad, ABDERRAHMANE YAKHOUB ISSA, who stood always on my side and pushed me for the best all the time.

Special dedication goes to my grandfather and grandmother, BAÃBA HAMAT HAROUN and AÃYA KALTAM MAKINE respectively.

Special dedication goes to all my sisters and brothers (KHADIDJA, ADOUM, OUMKALSOUM, NAFISSA, MADINA, AFFAF, ALDJINEH, KALTAM, ZEINAB, HABIBA, BICHARA, YOUSSOUF), to my nieces and nephews (MAHAMAT AMINE, MAHAMAT NAIM, HADJE ZAHRA, HAKKI and the new born RAHAMA), and all the rest of my family without any distinction. Thanks for your support and your commitment.

Special dedication goes to my beautiful JULIE ANN CURRAN for her love, support and her esteem and for treating me so especial all the time and be there with me regardless the distance between us.

Special dedication goes to my brothers, AHMADAY ABDERRAHMANE, MAHAMAT NAÏM ABDERRAHMANE, ALLAFOUZA LONI, ABDELAZIZ MOUSTAPHA, YASSINE BRAHIM DOUTOUM and HAMIT ALI.

This thesis is also dedicated to my deceased brother and uncle: SI ABOUBAKAR ASSIDIKH and ADOUM HAMAT HAROUN respectively; may Allah grant them paradise; we won't forget you!

ACKNOWLEDGEMENT

I would like to acknowledge the following people and Organisations for their contribution physically, spiritually, financially and academically towards the completion of this thesis:

- To my supervisor Prof. IRINA MASALOVA, for her infinite guide, encouragement, support, and determination through the whole research process till the completion of this thesis and the entry to my professional career.

- To AEL (African Explosives Limited) for their sponsorship and the permission to publish the results of the studies of my dissertation and for offering me a position within their Research and Technology Department.

- To Prof A. MALKIN for his helpful comments and suggestions.

- To my institution CAPE PENINSULA UNIVERSITY OF TECHNOLOGY, and to my Research unit FPRC (FLOW PROCESS RESEARCH CENTRE) as well as to my FACULTY and DEPARTMENT ENGINEERING CHEMICAL respectively.

- My sincerely thanks to my laboratory supervisor Mr NAZEEM GEORGE for his assistance and help.

- My sincere thanks to all my colleagues SIPHO, STEEVE, REZA, KARINA and BERNARD; and all my friends near or far distance from me (ROSIE, ARTHUR, RYAN, LUNGELWA, JAMIE, CYNTHIA, ZAKI, IBED, ABAKAR, AHMAT) and to CPUT and FPRC staffs for their endless support, assistance and motivation.

Hamat A. YAKHOUB

April 2009

NOMENCLATURE

Symbol	Description	Unit
A	Normalizing factor in gauss equation	---
ΔA	Change in interfacial area	m^2
C_m	Dispersed phase mass fraction	---
Ca	Capillary number	---
$Ca_{crit.}$	Critical Capillary number	---
d	Droplet size diameter	μm
D_{max}	Maximum droplet size diameter	μm
D_{50}	Volume median diameter or droplet size at 50% volume	μm
D_{32}	Sauter mean diameter	μm
$D_{crit.}$	Critical droplet diameter	μm
D_0	Initial droplet size diameter	μm
D	Pipe diameter	m
De	Deborah number	---
E_{ave}	Average error	%
E_ρ	Energy density	J/kg
G	Elastic modulus	Pa
G_0	Plateau elastic modulus	Pa
G'	Storage modulus	Pa
G''	Loss modulus	Pa
G*	Complex shear modulus	Pa
G_m	Mass flow rate	Kg/s
F	External driving force	N
$\tilde{F}_{max}$	Mean dimensionless contribution per drop to the yield stress	---
K	Fluid consistency index	$Pa.s^n$
K_G	Measure of elasticity	$Pa*\mu m^2$
L	Pipe length	m
n	Flow behaviour index	---
ΔG	Change in Gibbs energy	$J.mol^{-1}$
ΔH	Change in Enthalpy	$Kg.mol^{-1}.°C^{-1}$
ΔP	Pressure drop	Pa
ΔP_L	Laplace Pressure	Pa
ΔS	Change in Entropy	J/Kg
P	Pressure	Pa
Q	Volume flow rate	m^3/s
R	Radius of droplet size	m
R_{32} or R_{SV}	surface-area mean drop radius	m
R_1	Principal radii of curvature	m
R_2	Principal radii of curvature	m
T	Temperature	°C
$T_{crit.}$	Fudge point	°C
t_{obs}	Characteristic time of observation	s
V	Average flow velocity	m/s
V_E	Total Volume of emulsion	m^3
V_{DPh}	Volume of emulsion droplets	m^3
X	degree of crystallinity	%

Greek symbols

γ	Shear strain	%
γ_L	Limiting strain deformation	%
$\dot{\gamma}$	Shear rate	s^{-1}
$\dot{\gamma}_w$	Average or "bulk" shear rate	s^{-1}
η	Shear viscosity	Pa.s
η^*	Complex viscosity	Pa.s
η_C	Viscosity of the continuous phase	Pa.s
η_d	Viscosity of dispersed phase	Pa.s
η_0	Zero shear Newtonian viscosity	Pa.s
η_∞	Infinite shear Newtonian viscosity	Pa.s
f	Density of the distribution function	
τ	Shear stress	Pa
τ_w	Shear stress at the pipe wall	Pa
τ_y	Yield stress	Pa
τ_{deform}	Disruptive forces required to deform droplet	Pa
ϕ	Dispersed phase volume fraction	---
σ	Interfacial tension	$N.m^{-1}$
ρ	Density	$Kg.m^{-3}$
ρ_c	Density of continuous phase	$Kg.m^{-3}$
ρ_{DPh}	Density of dispersed phase	$Kg.m^{-3}$
θ	Characteristic time relate constant of the process	---
θ_D	Characteristic pumping parameter	---
θ_ω	Characteristic pumping parameter	---
λ	Viscosity ratio	---
Γ	Surface tension	$N.m^{-1}$
ω	Width of droplet size distribution	m
$\omega_{crit.}$	Critical width of distribution	m
ω_0	Initial width of distribution	m
ϖ	Angular velocity	s^{-1}

TERMS AND CONCEPTS CITED

Term		Definition
Breaking	:	An event where gross separation of the two phases (continuous & dispersed) occurs in which the identity of individual drop is lost; along with the physical and chemical properties of the emulsion (it is macroscopically apparent)
Coalescence	:	Spontaneous joining together of smaller droplets in an emulsion system to form larger ones (it may eventually lead to breaking of the emulsion system into two separate phases in the absence of a surfactant).
Congelation	:	Phase conversion of a thin waxy liquid into a thick congealed waxy material often affected by cooling.
Creaming	:	Form of gravitational separation described by an upward movements of droplets that caused by their lower density than the surrounding liquid.
Crystallization	:	Destabilization mechanism due to a change in the physical state of emulsion's dispersed phase – change from liquid state to crystal state.
Elastic	:	A conservative property in which part of the mechanical energy used to produce deformation is stored in the material and recovered on release of stress.
Elastic modulus	:	A modulus of a body that obeys Hooke's law.
Emulsion Explosive	:	High-internal-phase water-in-oil emulsion of a concentrated solution of nitrate salts in water emulsified into an oil base.
Flocculation	:	Cohesion of droplets in the formation of three-dimensional clusters without coalescence.

Hook's law : Provides that the quotient of stress and strain (i.e. the modulus) is a constant. A body obeying Hook's law can not be viscoelastic nor does flow occur

Instability : The ability of an emulsion to undergo changes in its properties over time – therefore the less stables the emulsion, the faster its properties change. This instability could be creaming, flocculation, coalescence, partial coalescence, phase inversion, crystallization and Ostwald ripening. However the occurrence of such destabilization phenomena depends on 3 things – composition, microstructure and environmental condition.

Loss Modulus : Its value is a measure of the deformation energy used up in the sample during the shear process and lost to the sample afterwards. This energy is either used up during the process of changing the sample's structure or dissipated into the surrounding environment in the form of heat.

Modulus : The quotient of stress and strain where the type of stress and strain is defined by the type of deformation employed.

Newtonian fluids : Fluids showing a flow behaviour in which the shear viscosity of the fluid remains constant irrespective of the amount of the stress or shear is applied. Mathematically, shear stress is linearly related to the rate of shear.

Non-Newtonian fluids: Fluids whose flow behaviour does not obey the Newtonian's law, i.e. viscosity is dependence to stress or shear rate.

Partial Coalescence: A destabilization mechanism whereby the droplets retain their shape, but there is a molecular contact between the droplets favoring, e.g. crystal growth.

Plastic : The property of a solid body that is in the elastic state when the stress is below a critical value, termed the yield stress, and in the plastic state when this value is exceeded. During ideal plastic flow, energy dissipation and stress are independent of the rate of deformation.

Relaxation time : A time characterizing the response of a viscoelastic material to the instantaneous application of a constant strain.

Rheology : The science of the deformation and flow of matter.

Rheometer : An instrument for measuring reological properties.

Rheopexy : An effect by which a material recovers some of its pre-sheared viscosity at a faster rate when it is gently sheared compared to when it is allowed to stand. Although rheopexy or thixotropy accompanies an isothermal structural change, which induced by mechanical disturbance to the fluids. When the mechanical disturbance is removed, these fluids recover their equilibrium structures. Therefore rheopectic behaviour is characterized by a gradually increasing viscosity when the fluid is subjected to a given stress.

Sedimentation : Form of gravitational separation described by downward movements of droplets due to difference in the density of Continuous & Dispersed phases

Shear Rate : Rate of shear deformation, change of shear deformation per unit time.

Shear Stress : Component of stress parallel or tangential to the direction of flow.

Shear Thinning : A reduction of the viscosity with increasing rate of shear in steady flow

Storage Modulus : Its value is a measure of the deformation energy stored in the sample during the shear process. After the load is removed, this energy is completely available and acts as the driving force for the reformation which partially or completely compensates the previous deformation.

Thixotropic behaviour : A reversible time dependence decrease in viscosity with time at a particular shear rate.

Yield Stress : A critical shear stress value below which an ideal plastic or viscoplastic material behaves like a solid (no flow). Once the yield stress is exceeded,

a plastic material yields (deforms plastically) while a viscoelastic material flows like liquid.

Viscoeleastic : A time-dependent property in which a material under stress produces both a viscous and an elastic response.

Viscosity : Resistance to flow. Qualitatively, the property of a material to resist deformation increasingly with increasing rate of deformation. Quantitatively, a measure of this property defined as the quotient of shear stress divided by shear rate in steady flow.

Viscous : The tendency of a liquid to resist flow as a result of internal friction. During viscous flow, mechanical energy is dissipated as heat and the stress that develops depends on the rate of deformation.

TABLE OF CONTENT

LIST OF FIGURES

LIST OF TABLES

CHAPTER 1
INTRODUCTION

The emulsion used in this study was of the "liquid explosive" type. Such an emulsion is classified as a highly concentrated water-in-oil emulsion, with the dispersed phase volume fraction exceeding the close packing limit of spherical droplets (up to 94% by mass). It consists of an aqueous solution of inorganic oxidizer salts (e.g. Ammonium nitrate) with the salt emulsified in melted form as supersaturated, supercooled droplets into a hydrocarbon oil base. The continuous phase or oil phase consisted of surfactant based on organic derivatives of *PIBSA* (an industrial acronym for poly(isobutylene) succinic anhydride).

Such emulsion products have numerous potential technological applications in the mining industries and other operations requiring blasting of rock or minerals and are used as re-pumpable materials. Therefore they are subjected to repeated handling or shearing action during their transportation, involving mixing, pumping, stirring and filling, which tends to alter and/or have a tremendous impact on their desired functionality and might reduce shelf-life and performance of the final product.

Some of their properties pertaining to sensitivity and stability may be improved slightly by passing the emulsion through a high-shear system to break the dispersed phase into even smaller droplets prior to adding other addictive (e.g. gassing solution). But the emulsion viscosity must remain low enough to allow for re-pumping at reasonable pressure. Or indeed repeated handling or shearing action tends to increase the emulsion's viscosity.

Thus, the challenge to manufacturers of industrial emulsion explosives is to produce emulsion products that have high desirable functionality and/or performance; hign stability to crystallisation once exposed to high shearing; but with more restrained refinement and less crystal content; which is often extremely difficult. Therefore it is hugely necessary to control the disruption of droplets and their instability in order to produce emulsions that have high stability once they have been exposed to high shearing.

The ability to do so therefore depends on an understanding of the major factors that govern the concept of disruption (break-up) of droplets through distortion; the viscous or elastic resistance of the droplet interior and of the interface layer to distortion; and their initiation towards instability (e.g. crystallisation, coalescence, etc.) during the shearing process.

Thus, the overall aim of this study is to investigate the effect of high shearing resulting from conditions of the manufacturing process, such as pumping, on the Rheological / Structural properties of emulsion explosives with various formulations of content. Various formulation content in this context also concerns how the excess concentration (effect of surfactant concentration); surfactant type (chemistry of surfactant head group); and ammonium nitrate concentration in the dispersed phase may affect the rheological properties, such as modulus and yield stress, of these materials during the pumping process.

It is well known that an emulsion's structure and rheology is directly relevant to its stability. Therefore, it is of great interest to use this knowledge as a basis for analysis of the effect of high shearing on the stability and structural properties of these emulsions. Knowledge of the mechanism of the deformation and disruption of emulsion droplets, refinement and destabilisation phenomena such as crystallisation, and coalescence has been the main focus for this study.

The structure and properties of emulsions have been studied from different points of view which are presented in many papers. Pioneering works published by Princen (1983, 1985) and Princen and Kiss (1986) demonstrated the role of the concentration of the dispersed phase and showed that the rheological properties are characterised by elasticity at low shear stresses and the existence of yielding behaviour. However, Masalova, Malkin, Slatter & Wilson (2003); Masalova, Taylor, Kharatiyan & Malkin (2005); Masalova, Malkin, Kharatiyan, Taylor & Haldenwang (2006) and Masalova & Malkin (2007a, b); Malkin, Masalova, Slatter & Wilson (2004a) and Malkin, Masalova, Pavlovski & Slatter (2004b) studied the rheological properties of highly concentrated w/o emulsions. They found that the emulsions are rheopectic materials and the shape of droplets is polygonal. They identified an incorrect prediction about the dependence of elastic modules on the droplet size when using the Princen-Kiss theory. They therefore proposed a new model based on either geometrical or dimensional arguments, which predicts that the elastic modules should be proportional to the concentration of a dispersed phase and squared reciprocal size of droplets. This model includes the width of an elastic layer as an additional geometrical factor.

There are several main types of instability in emulsions, namely creaming, flocculation, coalescence, crystallisation and disruption, which disturb and eventually destroy the microstructure of an emulsion (Mulder & Walstra, 1974; McClements, 2005). The physical stability of emulsions, in particular of the dispersed droplet phase, is an important factor when processing these colloidal materials (emulsions) (Hetzel, Nielsen, Wiesner & Brummer,

2000). They found that under these processing conditions, physical stability does not include the physical state of the dispersed emulsion droplets only; it also considers destabilisation phenomena such as flocculation or coalescence, where the droplets come into close contact with one another, which poses a certain threat to emulsion stability. In this case, both classical coalescence and crystallisation of the dispersed phase will lead to an additional destabilisation mechanism called partial coalescence: the emulsion droplets retain their shape, but there is molecular contact between the droplets leading to an exchange of the dispersed phase material between the droplets which, for instance, favour crystal growth (Fischer, Eugster, Windhab & Schuleit, 2007).

However, only very few publications concerning correlation through direct observation of the structural process during conditions of transportation of these emulsion materials with changes of their rheological properties can be found. Nevertheless, previous experimental studies were conducted in different emulsion systems, in order to investigate the influence of high shearing on the stability of an emulsion. In some cases, coalescence took place in some (Greene, Hammer & Olbricht, 1994; Saboni, Gourdon & Chesters, 1995; Loewenberg & Hinch, 1997; Rother *et al.*, 1997; Guido & Simeone, 1998; Hu, Pine & Leal, 2000; Park, Yamaguchi & Nakao, 2001; Yan, Thompson & Valsaraj, 2006; Zhou, Yue & Feng, 2008), crystallisation in others (Ziegleder, 1985; Narine & Marangoni, 1999; Sato, 2001; Mazzanti, Guthrie, Sirota, Marangoni & Idziak, 2004), and phase inversion also occurred (Shinoda & Friberg, 1986; Salager *et al.*, 2004). Additional destabilisation mechanisms such as partial coalescence have also been reported (Boode, Bisperink & Walstra, 1991; Boode & Walstra, 1993; Boode, Walstra & deGroot-Mostert, 1993; Fisher *et al.*, 2007). In addition to coalescence or other destabilisation phenomena, emulsion stability can also be affected by disruption of droplets (refinement) (Mulder & Walstra, 1974). Indeed, it was widely established that intense shearing causes refinement of droplets and this implies that the refinement induces an increase in rheological properties (viscosity, elastic modulus, yield stress).

The disruption of droplets was classified as a type of emulsion instability (Mulder & Walstra, 1974) where they found that droplets must first be deformed. The researchers stated that a droplet resists distortion, as this causes its internal pressure P to increase: the Laplace equation states that a pressure different ΔP_L exists between the two sides of a curved surface, the pressure being higher on the concave side (see Equation 1.1):

$$\Delta P_L = \sigma\left(\frac{1}{R_1}+\frac{1}{R_2}\right) \qquad \textbf{(Equation 1. 1)}$$

where σ is the interfacial tension and R_1 and R_2 are the principal radii of curvature – hence, the smaller the droplet, the greater its resistance to deformation. Since the stress is generally transmitted by the surrounding liquid via agitation, higher stresses need more vigorous agitation, hence more energy is needed to produce smaller droplets (Walstra, 1983). Other factors such as the viscous or elastic resistance of the droplet interior and of the interface layer (composed of surfactants) to distortion where this interfacial layer was considered to be strongly cohesive and may even have certain rigidity were also identified. These properties would hinder fluid circulation inside the droplet during deformation, probably increasing its resistance to distortion (Walstra, 1983).

Becher (1988) reported that such a melt (concentrated solution of inorganic salt) in emulsion explosives has a crystallisation point (more properly a fudge point) of around 70°C and therefore must be heated before inclusion into the emulsion. He advanced that this is one of the startling features of this system that in the properly formulated emulsion explosive the droplets of the melt phase remain liquid down to temperatures as low or lower than -20°C. Thus, such systems are considered to be thermodynamically unstable and have a simultaneous tendency to droplet crystallisation. Therefore it is essential for the proper functioning of emulsion explosives that these droplets remain liquid, and a great deal of research has been devoted to means of preventing crystal growth and its propagation through the emulsion (Becher, 1988).

However Masalova *et al.*, (2003, 2005, 2006); Malkin *et al.*, (2004a,b) and Masalova and Malkin (2007a,b; 2008), in their publications dedicated to rheology of w/o emulsion explosives, presented a clear correlation between stability and rheology. Masalova *et al.*, (2006) studied the ageing process of highly concentrated emulsions. They found that the origin of ageing of highly concentrated emulsions of the water in oil type (with volume fraction up to 90% by volume) consists primarily in slow crystallisation of the dispersed phase comprising of an overcooled highly concentrated aqueous solution, which leads to the increase of solid-like properties of a dispersion than can be considered as the emulsion-to-suspension transition. Their observation showed a significant shift of rheological properties to the solid-like behaviour; this was the result of the emulsion ageing, which shows itself as an increase of the storage modules and yield stress with time. The kinetic of crystallisation of

these emulsions was satisfied by the Johnson-Mehl-Avrami-Kolmogorov (JMAK) equation (see Equation 1.2) and the coalescence effects were excluded due to the fact that the size of droplets does not change in this ageing process, and before the initiation of crystal (Masalova et al., 2006; Kharatiyan, 2005).

$$X = 1 - e^{-(t/\theta)^n}$$ **(Equation 1. 2)**

where X is the degree of crystallinity, θ is the characteristic time related constant of the process, n is an empirical factor found to have a high value in their studies, exceeding the maximum-predicted theoretical value of 4 (Mandelkern, 1964). This later explained the probable mechanism responsible of the growth of crystallites out of the volume of a single droplet, thereby breaking through the inter-phase layers and combining with other crystals that appear in neighbouring droplets which, in turn, initiate acceleration of crystallisation (Masalova *et al.*, 2006; Masalova & Malkin, 2008).

From this, the current study continues to investigate the stability factors accounted for during the processing of these highly concentrated emulsion explosives. Thus the following questions contributed to the research question when exposing the emulsion materials to high shearing:

- How the excess concentration (effect of surfactant concentration); surfactant type (chemistry of surfactant head group); and ammonium nitrate concentration in the dispersed phase may affect the rheological properties such as modulus and yield stress of these materials during the shearing process?

- Do the droplets rupture to lead to more refinement, causing an increase in rheological properties?

- Do the droplets just start to crystallise when high shear is applied to the emulsion materials, again causing an increase in rheological properties?

- Do the droplets coalesce to lead to a decrease in rheological properties?

- Do both or multiple effects take place at the same time: Coalescence-crystallisation; or refinement-coalescence; or refinement-coalescence-crystallisation; etc.?

Prior to answering these research questions, it was necessary to set objectives for the study. These were as follows:

- To produce highly concentrated water-in-oil emulsions of the same drop size and similar size distribution using different types of surfactant (surfactant head group – MEA, UREA, IMIDE) and different surfactant concentrations in order to have the same starting point for the investigation of any destabilisation mechanism that might arise during the shearing process
- To shear the emulsion samples using a piston-pumping device which generates enough shear rate to alter the structure of these materials
- To determine the effect of surfactant type (surfactant head group) and surfactant concentration during the shearing process of such emulsion types.
- To find the criterion that determines any destabilisation mechanism that might arise during the pumping process, and finally
- To produce emulsions of different droplet sizes but the same oil and surfactant concentration and lower ammonium nitrate concentration in the dispersed phase in order to investigate the salt (ammonium nitrate) concentration during the shear stability of these materials.

The methodology that was used to achieve the above objectives is described below:

Pre-Test (Matrix of sample)

It is possible to obtain emulsions of different formulations and surfactant concentrations with same droplet size and distribution with the use of the Hobart N50 mixer through varying the speed of rotation of the stirrer and the time taken for stirring (deformation).

The emulsion samples consisted of the following:

- 4 different Surfactants based on organic derivatives of PIBSA with molecular weight of 900-1300 amu:
  - ✓ Pibsa-MEA
  - ✓ Pibsa-UREA
  - ✓ Pibsa-IMIDE
  - ✓ Pibsa-MEA/SMO
- Mosspar-H oil type
- Ammonium Nitrate as Oxidizer

The following constituted the emulsion formulation used in this study:

- Samples of four different surfactant types with each surfactant having two concentrations (8% and 14% surfactant concentration). This came to an overall number of 10 fresh samples prior to shearing:
  - ✓ Pibsa-MEA in Mosspar-H
  - ✓ Pibsa-UREA in Mosspar-H
  - ✓ Pibsa-IMIDE in Mosspar-H
  - ✓ Pibsa-MEA/SMO in Mosspar-H
- Three samples of different droplet size but the same formulation content (Pibsa-Urea in Mosspar-H)

The Shearing process – pumping

The pumping system consisted of a cylindrical chamber and an outlet orifice of small diameter. A piston-shaft was mounted into the chamber, to be moved downward under application of force. Therefore, during the operation of this device, the emulsion sample was forced out of the chamber of the piston by means of high pressure applied to the piston shaft through the small outlet of this instrument designed for pumping. In this manner, the "already produced and cooled to room temperature" emulsion sample was exposed to high shear, which was the result of the high friction generated between the orifice edge and the flow material.

Two (2) orifices of different diameters, namely 3 mm and 4 mm were to be used to shear the prepared emulsion samples. Each sample was to be pumped seven times at each orifice. That made a total of 141 samples for analysis.

Microscopy Observation

For the qualitative analysis of the sheared samples, it had to be seen whether sample droplets became refined, crystallised, or coalesced. This optical analysis was achieved with the use of a Leica optical microscope equipped with a digital camera and high magnification of 63 × 0.80.

Measurement of particle size distribution

A Malvern Mastersizer 2000 (light scattering technique) was used for measuring droplet size and droplet size distribution for all the emulsions: fresh samples as well as sheared samples. The measurement was achieved by measuring the angle distribution of the He-Ne laser light scattered by particles.

Rheological measurement

The rheological measurements were performed with the use of a rotational dynamic rheometer MCR 300 (Paar Physica).The geometry of the measurement unit was "plate-and-plate" with a sandblasted surface and a plate diameter of 50 mm, while the gap measurement between the two plates was 1 mm.

The type of rheological measurement conducted in this work was as follows:

- Amplitude Sweep Curve in order to define the Viscoelastic properties of the materials where the setting of the measurement parameters was done by keeping constant frequency of 1 HZ and strain was selected as the set variable and kept between 0.1 to 200 %.

- The flow curve measurement was performed at the downward sweeping shear rate mode; the shear rate was selected as the set variable and kept between 200 to $1x10^6$ 1/s.

All rheological measurements were conducted at 30°C, whereas the rheological investigation consisted of the following steps:

- Measuring of the flow and viscoelastic properties of the materials with
  - ✓ Fresh emulsions
  - ✓ Sheared emulsions
  - ✓ Different surfactant concentration after pumping
  - ✓ Different surfactant type after pumping
  - ✓ Low ammonium nitrate concentration in the dispersed phase

- Determining the rheological model to describe the flow behaviour of the fresh and sheared samples.

- Determining the characteristic rheological parameters in order to use them for the modelling of the structure change during the prolonged shearing and/or pumping.

- Correlation of the characteristic rheological parameters with emulsion formulation (surfactant concentration and surfactant type) and shearing action.

Although the following aspects were not covered in this research, it may be considered as future topics for investigation:

- The effect of high shearing on the evolution of rheological properties of this emulsion (highly concentrated emulsion explosives) with ageing.

- The effect of oil type on the rheological and structural properties of the highly concentrated emulsion under high shearing.

- The effect of variation of temperature during the high shearing process of emulsion.

However the following present the contribution of the research:

- Establishment of a valuable technique that mimics the transportation process conditions on a small scale in the laboratory so that correlation between rheological parameters such as viscoelastic properties (G') and flow properties (τ_y), droplet size characteristics (D_{32}) and pumping parameters (energy input) could be demonstrated.

- Obtaining data characterising the determination of destabilisation phenomena or refinement (e.g. disruption evolution) as function of surfactant concentration and surfactant type by means of droplet size distribution.

- Establishment of a methodology that might be applied directly to different techniques of shearing such as extrapolation to bigger scale pipeline transportation.

Rheology is a multidisciplinary field, and has wide applications in science, engineering and technology. Thus rheological properties of highly concentrated emulsion explosives dictate their structural behaviour, flowability, and stability during shelf life or processing. From the results of this study, the criterion that characterises the influence of high shearing on the parameters of structural change or final average droplet size and the width of their size distribution of emulsion explosives which results from conditions of the transportation process was determined.

This thesis is divided into five chapters, with each chapter dealing with a precise topic that constituted one of the compound through which the answers to the above research

questions, objectives, contributions and significance were achieved. Thus, the following characterized the chapters within this dissertation:

- Chapter 1 presents the main introduction to this research.

- Chapter 2 comprises a presentation of the relevant theory and literature studied to understand the fundamental concept of emulsion, emulsion explosives and their constituent components, and theory of emulsion stability, including previous studies of the shearing process. The chapter therefore covers relevant literature on theoretical rheological fundamentals of highly concentrated emulsions including relevant experimental work.

- Chapter 3 provides a comprehensive description of the materials used in order to manufacture the emulsion samples, the instrumentation and the experimental procedures used to achieve the objective of the research.

- Chapter 4 presents the core part of this thesis with the analysis and interpretation of the experimental results being presented, discussed and summarised.

- Chapter 5 comprises the overall conclusion of this research.

The principal results of this study were submitted to be published as a paper in the journal of *Chemical Engineering Communications* under the title "*HIGHLY CONCENTRATED EMULSIONS: ROLE OF DROPLET SIZE*" and authors (*H.A. Yakhoub, I. Masalova and R. Haldenwang*). Thus, this could be regarded as the contribution of this research project.

CHAPTER 2
THEORY AND LITERATURE REVIEW

2.1 INTRODUCTION

The basic definition and theory of emlsions is covered in the first section of this chapter. Following this, the relevant basics of emulsion explosives are detailed with more emphasis on the main components that constitute such types of emulsions and their particular features (i.e. high internal phase ratio). The notion of emulsion stability under a shearing process is highlighted, with a brief discussion of drop deformation and break-up. This is addressed in order to have a better understanding of the physical aspects of droplet behaviour and shearing in emulsions. The last section covers the essential and basic theory of the rheology of highly concentrated emulsions that involve flow and viscoelastic properties; the dependence of structural parameters, such as droplet size and droplet size distribution. The effect of the shearing process (which might induce drop refinement) on the rheological properties of the emulsions relevant to this research is also addressed.

The following topics and sub-topics that were investigated by means of the theory and literature review for this research project are discussed in this chapter:

- Definition of emulsions
- Emulsion explosives
- Main components of emulsion explosives
- Stability of emulsion during the shearing process
- Rheology of highly concentrated emulsions
- Herschel-Bulkley or yield-pseudoplastic flow model
- Viscoelastic behaviour of highly concentrated emulsions
- Rheology of emulsion explosives, including the correlation of their stability with their rheology.

2.2 GENERAL DEFINITIONS OF EMULSIONS

Emulsion is defined as a mixture of two immiscible liquids with one liquid being dispersed as small spherical droplets into the other (Figure 2.1). High specific surface areas resulting from the dispersion process are not energetically favoured, as in the simple example of the homogenisation of pure oil and pure water which rapidly result in separation into two separate layers that consist of a layer of oil (lower density) on top of a layer of water (higher density). This can be explained by the fact that the driving force behind this process is the contact between oil and water molecules, which is energetically unfavourable (Israelachvili 1992). Emulsions therefore are thermodynamically unstable and are supposed to break, i.e. to completely separate into two phases, after a finite amount of time.

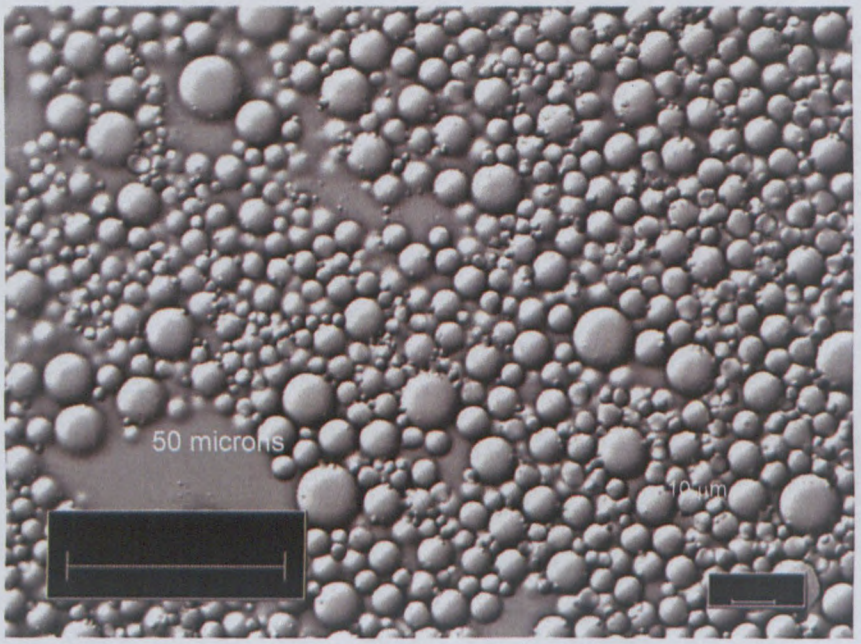

Figure 2.1: Microscopic image of an emulsion (McClements, 2005)

Emulsions can be classified conveniently according to the distribution of the oil and aqueous phases. A system consisting of oil droplets dispersed in an aqueous phase is called an oil-in-water, or O/W, or inverse emulsion. A system which consists of the water droplets dispersed in an oil phase is called a water-in-oil or W/O emulsion. The substance that makes up the droplets in an emulsion is referred to as the dispersed or internal phase, whereas the substance that makes up the surrounding liquid is called the continuous or external phase. It is also possible to prepare multiple emulsions of the oil-in-water-in-oil (O/W/O) or water-in-oil-in-water (W/O/W) type (Dickinson & McClements, 1995; Evison *et al.*, 1995). For example, a W/O/W emulsion consists of water droplets dispersed within larger oil droplets, which are themselves dispersed in an aqueous continuous phase (Evison *et al.*, 1995).

This example of pure water emulsified into pure oil broadly explained the thermodynamic instability illustration of emulsion systems. On the molecular level, however, oil molecules, mainly considered as nonpolar molecules, are incapable of forming hydrogen bonds (Israelachvili 1992, Evans & Wennerstrom 1994). Thus, when a nonpolar molecule is introduced into liquid water, the water molecules surrounding it change their orientation so that they can maximise the number of hydrogen bonds formed with neighbouring water molecules (McClements, 1999) (Figure 2.2).

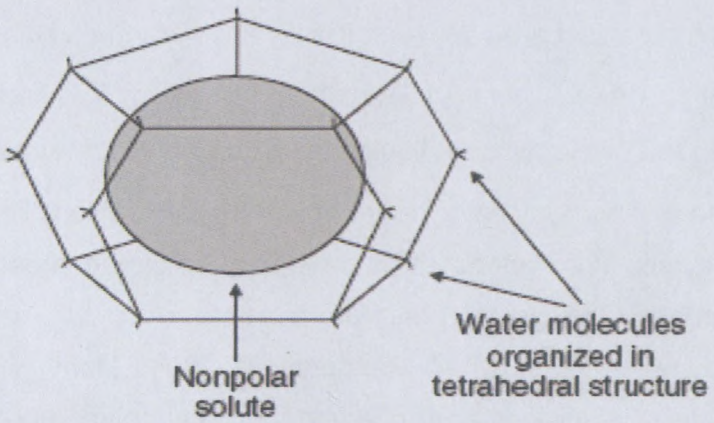

Figure 2.2: Schematic representation of the reorganisation of water molecules near a nonpolar solute (McClements, 1999)

Tanford (1980) illustrated the behaviour of nonpolar solutes in water, which can be understood as change in both the enthalpy ($\Delta H_{transfer}$) and entropy ($\Delta S_{transfer}$) of the system. The enthalpy change is related to the alteration in the overall strength of the molecular interactions, whereas the entropy change is related to the alteration in the structural organisation of the solute and solvent molecules (McClements, 1999). The overall free energy change ($\Delta G_{transfer}$) depends on the relative magnitude of these two contributions (Evans & Wennerstrom 1994):

$$\Delta G_{transfer} = \Delta H_{transfer} - T\Delta S_{transfer} \qquad \textbf{(Equation 2.1)}$$

Tunon, Silla & Pascual-Ahuir (1992) showed that the free energy associated with transferring a nonpolar molecule from an environment where it is surrounded by similar molecules to one in which it is surrounded by water molecules is the product of its surface area and the interfacial tension between the bulk nonpolar liquid and water (Equation 2.2). Therefore, an aqueous solution containing a nonpolar solute can decrease its free energy by reducing the

unfavourable contact area between the nonpolar groups and water, which is known as the hydrophobic effect (McClements, 1999):

$$\Delta G = \sigma_i \Delta A \qquad \textbf{(Equation 2.2)}$$

As the mixing of oil and water is strongly unfavourable because of the hydrophobic effect, it is necessary to supply energy to the system in order to increase the contact area between oil and water molecules. The amount of energy which must be supplied is proportional to the increase in contact area between the oil and water molecules, i.e. $\Delta G = \sigma_i \Delta A$ (Equation 2.2) (Hiemenz, 1986), where (ΔG) is the free energy required to increase the contact area between the two immiscible liquids by ΔA (at constant temperature and pressure), and σ_i is a constant of proportionality called the interfacial tension. The interfacial tension is a physical characteristic of a system which is determined by the imbalance of molecular forces across an interface: the greater the interfacial tension, the greater the imbalance of forces (Israelachvili 1992, Evans & Wennerstrom, 1994). Many of the most important macroscopic properties of emulsions are governed by this imbalance of molecular forces at an interface, including the tendency for droplets to be spherical, the surface activity of emulsifiers, the nucleation and growth of crystals and meniscus formation (McClements, 1999).

Although the formation of emulsions are thermodynamically unfavourable, it is possible to form emulsions that are kinetically stable (metastable) (Atkins, 1994) for a reasonable period of time (a few days, weeks, months, or years) by including substances known as emulsifiers and/or a thickening agent prior to homogenisation. Emulsifiers or, more particularly, surfactants, are surface-active molecules that adsorb to the surface of freshly formed droplets during homogenisation to form a protective membrane, which prevents the droplets from coming close enough to aggregate. Most emulsifiers (surfactants) are amphiphilic molecules (i.e., there are polar and nonpolar regions on the same molecule). Thickening agents are ingredients that are used to increase the viscosity of the continuous phase of the emulsion, and they enhance emulsion stability by retarding the movement of the droplets. A stabiliser is any ingredient that can be used to enhance the stability of an emulsion and may therefore be either an emulsifier or a thickening agent (McClements, 1999).

Kharatiyan (2005) highlighted that most emulsions are much more complex than the simple three-component (oil, water and emulsifier) system. The aqueous phase may contain a variety of water-soluble ingredients. The oil phase usually consists of a complex mixture of

oil-soluble components. The interfacial region may contain a mixture of various surface-active components. In addition, these components may form various types of structural entities in the oil, water or interfacial region (McClements, 1999).

Kharatiyan (2005) reported that knowledge of the concentration of droplets is important because the droplet concentration influences the appearance, texture, stability and cost (in terms of the concentration of the oil phase and, therefore, the surfactant) of emulsion-based products. The concentration of droplets in an emulsion is usually described in terms of the dispersed phase volume fraction (ϕ), which is equal to the total volume of the emulsion droplets (V_{DPh}) divided by the total volume of the emulsion (V_E): $\phi = \frac{V_{DPh}}{V_E}$. In some situations, it is more convenient to express the composition of an emulsion in terms of the dispersed phase mass fraction (C), which is related to the volume fraction by the following equation:

$$C_m = \frac{\phi \rho_{DPh}}{\phi \rho_{DPh} + (1-\phi)\rho_c} \quad \text{(Equation 2.3)}$$

where ρ_c and ρ_{DPh} are the densities of the continuous and dispersed phases, respectively. When the densities of the two phases are equal, the mass fraction is equivalent to the volume fraction. The dispersed-phase volume fraction of an emulsion is often known because the concentration of the ingredients used to prepare it are carefully controlled (McClements, 1999).

It is generally accepted that the volume fraction of the dispersed phase in a reasonably stable emulsion can be increased relatively easily up to a certain critical value, above which the emulsion tends to break or invert (Becher, 1988). In the case of a monodispersed emulsion, Ostwald's phase volume theory indicates that this point is reached at, or is close to, ϕ = 0.7405, i.e., the volume fraction that corresponds to the hexagonal close packing of undistorted spheres.

Quite stable emulsions of a considerably higher volume fraction of the dispersed phase are known to exist under the following conditions:

- When the emulsion is strongly heterodispersed, the interstices between the spherical droplets can be filled successively by smaller ones. This would, in principle, allow the dispersed phase volume fraction to closely approach unity.

- Under the influence of a centrifugal force field, the emulsion can be compressed considerably (Mittal, 1975). The droplets are forced to deform, i.e., they flatten in those areas where they make "contact" and assume the shape of polyhedra with rounded edges and corners. In the case of centrifuged emulsion, the imposed deformation will normally relax as soon as the centrifugal force field is removed. The continuous phase that was squeezed out during centrifugation will re-enter the emulsion matrix until $\phi \leq 0.7405$.

- Emulsions with a dispersed phase volume fraction as high as 0.99 have been reported in the literature from time to time. These systems have been studied in some detail, particularly by Lissant (1966), Lissant & Mayhan (1973), Lissant *et al.*, (1974), Princen (1979), and Princen *et al.* (1980). The high values of the dispersed phase volume fraction were attained in the absence of a centrifugal force field and cannot be explained on the basis of heterodispersity. The authors stress the importance of the surfactant. Lissant (1966, 1974) has postulated and demonstrated that the droplets are deformed into polyhedral structures of particular types.

2.3 EMULSION EXPLOSIVES

Emulsions Explosives are classified as highly concentrated Water – in – Oil emulsions of a concentrated solution of nitrate salts in water emulsified into an oil base. The internal phase volume fraction of such emulsions was approximated to 94%, i.e. far beyond the close packing limit of spherical droplets of 74%. In general, commercial explosives consist of an intimate mixture of condensed oxidizer, almost invariably the nitrate salts of ammonia, sodium and calcium, which are mixed with a fuel and other additives. The purpose of the latter is to control the rheology and to provide the correct reactivity, physical form, and density to ensure reliable detonation. It is also the most technically sophisticated, as it must meet requirements of shelf life, resistance to handling, immunity to changes in temperature, etc. (Becher, 1988).

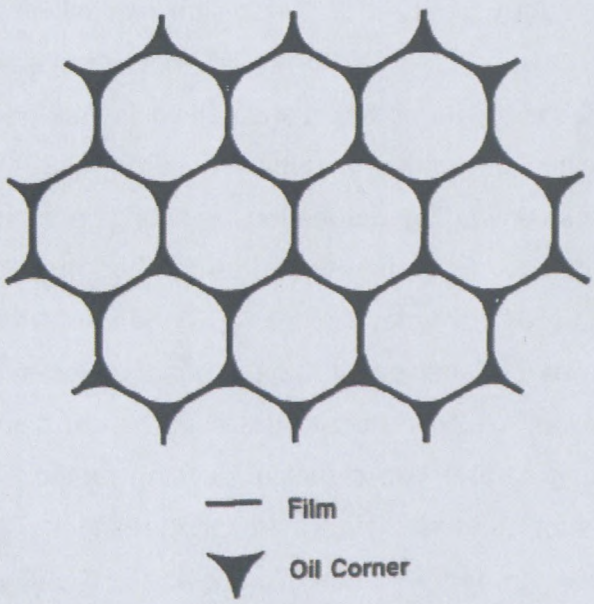

Figure 2.3: Idealised geometric model of an emulsion explosive (Becher, 1988)

Becher (1988) highlighted that the detonation capacities and particularly the high velocities of detonation of emulsion explosives depend on maintaining a very intimately mixed, all-liquid system. In practice, this requires droplet sizes of the order of 1 μm. Since water is an effective detonation inhibitor, the desired sensitivities are achieved by controlling water levels in the formation. Finally, the requirements of redox stochiometry create a situation that can be resolved only by the use of a large volume of supersaturated (and therefore metastable) salt solution, dispersed in a small volume of hydrocarbon oil.

Thus the dispersed phase of the emulsion explosives is constituted of droplets of supercooled concentrated aqueous solutions of inorganic salts, mainly ammonium nitrate (AN) (the major ingredient about 70% by mass of the overall composition) with a minor proportion of *Ca* and *Na* nitrates. The water solution consists of less than 20% of this phase. It is important that, at room temperature, the aqueous phase is supersaturated with the nitrates remaining in a state of solution while the emulsion is stable. The continuous phase is a solution of an emulsifier made up of hydrocarbon oils, which comprises approximately 15% of the oil phase (Malkin *et al.*, 2004a; Masalova *et al.*, 2005). Additional solid ingredients (generally less than 15% by mass) include glass or plastic microbubbles, aluminium powder as an energetic fuel, and some quantities of particulate salts. A variety of other ingredients, e.g., sensitiser, may be added to perform specific functions (Becher, 1988).

Da Silva *et al.*, (2006) reported that emulsion explosives are inherently safer than other common mining explosives, as they will not detonate before they are sensitised. Sensitisation requires the introduction of small voids into the emulsion matrix, typically either air, or some hollow or porous material (Xuguang, 1994). These void spaces undergo adiabatic compression during detonation, resulting in rapid heating to temperatures that exceed the explosive's detonation temperature, thus propagating the explosive shockwave (Bourne & Field, 1991; Bourne & Milne, 2003; Mader, 1965; Sychev, 1985, 1995, 1997). Traditional methods of sensitisation have their drawbacks as they are typically expensive, and often require an explosive to be sensitised before being introduced into its blast hole, thus compromising safety. The chemical gassing method circumvents these problems by generating gas bubbles in situ, via a nitrosation reaction. The resultant gas bubbles form a stable three-phase foamed emulsion (Turner *et al.,* 1999), with bubbles of around 80 μm in diameter (Swayambunathan *et al.*, 1993) and aqueous droplets of around 10 μm in diameter. Foamed emulsions of this type provide excellent sensitisation to detonation, and are highly resistant to pressure desensitisation (Sumiya, Hirosaki & Kato, 2002; Nie, 1997). Chemical gassing utilises inexpensive reagents, and can be performed while the explosive is being loaded into a blast hole. These advantages have installed chemical gassing as the process of choice for the sensitisation of the majority of bulk emulsion explosives (Da Silva *et al.*, 2006).

Chemical gassing is initiated by adding a concentrated nitrite ion solution to an emulsion explosive. Upon mixing, nitrite reacts with ammonia (a component of the explosive) to produce nitrogen gas (Da Silva *et al.*, 2006).

The reaction is sometimes written as (Xuguang, 1994:128-132)

$$NH_4NO_3 + NaNO_2 \rightarrow NH_4NO_2 + NaNO_3 \qquad \textbf{(Formula I)}$$

$$NH_4NO_2 \rightarrow 2H_2O + N_2 \qquad \textbf{(Formula II)}$$

But since it takes place in aqueous solution it is more properly written as:

$$NH_4^+{}_{(aq)} + NO_2^-{}_{(aq)} \rightarrow 2H_2O_{(l)} + N_{2(g)} \qquad \textbf{(Formula III)}$$

This process proceeds slowly at ambient temperatures, which constitutes its major drawback (Manka, 2004). Even in the presence of powerful catalysts such as thiocyanate (Williams, 1977) explosives may still take over an hour to sensitise, which can cause costly delays. An alternate gassing process has been developed utilising the accelerant thiourea (Pare, 1981), though this process does not sufficiently increase the rate of the ammonia gassing process. Furthermore, the mechanism by which thiourea accelerates chemical gassing is still not clear; due to the multiple roles that thiourea can play in nitrosation reactions. Within this context, the explosives industry seeks to better understand existing gassing technology, and to develop new approaches to accelerate the rate of ammonia and/or thiourea nitrosation, in order to rapidly produce gassed emulsion explosives at temperatures below 25°C (Da Silva *et al.*, 2006).

The chemical gassing of emulsion explosives proceeds via a nitrosation mechanism, by which the nitrosonium cation ($O=N^+$) is transferred from some nitrosating agent to a substrate: The Nitrosation reactions proceed through initial formation of nitrous acid, HNO_2. Nitrous acid may subsequently react with a nitrite ion (NO^-_2) to form dinitrogen trioxide (N_2O_3), or with a hydrogen ion (H^+) to form the nitrosonium cation (ON^+, or ON^+OH_2). These two species both act as powerful nitrosating agents, which are capable of reacting with primary amine substrates, such as ammonia. After being nitrosated, primary amines rapidly decompose to yield nitrogen gas. A further mechanism of nitrosation involves the reaction of nitrous acid with a strong nucleophilic species (designated X^-), to produce a nitrosating agent of the form ONX. Nucleophilic species such as thiocyanate, thiourea and iodide are all known to catalyse nitrosation via this mechanism (Da Silva *et al.*, 2006). Any of the reaction mechanisms discussed above could be operating during both the ammonia and thiourea gassing processes.

Postulated reaction mechanisms for the ammonia gassing process (Da Silva *et al.*, 2006: 3186-3197):

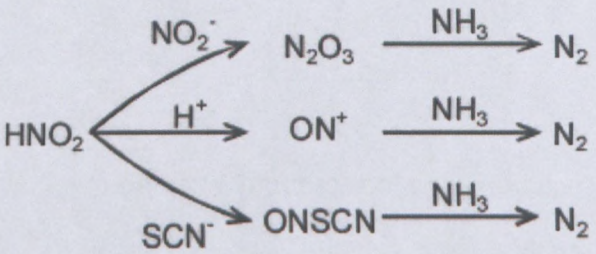

(Formula IV)

The sensitisation process of the emulsion explosives such as the chemical gazing (nitrosation reaction) and the addition of other additives, such as the density control agents, have only one main real effect, to make these compositions detonable. But the main component that influences the emulsion structure, final performance (detonation properties), shelf-life and stability, is the aqueous phase (solution of inorganic oxidizer salts in water), the oil phase (hydrocarbon oil) and the emulsifiers (Surfactants). Thus, these will be described in greater detail in the following section of this chapter.

2.4 MAIN COMPONENTS OF EMULSION EXPLOSIVES

Emulsion explosives, like any other emulsions, are composed of fine dispersions of one liquid in the form of small droplets into another (continuous phase), both liquids being mutually immiscible and resulting in an increase in contact area between the molecules of the two liquids, which make them thermodynamically unfavourable but kinetically stable if a third component is added, namely surfactants/emulsifiers. Water-in-oil emulsion explosives, hereafter referred to as "emulsion explosives", are well known in the industry (Hales, Cranney, Hurley & Preston, 2004). Such systems have been studied in some detail, particularly by Masalova *et al.* (2003, 2005, 2006); Malkin *et al.* (2004a, b); Hales *et al.* (2004); and Becher (1988). Thus, the emulsion explosives were water-in-oil emulsions of a supercooled concentrated solution/melts of inorganic salts in water (aqueous phase) emulsified into a hydrocarbon oils (oil phase), stabilised by surfactants that consisted of organic derivatives of PIBSA, the industry's acronym for poly isobutylene succinic anhydride (Masalova, 2006).

These three components (aqueous phase, oil phase and surfactants) influence and have real effect on the emulsion structure, which is, in turn, directly relevant to its rheology, stability, and detonation properties (Becher, 1988).

2.4.1 AQUEOUS PHASE

The aqueous phase makes up some 90% or more of the emulsion formulation and conventionally consists of a melt of ammonium nitrate, sodium nitrate, and calcium nitrate with a little water to lower the melting point. A typical composition contains from 10 to 20% water and is usually made up so that the composition is close to a eutectic point (lowest freezing point) (Becher, 1988). For example, most packaged explosives are made from an ammonium nitrate/sodium nitrate/water melt of a composition approximately 73/14/13 (Sudweeks & Jessop, 1980a; Sudweeks & Lawrence, 1980b; Wade, 1978), although each manufacturer has a preferred ratio. Becher (1988) advances, for argument's sake, that such a melt has a crystallisation point (more properly a fudge point) of around 70°C and therefore must be heated before inclusion into the emulsion. He added that this is one of the startling features of this system, that, in the properly formulated emulsion explosive, the droplets of the melt phase remain liquid down to temperatures as low or lower than -20°C. Thus he concluded that it is essential for the proper functioning of emulsion explosives that these droplets remain liquid, and a great deal of research has been devoted to means of preventing crystal growth and its propagation through the emulsion.

2.4.2 OIL PHASE

Early in the evolution of emulsion explosives it was realised that the oil phase (continuous phase) played a highly important role in stabilising these systems (Becher, 1988). Indeed, Bluhm's early patent (1969) calls for the use of highly refined (highly paraffinic or naphthenic) paraffin oils and waxes in order to make stable products, and Brockington (1980) and Wade (1978, 1979a,b) showed that the use of such refined waxes was essential to obtaining long-term stability under a variety of conditions. A number of types of waxes have been claimed to be effective in this system, including microcrystalline waxes (Wade, 1978; 1979a, b), insect waxes (Wade, 1979a, b), and paraffin (Bampfield, 1984). Since stability is less of a concern in bulk-delivered explosives, it has proved possible to make bulk products from less refined materials (Mitchell, 1984) or even waste products. Yorke *et al.*, (1983) have shown recently that a wide range of crude or partially refined petroleum products can give results as good as (or even better than) the refined products commonly used.

2.4.3 SURFACTANTS AND THEIR ROLES

As it is well known, emulsion explosives are high internal phase water-in-oil emulsions of a concentrated solution of nitrate salts in water emulsified into an oil base (Masalova *et al.*, 2003, 2005, 2006, 2007a, b; Malkin *et al.,* 2004a, b & Becher, 1988). This dispersion or emulsion phase is held in place by a water-in-oil emulsifier (hereafter "surfactant") provided the emulsified state remains stable (Hales *et al.*, 2004). Thus the principal role of surfactants in emulsions is to enhance their formation and stability (Dickson & McClements, 1995; Bergenstahl, 1997).

Becher (1988) found that surfactants in emulsion explosives have two roles to play: to form and stabilise the high internal phase W/O emulsion at processing temperatures and prevent the droplets that are inevitably nucleated from crystallising the rest of the emulsion. He added that these systems, however, once formed, are cooled thereby supercooling the internal phase; this requires that the surfactant also be capable of maintaining this supercooled state, which implies that the surfactant must not nucleate the nitrate salts.

Chattopadhyay (1996) found that the selection of the surfactant used to prepare an emulsion explosive is of major importance in providing an emulsion which emulsifies easily, has a suitable discontinuous phase droplet size, and is stable during storage to prevent or lower the tendency for the oxidizer salt to crystallize or coalesce, since crystallization or coalescence will adversely affect the explosive properties of the emulsion explosive.

The surfactant will now be further described by means of the following: its definition (what is a surfactant?); its properties in solution/micelles; its role in interfacial properties; and interfacial tension.

2.4.3.1 Definition

As is well known to those skilled in the art, a key to a good emulsion product is the surfactant, which is a chemical whose molecules preferentially occupy the interface between the two phases, thereby forming a barrier layer and preventing coalescence of the dispersed phase droplets. The emulsion is thus rendered stable (Boer, 2003).

Surfactants therefore are amphiphilic molecules that have a hydrophilic head group which has a high affinity for water and a lipophilic tail group which has a high affinity for oil (Myers, 1988).

Figure 2.4, below, is a schematic representation of a surfactant molecule, showing the hydrophilic head and the lipophilic tail.

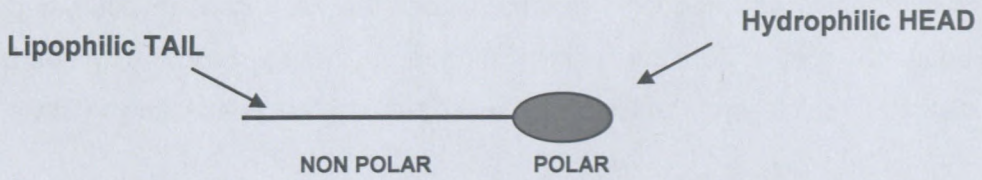

Figure 2.4: Schematic representation of a surfactant molecule

The characteristics of a particular surfactant depend on the nature of its head and tail. The head group may be anionic, cationic, amphoteric or non-ionic. The tail group usually consists of one or more hydrocarbon chains, with between 10 and 20 carbon atoms per chain (St Angelo, 1989; Bergenstahl, 1997); the chain may be saturated or unsaturated, linear or branched, aliphatic or aromatic.

A number of classification schemes have been proposed to facilitate the rational selection of surfactants for particular applications. Classification schemes have been developed that are based on a surfactant's solubility in oil and/or water (Bancroft's rule), its ratio of hydrophilic to lipophilic groups (hydrophile-lipophile balance [HLB] number), and its molecular geometry (Israelachvili, 1992, 1994; Davis, 1994; Bergenstahl, 1997). Ultimately, all of these properties depend on the chemical structure of the surfactant, so different classification schemes are often closely related to each other (McClements, 2005).

Bancroft's rule: One of the first empirical rules developed to describe the type of emulsion that could be stabilised by a given surfactant was proposed by Bancroft (Davis, 1994, Bergenstahl, 1997). Bancroft's rule states that the phase in which the surfactant is most soluble will form the continuous phase of an emulsion. Hence, a water soluble surfactant should stabilise O/W emulsions, whereas an oil-soluble surfactant should stabilise W/O emulsions. It has recently been highlighted that the solubility should be determined by the total surfactant concentration (monomers + micelles) in a phase, not just the monomers (Binks, 1998). This rule works well for a wide range of surfactants, although there are a number of exceptions (McClements, 2005).

Hydrophile-lipophile balance (HLB): The HLB concept is a semi-empirical method that is widely used for classifying surfactants (Bergenstahl, 1997). The hydrophile-lipophile balance is described by a number that gives an indication of the relative affinity of a surfactant molecule for the oil and aqueous phases (Davis, 1994). McClements (2005) stated that each surfactant is assigned a HLB number according to its chemical structure. A molecule with a high HLB number has a high ratio of hydrophilic groups to lipophilic groups, and vice versa. The HLB number of a surfactant can be calculated from knowledge of the number and type of hydrophilic and lipophilic groups it contains, or it can be estimated from experimental measurements of its cloud point (Shinoda & Friberg, 1986). A widely used semi-empirical method of calculating the HLB number of a surfactant is as follows (Davis, 1994):

$$\mathbf{HLB = 7 + \Sigma\,(hydrophilic\ group\ numbers) - \Sigma\,(lipophilic\ group\ numbers)} \qquad \textbf{(Equation 2.4)}$$

The HLB number of a surfactant gives a useful indication of its solubility in either the oil and/or water phases, and can be used to predict the type of emulsion that will be formed by a surfactant (Table 2.1). A surfactant with a low HLB number (3 to 6) is predominantly hydrophobic, dissolves preferentially in oil, stabilises W/O emulsions, and forms reverse micelles in oil. A surfactant with a high HLB number (10 to 18) is predominantly hydrophilic, dissolves preferentially in water, stabilises O/W emulsions, and forms micelles in water. A surfactant with an intermediate HLB number (7 to 9) has no particular preference for either oil or water, and is considered a good "wetting agent". Molecules with HLB numbers below 3 (very hydrophobic) and above 18 (very hydrophilic) are often not particularly surface-active since they tend to accumulate preferentially in bulk oil or bulk water, rather than at an oil–water interface (McClements, 2005).

Table 2.1: Comparison of functional attributes of different general classes of emulsifiers (McClements, 2005)

Chemical Name		Solubility	Emulsion Type	Usage Level (g/g_{oil})	pH Stability	Salt Stability	Temperature Stability
Surfactants	Nonionic (low HLB)	Oil	W/O	~0.05	Good	Good	–
	Nonionic (high HLB)	Water	O/W	~0.05	Good	Good	Poor at T~PIT
	Ionic	Water	O/W	~0.05	Good	Poor at I>CFC	Poor at T~PIT
Proteins		Water	O/W	~0.05	Poor at IEP	Poor at I>CFC	Poor at $T>T_m$
Polysaccharides		Water	O/W	~1-1.5	Good	Good	Good

The symbols in the table are PIT = Phase inversion temperature; T_m = thermal denaturation temperature; IEP = isoelectric point; I = ionic strength; and CFC = critical flocculation concentration

McClements (2005) explained that the empirical observations suggest that maximum emulsion stability is obtained for W/O emulsions using surfactants with a HLB number around 3 to 5. This is because the surfactants are surface-active, but do not lower the interfacial tension sufficiently for the droplets to be easily disrupted. He continued that one of the major drawbacks of the HLB concept is that it does not take into account the fact that the functional properties of a surfactant molecule are altered significantly by changes in temperature or solution conditions (Davis, 1994; Binks, 1998). Thus, a surfactant may be capable of stabilising O/W emulsions at one temperature, but W/O emulsions at another temperature, even though it has exactly the same chemical structure. The HLB concept could be extended to include temperature effects by determining the group numbers as a function of temperature, although this would be a rather tedious and time-consuming task. Another limitation is that the optimum HLB number required for a surfactant to create a stable emulsion often depends on the oil type. Hence, the optimum "required" HLB number has to be empirically established for different kinds of oil (McClements, 2005).

When surfactant molecules associate with each other, they tend to form monolayers that have a curvature that allows the most efficient packing of the molecules. At this *optimum curvature* the monolayer has its lowest free energy, and any deviation from this curvature requires the expenditure of free energy (McClements, 2005). The optimum curvature (H_0) of a monolayer depends on the packing parameter of the surfactant: for $p = 1$, monolayers

with zero curvature ($H_0 = 0$) are preferred; for $p < 1$, the optimum curvature is convex ($H_0 < 0$); and, for $p > 1$, the optimum curvature is concave ($H_0 > 0$) (Figure 2.5). Simple geometrical considerations indicate that spherical micelles are formed when p is less than 1/3; non-spherical micelles when p is between 1/3 and 1/2, and bilayers when p is between 1/2 and 1 (Israelachvili, 1992, 1994). Above a certain concentration, bilayers join up to form vesicles because energetically unfavourable end effects can be eliminated. At values of p greater than 1, reverse micelles are formed, in which the hydrophilic head groups are located in the interior (away from the oil), and the hydrophobic tail groups are located at the exterior (in contact with the oil). The packing parameter therefore gives a useful indication of the type of association colloid that a surfactant molecule forms in solution.

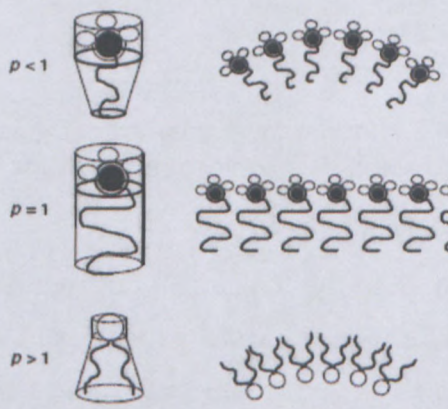

Figure 2.5: The physicochemical properties of surfactants can be related to their molecular geometry (McClements, 2005)

Becher (1988) highlighted that the vast majority of industrial emulsion explosives have been formulated with conventional W/O surfactants. The most commonly used are oleic acid esters of sorbitol; glycerides and oxazoline derivatives have also proved popular.

Emulsion explosives are water-in-oil emulsions of a supercooled concentrated solution/melts of inorganic salts in water (aqueous phase) emulsified into hydrocarbon oils (oil phase), stabilised by surfactants that consist of organic derivatives of PIBSA, the industry acronym for poly isobutylene succinic anhydride (Masalova *et al.*, 2003, 2005, 2006).

The use of polyisobutenyl succinic anhydride ("PIBSA") derivatives as superior surfactants for emulsion explosives was commenced during the 1970s/1980s. The main classes of organic chemicals that will form an adduct with PIBSA are alcohols, polyols, amines and alkanolamines. Surfactants in the form of the adduct of monoethanolamine of PIBSA have been sold and exploited since the 1980s (Boer, 2003).

The polyalk(en)yl succinic of formula V (see formula V, below) preferably comprises polyisobutenyl succinic anhydride (PIBSA). The PIBSA may have a molecular weight from about 270 to about 2500; from about 950 to about 1200 is preferable (Boer, 2003):

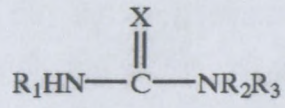

(Formula V)

Wherein

R_1 is hydrogen, hydroxyl, hydrocarbyl, hydroxyhydrocarbyl, carbamyl, 1-acetyl, amino, or nitro;

R_2 is hydrogen, hydroxyl, hydrocarbyl, hydroxyhydrocarbyl, carbamyl, 1-acetyl, amino, or nitro;

R_3 is hydrogen or hydrocarbyl, hydroxyhydrocarbyl;

X is O, S or NH; Or a derivative of such an adduct.

Hales *et al.* (2004) used a polymeric surfactant in forming the emulsion and this typically is present in an amount of from about 0.2% to about 5% by mass of the emulsion phase. The polymeric water-in-oil surfactants are molecules which have a polymeric hydrophobic portion and a polar moiety that serves as the hydrophilic portion. Hales *et al.* (2004) have stressed that the polymer can be derived from any of a number of monomers such as ethylene, propylene, and isobutene. The hydrophilic moiety can be any polar moiety which is attracted to water, or ionic solutions of water such as carboxyl groups, esters, amides, and imides (Hales *et al.*, 2004). McKenzie & Lawrence (1990) described a polymeric surfactant derivatised from trishydroxymethylaminomethane and polyisobutenyl succinic anhydride ("PIBSA"), which is particularly effective in combination with organic microspheres and is a preferred surfactant.

When surfactant molecules are mixed with a solution of polymer molecules, they may exist in either a free or a bound state (Figure 2.6 below). In either of these states, the surfactant may exist as individual monomers or molecular clusters (e.g., micelles). The partitioning of surfactant molecules between these different molecular forms depends on the concentration and molecular characteristics of the biopolymer and surfactant (e.g., molecular weight, hydrophobicity, electrical charge, flexibility), as well as the prevailing solution and environmental conditions (e.g., temperature, pressure, pH, ionic strength, and external forces) (McClements, 2005). A variety of different physicochemical mechanisms may either favour or oppose binding, for example, hydrophobic interactions, electrostatic interactions, configurational entropy, conformational entropy, and hydrogen bonding. In a system comprising a fixed biopolymer concentration and increasing amounts of surfactant, it is possible to define two critical surfactant concentrations: "*C*1" and "*C*2". *C*1 is usually referred

to as the *critical aggregation concentration* (CAC) and represents the onset concentration at which the interaction between the surfactant and the biopolymer first occurs. Above this concentration, the surfactant molecules may either bind as monomers or as micelle-like clusters. *C*2 is the surfactant concentration at which the polymer becomes saturated with surfactant. Above this concentration, additional surfactant goes into the aqueous phase and forms monomers or micelles, depending on whether or not the free surfactant concentration is below or above the CMC, respectively. *C*1 is generally well below the CMC of the surfactant and is only weakly dependent on the amount of polymer in solution. On the other hand, *C*2, which represents the surfactant concentration at saturation of the polymer, is usually proportional to the polymer concentration (McClements, 2005).

Myers (1992) stipulated that surfactants, when they adsorb at the interface between immiscible liquids, lower the interfacial tension and form a monolayer film in which the stability of all the systems lie, by forming a barrier between emulsion droplets.

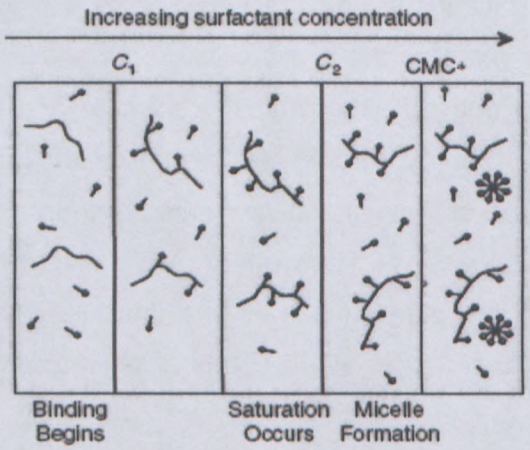

Figure 2.6: Schematic representation of surfactant binding to biopolymers (assuming that the surfactants do not form micelle-like structures on binding, which is often the case) (McClements, 2005).

In the above figure, C1 is the surfactant concentration where binding begins; C2 is the surfactant concentration where the biopolymer becomes saturated with surfactant; CMC* is the effective CMC of the surfactant in the presence of the biopolymer (McClements, 2005).
In summary, surfactants must have three characteristics to be effective at enhancing the formation and stability of emulsions. First, they must rapidly adsorb to the surface of the freshly formed emulsion droplets during homogenisation. Second, they must reduce the interfacial tension by a significant amount. Third, they must form an interfacial layer that prevents the droplets from aggregating (McClements, 2005).

While it may be tempting to attribute emulsion stability to the existence of low interfacial tension, it is generally felt today that interfacial tension effects are less important to overall long-term emulsion stability than are the effects of the nature of the interfacial film (McClements, 1999; Myers, 1992).

2.4.3.2 Properties of surfactant in solution / Micelles

Surfactants aggregate spontaneously in solution to form a variety of thermodynamically stable structures known as association colloids (like micelles, bilayers, vesicles and reverse micelles). Micelles are the most encountered type of association colloid. These structures are adopted because they minimise the unfavourable contact area between the non-polar tails of the surfactant molecules and water (Hiemenz, 1986; Evans & Wennerstrom, 1994). The different types of association colloids are held together by physical interactions that are relatively weak compared to the thermal energy, and therefore they have highly dynamic and flexible structures (Israelachvili, 1992). In addition, their structures are particularly sensitive to changes in environmental conditions, such as temperature, pH, ionic strength, and ion type (McClements, 1999).

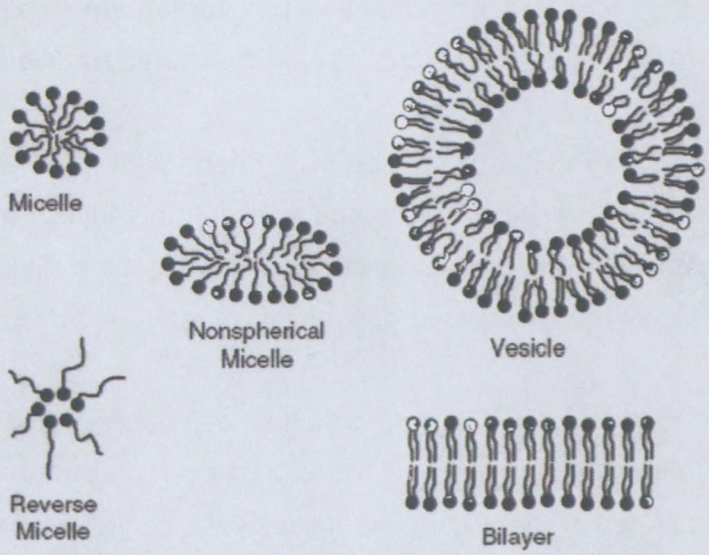

Figure 2.7: Some typical structures formed due to the self-association of surfactant molecules (McClements, 1999)

Micellation, therefore, is an alternative mechanism to absorption by which the interfacial energy of a surfactant solution might decrease. Many non-ionic surfactants form micelles, often at very small concentrations of around 0.0001 mol/dm^3 (Shaw, 1970).

Hartley (1936) proposed a spherical shape for the micelle structure, and suggested that they are essentially liquid droplets of colloidal dimensions with the charged groups situated at the surface; most of the available evidence favours this model.

In contrast, McBain *et al.* (1961) believed that a laminar form also exits, and Harkins (1952) considered the possibility of a cylindrical micelle. But, the spherical type of micelle tends to be the most reasonable suggestion.

2.4.3.2.i Micelles in non-aqueous media

The formation of micelle-like aggregate in non-aqueous solvents has received far less attention than the related phenomena in water. In fact, there is some controversy as to whether such a phenomenon in fact occurs in the same sense as in aqueous solutions. There can be no doubt that some chemical species, many surfactants included, do undergo an aggregation process in hydrocarbon and other non-polar solvents (Myers, 1992).

Overwhelming experimental evidence, however, points to the fact that many other chemical types not only dimerise, but form relatively large aggregates in nonpolar solvents which must be considered to be related, if not identical to, micelle formation in aqueous systems (Kertes & Gutmann, 1976). Such species can be called reversed micelles, or inverted micelles.

In non-aqueous media, the orientation of the surfactant relative to the bulk solvent will be opposite to that in water (hence "reversed" micelle). In addition, the micelle, regardless of the nature of the surfactant, will be un-ionized in solvents of low dielectric constant, and thus will have no significant electrical properties relative to the bulk solvent (Myers, 1992).

The primary driving force for the formation of micelles in an aqueous solution is the hydrophobic effect – they drive to minimise the unfavourable interactions between water and the hydrophobic tail of the surfactant molecule. In non-aqueous solvents, it is unlikely that there will be any significant change in the interfacial energy between surfactant tail and solvent, even if the one is hydrocarbon and the other aromatic. A more significant energetic consequence of non-aqueous micelle formation is the reduction of unfavourable interactions between the ionic head group of the surfactant and the nonpolar solvent molecules. By analogy, such an effect might be called a "hydrophilic effect" (Myers, 1992).

Unlike the situation for the aqueous micelles in which interactions between the hydrophobic tails contribute little to the overall free energy of micelle formation, ionic, dipolar, or hydrogen

bonding interactions between head groups in reversed micelles are one primary driving forces favouring aggregation (Myers, 1992).

Moreover, in the two-phase, or pseudo-phase, theory the micelle is treated as a separate but soluble phase, which begins to form at the CMC. Hence the CMC is the saturation concentration for monomers, and the concentration or activity of the monomers should increase above it (Shaw, 1970).

2.4.3.2.ii Critical micelle concentration (CMC) and its determination

A surfactant forms micelles in an aqueous solution when its concentration exceeds some critical level, known as the Critical Micelle Concentration or CMC (Myers, 1988). Below the CMC, the surfactant molecules are dispersed predominantly as monomers, but once the CMC is exceeded, any additional surfactant molecules form micelles, and the monomer concentration remains fairly constant (Hiemenz, 1986). This is because the properties of the surfactant molecules dispersed as monomers are different from those in micelles. For example, surfactant monomers are amphiphilic and have a high surface activity, whereas micelles have little surface activity because their surface is covered with hydrophilic head groups. Consequently, the surface tension of a solution decreases with an increasing surfactant concentration below the CMC, but remains fairly constant above it.

Despite the highly dynamic nature of their structure, surfactant micelles have a fairly well-defined average size and shape under a given set of environmental conditions. Thus, when surfactant is added to a solution above the CMC, the additional surfactant molecules tend to go into micelles, therefore the number of micelles tends to increase, rather than the size or shape of the individual micelles (Adamson, 1997).

The general way to measure the CMC is to plot some physico-chemical properties (osmotic pressure, conductance, surface and interface tension, density) versus the concentration of surfactant micelles of interest and observe the break, as illustrated in Figure 2.8 (Kruss, 2005). The CMC will be determined by plotting interfacial tension versus logarithm of concentration of the surfactants. The curve has the following characteristic shape:

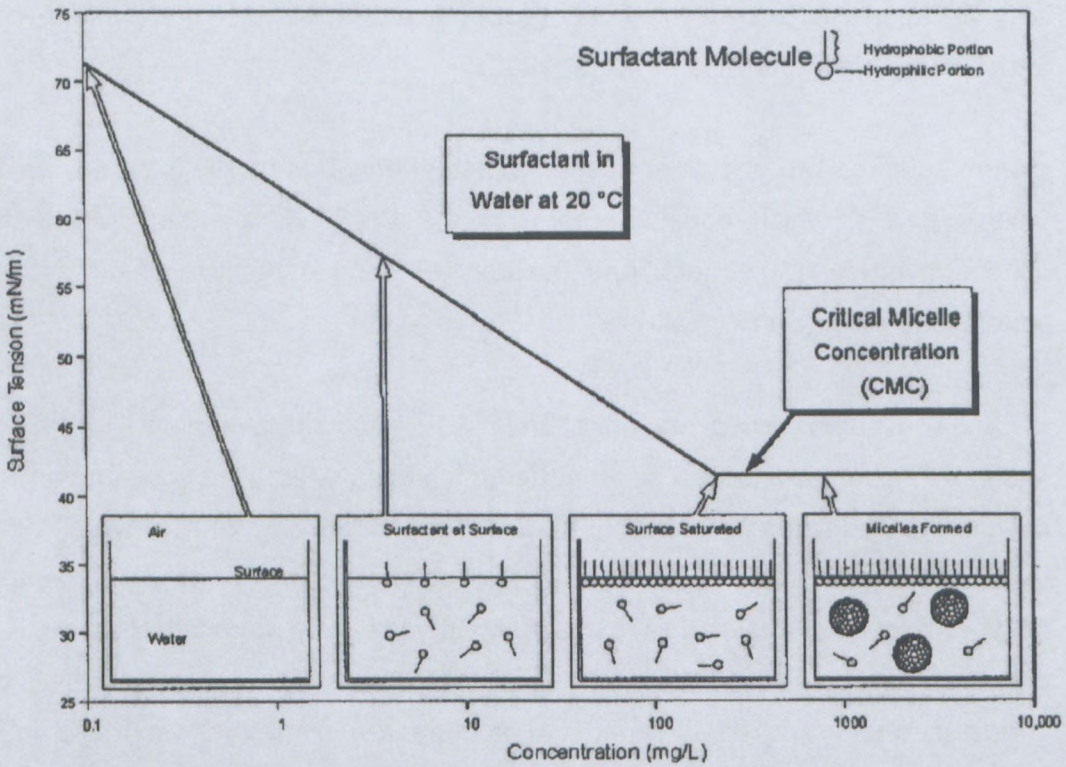

Figure 2.8: Determination of the critical micelle concentration, CMC (Kruss, 2005); the curve obtained shows how surfactant molecules lower the interfacial tension of the aqueous solution.

- At low surfactant concentrations, the hydrophobic portion of some molecules will be above the liquid surface. As some of the surface becomes covered by adsorbed surfactant molecules, the surface tension decreases. When the surface becomes saturated with surfactant, the surface tension remains fairly constant.

- If the surfactant concentration is increased, the monomer molecules are organised into micelles. The concentration where the micelle formation starts is referred to as the critical micelle concentration (CMC). The CMC is a characteristic for a given surfactant in a specific solvent at a defined temperature (Kruss, 2005).

2.5 EMULSION STABILITY UNDER SHEAR

From the above section presenting the general definition, an emulsion is considered to be a dispersion of one liquid in another; and from the thermodynamic point of view, it is a two-phase system: a dispersed phase and a continuous phase. Such a system is never completely stable in the absolute sense, because the interface between phases is the seat of surface free energy, and if two droplets join together there is a net reduction in interfacial area (Kitchener & Mussellwhite, 1968). However, McClements (1999:185-233) defined the term "emulsion stability" as the ability of an emulsion to resist changes in its properties over time: the more stable the emulsion, the more slowly its properties change. He advanced that an emulsion may become unstable due to a number of different types of physical, chemical and, sometimes, even microbiological processes and changes. The most accounted everyday case is the physical one which is discussed in more detail in this work.

The droplets in an emulsion are in a continual state of motion and frequently collide with one another, thereby initiating physical instability which can be defined as the result of alteration in the spatial distribution or structural organisation of the molecules, and examples of such instability are creaming, flocculation, coalescence, partial coalescence, phase inversion, and Ostwald ripening (Dickinson & Stainsby, 1982; Dickinson, 1992; Myers, 1992; Walstra, 1996a, b) – see Figure 2.9, below. For chemical instability, oxidation and hydrolysis are the commonly found causes.

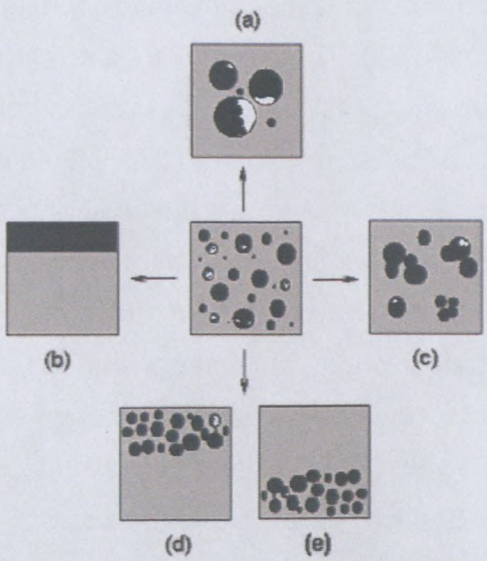

Figure 2.9: (a) Coalescence (Droplet aggregation), (b) Breaking, (c) Flocculation (Droplet aggregation), (d) Creaming (gravitational separation) and (e) Sedimentation (gravitational separation) (Myers, 1992)

It is worth mentioning *thermodynamic* and *kinetic stability* when considering stability of an emulsion in general. Thermodynamics have to do with whether or not a given process will occur, whereas kinetics is about the rate at which it will proceed if it does occur (Atkins, 1994). Unfavourable thermodynamic aspects during the formation of emulsion were described in Section 2.2, but the kinetic aspect is detailed here. According to McClements (1999:185-233), the kinetic stability of emulsions is of more interest to scientists than their thermodynamic stability because of the following:

- The kinetic effect can be highlighted as the shelf-life of the emulsion, therefore many emulsions are thermodynamically unstable but remain kinetically stable (metastable) for months or even years.
- Kinetic stability is attributed to an activation energy (ΔG^*) which must be overcome before an emulsion can reach its most thermodynamically favourable condition.
- An emulsion which is kinetically stable must have an activation energy which is significantly larger than the thermal energy of the system (kT).
- For most emulsions, an activation energy of about 20 kT is sufficient to provide long-term stability (Friberg, 1997).

So, roughly, the kinetic stability of emulsions is largely determined by the dynamics and interactions of the droplets they contain, and the rate at which destabilisation takes place in such a system depends on three things: its composition, microstructure and environmental conditions (temperature variation, mechanical agitation and storage conditions) (McClements, 1999:185-233). Therefore it is clear that shearing can be considered as one kind of mechanical agitation that influences instability and many experimental studies have been conducted in order to investigate the influence of high shearing resulting from manufacturing process conditions on the stability of an emulsion. In some cases, coalescence was found to take place, in others crystallisation and phase inversion occurred; an additional destabilisation mechanism that has also been reported was partial coalescence. For convenience, only shear-induced coalescence is considered in this chapter. However, the remaining instability phenomena (i.e. partial coalescence, phase inversion and crystallisation) that might also be induced by shear action, are discussed in detail in Chapter 4 (Section 4.2.2) of this thesis. But prior to engaging in shear-induced instability, a brief discussion of drop deformation and break-up will be presented in order to have a better understanding of the physical concept behind emulsion droplets and shear.

2.5.1 DROP DEFORMATION AND BREAK-UP

The theory of deformation and disruption of emulsion droplets has been the subject of many studies conducted in this field. Early work by Taylor (1934) investigated the break-up of single droplets in a laminar simple shear flow field. Further development was reported with many models derived for different flow conditions (laminar, turbulent, cavitational), different flow profiles (parallel, simple shear, rotational and hyperbolic) and different compositions (in the presence / absence of emulsifiers, soluble / insoluble emulsifiers) and fluid types (Newtonian / non-Newtonian). However, this section of the thesis will highlight and discuss only the basic principle (the classical analysis of Taylor and the later significant experimental and theoretical studies (Rumscheidt & Mason, 1961; Taylor, 1964; Torza, Cox & Mason, 1972; Barthes-Biesel & Acrivos, 1973; Acrivos & Lo, 1978; Rallison, 1980; Grace, 1982) which were found to be the groundwork for the most important principles of the disruption of larger droplets into smaller ones.

Walstra (1983, 1993b) reported that the break-up of a droplet is determined by a balance between two forces: *interfacial forces*, which tend to hold the droplets together; and *disruptive forces* generated within external forces, which tend to pull them apart.

2.5.1.1 Interfacial forces

An emulsion droplet tends to be spherical because this shape minimises the energetically unfavourable area between the oil and aqueous phases. Changing the shape of a droplet or breaking it up into a number of smaller droplets increases this contact area and therefore requires an energy input (Walstra, 1993b). Therefore, in order to deform and disrupt a droplet, it is necessary to apply an external force which is significantly larger than the interfacial force (Walstra, 1983, 1996b). However, the interfacial force (responsible for holding the droplets together) is characterised by the *Laplace pressure* (ΔP_L), which acts across the oil-water interface toward the centre of the droplet so that there is a larger pressure inside the droplet than outside of it:

$$\Delta P_L = \frac{4\sigma}{d}, \qquad \textbf{(Equation 2.5)}$$

where σ is the interfacial tension between oil and water, and d is the droplet diameter.

Thus, Equation 2.5 indicates that ΔP_L increases as the interfacial tension increases or as the droplet size decreases.

2.5.1.2 Disruptive forces

For a droplet to be broken up during a process (e.g. homogenisation), the disruptive forces which tend to pull droplets apart must exceed the interfacial forces, and their duration must be longer than the time required to deform and disrupt the droplet (τ_{deform}) (Stone, 1994; Karbstein & Schubert, 1995). Different processes have different flow conditions (laminar, turbulent, or cavitational). Meanwhile the nature of disruptive forces depends on the flow conditions experienced (Phipps, 1985; Walstra, 1993b). These flow conditions of an emulsion within a process are usually extremely complex and are therefore difficult to model mathematically (Phipps, 1985). Nevertheless, studies have been conducted for different flow conditions, particularly laminar and turbulent ones in order to gain insight into the factors that influence and characterised droplet deformation and break-up.

2.5.1.2.i Laminar flow fields

This type of flow profile develops at low flow rates, and is governed by the deforming viscous stresses τ acting on the surface of emulsion droplets (acting shear and elongation rates) and the related viscosity of the continuous fluid phase (Taylor, 1932). Hence, some dimensionless stress ratio, capillary number, *Ca,* and/or Weber number, *We* (the latter differs from the former by a factor of 2 – Equation 2.6), which is the ratio between viscous forces and interfacial forces, characterised disruption of emulsion droplets.

There is different type of deformation behaviour of emulsion drops in laminar flow fields. Such behaviour depends on the direction and velocity at which different regions within the fluid move relative to one another. And this involves (parallel, simple shear, rotational, and hyperbolic flow), which is schematically shown in the following figure (Windhab, Dressler, Feigl, Fischer & Megias-Alguacil, 2005):

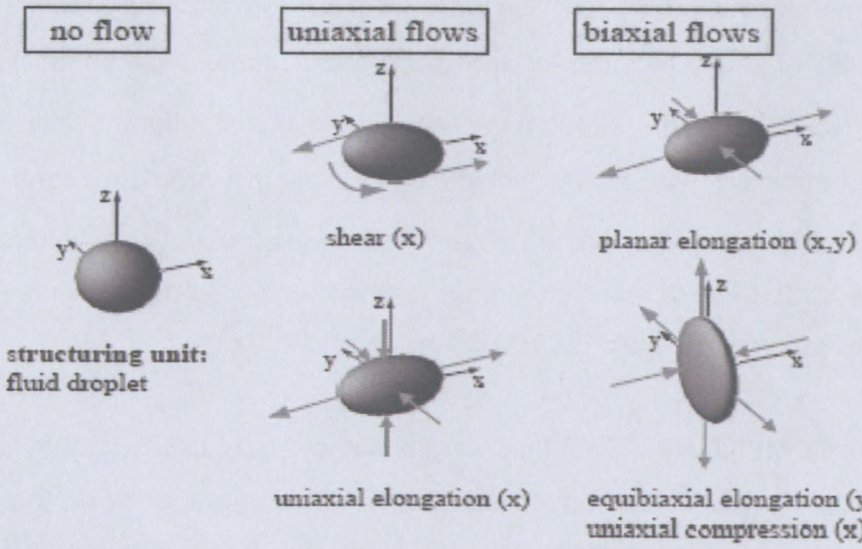

Figure 2.10: Drop deformation characteristics in different laminar shear and elongation flow fields (Windhab *et al.*, 2005)

$$Ca = \frac{Shear\ forces}{\text{int}erfacial\ forces} = \frac{\dot{\gamma}\eta_c d}{2\sigma} = \frac{\tau R}{\sigma} \qquad \textbf{(Equation 2.6)}$$

and the viscosity ratio:

$$\lambda = \frac{\eta_D}{\eta_C}, \qquad \textbf{(Equation 2.7)}$$

where $\dot{\gamma}$ is the shear rate, η_c and η_D the viscosity of the continuous phase and emulsion respectively, d and R are the diameter and radius of the droplets respectively, and σ is the interfacial tension.

As an example, only simple shear flow conditions were taken into consideration in this chapter and are described as follows:

In the presence of a simple shear field, a droplet experiences a combination of normal and tangential stresses (Loncin & Merson, 1979; Yu & Bousmina, 2003; Windhab *et al.*, 2005). These stresses cause the droplet to rotate and become elongated, as well as causing the liquid within the droplet to circulate (Figure 2.10). At sufficiently high shear rates, the droplet becomes so elongated that it is broken into a number of smaller droplets (Stone, 1994;

Williams, Janssen & Prins, 1997). The manner in which the droplets break up depends on the ratio of the viscosities of the droplet and continuous phase (η_D / η_c) (McClements, 1999:185-233). Some experiments conducted under different flow conditions have shown photographically that at low values of η_D / η_c the droplets break up at their edges, at intermediate value they break up near their middle, and at high values they may not break at all, because there is insufficient time for the droplets to deform during the application of the disruptive forces (Gopal, 1968; Williams *et al.*, 1997).

It was shown (Grace, 1982) that there is some critical capillary number value $Ca_{crit.}$, at which the droplet rupture can happen and this $Ca_{crit.}$ value depends on the ratio of viscosities λ of both components of an emulsion: if an emulsion has a capillary number above this critical value (i.e., high shear rates or large droplets), the droplets will be broken up; otherwise they will remain intact (Figure 2.11).

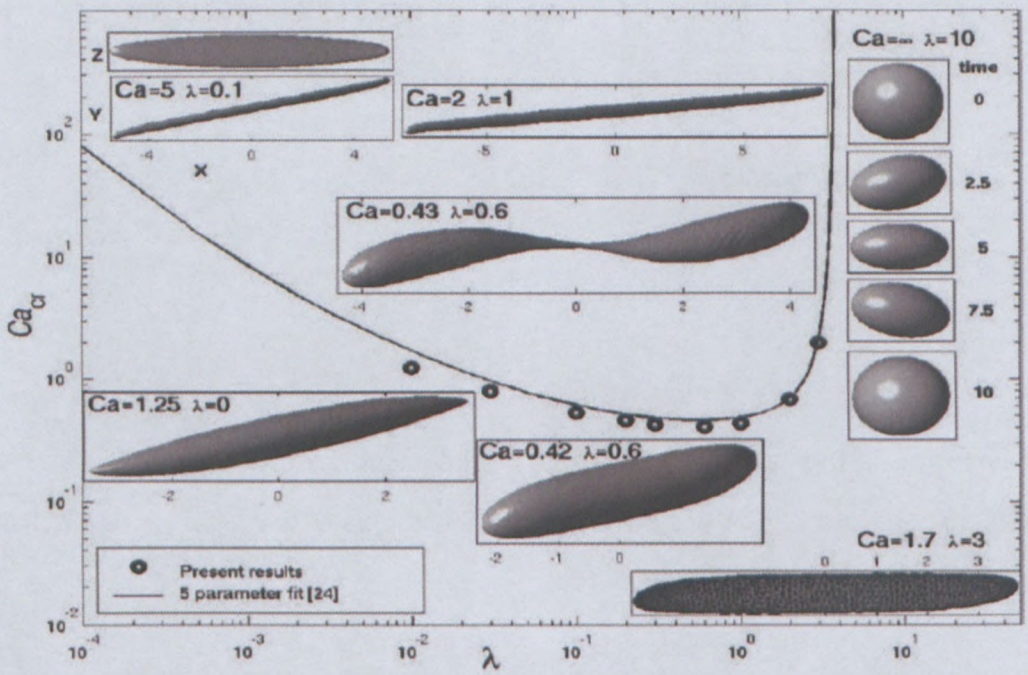

Figure 2.11: Critical capillary number for simple shear flow as a function of viscosity ratio (Bazhlekov, Anderson & Meijer, 2006)

Research studies reveal that the behaviour of droplets in a flow field is different for an emulsion consisting of emulsifiers and one that does not have any at all (absence of emulsifiers). In the latter (absence of emulsifiers), droplets are resistant to break-up at low viscosity ratios (< 0.05) because they are able to become extremely elongated before any

disruption will occur. They are resistant to break-up at high viscosity ratios (> 5) because they do not have sufficient time to become deformed before the flow field causes them to rotate to a new orientation and therefore alter the distribution of disruptive stresses acting on them. At intermediate viscosity ratios, the droplets tend to form a dumbbell shape just prior to breaking up.

But in the presence of emulsifiers, where the emulsifiers were found to have an influence on the rheology of the interfacial membrane (Lucassen-Reynders & Kuijpers, 1992; Jansen, Boon & Agterof, 1994, Williams *et al.*, 1997), the droplets are more difficult to disrupt than would be expected from their equilibrium interfacial tension. Therefore, emulsifiers increase droplet resistance to tangential stresses because of their influence on the interfacial rheological properties of such liquid-liquid dispersions.

2.5.1.2.ii Turbulent flow conditions

These occur when the flow rate of a fluid exceeds some critical value, which is largely determined by its viscosity (Curle & Davies, 1968; Walstra, 1983, 1993b; Phipps, 1985). Turbulence is characterised by rapid and chaotic fluctuations in the velocity of the fluid with time and location (McClements, 1999:185-233). According to Walstra (1993b), the disruption of droplets under turbulent flow conditions is caused by the extremely large shear and pressure gradients associated with the eddies generated in the fluid. Thus, large eddies are believed to be ineffective at disrupting emulsion droplets. Very small eddies are also believed to be ineffective at breaking up droplets because they generate such high shear stresses that most of their energy is dissipated through viscous losses rather than through droplet disruption. For these reason, intermediate-sized eddies are thought to be largely responsible for droplet disruption under turbulent flow condition (Walstra, 1983, 1993b). When a droplet is in the vicinity of one of these intermediate-sized eddies, it is deformed and disrupted because of the large shear gradient acting across it (Gopal, 1968). Early studies suggested that the viscosity of the liquid does not influence the droplet size under turbulent flow conditions. However, recent studies (Braginsky & Belevitskaya, 1996) have shown that the viscosities of the dispersed and continuous phases do influence the maximum droplet size that can persist during processes such as homogenisation, with a minimum in d_{max} when η_D / η_c is between about 0.1 and 5. Therefore, in some processes, the dependence of droplet size on viscosity ratio produced under turbulent flow conditions is similar in form to that produced under laminar flow conditions (Figure 2.11).

As a summary to this section, the evidence shows that energy is needed to increase the specific surface area of a collective of droplets by a certain amount of area, whether or not droplet break-up is mainly governed by the balance between viscous forces (resulting from external stress) and interfacial forces (Laplace pressure); which, in turn, is characterised and quantified by a dimensionless capillary number. Thus the mechanism of droplet disruption is characterised by the critical capillary number value, $Ca_{crit.}$, at which the droplet rupture can occur and this $Ca_{crit.}$ value depends on the ratio of viscosities λ of both components of an emulsion: viscosities of the droplet and of the continuous phase. The efficiency of droplet disruption in a process depends on the type of forces acting on the droplet and, therefore, on the flow pattern, though. However, the presence of emulsifiers has an influence on the rheology of the interfacial membrane, and is expected to decrease droplet disruption efficiency by increasing droplet resistance to tangential stresses.

The next step is to find out whether the shearing process or external stress influences droplet stability. Section 2.5.2 presents a discussion of some experimental studies conducted in order to investigate the influence on the stability of an emulsion of high shearing resulting from manufacturing process conditions.

2.5.2 SHEAR-INDUCED COALESCENCE

Coalescence is the result of the liquid within two or more emulsion droplets coming into molecular contact (Evans & Wennerstrom, 1994; Kabalnov & Wennerstrom, 1996; Walstra 1996a, b). This occurs only when the droplets are close to each other and the interfacial membranes are disrupted (McClements, 1999:185-233). McClements advanced that the fact that droplets have to be in close contact means that coalescence is much more dependent on short-range forces, and therefore on the precise molecular details of a system, than on either gravitational separation or flocculation. However, many theoretical and empirical studies (Saboni, Gourdon & Chesters, 1995; Rother, Zinchenko & Davis, 1997; Yan, Thompson & Valsaraj, 2006) have revealed that the coalescence behaviour of approaching emulsion droplets is controlled by the dynamics of the film between their surfaces. Thus their results on the film drainage process under constant approaching velocity or constant driving force indicated that its (film drainage) rate is mainly controlled by the interfacial tension σ, the viscosity ratio between the dispersed and suspending phases λ and the external driving force F. These factors have a profound effect on the drainage rate, which often depends on the deformability and tangential mobility of the droplet surface (Yan *et al.*, 2006). Then, it was advanced, the coalescence behaviour of emulsion droplets upon collision depends on

the interplay between two forces: hydrodynamic forces (due to viscous friction) and intermolecular forces (disjoining pressure). Thus, if the total interaction is very repulsive, the droplets can rebound; if the intermolecular repulsive forces can hold the film at an equilibrium separation, the droplets may flocculate; and if the total interaction is attractive, the film will become thinner and finally rupture, i.e., the droplets coalesce (Yan *et al.*, 2006).

Interesting studies conducted in unbounded simple shear flow (Loewenberg & Hinch, 1997; Guido & Simeone, 1998; Hu, Pine & Leal, 2000; Zhou, Yue & Feng, 2008) to quantify the coalescence phenomenon in such flow condition may add much insight into the understanding of shear-induced coalescence. Zhou *et al.* (2008) showed that the coalescence behaviour of two droplets in such flow conditions (simple shear) depends on capillary number, *Ca*, as it only occurs at a capillary number that is lower than a critical value, $Ca_{critical}$.

On the other hand, Greene, Hammer and Olbricht (1994) found in their empirical studies that, when the flow was bounded (i.e. in flows of porous media), the hydrodynamic resistance experienced by emulsion droplets in porous media differs significantly from that in an unbounded flow because of the strong hydrodynamic interaction between the droplets and the pore walls. They therefore concluded that, besides the factors mentioned on the unbounded flow, geometric-related parameters are also important in predicting the behaviour of emulsion droplets in such flow conditions. Afterwards, many studies confirmed this observation, particularly in this millennium (Cumming, Holdich & Smith, 2000; Park, Yamaguchi & Nakao, 2001; Hong, Fane & Burford, 2003).

2.6 RHEOLOGY OF HIGHLY CONCENTRATED EMULSIONS

The rheology of emulsions is reviewed in this section, with rheology defined as the science of the deformation and flow of materials. It has a key position in emulsion research, being an important link in the correlation chain from emulsion structure, flowability and stability to performance of the final product and design processing operations. Thus, according to Fredrickson (1964), "the goal of rheology is prediction of the force system necessary to cause a given deformation or flow in a body, or conversely, prediction of the deformation or flow resulting from the application of a given force system to a body". The application of a force to a fluid produces flow. When this force is removed, the fluid does not return to its original state – it undergoes irreversible deformation. The response of a solid to an applied force depends on whether it shows elastic or plastic behaviour. An elastic solid undergoes deformation but it does not flow. When the force is removed it returns to its original state so that it exhibits reversible deformation. A plastic solid behaves in a similar way provided the applied force does not exceed a critical value. If this critical value is exceeded, however, it flows as a fluid and when the applied force is removed it does not return completely to its original state (Malkin, 1994; McClements, 1999).

Emulsions exhibit a wide range of different rheological properties, ranging from low viscosity liquids to fairly rigid solids. Therefore the rheological behaviour of an emulsion depends on the type and concentration of ingredients it contains, as well as the processing and storage conditions it has experienced (McClements, 1999:235-266). Thus it is more convenient to classify emulsions and emulsion rheology into two broad categories, namely dilute emulsions (and the rheology of dilute emulsions) which behave like simple liquids and exhibit Newtonian flow; and concentrated emulsions where the droplets interact with one another, thus showing viscoelastic behaviour (Sherman, 1968; Dickinson, 1992).

However, this study was devoted to highly concentrated emulsions where the internal phase volume fraction is far beyond the close packing limit of spherical droplets of 74%, and thus it (HCE) exhibits a plastic-like response to shear deformation or plasticity behaviour: for small deformations, they resist the shear elastically, with the stress being linearly proportional to the strain; for large enough deformations they flow, offering comparatively much less additional resistance (Webber, 1999; Masalova *et al.*, 2003a). It is clear that such a material starts to flow only after the applied stress reaches some range known as the "yield stress", and the fluid exhibited non-Newtonian behaviour (e.g., pseudoplastic, dilatant) – see Figure 2.12 for the typical rheograms for classes of fluids (Slatter & Chhabra, 2002).

Before getting to the core of this section, though, it is convenient to highlight flow properties of non-Newtonian fluids which happen to characterise the flow behaviour of the material subject to this investigation.

2.6.1 FLOW MODELS OF NON-NEWTONIAN FLUIDS

Numerous flow and structural mathematical equations (models) describing the flow behaviour of non-Newtonian fluids have been proposed by various authors (Figure 2.12). Some of the most popular and most commonly used models are:

a) Herschel-Bulkley or yield-pseudoplastic flow model:

$$\tau = \tau_y + K\dot{\gamma}^n \qquad \textbf{(Equation 2.8)}$$

b) Power law or pseudoplastic flow model:

$$\tau = K\dot{\gamma}^n \qquad \textbf{(Equation 2.9)}$$

c) Bingham plastic model:

$$\tau = \tau_y + \eta_{pl}\dot{\gamma} \qquad \textbf{(Equation 2.10)}$$

d) Cross-structural viscosity model:

$$\eta\left(\dot{\gamma}\right) = \eta_\infty + \frac{\eta_0 - \eta_\infty}{1 + \left(\lambda.\dot{\gamma}\right)^n} \qquad \textbf{(Equation 2.11)}$$

e) Carreau structural viscosity model:

$$\eta\left(\dot{\gamma}\right) = \eta_\infty + \frac{\eta_0 - \eta_\infty}{\left[1 + \left(\lambda.\dot{\gamma}\right)^2\right]^{-p}} \qquad \textbf{(Equation 2.12)}$$

f) Windhab model:

$$\tau\left(\dot{\gamma}\right) = \tau_{y0} + \eta_{\infty}\,\dot{\gamma} + \left(\tau_{y1} - \tau_{y0}\right)\left\{1 - \exp\left\{\frac{-\dot{\gamma}}{\dot{\gamma}^{*}}\right\}\right\} \qquad \textbf{(Equation 2.13)}$$

$$\dot{\gamma}^{*} = \dot{\gamma}\,\tau^{*} = \left[\tau_{y0} + \left(\tau_{y1} - \tau_{y0}\right)\left(1 - \frac{1}{e}\right)\right]$$

τ is the shear stress (Pa); τ_y is yield stress (Pa), $\dot{\gamma}$ is the shear rate (s^{-1}); η_0 is the zero shear Newtonian viscosity (Pa.s); η_∞ is the infinite shear Newtonian viscosity (Pa.s), and all the other symbols represent empirical or semi-empirical parameters.

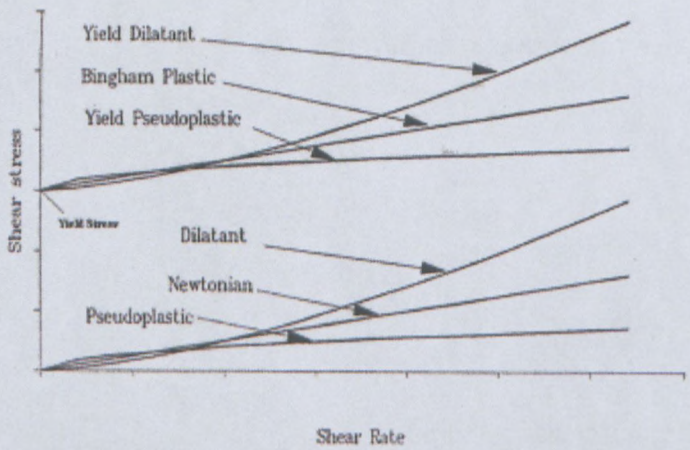

Figure 2.12: Types of time-independent (and/or shear-rate dependent) flow behaviour (Slatter & Chhabra, 2002)

For convenience, only the Herschel-Bulkley or yield-pseudoplastic flow model is considered in this chapter. It has been described (Kharatiyan, 2005) as follows:

2.6.1.1 Herschel-Bulkley or yield-pseudoplastic flow model

This three-parameter constitutive rheological model is given above by Equation 2.8:

$$\tau = \tau_y + K\,\dot{\gamma}^{n}, \qquad \textbf{(Equation 2.8)}$$

where τ is the shear stress (Pa), $\dot{\gamma}$ is the shear rate (s^{-1}), τ_y is the yield stress (Pa), K is the fluid consistency index ($Pa.s^n$), and n is the flow behaviour index.

The Herschel-Bulkley model accommodates both the yield stress (τ_y) and the shear-thinning behaviour of the overall fluid flow behaviour, and it describes the behaviour of yield pseudoplastics with reasonable accuracy. The shear thinning behaviour shows non-linearity of the flow behaviour, as can be seen clearly in Figure 2.12 from the convexity of the rheogram curvature. The fluid consistency index (K) and the flow behaviour index (n) describe the rheogram curvature. All the flow model constants are empirical, which means that they are not related to the structure of the material, in fact, the τ_o value obtained often differs from the value of the ' true' dynamic and static yield stresses (Larson, 1999).

The advantage of the Herschel-Bulkley is that it incorporates the features of the pseudoplastic model (rheogram curvature) and the Bingham plastic model (yield stress), (Slatter, 1999). In fact, this model can be used to characterise all time-independent flow behaviour illustrated in Figure 2.11, above. Referring to this figure, the following rheological relationships can be accommodated in the yield pseudoplastic model:

- Yield dilatant $\{\tau_y > 0, n > 1\}$
- Bingham plastic $\{\tau_y > 0, n = 1\}$
- Yield pseudoplastic $\{\tau_y > 0, n < 1\}$
- Dilatant $\{\tau_y = 0, n > 1\}$
- Pseudoplastic $\{\tau_y = 0, n < 1\}$
- Newtonian $\{\tau_y = 0, n = 1\}$

2.6.1.2 Prediction of pipeline transportation of emulsion

The understanding of the rheological behaviour of emulsions is of importance in many industrial applications (Pal, 1996a). In the pipeline transportation of emulsions, knowledge of the rheological properties of emulsions is required for the design, selection, and operation of the equipment involved (Tanner, 2000; Slatter, 1999 and 2002; Slatter & Wasp, 2002). The central position in this problem is occupied by fitting experimental data (flow curves) to an approximating equation (Herschel-Bulkley equation, power law equation, etc.) (Malkin *et al.*, 2004b). The equation is then integrated to predict the relationship between pressure and velocity, or – in the case of flow through a pipe – between pressure drop, ΔP, and volume flow rate, Q, or mass flow rate, G_m. Once the $\dot{\gamma}(t)$ dependence has been measured, the Q (ΔP) dependence can be computed by direct numerical integration of the well-known Rabinowitsch-Weissenberg equation, which is generally valid for any non-Newtonian liquid. This equation connects the so-called "average" or "bulk" shear rate $\gamma_{av} = 8V / D = 8Q / \rho D^3$

with the shear stress at the pipe wall $\tau_w = \Delta PD / 4L$. Here V is the "average" velocity, Q is volume flow rate and D and L are pipe diameter and length, respectively.

The Rabinowitsch-Weissenberg equation takes the following closed integral form:

$$\gamma_{av} = \frac{4}{\tau_w^3} \int_0^{\tau_w} \tau^2 \dot{\gamma}(\tau) d\tau \qquad \textbf{(Equation 2.14)}$$

In this equation, $\dot{\gamma}(t)$ is the measured flow curve. Note that this relationship shows that, provided there is no slip at the pipe wall, $\dot{\gamma}_{av}$ is a unique function of τ_w and independent of pipe diameter. Indeed, this provides a practical method of detecting slip at the pipe wall Malkin *et al.* (2004b), answering the question "Is the choice of flow curve fitting equation crucial for the estimation of pumping characteristics?" by using the Cross equation, the Herschel-Bulkley equation, the power law equation and the direct numerical method (using Rabinowitsch-Weissenberg integral) for the calculation of the laminar pipe flow transport characteristic and comparing the results with the experimental pipe flow data. The difference in the accuracy of the fitting equation relates mainly to the low shear rate domain. It was shown by authors that in all cases the choice of the flow curve fitting equation was unimportant on condition that applied pressure (the pressure drop) is sufficiently high (Malkin *et al.*, 2004b).

Rheological studies of emulsion systems are not restricted to measuring the viscosity, but can yield other rheological parameters (e.g. storage and loss moduli, denoted by G' and G'' respectively), which are characteristic properties of the concentrated emulsion system like viscoelasticity and time dependency (rheopexy). Highly concentrated emulsions showed viscoelastic behaviour at low shear due to the compressed droplet configuration; such systems have been widely studied both experimentally and theoretically (Barry, 1975; Princen, 1979, 1983, 1985, 1988; Princen *et al.*, 1980; Princen & Kiss, 1986, 1989; Bibette, 1992; Aronson & Petko, 1993; Benali, 1993; Reinelt & Kraynik, 1993; Otsubo & Prud'homme, 1994b; Babak, Langfield & Stebe, 2001). It has been shown that concentrated emulsions behave like solids in the initial stages of shear and subsequently exhibit shear-thinning fluid flow behaviour "in the sense that the work of shearing deformation is not conserved, as in solids, nor is it completely dissipated as in fluids" (Sherman, 1968); their viscoelastic properties depend on mean the diameter of dispersed particles, polydispersity, interfacial tension, and particularly on the dispersed volume fraction.

2.6.2 VISCOELASTIC PROPERTIES

Malkin (1994) showed that rheological behaviour related to viscoelasticity is the most relevant for the description of a majority of real materials. In general, viscoelasticity is a combination (or superposition) of characteristic properties for liquids (viscous dissipative losses) and solids (storage of elastic energy). Therefore, a general definition of viscoelastic materials includes two components – elastic potential and intensity of dissipative losses. Viscoelastic behaviour can be considered as a delayed development of stresses and deformations in time, and this delay must not be confused with inertial effects also characterised by a specific lag time.

The time of observation of the viscoelastic processes is very important. The dimensionless criterion called the Deborah Number, De, was introduced to be a measure of a ratio between characteristic time of observation, t_{obs}, and the time scale of inherent processes in material, t_{inh}. The Deborah Number is especially important for viscoelastic phenomena because they always proceed in time. Since the time interval is very wide, it must be encountering a situation when the Deborah Number is of order of 1 (Malkin, 1994).

There are three fundamental experiments, which are treated as reflections of viscoelastic behaviour of a matter. But only the periodic oscillations experiment is described in this chapter:

- Creep – delayed development of deformations under action of constant force (or stress).
- Relaxation – slow delay of stresses at preserving constant deformation.
- Periodic oscillations – harmonic changing of stresses or deformations with relative shift of deformation in relation to stress.

2.6.2.1 Oscillatory Tests

Oscillatory tests are used to examine all kinds of viscoelastic materials, from low viscosity liquids to fairly rigid solids. Such kinds of test are referred to as "Dynamic Mechanical Analysis" (DMA) (Thomas, 2002).

Basic Definition

Complex Shear Modulus G': This is described by the complex form of Hooke's law as follows

$$G^* = \frac{\tau(t)}{\gamma(t)}, \qquad \textbf{(Equation 2.15)}$$

with G^* the complex shear modulus [Pa] and $\tau(t)$ the sinusoidal function [Pa] and $\gamma(t)$ the sinusoidal function [1] or [%];

Storage Modulus G' [Pa]: Its value is a measure of the deformation energy stored in the sample during the shear process. After the load is removed, this energy is completely available and acts as the driving force for the reformation which partially or completely compensates the previous deformation. Thus, G' represents the elastic behaviour of a sample (Thomas, 2002);

Loss Modulus G" [Pa]: Its value is a measure of the deformation energy used up in the sample during the shear process and lost to the sample afterwards. This energy is either used up during the process of changing the sample's structure or dissipated into the surrounding environment in the form of heat. Thus, G" represents the viscous behaviour of a sample (Thomas, 2002);

Complex Viscosity η^*: This is also termed "dynamic viscosity" or "absolute dynamic viscosity". It appears when Newton's law is given in complex form (Equation 2.16):

$$\eta^* = \frac{\tau(t)}{\dot{\gamma}(t)}, \qquad \textbf{(Equation 2.16)}$$

with η^* as complex viscosity, $\tau(t)$ and $\dot{\gamma}(t)$ as sinusoidal functions in [Pa] and [1/s] respectively.

2.6.2.2 Amplitude Sweep

An amplitude sweep is an oscillatory test with variable amplitude and constant frequency value. It is mostly carried out for the sole purpose of achieving the following three aims:

- Determination of the limit γ_L of the linear viscoelastic range (LVE range). The limit of this range is exceeded at the point at which the first of the two curves (G' or G" function) begins to leave the constant plateau value significantly, whereas this constant plateau region means that the structure of the sample is stable under this low-deformation condition.

- Characterisation of the material structure indicating that the material has solid-like or liquid-like behaviour.

- Evaluation of the structural strength as the G' value in the LVE range (called also "Rigidity".

At amplitudes higher than γ_L, the limit of the linear viscoelastic range is exceeded (this range is also called Non-Linear Viscoelastic Range) so that the structure of the sample has been irreversibly changed or even completely destroyed (Figure 2.13 below) (Thomas, 2002).

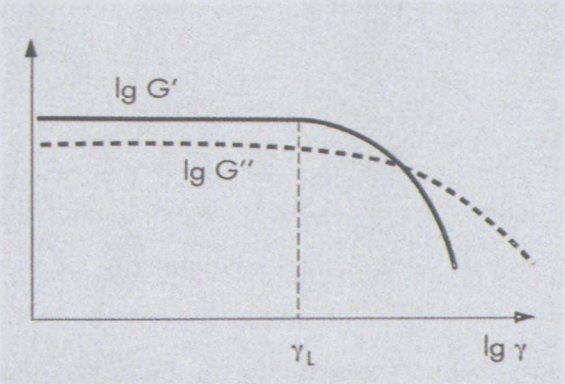

Figure 2.13: G'(t) and G''(t) with the limiting value γ_L of the linear viscoelastic deformation range (Thomas, 2002)

2.6.2.3 Frequency sweep

A frequency sweep (the so-called "Dynamic Oscillation") is an oscillatory test with variable frequency and constant amplitude values where time-dependent shear behaviour is examined:

- Short-term behaviour is simulated by rapid movements (at high frequencies) and
- Long-term behaviour by slow movements (at low frequencies)

However, before performing a frequency sweep, the limit γ_L of the linear viscoelastic range must be determined for each new unknown sample, therefore an amplitude sweep must always be carried out first. After this test, the test conditions for the frequency sweep can be selected to ensure that the test is really in the linear viscoelastic range (see Figure 2.14) (Thomas, 2002).

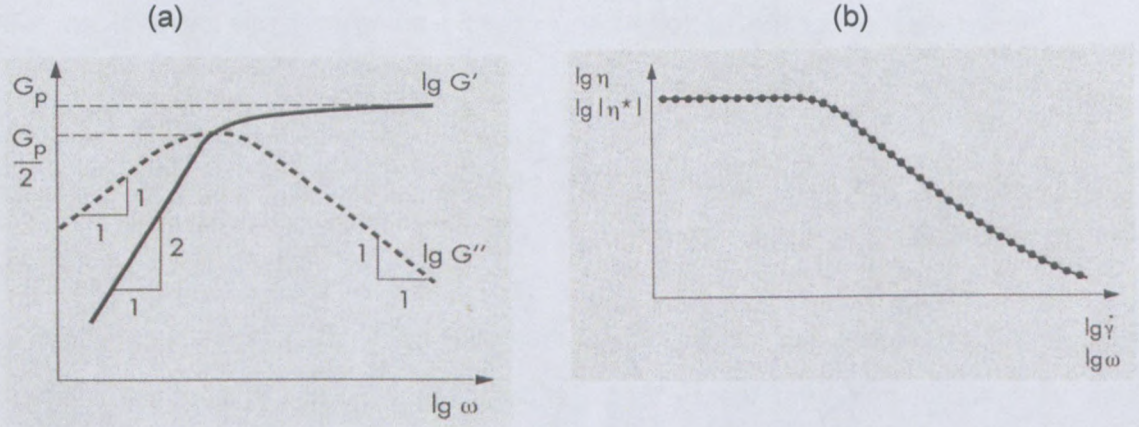

Figure 2.14: (a) G'(ω) and G''(ω) of a Maxwell Liquid, (b)The Complex Viscosity (Thomas, 2002)

2.6.3 RHEOLOGICAL PROPERTIES OF EMULSION EXPLOSIVES

Emulsion explosives are highly concentrated emulsions which can be classified as high internal phase ratio emulsions, where the dispersed phase droplets are arranged in a closely packed hexagonal configuration (i.e. far beyond the close packing limit of spherical monodispersed droplets of 74%). This closely packed configuration and the profound hydrodynamic interaction between neighbouring droplets induce mechanical interference between the droplets, thus prohibiting their free movement. In such systems, extensive aggregation of dispersed phase droplets occur, which results in a stable weak gel-like particulate network (Jager- Lézer *et al.*, 1998; Partal, Guerrero, Berjano & Gallegos, 1997).

2.6.3.1 Flow Properties

As mentioned in section 2.6.3, a high internal phase ratio emulsion system exhibits strong non-Newtonian behaviour, which is characterised by both shear thinning and elastic effect. This non-Newtonian behaviour is characterised by the existence of a yielding behaviour and a strong shear-thinning region, in which the apparent shear viscosity is dependent on the rate of shear or shear stress. Mason, Bibette & Weitz (1996) revealed in their study that the flow properties of compressed, elastic emulsions can be broadly divided into two categories, yielding and steady shear flow. They proposed that the change from a linear to nonlinear stress-strain relationship can be crudely characterised by a yield stress, which marks the significant departure of the microscopic droplet structure from its initial, unsheared configuration. For shear stresses higher than the yield stress, the emulsion flows irreversibly, creating a residual deformation after the stress has been removed which cannot be attributed to the equilibrium dissipation of fluctuations. During steady shear flow, the strain rate dependence of the additional viscous stress above the yield stress reflects the

interplay of dissipative mechanisms like fluid flow and droplet rearrangements with storage mechanisms like deformation. Thus the flow properties of the compressed emulsions depend sensitively on the packing and the deformation of the droplets, and on their intrinsic elasticity. The elasticity of the droplets, and the degree of deformation, are controlled by their internal pressure (Laplace pressure) (see Equation 2.5). The effect of interfacial tension on the steady-flow of emulsions was studied experimentally by Otsubo and Prud'homme (1994a). These authors showed that emulsions show a remarkable elasticity resulting from the interfacial energy associated with the deformation of liquid films: the viscosity is proportional to the interfacial tension.

However Masalova *et al.* (2003, 2005, 2006); Malkin *et al.* (2004a,b) and Masalova and Malkin (2007a, b; 2008) demonstrated in their publication dedicated to rheology of w/o emulsion explosives where they presented a complete rheological characterisation of highly concentrated emulsion types with a full set of rheological measurements including steady flow, transient regimes of deformation and viscoelastic measurements. In their publication of the peculiarities of rheological properties and flow of emulsions Masalova and Malkin (2007a) suggested two mechanisms of flow of emulsions, at low and high shear rates, which was identified from the point of view of analysis done on photographic observations. They clearly demonstrated that the movement of an emulsion at low shear rate presented the rolling of large droplets over smaller ones without any noticeable distortions of their shape; meanwhile at high shear rates serious distortions of the droplet shape took place. Although, the authors stressed that droplets slid between other droplets, when they did not mount over each other (and the effect of Reynolds' dilatancy did not appear).

Other authors explained that shearing causes the emulsion droplets to deform in the direction of flow, and of the flow gradient, inducing droplet deflocculation with an increase in shear stress or in the rate of shear, subsequently resulting in a slacker configuration, which is associated with decrease in flow resistance (Jager-Lézer, 1998; Pal, 1996b and 1999; Partal *et al.*, 1997, Thomas, 2002). It was also found that the yield stress, shear viscosity and elastic modulus increase significantly with decrease in droplet size (Pal, 1996b).

The flow properties of highly concentrated emulsion systems are governed by the different interaction forces (Sherman, 1968) that occur within them, and depend on the following:

- Volume fraction of the dispersed phase
- Concentration and nature of the emulsifiers
- The chemical composition of the continuous phase
- The interfacial properties

Other structural parameters which also exert some effect include the droplet size and shape, the polydispersity of the droplet size distribution and the rheological properties of the continuous phase (Partal *et al.*, 1997; Princen, 1983, 1985; Princen & Kiss, 1986a, b; Khan & Armstrong, 1987)

When the influence of droplet size on viscous properties of w/o emulsions was studied by Otsubo and Prud'homme (1994a) they found that viscosity of the highly concentrated of dispersed phase strongly depends not only on average droplet size but also on the width of droplets size distribution. However, for relatively narrow distributions, this effect can be neglected (Lacroix, Bousmina, Carreau, Favis & Michel, 1996). The influence of droplet size and the internal phase ratio on the viscosity of emulsions was also demonstrated, among others, by Pal (1996b).

Some experimental work devoted to studying the effect of the volume fraction on rheological properties of emulsions demonstrated that both yield stress and the apparent viscosity increase with an increasing volume fraction of the dispersed phase (Bikerman, 1973; Lissant, 1966). Early in 1887, Thomson reported that, at the limit of the very high volume fraction, the emulsion is composed of a network of thin films and its stability under shear is determined entirely by the mechanical stability of the intersection of these films at the plateau borders; three continuous phase films which meet at an edge must be separated by 120^0 angles, and four films which meet at a corner must meet at tetrahedral angles. Thus, the increase in yield stress values with increase of volume fraction of dispersed phase indicates that it is the geometry of the droplets' packing, and their resultant deformations, that are responsible for the volume fraction dependence of the yield stress. The rise of the yield stress with droplet concentration is due to increased packing constraints, which influence the thickness of the interdroplet thin oil film. The rheological behaviour of emulsions depends on the response of the thin liquid films and the plateau borders during

shear (Edwards & Wasan, 1988). Several researchers have determined the static and dynamic interfacial properties of liquid/liquid interfaces in the presence of surfactants, using a number of methods (Defay & Petre, 1979; Edwards, Brenner & Wasan, 1991). The assumption in these studies is that the behaviour of the film can be derived from the properties of its interfaces (Kim, Koczo & Wasan, 1997).

While experimental work on the rheology of these systems was scant, there appeared to be a virtual lack of theoretical understanding of how the rheological properties are linked in a quantitative way to a system parameter such as volume fraction of dispersed phase (Princen, 1979; Princen *et al.*, 1980; Aronson & Princen, 1980, 1982; Aronson & Petko, 1993).

Princen and Kiss (1986) theoretically and experimentally demonstrated that the yield stress could be related to the volume fraction. Their studies made it possible to derive the exact stress versus strain relationships in the elastic region as a function of the volume fraction of dispersed phase, ϕ. Thus an exact prediction can be made of the yield stress, τ_y. The expression for real, polydispersed emulsion is:

$$\tau_y = \frac{\sigma}{R_{32}} \phi^{1/3} Y(\phi) \qquad \textbf{(Equation 2.17)}$$

$$Y(\phi) = C_1 \cdot \tilde{F}_{max}(\phi), \qquad \textbf{(Equation 2.18)}$$

where C_1 is numerical constant, R_{32} is surface-area mean drop radius and $\tilde{F}_{max}(\phi)$ is the mean dimensionless contribution per drop to the yield stress. The dependence of the yield stress on the volume fraction of the dispersed phase is complex because of the term $\tilde{F}_{max}$, but the overall effect is that the yield stress increases sharply with an increasing volume fraction of the dispersed phase in most cases. The yield stress has been determined experimentally for a series of well-characterised, highly-concentrated w/o emulsions (ϕ>0.74) and the same general relationship was applied.

2.6.3.2 Viscoelastic Properties of HCE

Viscoelastic properties of high internal phase ratio emulsions have been widely studied, both experimentally and theoretically (Barry, 1975; Princen, 1979, 1983, 1985, 1988; Princen *et al.*, 1980; Princen & Kiss, 1986, 1989; Bibette, 1992; Aronson & Petko, 1993; Benali, 1993; Reinelt & Kraynik, 1993; Otsubo *et al.*, 1994b; Babak *et al.,* 2001). It has been shown that the viscoelastic properties depend on mean diameter of dispersed particles, polydispersity, interfacial tension, and particularly on the dispersed volume fraction.

Some previous oscillatory experiments on highly concentrated emulsions showed the appearance of a constantly high plateau region as the strain increased, but G' decreased as strain increased further. Therefore the mechanical properties of these materials were linear until $\gamma_{limiting}$, above which (higher deformation) dependence of the dynamic moduli on the amplitude appeared, and a transition from the linear to the non-linear domain was observed. According to some authors and studies, this plateau region that appeared with increased strain can be explained by means of the samples' structure which was undisturbed by the shear at this strain where the particles were crowded and could not move freely (Thomas, 2002; Kharatiyan, 2005), or may be related to the formation of an elastic structural network due to interactions among the emulsifier molecules located at the oil-water interface of adjacent droplets (Dickinson, 1989; Franco, Guerrero & Gallegos, 1995; Guerrero, Partal & Gallegos, 1998). It may also be related only to the equilibrium microscopic structure, forces, and inherent dissipation of fluctuations (Bird *et al.*, 1987). However, Masalova and Malkin (2007a) demonstrated "the rolling mechanism of larger droplets over smaller ones" to explain this constant plateau region as the strain increased, and some serious distortion of droplet shape occurring at the non-linear domain.

However, the structure and properties of emulsions were studied in many papers and from different points of view. Pioneering works were published by Princen (1983, 1985). Princen and Kiss (1986) carried out step-strain measurements on emulsions of paraffin oil droplets which were polydispersed in size and in the continuous phase contained a surfactant as stabiliser. They showed that the modulus G' of these dense emulsions can be represented by the simple formula:

$$G = A\frac{\Gamma}{R_{SV}}\phi^{1/3}\left(\phi - \phi^{*}\right) \qquad \textbf{(Equation 2.19)}$$

where R_{SV} is the mean (by the volume-to-surface ratio) characteristic size of dispersed droplets and A is the coefficient, ϕ^* represents the "limiting" degree of the filling of system volume with dispersed particles, ϕ is the volume concentration of dispersed particles (irrespective of their sizes), G is elastic modulus and Γ is the surface tension.

Another rheological model for highly concentrated emulsions containing 77 to 98% of the dispersion phase was proposed by Babak *et al.* (2001). Their model relates the macroscopic functional properties of these systems (elasticity modulus, yield stress and yield strain) to the microscopic physicochemical parameters (droplet size, interfacial tension, surface forces acting in thin liquid films, specific surface of these films, adhesion force between the droplets, their deformability, etc.). Whereas Princen's model describes the effect of the capillary pressure and the volume fraction of the internal phase on the elasticity modulus of such emulsions, the Babak *et al.* (2001) model also predicted the effect of the adhesion-free energy between the droplets (or the contact angle between the droplets) on the elasticity modulus and the yield stress and strain of these emulsions.
Experimental studies on the concentration dependence of viscoelastic properties of highly concentrated emulsions were discussed on the basis of Princen's theory (Ponton, Clement & Grossiord, 2001; Jager-Lézer *et al.*, 1998; Pons, Solans & Tadros, 1995) and a comparison of their experimental data with Princen's theoretical model showed good agreement.

Masalova *et al.*, (2003, 2005, 2006); Malkin *et al.*, (2004a,b) and Masalova and Malkin (2007a,b; 2008), however, demonstrated in their studies on highly concentrated w/o emulsions that the elasticity of their emulsion material was determined by the surface of the droplets (Malkin *et al.*, 2004a – Equation 2.20). This observation was found to be in contradiction with the theoretical models proposed earlier (by Princen and Kiss. 1986; Babak *et al.*, 2001; Pal, 2002), where the elastic modulus was expected to depend on reciprocal diameter. The argument given for such discrepancy of their experimental results was related to the type of emulsion used (highly concentrated emulsion), as well to differences in the averaging procedure for polydispersed samples.

$$G = K_G D^{-2} \qquad \textbf{(Equation 2.20)}$$

2.7 RESEARCH ISSUES IDENTIFIED

Emulsion explosives mainly consist of an aqueous phase of supersaturated nitrate salt solution. Such materials are freshly stable at room temperature while the droplets' salt solution ("Fudge Point" or crystallisation point) was approximated to be higher (for instance at > 80% Ammonium nitrate concentration of the dispersed phase, $T_{crit} \approx 58\ ^{0}C$). Therefore the instability of this type of emulsion mostly derives from the crystallisation of the metastable aqueous phase. Little work on such materials in terms of their stability and their rheological properties has been reported, except for some interesting studies conducted by Masalova *et al.* (2003, 2005, 2006); Malkin *et al.* (2004a, b); Masalova and Malkin (2007a, b, 2008); Kharatiyan (2005) and Nkomo (2005) on this specific field of emulsion types in which rheology and stability were correlated. Masalova *et al.*, (2006) and Kharatiyan (2005) studied the instability of these emulsion systems during the ageing process and found it to be true that aging of HCE explosives is reflected in the change of the emulsion's rheological properties which resulted from an increase in storage modulus with time, as well as yield stress measured in the upward sweeping shear rate mode (See Figures 2.15 and 2.16, below). They proved that the kinetic of crystallisation was satisfied by the Johnson-Mehl-Avrami-Kolmogorov (JMAK) equation:

$$X = 1 - e^{-(t/\theta)^n}, \qquad \textbf{(Equation 2.21)}$$

where X is the degree of crystallinity, θ is the characteristic time-related constant of the process, n is an empirical factor found to have a high value in their studies, exceeding the maximum predicted theoretical value of 4 (Mandelkern, 1964). This later explained the probable mechanism responsible of the growth of crystallites out of the volume of a single droplet, thereby breaking through the interphase layers and combining with other crystals that appear in neighbouring droplets which, in turn, initiate acceleration of crystallisation (Masalova *et al.*, 2006; Masalova & Malkin, 2008)

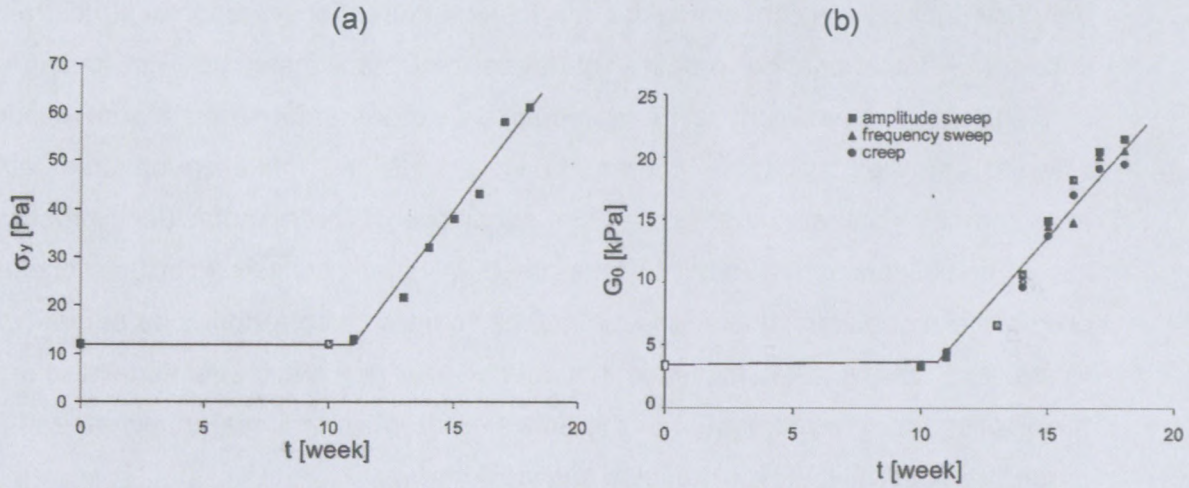

Figure 2.15: Evolution of yield stress (a) and elastic modulus (b) of HCE in aging (Masalova *et al.*, 2006)

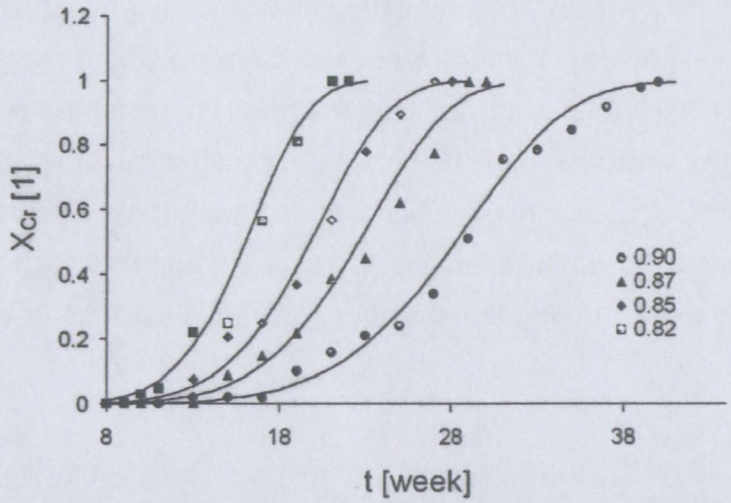

Figure 2.16: Change in relative crystallinity with aging time for emulsions with different volume fractions obtained from x-ray analysis (Masalova *et al.*, 2006).

Highly concentrated emulsions of this type have numerous potential technological applications in cosmetics, mining, oil recovery and explosives and are used as a re-pumpable material. Emulsion explosives are therefore subjected to repeated handling or shearing action during their transportation, which tends to have a tremendous impact on their desired functionality and might reduce shelf-life and performance of the final product.

Some of their sensitivity properties and stability may be improved slightly by passing them through a high-shear system to break the dispersed phase into even smaller droplets prior to adding other additives, but the emulsion's viscosity must remain low enough to allow for re-pumping at reasonable pressure. Repeated handling or shearing action tends to increase the emulsion viscosity.

Very few publications concerning the correlation of direct observation of structural processes during the transportation process of these emulsion materials with changes of their rheological properties can be found. Previous experimental studies were conducted with different emulsion systems, in order to investigate the influence on the stability of an emulsion of high shearing resulting from conditions of the manufacturing process. In some cases, coalescence was found to take place, in others crystallisation and phase inversion occurred. An additional destabilisation mechanism was also reported as partial coalescence. However, it was widely established that intense shearing causes refinement of droplets, and this implies that the refinement of the emulsion droplets induces an increase in rheological properties (viscosity, elastic modulus and yield stress).

Because of the lack of information identified in the previous paragraph, the main goal of this current research is to present and understand the effect of high shearing caused by manufacturing process conditions such as pumping on the rheological / structural properties of emulsion explosives with various formulation contents. Various formulation content in this context also concerns how the excess concentration (effect of surfactant concentration), surfactant type (chemistry of surfactant head group) and ammonium nitrate concentration in the dispersed phase may affect the rheological properties, such as modulus and yield stress, of these materials during the shearing process. Questions to which answers were sought, were:

- Does droplet rupture to lead to further refinement, causing an increase in rheological properties?

- Do the droplets just start to crystallise when high shear is applied to the emulsion materials, causing, again, an increase in rheological properties?

- Do the droplets coalesce to lead to a decrease in rheological properties?

- Do both or multiple effects take place at the same time: Coalescence-crystallisation; or refinement-coalescence; or refinement-coalescence-crystallisation; etc.?

CHAPTER 3
MATERIALS AND EXPERIMENTAL PROCEDURE

3.1 INTRODUCTION

This chapter presents a comprehensive description of the materials used in order to manufacture the emulsion samples, followed by the instrumentation and the experimental procedure used to achieve the objective set in the introduction of this thesis.

The emulsion samples used for this study were highly concentrated water-in-oil emulsions that had a dispersed phase volume fraction that exceeded the close packing limit of spherical droplets and consisted of a concentrated solution of ammonium nitrate. The oil phase consisted of surfactants emulsified in hydrocarbon oil. The first section of this chapter lists complete details of the materials used, including the type of surfactants (chemical structure, molecular weight and the HLB number), type of hydrocarbon oil and the composition of the dispersed phase.

A full description of the instruments used to shear, analyse microscopically, and measure size distribution and rheology of the emulsions is given. This includes the experimental technique or procedure that has been used in order to achieve these measurements. The following objectives were set prior to the description of the composition of these emulsions and the experimental procedure.

3.2 OBJECTIVES

The objectives of this experimental investigation including the following:

- To produce highly concentrated water-in-oil emulsions of the same drop size and similar size distribution using different surfactant types (surfactant head group – MEA, UREA, IMDE) and different surfactant concentrations in order to have the same starting point for the investigation of any destabilisation mechanism that might arise during the shearing process.

- To shear the emulsion samples using the piston-pumping device which generates enough shear rate to alter the structure of these materials.

- To determine the effect of surfactant type (surfactant head group) and surfactant concentration during the shearing process of such emulsion types.

- To find the criterion that determines any destabilisation mechanism that might arise during the pumping process.

- And finally, to produce emulsions of different droplet sizes but the same oil and surfactant concentration and lower ammonium nitrate concentration in the dispersed phase in order to investigate the effect of salt (ammonium nitrate) concentration during the shear stability of these materials.

3.3 METHODOLOGY

The following describes the methodology used to achieve the above objectives:

- By using the Hobart N50 mixer and varying the speed of rotation of its stirrer and the duration of stirring (deformation), it was possible to obtain emulsions of different formulations and surfactant concentrations with same droplet size and distribution.

- The sheared emulsion sample was examined through a Leica Optical microscope equipped with a digital camera and high magnification, for the purpose of qualitative analysis.

- The Droplet Size Distribution (DSD) for the fresh and sheared emulsion samples was determined through using the Malvern Mastersizer 2000.

- The rheological properties of the fresh and pumped emulsions were determined by means of the rotational rheometer MCR-300 (Paar Physica).

3.4 MATERIALS

The studied emulsion was of the "liquid explosive" type. Such emulsions are classified as highly concentrated water-in-oil emulsions where the dispersed phase volume fraction exceeds the close packing limit of spherical droplets. It consists of an aqueous solution of inorganic oxidizer salts (ammonium nitrate) with the salt emulsified in melt form as supersaturated, supercooled droplets in a hydrocarbon oil base. The continuous phase or oil phase consists of surfactant based on organic derivatives of *PIBSA* (the industrial acronym

for poly(isobutylene) succinic anhydride) and is dissolved in high concentrations in Parprol 32 (a paraffinic petroleum oil with no additives), prior to being diluted with hydrocarbon fuel of Mosspar-H to achieve the desired concentration and viscosity.

3.4.1 DISPERSED PHASE

The dispersed phase of the emulsion samples used in this study consisted of a solution of inorganic salt of ammonium nitrate emulsified in melt form as a supersaturated solution in a hydrocarbon oil base of the continuous phase. For the first part of this work, the water content of the dispersed phase was less than 20% by mass. Therefore, the remainder of the aqueous phase was ammonium nitrate salt, which strengthened the ion charge within the solution. Such a solution has a "Fudge Point" or crystallisation point of approximately 58 ^{0}C. In second part of the study, emulsion samples were prepared with the ammonium nitrate concentration reduced to less than 65% by mass for the investigation of the effect of this on the shear stability, as stated in the objectives. However, the dispersed phase solution was still supersaturated, with a decrease of the Fudge Point from the previous solution (where water content was less than 20 wt.%) to approximately 18 ^{0}C. Such conditions produced an emulsion of supercooled droplets of supersaturated ammonium nitrate solution emulsified in the hydrocarbon oil base (which is explained in detailed in the next section on surfactants and fuel oil).

During the emulsification process in the Hobart N50 mixer prior to the addition of the oil compound (which comprised surfactant and hydrocarbon oil), some buffer and acid were added in order to control the pH of the final product (emulsion). In all cases, less than 0.5% of pH-buffering additives and acids were added in the formulation. The concentration of the dispersed phase after emulsification was 92% by mass for all emulsions of different formulations used in the study, and their density was approximated to be 1347 kg/m^3.

3.4.2 SURFACTANTS

The surfactants used to stabilise the emulsion samples for this work was manufactured and provided by Lake International Technologies (Lake). They were described, in the information given by "Lake – international" as organic derivatives of *PIBSA* (the industrial acronym for poly(isobutylene) succinic anhydride) which formed an open-chain carboxylate in its derivative form. Four surfactants were used, these were Pibsa-MEA, Pibsa-IMIDE, Pibsa-UREA and a mixture of Pibsa-MEA/SMO, where the SMO was a sorbitan ester. When originally synthesised, the surfactants were dissolved or dispersed in *Parprol 32*, a paraffinic

petroleum oil with no additives. Further dilution with Mosspar-H hydrocarbon-based oil was used to achieve the desired concentration and viscosity.

The hydrophobic moiety for the three Pibsa derivatives (Pibsa-MEA, Pibsa-IMIDE and Pibsa-UREA) was the polyisobutylene group, with an approximate relative molecular weight of 1050. The hydrophilic moiety was the modified succinic anhydride group, with an approximate relative molecular weight of 150. Thus the hydrophilic-lipophilic balance (HLB) lay heavily towards lipophilicity (i.e. hydrophobicity), and the surfactants were soluble in hydrocarbon oils, but insoluble in water. For the SMO, the hydrophobic moiety was an oleic group, with an approximate relative molecular weight of 280, with the hydrophilic moiety was the sorbitan group with a relative molecular weight of 160. Therefore the balance was also towards lipophilicity.

3.4.2.1 Pibsa-MEA

It was the poly(isobutylene succinic) anhydride that reacted in approximately 1:1 ratio with monoethanolamine to an uncondensed amide/acid head group.

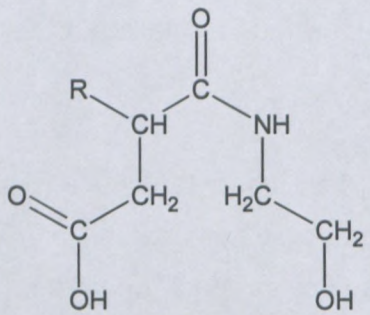

PIBSA MEA

The *R* indicates polyisobutylene, the repeat unit of which was $-(CH_2\text{-}(CH_3)_2\text{-}CH_2)-$ i.e. a chain of carbon atoms with two methyl side groups attached to every second one, to give a molecular weight of 1048. Thus, there would have to be about 17 repeat units in the chain. If these were contained in a single chain, the length would be 34 carbon atoms with an additional 34 in the methyl side groups (the chain may be attached to the carbon atom adjacent to the carboxylic acid group, rather than the one adjacent to the amide group as shown). The overall molecular weight would be about 1109.

3.4.2.2 Pibsa-IMIDE

This was described as Pibsa-MEA condensed to an N-substituted pyrrolidinedione (succinimide) structure, see figure below.

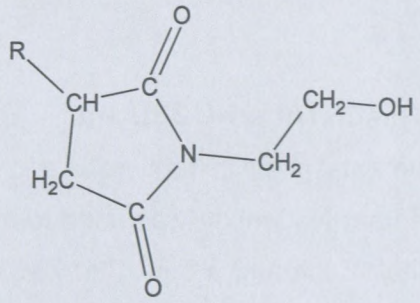

PIBSA IMIDE

The overall molecular weight would be 1091

3.4.2.3 Pibsa-UREA

The following described its structure:

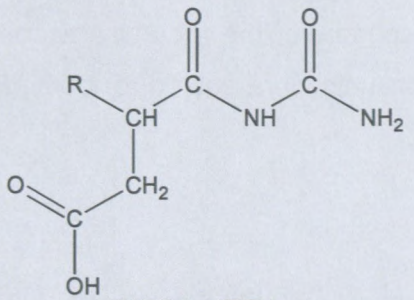

PIBSA UREA

The overall molecular weight was about 1047

3.4.2.4 SMO (in mixture of Pibsa-MEA/SMO)

SMO was an ester formed between sorbitan and oleic acid (oleic acid is a C18 fatty acid with a single *cis* double bond, written as C18:1). Its molecular weight was 428, and its structure was given below.

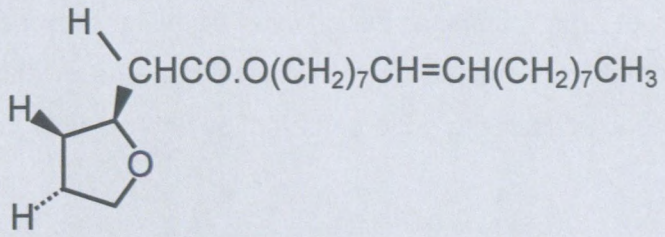

SMO

In the mixture of Pibsa-MEA/SMO the ratio was taken as 10:1 respectively.

3.4.3 HYDROCARBON OIL

The surfactants in the continuous phase were preliminarily dissolved at high concentrations in Parprol 32, prior to being diluted with hydrocarbon fuel of Mosspar-H to achieve the desired concentration and viscosity.

3.5 INSTRUMENTATION AND EXPERIMENTAL PROCEDURE

This section addresses the instruments used in this work and the procedure followed to operate them. Thus, to start, the Hobart N50 mixer was used to manufacture all the samples under study. It consisted of an agitator unit and a bowl that was heated to 85°C prior to the addition of the continuous phase, which consisted of fuel oil (Mosspar-H) and surfactant; and the dispersed phase solution that included: the ammonium nitrate solution and other substances such as buffers and acid. While agitating the system, water-in-oil emulsions of a highly concentrated dispersed phase of 92% by mass were formed. The formulations differed in terms of surfactant type, surfactant concentration, and salt concentration in the dispersed phase, but the type of emulsion (water-in-oil) formed, the dispersed phase volume fraction (92 wt.%) and the polydispersity of the droplet size remained the same for all the samples formed. The prepared products were cooled to room temperature prior to shearing them by using a pumping device.

3.5.1 PUMPING SYSTEM

The pumping system consisted of a cylindrical chamber with an outlet orifice of small diameter. A piston shaft was mounted into the chamber, which was moved downward under application of force acting upon it (see Figure 3.1, below). This system was connected to a panel consisting of control valves: a distributor block and regulator (as shown in Figure 3.1) was fixed to a wall and served as the pressure function control of this pumping device.

During the operation of this device, the emulsion sample under high pressure applied to the piston-shaft was forced out of the chamber of the piston through the small orifice designed as the outlet of this pumping instrument. Thus, the "prepared and cooled to room temperature" emulsion sample was exposed to high shear which was the result of the high friction generated between the edge of the orifice and the flow material.

3.5.1.1 Operation procedure for the pumping device

The procedure that was followed is explained below.

- Load the emulsion sample into the piston chamber, and then screw back the outlet of the chamber using the small orifice (3 and 4 mm in diameter for this study).

- Switch on the air compressor (used to provide pressure) and adjust the pressure to 3 bar, using the pressure regulator in the control panel.

- Ensure that the pressure lines (from the compressor into the control panel and from the control panel to the piston device) are connected properly.

- Ensure also that the control valve in the distribution block and the release valve are open.

- To start pumping or shearing the samples, close the release valve on the top of the distribution block. Be sure to place a receptacle underneath the device as it faces downward to collect the sheared emulsion coming out of the device for further analysis, as indicated in the picture.

3.5.1.2 Caution

The following identifiable risks and hazards were foreseen as possibly arising during the operation of this pumping device:

- High pressure on the line

- Pinch points

- Emulsion's classification as a chemical products makes it necessary to wear gloves, overall and goggles to avoid bio-chemical contamination (e.g. of eyes).

- Spills need to be minimised during the pumping process to avoid and lower the risk of slipping.

- Operation of the air compressor needs to be properly understood prior of the use of this shearing device

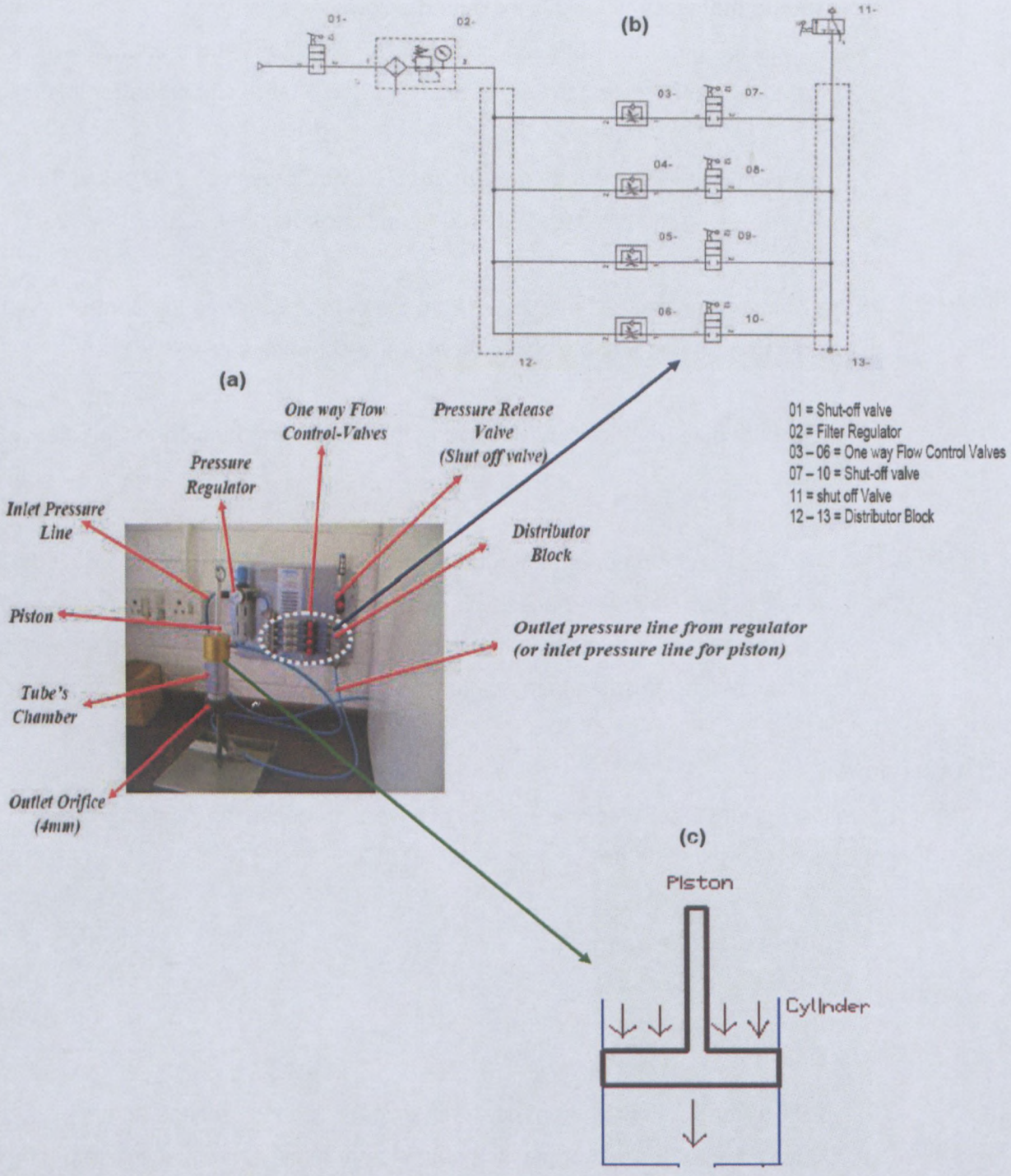

Figure 3.1: Function control and components of pumping device: (a) Overall pumping device. (b) Schematic presentation of pressure control panel. (c) Schematic presentation of the piston during the pumping process

3.5.2 MICROSCOPY OBSERVATION

For the qualitative analysis of the sheared samples it had to be seen whether sample droplets had become refined or crystallised or had coalesced. Such optical analysis was achieved through the use of Leica optical microscope equipped with a digital camera and high magnification. The following figure is a photographic image of the microscope:

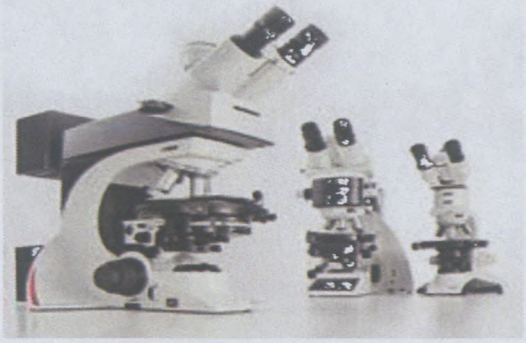

Figure 3.2: Leica optical microscope

3.5.3 MALVERN MASTERSIZER 2000 (PARTICLE SIZE DISTRIBUTION)

This is another optical method used to determine the particle size distribution within the emulsion. The measurement is achieved by measuring the angle distribution of the He-Ne laser light scattered by particles. The angle at which the light is scattered is inversely proportional to the size of the particles. Particle sizes in the range from 0.02 to 2000 μm can be measured by this Mastersizer; this range, however, is much wider than the droplet size distribution of the actual samples used in this thesis. The sized distribution calculations were based on the rigorous Mie theory. The following illustrates the experimental procedure carried out during the measurement:

- A small amount of sample was diluted with an oil hydrocarbon (*Ash 1925* was used for this work).

- The agitation vessel in which the diluted sample was poured, had preliminarily been filled with the same oil that was used for dilution, prior to the addition of sample.

- During the above process, the sample dispersion measurement was controlled by means of special software designed for this instrument and the angle depended on the intensity of scattering of the He-Ne laser beam.

Figure 3.3: Malvern Mastersizer 2000 (Cape Peninsula University of Technology – Rheology laboratory)

3.5.4 RHEOMETER – MCR 300 SYSTEM (RHEOLOGICAL ANALYSIS)

The rheological measurements were performed with the use of a rotational dynamic rheometer MCR 300 (Paar Physica) at the Rheology Laboratory of CAPE PENINSULA UNIVERSITY OF TECHNOLOGY (Cape Town Campus). The geometry of the measurement unit was "plate-and-plate" with a sandblasted surface (see Figure 3.5, below) and plate diameter of 50 mm. The gap between the two plates measured 1 mm.

The function controls and components of MCR 300 are detailed in Figure 3.4, below. All the rheological data were obtained from the rheometer MCR 300; the rheological parameters (such as G_0', τ_y, $\gamma_{limited}$) were determined directly by the *Paar Physica* Software and then converted to Microsoft Excel for further modelling.

The following describe the type of rheological measurement conducted in this work:

- Amplitude Sweep Curve to define the viscoelastic properties of the materials, with the setting of the measurement parameters done by keeping a constant frequency of 1 HZ, and strain was selected as the set variable and kept between 0.1 to 200 %.

- The flow curve measurement was performed in the downward sweeping shear rate mode, the shear rate was selected as the set variable and kept between 200 to $1x10^{-6}$ 1/s.

All rheological measurements were conducted at 30°C.

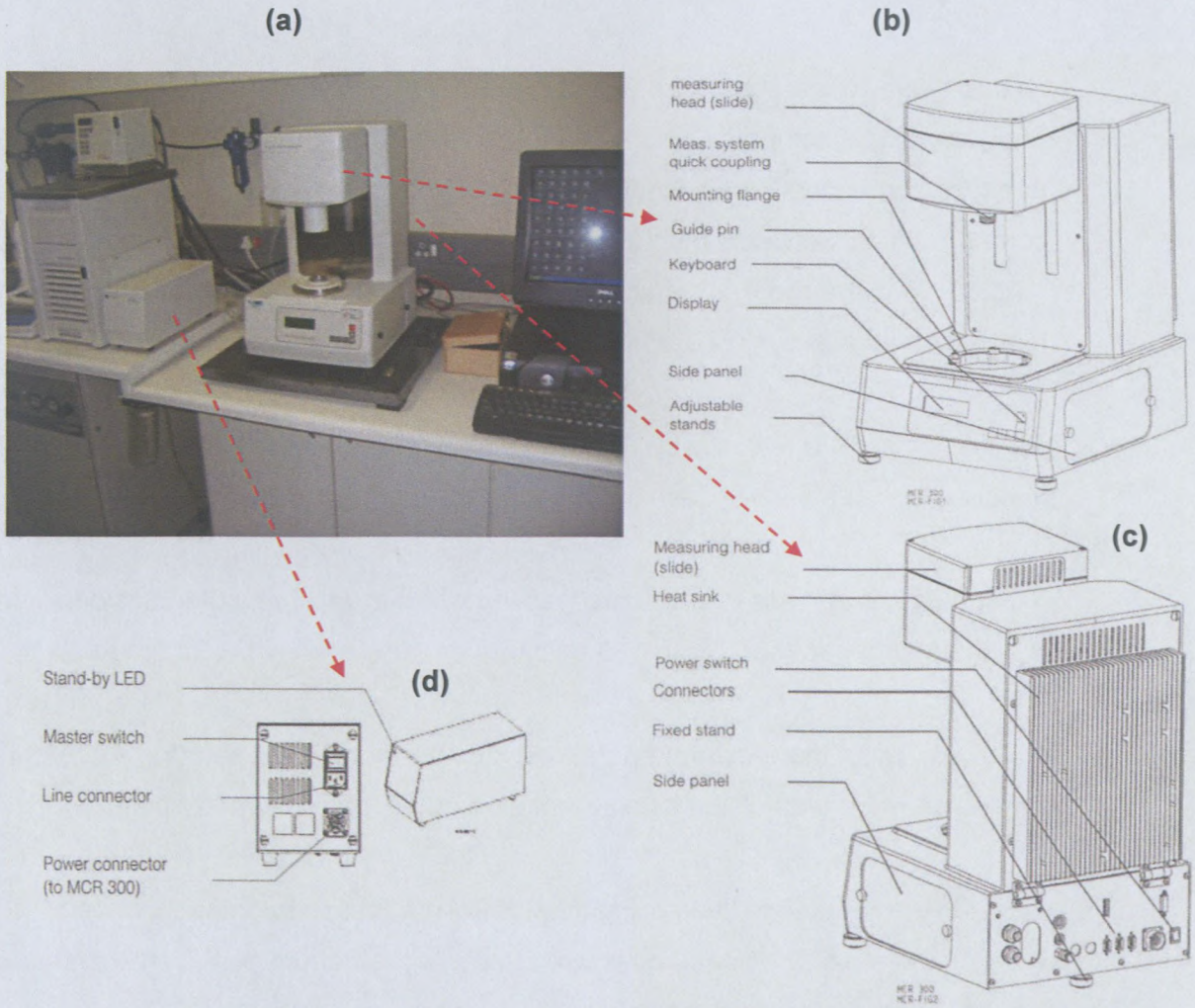

Figure 3.4: (a) The MCR 300 rheometer System, the Power Supply Unit & the computer system
(b) Front View of MCR 300 System with its function control & Component
(c) Rear View of MCR 300 System with its function control & Component
(d) Function control of the Power Supply unit (PS 1)

3.5.4.1 Experimental Procedure

The experimental procedure for the rheological analysis using the MCR 300 Rheometer was conducted as follows:

- The pressure valve on the air compressor was open, and pressure was adjusted to 4 bar using the "air regulator" situated on the same line next to the pressure valve.

- Now the MCR 300 system was switched on with the "master switch" situated on the Power supply unit [see Figure 3.4, (d)]. At this stage, the system was in "Stand-by Mode".

- The Rheometer was switched on with the "power switch" situated at the MCR 300 System [see Figure 3.4 (c)].

- At this stage, once again, the whole Rheometer was powered, but not operational yet. The use of the computer data generation system [connected to the MCR 300 system through "connectors" (see Figure 3.4 (c)) becomes useful at this stage. To do so, the communication between the Computer (PC) and the MCR 300 was set up using the "US200 Software program" that is installed in the C-drive of the Computer. At this point, the rheometer was fully operational through the computer using the US200 program.

- Before starting the test, the system was first initialised, then the "measuring system" was installed to the "meas. System quick coupling" (Figure 3.4 (b)).

- Then the system was run to "zero gap" to set the gap measurement between the two plates at 1mm gap (see Figure 3.5 below).

- Following this, the desired operational temperature was set (to 30°C) through the computer and the emulsion sample was poured into the rheometer plate.

- Next, the "measuring head" (Figure 3.4 (b)) was set to "measuring position", which brought the measuring head downward towards the bottom plate of the rheometer where the emulsion sample was located.

- Finally, the test was started through the Computer, but before engaging the "play button", the rheological parameters which determined what type of test was to be run (amplitude sweep or flow curves) had to be set. Then, by clicking on the "play button" that is shown on the computer screen, the test was started.

3.5.4.2 Measuring unit & Zero gap

As stated at the beginning of this section, the geometry of the measurement unit was "plate-and-plate" with the plate's diameter being 50 mm and the gap measurement between the two plates being 1 mm. This measurement unit was composed of a bottom plate, which was mounted to "the mounted flange" of the rheometer MCR 300 through the "guide pin" (see Figure 3.4 (b)), and of a "measuring system" that comprised a "shaft" with a 50-mm circular head.

The "zero gap" setting during the measurement defined the gap measurement between the two plates, and was set to 1 mm for this study analysis. The following was found true to demonstrate the basic concept behind zero gap setting:

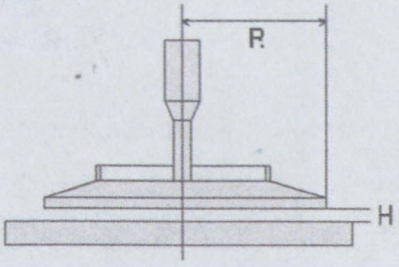

Figure 3.5: PP-50 Measuring system

H	gap (mm)
R	Plate Radius (mm)
τ	Shear stress (Pa)
M	Torque (mNm)
γ	Strain (%)
φ	Deflection angle (mrad)
n	Speed (min^{-1})
ω	Angular velocity (s^{-1})
$\dot{\gamma}$	Shear rate (s^{-1})

$$\gamma_{max} = \frac{1}{10} \cdot \frac{R}{H} \cdot \varphi \qquad \textbf{(Equation 3.1)}$$

$$\tau_{max} = \frac{2}{1000} \cdot \frac{M}{\pi R^3} \qquad \textbf{(Equation 3.2)}$$

$$\dot{\gamma}_{max} = \frac{2\pi}{60} \cdot \frac{R}{H} \cdot n \qquad \textbf{(Equation 3.3)}$$

$$\omega = \frac{2\pi}{60} \cdot n \qquad \textbf{(Equation 3.4)}$$

3.6 SUMMARY

This chapter has presented a full description of the substances that constituted these highly concentrated emulsion materials in which the dispersed phase concentration was 92 wt %, and consisted of supersaturated, supercooled droplets of ammonium nitrate solution dispersed in an oil phase consisting of a surfactant based on organic derivatives of *PIBSA* emulsified into Mosspar-H hydrocarbon oil.

This was followed by the description of the instrumentation and the experimental procedure used to achieve the objectives of the research. This included a newly designed piston-pumping instrument which served to shear the freshly manufactured emulsion samples (through the agitation process of a Hobart N50 mixer) by which the materials, under the high pressure applied to the piston-shaft, were forced out of the chamber of the piston through a small orifice which was set as the outlet. Thereafter, two optical analyses were described. One was a qualitative microscopic analysis that was achieved by using a Leica optical microscope equipped with digital camera and high magnification; the other determined the particle size distribution within the emulsion material and this was done through laser diffraction using a Malvern Mastersizer instrument. Finally, the rheological measurement that was performed with the use of a rotational dynamic rheometer MCR 300 (Paar Physica) involved an amplitude sweep test by which the viscoelastic properties of the materials were determined; and a flow test for the characterisation of the flow properties of the emulsion materials used in this project.

CHAPTER 4
RESULTS AND DISCUSSION

4.1 INTRODUCTION

This chapter presents the analysis and interpretation of the experimental results whereas the method and procedure of measurement that were followed have been discussed in the previous chapter, Chapter 3 of this thesis.

The results of the study have been subdivided into three (3) Parts which, in turn, consist of subsections with subtitles: Part A consists of the analysis of droplet size and their distribution where a quantitative correlation between these parameters and the factors that influenced them (surfactant type and concentration; and process factors such as device geometry and energy) was achieved. Part B, in which all the rheological results and analyses are presented, includes a discussion of viscoelastic properties and flow curves. And Part C presents a discussion of the effect of ammonium nitrate salt concentration in dispersed phase on the stability of these materials under high shear conditions.

However, the main goal of this study was to investigate the effect of the shearing process (pumping) on the structure and rheological stability of these highly concentrated emulsions. To achieve the objectives, measured constants from different measurement techniques (G'_0, τ_y, D_{50}, D_{32}, ω, $\gamma_{limiting}$) were correlated with one another to give a better scientific interpretation and understanding of this colloidal system where its stability under shear still remains unsolved. Four types of surfactants of PIBSA derivative were used in the emulsion formulation, each in two different concentrations. Two different orifice diameters for every formulation were used in the shearing process. Furthermore, three samples of the same surfactant content (type and concentration) but with a lower ammonium nitrate salt concentration in the dispersed phase were used to investigate the effect of the latter (salt concentration) on the shear stability of such emulsion materials. However, their difference (3 samples) was on their droplet size.

4.2 PART A – CHARACTERISATION OF DROPLET SIZE, CRITICAL DROPLET DIAMETER AND ENERGY : EFFECT OF SURFACTANT CONCENTRATION, SURFACTANT TYPE AND ORIFICE GEOMETRY

Emulsions are defined as fine dispersions of one liquid in the form of small spherical droplets in another (the continuous phase), both liquids being mutually immiscible (more detail on the general definition of emulsions are discussed in Section 2.2 of Chapter 2 – Theory and literature review). The size of the droplets in the dispersed phase within emulsions determines many of an emulsion's most important properties such as stability and appearance (Dickinson & Stainsby, 1982; Dickinson, 1992). Therefore it was of extreme necessity to be able to report and control the size and disruption of droplets in emulsions, when exposed to high shear during transportation involving pumping, which can cause significant alterations in their overall properties. Thus, McClements (1999:8) stressed the fact that it was convenient to represent the size of the droplets in a polydispersed emulsion (such as the emulsions in this study – highly concentrated w/o emulsions) by their mean diameter ($\bar{d}$), which is a measure of the central tendency of the distribution, and the width of their distribution.

4.2.1 DROPLET SIZES AND THEIR DISTRIBUTIONS (FRESH AND SHEARED SAMPLES)

The droplet size can be expressed in a number of ways, with each of them having the dimension of length (metres) but stressing a different physical aspect of the distribution (McClements, 1999:8-9). The volume median diameter used throughout this study were the D_{50}, which is the diameter at 50% volume (Malkin, Masalova, Slatter & Wilson, 2004a; Masalova & Malkin 2007a, 2007b) and the surface area mean diameter D_{32} sometimes expressed as the Sauter mean diameter (Equation 4.1) (Jafari & Bhandari, 2007; Romero, Cordobes, Puppo, Guerrero & Bengoechea, 2008; Masalova & Malkin, 2008), which was the mean diameter related to the surface area of droplets exposed to the continuous phase per unit volume of emulsion (McClements, 1999:9):

$$D_{x,y} = \frac{\sum n_i d_i^x}{\sum n_i d_i^y} \quad \Leftrightarrow \quad D_{32} = \frac{\sum n_i d_i^3}{\sum n_i d_i^2} \qquad \textbf{(Equation 4.1)}$$

This difference in expression of droplet diameter can be explained by the difference of the experimental techniques used to measure it, which, in turn, were sensitive to different mean values (Orr, 1988: Chapter 3). Thus, analysis of the size distribution of the emulsions of this

study was achieved using a Malvern Mastersizer 2000 that gave information about the surface area mean diameter (D_{32}) and volume median diameter (D_{50}).

For the characterisation of width of DSD, the standard Gauss equation (Equation 4.2) was used to fit all the emulsion droplet size distributions (Masalova & Malkin, 2007b):

$$f = \frac{A}{\omega\sqrt{\pi/2}} e^{-\frac{2(D-D_0)^2}{\omega^2}}, \qquad \textbf{(Equation 4.2)}$$

where f represents the density of the distribution function, D is the argument (droplet size), D_{50} is the position of the maximum (in semi log scale), ω is the dispersion characterising the width of the distribution, and A is a normalising factor.

4.2.1.1 Droplet sizes and their distributions for fresh emulsions

The first step in this study was to produce highly concentrated water-in-oil emulsions emulsified with organic derivatives of the PIBSA family as described previously (in Chapter 3: Materials and experimental procedure).

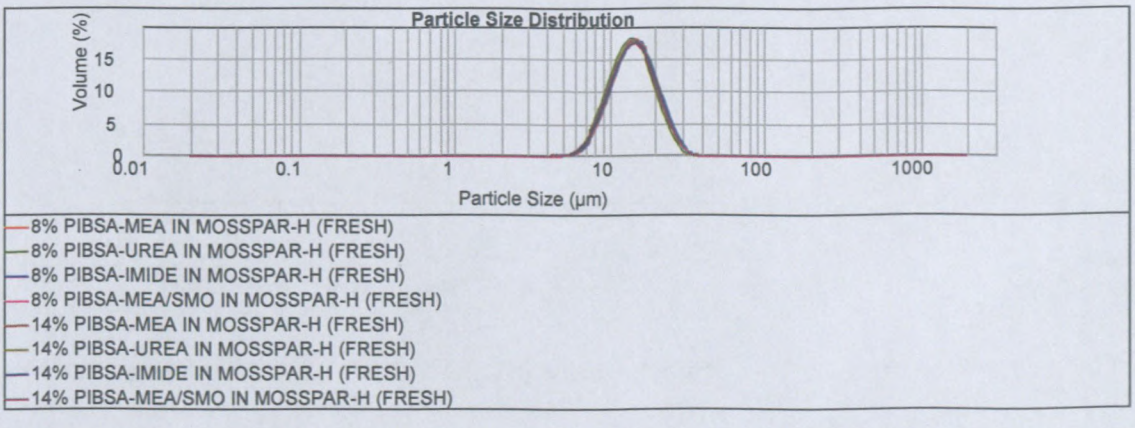

Figure 4.1: Histogram of drop size distribution in fresh emulsion of all formulations. Droplet size approximately ($D_{32} \approx 13$mm).

Figure 4.1 above shows the size distributions for the fresh emulsion of all formulation performed by means of the *Mastersizer-2000* instrument, while Figure 4.2 shows the "Good fit" of the size distribution of 8% PIBSA MEA in Mosspar-H of fresh emulsion using the Gauss equation. This fitting of the size distribution was identical for all fresh emulsions with different formulation content (See Appendix B for the rest of the fresh emulsion fittings). This information is summarised in Table 4.1 below. All size distributions of these fresh emulsions

were of the Gaussian type. They were wider, and similar for all samples of the formulation with approximately equal droplets size (D_{32}) of 13 μm, referred to in this study as the starting point of refinement. Thus, the size distributions for all fresh samples did not depend on the surfactant type or surfactant concentration in these emulsions. Such a trend should be stressed as it confirms findings from previous studies by Masalova *et al.* (2005 & 2007b) and Malkin *et al.* (2004a) in which the size distributions of samples did not depend on the content of the dispersed phase in an emulsion.

This close size of D_{32} in all formulations was achieved by the technology followed in emulsion preparation, as stressed by Malkin *et al.* (2004a), where the size of droplets depended on the conditions of mixing in a vessel. In the case of the present study this was determined by the HOBART N50 mixer's speed of rotation of the stirrer and time of stirring (deformation). By varying these factors, it is possible to obtain emulsions of different formulations and surfactant concentrations with the same droplet size.

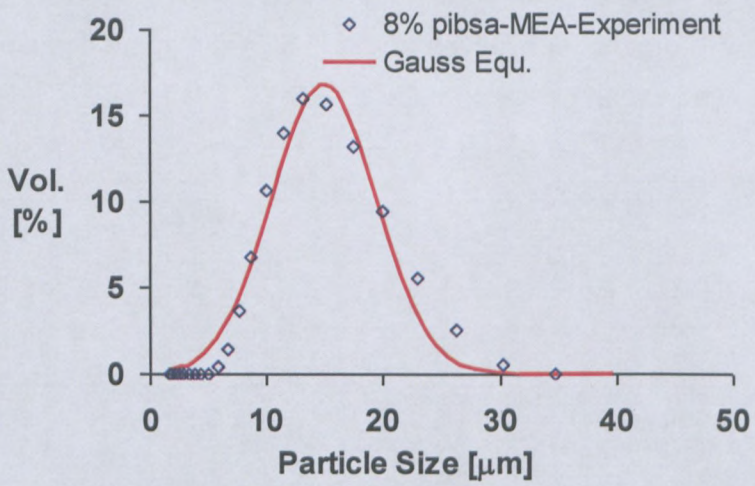

Figure 4.2: Characterisation of DSD of 8% PIBSA-MEA in Mosspar-H fresh emulsion.

Table 4.1: The width of the size distribution of droplets was wider in all the fresh emulsion samples of different formulation content; their characteristics using the Gauss equation are summarised as follows:

Emulsion Formulation	Surfactant Concentration	$D_{32,\ Fresh}$ (μm)	$D_{50,\ Fresh}$ (μm)	ω	A
PIBSA-MEA	8%	13.65	14.63	8.8	186
	14%	13.84	14.89	7.2	159
PIBSA-UREA	8%	13.94	15	9.2	190
	14%	13.7	14.9	9.1	187
PIBSA-IMIDE	8%	13.01	13.99	8.4	177
	14%	13.34	14.39	8.7	182
PIBSA-MEA/SMO	8%	13.56	14.5	8.7	184
	14%	13.35	14.5	8.9	182

4.2.1.2 Droplet size distributions for sheared emulsions

Figures 4.3 and 4.4 illustrated the droplets size distribution profiles for sheared emulsion samples using two orifices of different diameter (3 and 4 mm) respectively. In all cases, an evolution toward smaller droplet size was observed as the number of pumpings increased and/or energy increased (see Tables 4.2 and 4.3). All the other formulations followed similar trends and are presented in Appendix A.

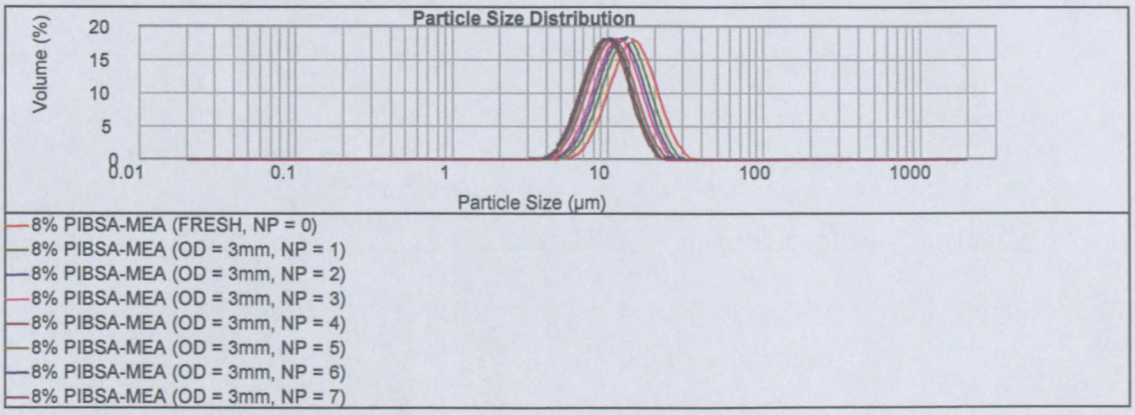

Figure 4.3: Histogram of drop size distribution of 8% PIBSA-MEA in MOSSPAR-H (Orifice Diameter = 3 mm)

Thus, it was clearly seen that, by subjecting the fresh samples of different formulation but at same starting point of refinement ($D_{32} \approx 13\mu m$) to shearing action led to a reduction in droplet size, as confirmed by the qualitative analysis under high magnification of the optical microscope, as pictured in Figure 4.5 below. This trend has also been observed in many

other studies; however the technique of shearing may have differed, the tendency of the emulsion droplets to refinement and/or disruption nevertheless remained the same (e.g., in emulsification processes using modern or traditional emulsifying devices in investigations by Robin, Kalab, Britten & Paquin, 1996; Forgiarini, Esquena, Gonzalez & Solans, 2001; Masalova, Malkin, Slatter & Wilson, 2003; Olson, White & Richter, 2004; Salager, Forgiarini, Marquez, Pena, Pizzino, Rodriguez & Gonzalez, 2004; Malkin, Masalova, Slatter & Wilson, 2004a; Malkin, Masalova, Pavlovski & Slatter, 2004b; Windhab, Dressler, Feigl, Fischer & Megias-Alguacil, 2005; Masalova & Malkin 2007a, 2007b; Jafari & Bhandari 2007; Fradette, Brocart & Tanguy, 2007).

Neither crystallisation nor any other destabilisation phenomena (e.g. coalescence, phase inversion, partial coalescence) occurred during the shearing process of these emulsions regardless of their formulation content. The absence of such emulsion instability during shearing in this study should be stressed, as opposed to some other studies (e.g. Salager *et al.*, 2004) where the phase inversion was sensitive to shear and the formulation concentration's content.

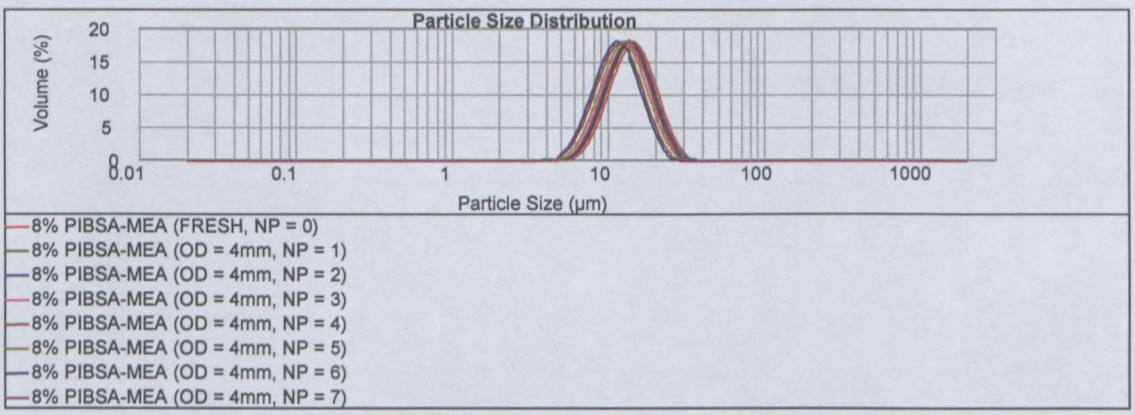

Figure 4.4: Histogram of drop size distribution of 8% PIBSA-MEA in MOSSPAR-H (Orifice diameter = 4 mm)

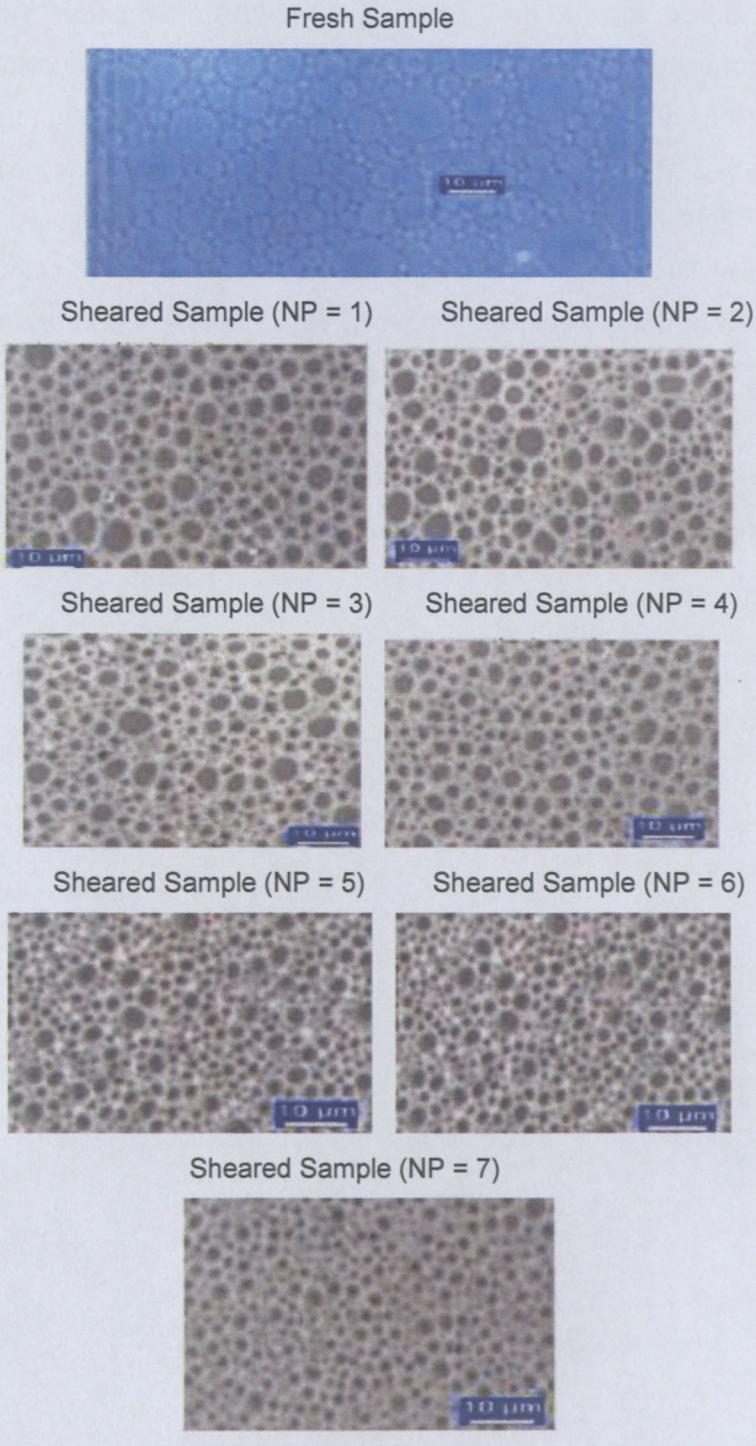

Figure 4.5: Microscopic image of fresh and sheared emulsion samples of 8% PIBSA-MEA in Mosspar-H.

Figure 4.6 below showed the "Good fit" of the size distribution of droplets of sheared and/or pumped emulsion samples using the Gauss equation. They were of Gaussian type and revealed wider distribution. All the sheared samples of different formulation contents showed a similar trend and are represented in Appendix B. The fitting characteristics of distribution for 8% PIBSA-MEA and 8% PIBSA-UREA are summarised in Tables 4.2 and 4.3 respectively. They have indicated that the width of the distribution, the D_{50} and/or D_{32} decreased with the increasing number of pumpings (NP) and/or energy, and had a tendency to approach a constant value as the number of pumping increased further (see Appendix B for the Table summarising the rest of the formulations that showed a similar trend to those presented in this chapter). It was of huge interest to illustrate the evolution of these parameters with the increase in number of pumpings or prolonged shearing action.

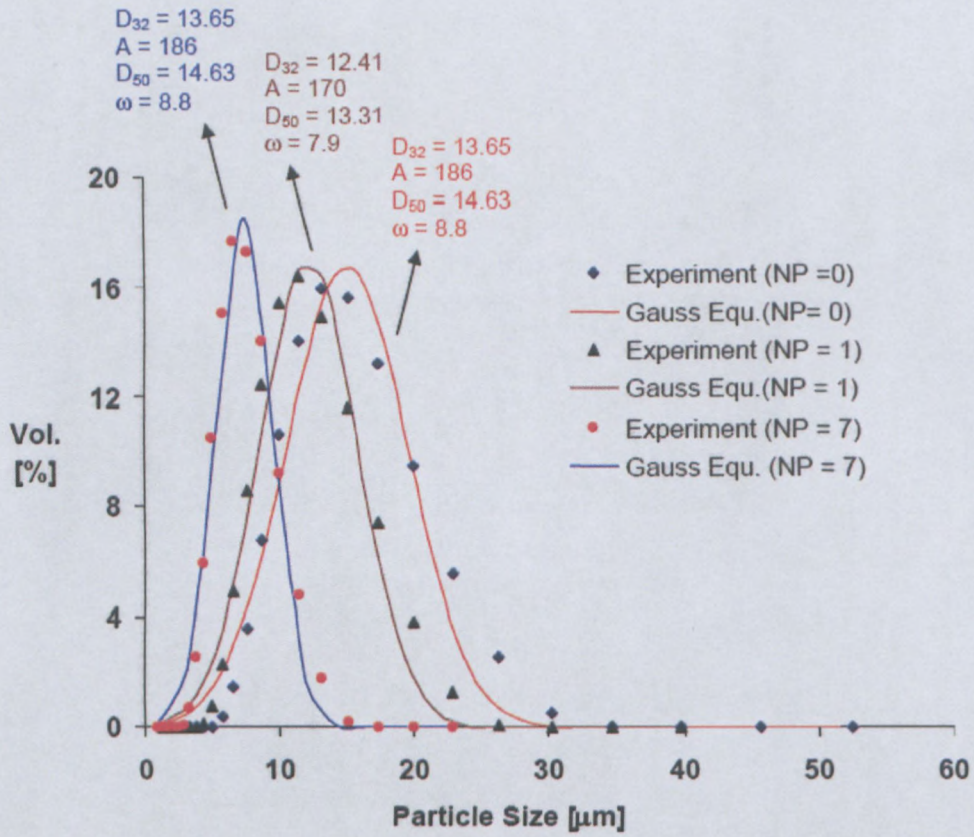

Figure 4.6: Characterisation of DSD of 8% Pibsa-MEA in Mosspar-H of sheared emulsion using the standard Gauss equation (Equation 4.2).

Table 4.2: Summary of table of the characterisation of the width of DSD of sheared emulsion of formulation – 8% PIBSA-MEA in MOSSPAR-H

OD	NP	D_{50}	ω	A
3 mm	0	14.63	8.8	186
	1	13.31	7.9	170
	2	12.3	7.3	157
	3	11.63	6.9	148
	4	10.7	6.4	136
	5	10.18	6	129
	6	10.07	6	128
	7	9.7	5.7	123
4 mm	0	14.63	8.8	186
	1	14.12	8.4	179
	2	13.87	8.3	176
	3	13.53	8	172
	4	13.22	7.9	168
	5	12.72	7.6	161
	6	11.95	7.2	151
	7	11.51	6.9	146

Table 4.3: Summary of table of the characterisation of the width of DSD of sheared emulsion of formulation – 8% PIBSA-UREA in MOSSPAR-H

OD	NP	D_{50}	ω	A
3 mm	0	15	9.2	190
	1	12.2	7.2	155
	2	10.6	6.4	134
	3	10.2	5.6	131
	4	9.0	5.0	115
	5	8.1	4.5	104
	6	8.0	4.5	102
	7	7.4	4.1	96
4 mm	0	15	9.0	190
	1	13.5	8.1	172
	2	12.9	7.7	164
	3	11.8	7.0	150
	4	11.4	6.8	145
	5	11.1	6.2	143
	6	10.8	6.0	139
	7	10.6	5.9	135

4.2.2 CHARACTERISATION OF CRITICAL DROPLET DIAMETER

Figures 4.7 and 4.8, below, show the evolution of the volume median diameter (D_{50}) and the width of the DSD as a function of the number of pumpings. The curves show an exponential decrease of the average droplet size and the width of the distribution as the number of pumpings increased, and approaching a constant value referred here as the critical width ($\omega_{critical}$) and critical diameter ($D_{crit.}$). The latter can be defining as the emulsion droplet diameter where no further refinement can be observed (see Appendix C for the rest of formulation fittings).

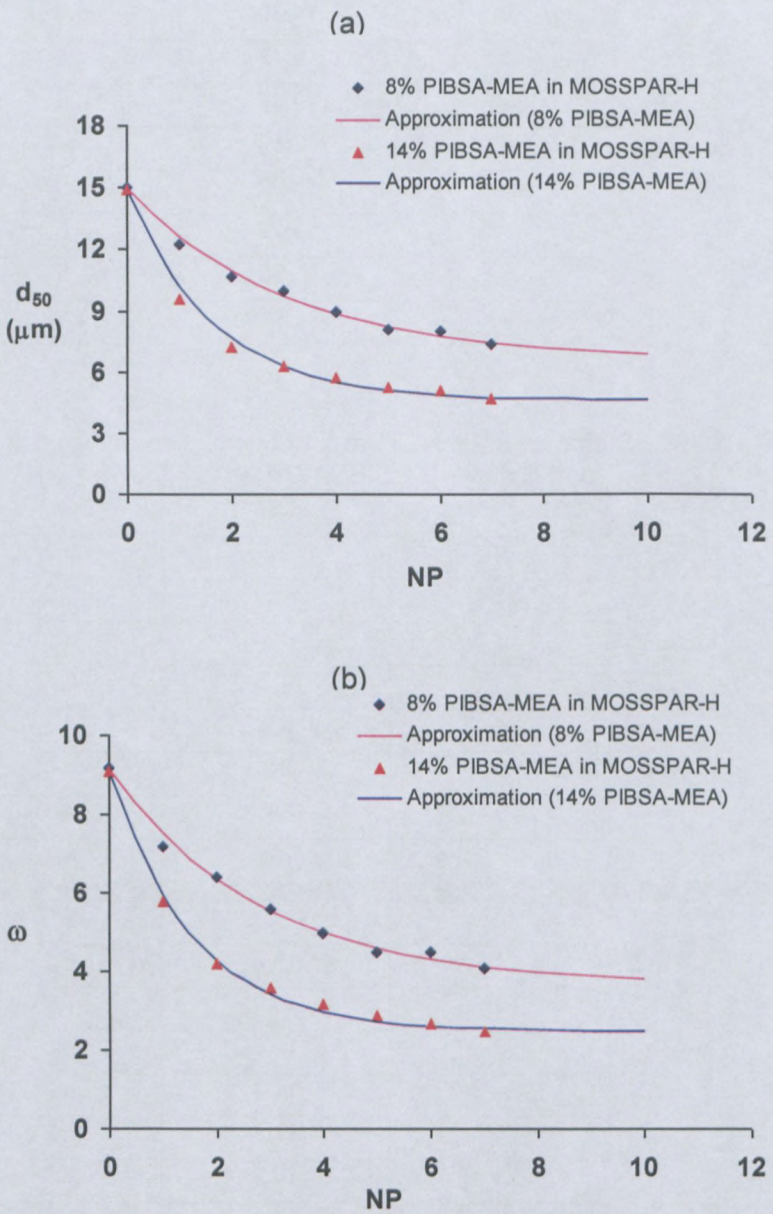

Figure 4.7: Evolution of the volume median diameter (a) and the width of DSD (b) as functions of the number of pumpings – Effect of surfactant concentration.

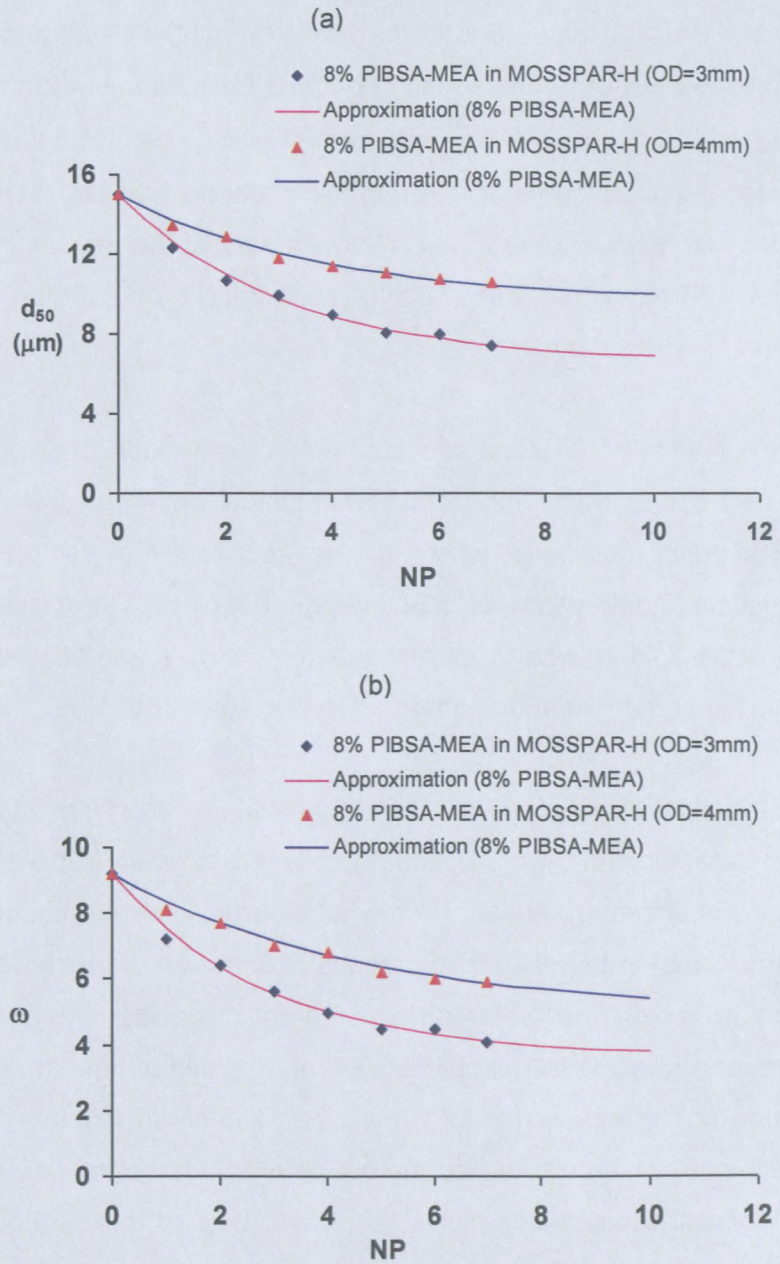

Figure 4.8: Evolution of the volume median diameter (a) and the width of DSD (b) as a function of the number of pumpings – Effect of orifice diameter.

The following models were proposed and used to fit the experimental results and the determination of D_{crit} and $\omega_{crit.}$ as shown in Figures 4.7 and 4.8:

$$D_{cal} = D_{crit.} + e^{-(N/\theta_D)}\left(D_0 - D_{crit.}\right) \qquad \textbf{(Equation 4.3)}$$

and

$$\omega_{cal} = \omega_{crit.} + e^{-(N/\theta_\omega)}\left(\omega_0 - \omega_{crit.}\right), \qquad \textbf{(Equation 4.4)}$$

where D_0, ω_0, $D_{crit.}$, $\omega_{crit.}$, θ_D and θ_ω were the fitting parameters. The experimental D_{50} and $\omega_{exp.}$ obtained from the Gauss fitting of DSD (see Tables 4.2 and 4.3) must be fitted by D_{cal} and ω_{cal} with the above fitting parameters. Using these models, θ_D and θ_ω which were the characteristic pumping parameters of the shearing process, were obtained. Their values did not necessarily have to be equal. The summary of the results is tabulated in Tables 4.4 and 4.5, below, from which the effect of surfactant concentration, surfactant type and orifice diameter can be clearly estimated.

Figure 4.7 shows the effect of surfactant concentration and it can be seen that the higher surfactant concentration provided lower critical diameter and width. Figure 4.8 shows the effect of orifice geometry, where greater refinement and more narrowing of the emulsion droplets and their width of DSD were observed with the small orifice diameter. This demonstrated, that when using the 3 mm orifice diameter, the emulsion samples were exposed to higher shearing compared to the 4 mm one.

Indeed, both Walstra (1983:57-127) and McClements (1999:161-184) have emphasised the role of surfactants in the disruption process of emulsion droplets, and the factors determining their effectiveness on the latter. They afterwards reported that one of the roles of emulsifiers (or surfactants) in the disruption process of emulsion droplets was to decrease the interfacial tension in the-oil-and water phase, thereby reducing the amount of energy required to deform and disrupt the droplets. But at the same time, they stressed the factors that influence the effectiveness of emulsifiers and/or surfactants on reducing the emulsion's droplets size, which concerned the emulsifiers' adsorption rate and their concentration: thus the quicker the emulsifier (surfactant) adsorbed to the surface of the droplets during the disruption process, the smaller the droplets produced and the greater the amount or concentration of emulsifiers (surfactant) accumulated at the surface, the easier the droplets disrupted or, in other words, the less energy required for the reduction of droplets size.

Tables 4.4 and 4.5, below, illustrate the effect of surfactant type on the shear stability of the emulsions where the following trend with regard to the critical diameter ($D_{crit.}$), critical width ($\omega_{crit.}$) and characteristic pumping parameters of the shearing process θ_D and θ_ω, was observed:

PIBSA-MEA > PIBSA-IMIDE > PIBSA-UREA > PIBSA-MEA/SMO

This observation clearly outlined the concept of energy of adsorption (Robin *et al.*, 1992) and the trend for the different surfactant head group used in this study followed (PIBSA-MEA > PIBSA-IMIDE > PIBSA-UREA > PIBSA-MEA/SMO) – with the PIBSA MEA showing the highest resistance to disruption. However, Darling and Birkett (1987) and Robin *et al.*, (1992, 1996) reported on the surfactant's molecular weight, which was proportional to the rate of adsorption where the lower molecular weight surfactant affected the refinement or disruption of the emulsion droplets during the shearing process by reducing interfacial tension more rapidly, thereby allowing the production of smaller-sized dispersed particles.

A synergistic effect was observed in the case of the mixture of SMO and PIBSA-MEA, where a competitive adsorption between the two surfactants head group (SMO and PIBSA-MEA) leading to a faster reduction of emulsion droplets size.

Table 4.4: Summary of the characterisation of critical droplet diameter when using the 3 mm diameter orifice during the shearing process (OD = 3 mm)

Surfactant Type	Surfactant Con. (%)	$D_{critical}$	θ_D	Error	$\omega_{critical}$	θ_ω	Error
PIBSA MEA in Mosspar	8	8.64	3.97	0.003	4.91	4.30	0.004
	14	7.10	2.29	0.009	3.70	3.68	0.008
PIBSA IMIDE in Mosspar	8	8.13	3.18	0.006	4.15	3.99	0.009
	14	6.12	2.12	0.006	3.26	2.06	0.005
PIBSA UREA in Mosspar	8	6.58	3.10	0.007	3.68	2.80	0.008
	14	4.60	1.66	0.01	2.48	1.55	0.01
PIBSA MEA/SMO	8	6.20	2.90	0.009	3.38	2.65	0.007
	14	4.52	1.86	0.007	2.00	2.02	0.02

Table 4.5: Summary of the characterisation of critical droplet diameter (OD = 4 mm)

Surfactant Type	Surfactant Con. (%)	$D_{critical}$	θ_D	Error	$\omega_{critical}$	θ_ω	Error
PIBSA MEA in Mosspar	8	10.95	5.84	0.009	6.79	5.31	0.009
	14	8.90	3.99	0.01	5.24	4.58	0.007
PIBSA IMIDE in Mosspar	8	10.03	5.77	0.005	6.00	4.95	0.006
	14	7.93	3.89	0.01	4.35	3.29	0.007
PIBSA UREA in Mosspar	8	9.64	3.77	0.004	4.95	4.62	0.007
	14	6.49	2.90	0.01	3.58	2.35	0.01
PIBSA MEA/SMO	8	9.47	3.47	0.008	4.68	3.87	0.008
	14	6.35	2.78	0.02	3.52	2.15	0.01

It is also worth mentioning some other experimental studies conducted in order to investigate the influence of high shearing resulting from the conditions of the manufacturing process on the stability of an emulsion (see Section 2.5 of Chapter 2: Theory and Literature Review.

In some case, coalescence took place where its behavior of approaching emulsion droplets was controlled by the dynamics of the film between their surfaces (Yan *et al.*, 2006). Many results from different studies indicated that the film drainage rate was mainly controlled by the interfacial tension σ, the viscosity ratio between the dispersed and continuous phases λ and external driving force F (Yiantsios & Davis, 1991; Saboni *et al.*, 1995; Rother *et al.*, 1997; Hu *et al.*, 2000). Although Zhou *et al.* (2008) observed that the coalescence behaviour of two droplets in simple shear flow strongly depends on the capillary number, which is the ratio between viscous forces and interfacial forces that characterises the droplet deformation, coalescence only occurred at a Ca that was lower than the critical value, Ca_c. Besides the above-mentioned coalescence factors, other authors stressed the geometry-related parameters which were also important in predicting the behaviour of emulsion droplets with regard to coalescence (Yan *et al.*, 2006), particularly in the experimental membrane studies (Cumming *et al.*, 2000; Park *et al.*, 2001; Hong *et al.*, 2003). Yan *et al.* (2006), however, pointed out the coalescence behaviour of emulsion droplets in porous media where coalescence upon collision of droplets depends on the interplay between two forces, hydrodynamic forces and intermolecular forces (disjoining pressure). They explained that, if the total interaction is very repulsive, the droplets can rebound; if the intermolecular repulsive forces can hold the film at equilibrium separation, the droplets might flocculate; and if the total interaction was attractive, the film will become thinner and finally rupture, i.e., the droplets will coalesce.

In others, crystallisation occurred, particularly polymorphic crystallisation being determined by the rate of nucleation, which, in turn, is governed by thermodynamic and kinetic factors (Sato, 2001). Such nucleation might be induced under large kinetic factors, e.g., supercooling or super saturation, where the Ostwald step rule or "law" predicts the phase change that occurred step-by-step by way of successively more stable phases (Mutaftschiev, 1993). For most of the time this law was broken when the more stable crystal forms were nucleated under application of external influences (pressure, temperature fluctuation, ultrasonic stimulation, template, seeding) (Sato, 2001). Although the shearing flow process induces crystallisation (Ziegleder, 1985; Narine & Marangoni, 1999; Mazzanti *et al.*, 2004), most of the related experiments were conducted on food and/or pharmaceutical emulsion

products. Nevertheless, it was argued that the initiation of crystals was due to the probability of interaction of the small oil molecules, which was enhanced by the flow (Kumaraswamy, 2005). Vanapalli *et al.* (2002) reported that the oils in food emulsions consist of mixtures of triacyl glycerol molecules which were crucially less stable to freeze-thaw than the alkane systems. From this, one could expect high affinity to shear-induced crystallisation in a system consisting mainly of alkane compounds in the oil phase.

Contrary to the crystallisation mechanism in emulsion systems, the shear-induced crystallisation in melt polymers was assumed to originate from the alignment of polymer coils which, in turn, develop due to shear or strain (Zhang *et al,* 2008; Varga & Karger-Kocsis, 1996; Kumaraswamy, 2005). During the shearing process, the polymer coil conformations were significantly distorted from their equilibrium isotropic state, and crystallised directly from this distorted state (Elmoumni *et al.*, 2003). According to certain model (Kawakami *et al.*, 2004, 2006) three stages of the crystallisation mechanism are described during the shearing of melt polymers: i) molecular orientation occurring due to strong molecular interaction – "orientation" stage; ii) nucleus starting to appear as a result of molecular orientation – "nucleation" stage; and iii) crystallisation developing through a growth process – "growth" stage. Kumaraswamy (2005) reported that the large size of a polymer molecule and chain-chain entanglements resulted in slow time scales for relaxation relative to small molecules. Therefore the overall crystallisation rate was enhanced when a polymer crystallised from an incompletely relaxed melt. On one hand, Wolkowicz (1978) explained that the nucleation density was enhanced at low shear rates and a large number of crystals were formed. On the other hand, different crystal morphological structures, the so-called shish-kebab structures, were formed at higher shear rates (Coppola *et al.*, 2001; Somani *et al.*, 2005a, b; Vleeshouwers & Meijer, 1996; White & Bassett, 1997; Keller & Kolnaar, 1997; Bashir, Odell & Keller, 1984; Monks, White & Bassett, 1996).

An additional destabilisation mechanism that was also reported was partial coalescence (Van Boekel & Walstra, 1981a-b; Jeelani & Hartland, 1993; Fisher *et al.*, 2007), where shear action was cited to be one of the susceptibility factors (Boode *et al.*, 1991, 1993), thereby their presence (shear forces) increases the rate of collision between droplets and therefore leads to greater tendency towards partial coalescence. Although Van Boekel and Walstra (1981b) and Vanapalli *et al.* (2001) observed that the rate of heterogeneous interdroplet nucleation can be described as a product of collision rate and collision efficiency.

In the case of phase inversion, McClements (1999:229-233) had reported that, high shear action being a necessity for the occurrence of phase inversion, the higher the shearing force, the more likely phase inversion is to occur. Or, indeed, that, prior to subjecting the emulsion to shearing in order to invert it from one phase to another, some alteration in composition or environmental conditions of the emulsion (such as dispersed-phase volume fraction, emulsifier type, emulsifier concentration, temperature) had to be reached (Shinoda & Friberg, 1986; Dickinson, 1992; and Campbell, Norton & Morley, 1996). Thus, only certain types of emulsion are capable of undergoing phase inversion, and its physiochemical basis was found to be complex, involving aspects of flocculation, coalescence, partial coalescence, and emulsion formation (McClements, 1999:229-230; Boode *et al.*, 1993).

However, shear-induced instability was not observed in this work during this process of shearing. Nevertheless, the stability of such emulsion systems (highly concentrated w/o emulsion) where the dispersed phase consists of supercooled aqueous solutions of inorganic salts usually was threatened by the crystallisation phenomenon. Masalova *et al.* (2006) investigated the effect of aging on the rheological properties and physical structure of highly concentrated w/o emulsions and found that crystallisation took place within the emulsion droplets during aging where the kinetics of this process were satisfied by the Johnson-Mehl-Avrami-Kolmogorov (JMAK) equation:

$$X = 1 - e^{-(t/\theta)^n}, \qquad \textbf{(Equation 4.5)}$$

where X is the degree of crystallinity, θ is the characteristic time, n an empirical factor.

The results obtained in this experiment study so far has shown that the high shear applied to the emulsions led to the rupture of large droplets into smaller ones. A very small number of publications have reported on the effect of high shearing on highly concentrated w/o emulsion properties. The following sections outline the energy characterisation where, again, the effect of surfactant concentration, surfactant type and orifice diameter are estimated.

4.2.3 ENERGY DENSITY CHARACTERISATION

An interesting engineering illustration based on basic principles of physics where energy density (or energy per kilogram) was derived and found to be the ratio of applied pressure to the density of the material.

It is well known from the theory of physics that Work is defined as force times distance (Equation 4.6) where the work is a measure of the energy expended in applying a force to move an object. While work is done on a body, there is a transfer of energy to the body, and so work can be said to be energy in transit (Boxer, 1987; Balian, 2007 and an internet online definition: The physics classroom. [1996-2009] *Definition and mathematics of work*, http://www.physicsclassroom.com/Class/energy/U5L1a.ht).

$$Work = Force \times Distance = Energy \qquad \textbf{(Equation 4.6)}$$

In this study, it will be described as the pressure acting upon the piston shaft to cause the flow of emulsion material through the small orifice (see Chapter 3: Apparatus and experimental procedure). Therefore the work (or energy in transit) done by the piston shaft on the emulsion material during the pumping process can be expressed as follows:

$$Energy = Force \times Distance$$

$$\Rightarrow Energy = \frac{Force}{Area} \times Area \times Distance \qquad \textbf{(Equation 4.6.1)}$$

$$\Rightarrow Energy = Pressure \times Volume \qquad \textbf{(Equation 4.6.2)}$$

$$\Rightarrow \frac{Energy}{Mass} = \frac{Pressure \times Volume}{Mass} = \frac{Pressure}{Density} = \frac{P}{\rho} \qquad \textbf{(Equation 4.6.3)}$$

This means that every time a sample of emulsion is pumped, P/ρ joule per kilogram energy is applied on the sample. So, if the pumping procedure is applied N times, the total energy density would be:

$$E_\rho = \frac{NP}{\rho}, \qquad \textbf{(Equation 4.7)}$$

where P is the pressure applied on the piston shaft creating the motion of the emulsion, ρ is the density of the emulsion to be pumped and N is the number of pumpings that the material experiences during the pumping process.

Figures 4.9 to 4.11 illustrate the value of this argument, through the dependencies of the Sauter average diameter of the emulsion sample against energy density shown for samples with different surfactant concentrations and surfactant types (Appendix D presents the rest of the fitting). It is clear to see that the experimental data was successfully fitted using log-scale by the following power-law equation proposed and used previously by other authors (Walstra, 1983; Schubert & Engel, 2004; Romero *et al.*, 2008):

$$D_{32} = CE_{\rho}^{\ b} \qquad \textbf{(Equation 4. 8)}$$

where the constant C and b depend on the type of surfactant, surfactant concentration and orifice geometry.

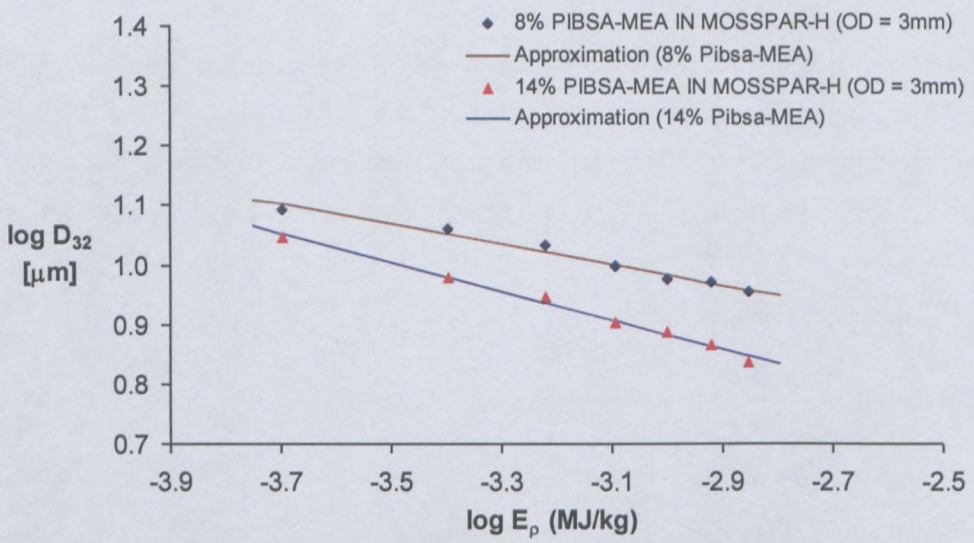

Figure 4.9: Dependencies of the Sauter average diameter of droplets against energy density: effect of surfactant concentration (OD = 3 mm)

First, the values of the coefficient C and exponent b are used to estimate the effect of surfactant concentration (see Table 4.6, below, where an overall summary is presented): the coefficient C increased with the decrease of surfactant concentration. On the other hand, the inverse trend was found where the exponent b decreased with the decrease of surfactant concentration. Therefore these results were in line with those reported in the previous section on the characterisation of critical droplet diameter where it was detailed that the surfactant concentration is one of the factors that influence the effectiveness of emulsifiers and/or surfactants. Thus the greater the concentration of emulsifiers (surfactants) accumulated at the surface of the droplets, the easier the droplets disrupt, or, in other words,

the less energy is required for the reduction of droplet size (Walstra, 1983:57-127; McClements, 1999:161-184).

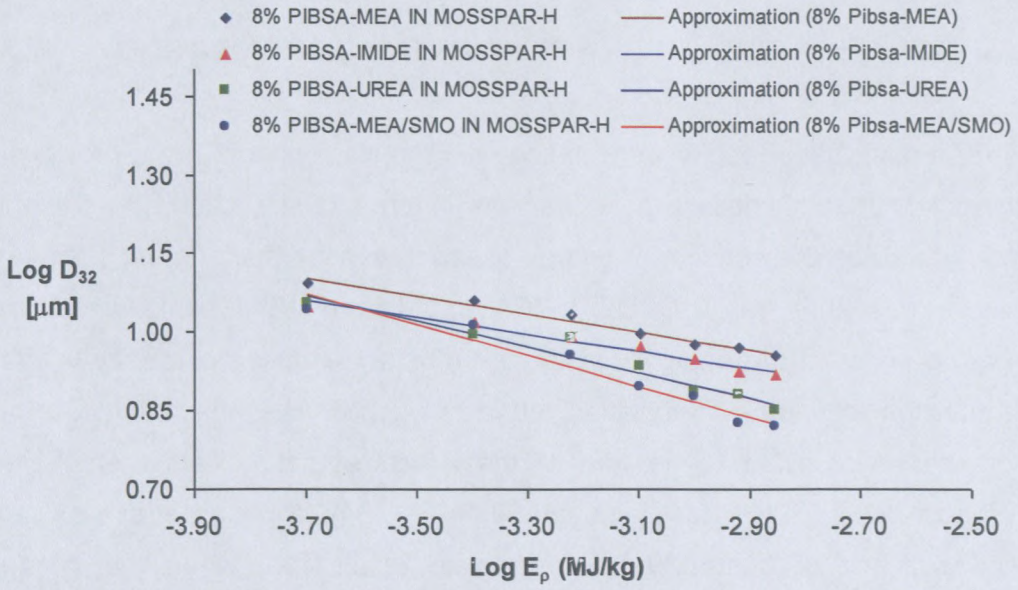

Figure 4.10: Dependencies of the Sauter average diameter of droplets against energy density – effect of surfactant types (OD = 3 mm)

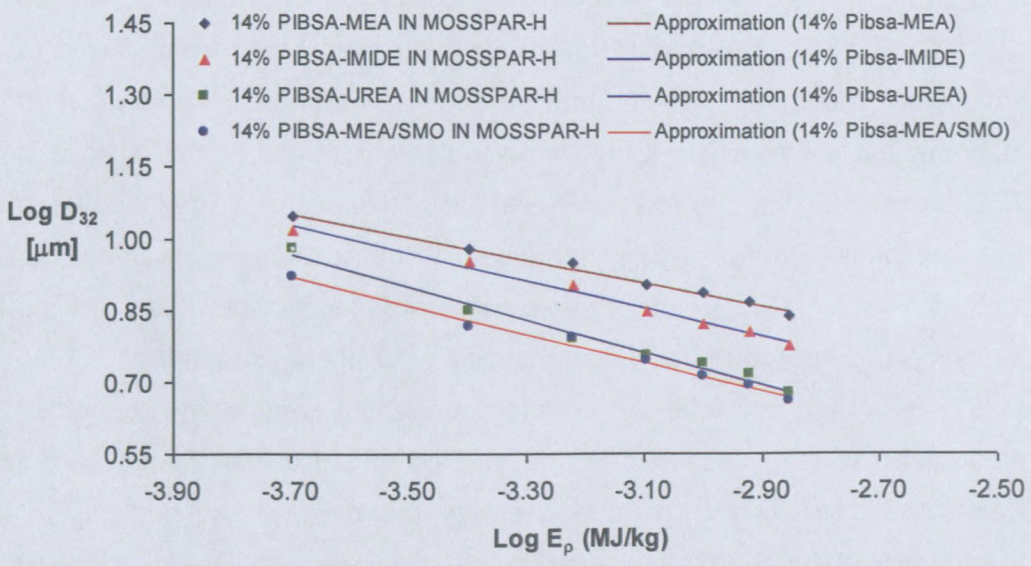

Figure 4.11: Dependencies of the Sauter average diameter of droplets against energy density – effect of surfactant types (OD = 3 mm)

Secondly, the above tendency (lower C indicated higher efficient of droplet refinement) was also observed when it came to the effect of surfactant type. Thus, the following trend was observed for surfactant type:

PIBSA-MEA > PIBSA-IMIDE > PIBSA-UREA > PIBSA-MEA/SMO

Here, again, these results were in line with results reported in the previous section on the characterisation of critical droplet diameter in terms of surfactant type. Thus this observation clearly outlines the concept of energy of adsorption for the different surfactant head groups used in this study (MEA, IMIDE, UREA and Mixture MEA/SMO). This also means that, by keeping constant the energy density, the droplet disruption efficiency differed from sample formulation to sample formulation (surfactant type). The adsorption rate of emulsifiers or surfactant was cited to be one of main factors that influence emulsifier effectiveness (Walstra, 1983:57-127; McClements, 1999:161-184). Windhab *et al.* (2005) also mentioned the efficiency of interfacial coverage with emulsifiers, when the interfacial area was decreased by drop deformation and break-up during processing conditions where they found that the efficiency of the latter strongly depends on the adsorption kinetics of emulsifier and/or surfactant molecules at the interface. Although, many authors of research articles on food emulsion (e.g. Walstra & Oortwijn, 1982; Dickinson, Euston & Woskett, 1990; Robin *et al.*, 1992; Darling & Birkett, 1987) have discussed on the major role of two classes of molecules within emulsifiers and/or surfactants in the adsorption rate: amphiphilic macromolecule emulsifiers and low molecular weight emulsifiers (such as monoglycerides). They advanced that the low molecular weight emulsifiers reduced the interfacial tension between phases more rapidly than would the macromolecules alone; thus leading to the formation of smaller sized droplets. This was associated with the greater energy of adsorption compared to the macromolecule emulsifiers (Robin *et al.*, 1992). Dickinson *et al.* (1990) reported on food oil-in-water emulsions where the proteins (macromolecule emulsifiers) were dislodged from the surface of the dispersed particles by low molecular weight emulsifiers, which was due to their greater energy of adsorption. But at the same time they observed that the proteins were better stabilisers compared to the low molecular weight emulsifiers due to the tendency of the emulsion material towards instability after the dislodgement of proteins from the surface of the droplets.

Finally, the effect of orifice diameter can be illustrated from the results tabulated below. It can be seen that the efficiency of droplet disruption was greater (lower value of C) when the orifice diameter was smaller. This was associated with the high shear results from the higher

friction generated between the edge of the orifice and the flowing emulsion materials during the pumping process; it increased with the decreasing of orifice diameter.

Table 4.6: Coefficient C and b values for all emulsion formulations used in this study

Orifice Diameter	Surfactant Concentration	Emulsion Materials	C	b	Average Error, E
3 mm	8%	PIBSA MEA	2.97	0.17	0.003
		PIBSA IMIDE	2.94	0.16	0.003
		PIBSA UREA	1.51	0.24	0.003
		PIBSA MEA/SMO	1.03	0.29	0.003
	14%	PIBSA MEA	1.45	0.24	0.003
		PIBSA IMIDE	0.91	0.29	0.004
		PIBSA UREA	0.67	0.30	0.005
		PIBSA MEA/SMO	0.49	0.34	0.003
4 mm	8%	PIBSA MEA	5.70	0.10	0.003
		PIBSA IMIDE	5.21	0.11	0.003
		PIBSA UREA	4.64	0.12	0.003
		PIBSA MEA/SMO	2.79	0.19	0.002
	14%	PIBSA MEA	5.59	0.10	0.003
		PIBSA IMIDE	3.25	0.15	0.004
		PIBSA UREA	2.50	0.18	0.004
		PIBSA MEA/SMO	1.60	0.23	0.004

4.2.4 SUMMARY

As a summary to this part of the results and discussion, the first objective of this study was achieved by producing highly concentrated water-in-oil emulsions emulsified with organic derivatives of the PIBSA family (MEA, UREA, IMIDE and MEA/SMO) at different concentrations. The droplet size distribution for all these fresh emulsions was approximately similar, wider and of Gaussian type where the surface area mean droplet size (D_{32}) found to be approximately 13 μm (referred to in this study as the starting point of refinement).

Neither crystallisation nor other destabilisation phenomena such as coalescence, partial coalescence or phase inversion occurred during the shearing process of these emulsions, regardless their formulation content. The pumping process subjected the fresh emulsion materials to high shearing action that led to a reduction in droplet size, which was confirmed by the qualitative analysis under high magnification of the optical microscope. Following this, the size distribution of these sheared materials was fitted again by the Gauss equation and showed a narrower distribution with increased pumping. Thus, two models were proposed and used to fit the evolution of the volume median diameter and the width of the Droplet Size Distribution as a function of the number of pumpings. The models showed an exponential decrease of the average droplet size and the width of the distribution as the number of pumpings increased and approached a constant value here referred to as the critical width ($\omega_{critical}$) and critical diameter ($D_{crit.}$). Using these models, some characteristic pumping parameters of the shearing process were obtained and their values clearly estimated the effect of surfactant concentration, surfactant type and orifice diameter.

Meanwhile, an interesting engineering illustration of the work done on the material during the pumping process was derived in term of energy density (the ratio of applied pressure to the density of the material). Thus a power law equation illustrating the dependencies of the Sauter average diameter of the emulsion sample against energy density estimated, through its coefficients, the effect of surfactant type and surfactant concentration during the shearing process.

It is well known that surfactant concentration is one of the factors that influence the effectiveness of emulsifiers and/or surfactants. During the shearing process, lower surfactant concentrations possessed higher characteristic pumping parameters (θ_D and θ_ω) and a lower coefficient C from energy dependence of D_{32}, compared to higher concentration. Thus, the greater the concentration of emulsifiers (surfactants) accumulated at the surface of the

droplets, the easier the droplets disrupted or, in other words, the less energy was required for the reduction of droplets.

For the effect of surfactant type, the droplet disruption efficiency differed from one type of surfactant to another type. Therefore the adsorption rate was assumed to be the driving force in such behaviour, which, in turn, depended on the surfactant's molecular weight. Thus the following trend was observed, with PIBSA-MEA/SMO possessing the highest refinement efficiency:

PIBSA-MEA > PIBSA-IMIDE > PIBSA-UREA > PIBSA-MEA/SMO

Besides the two factors above, the geometry of the orifice also influenced the refinement efficiency of droplets, with the smaller diameter providing higher droplet reduction. This is explained by the fact that, during pumping, high friction was generated between the orifice edge and the flowing emulsion materials. Thus, with the orifice edge shrinking, the material was exposed to higher shearing, which led to greater droplet disruption.

4.3 PART B – RHEOLOGICAL PROPERTIES

This section outlines the rheological properties of the emulsion samples used in this study, with the factors that influence them within the experimental window, such as surfactant type and concentration and droplet size as shearing action takes place, are discussed in greater detail.

The rheological measurements were carried out with the use of a dynamic rotational MCR 300 rheometer (see Chapter 3 under the instrumentation section 3.5). The geometry of the measuring unit was "plate-and-plate" with a sandblasted surface (the plate diameter was 50 mm) and the gap measurement between the two plates was 1 mm. All rheological measurements were conducted at 30°C.

The investigation of the rheological characterisation including the following:

- An Amplitude Sweep Curve in order to define the viscoelastic properties of the materials where the setting of the measurement parameters was done by keeping a constant frequency of 1 HZ and strain was selected as the set variable and kept between 0.1 to 200%.

- The flow curve measurement was performed at the downward sweeping shear rate mode; the shear rate was selected as the set variable and kept between 200 to 1 x 10^{-6} 1/s.

4.3.1 VISCOELASTIC PROPERTIES

Figures 4.12 and 4.13, below, illustrate the evolution of the storage modulus during the pumping process (See Appendix E for the remaining sample formulations).

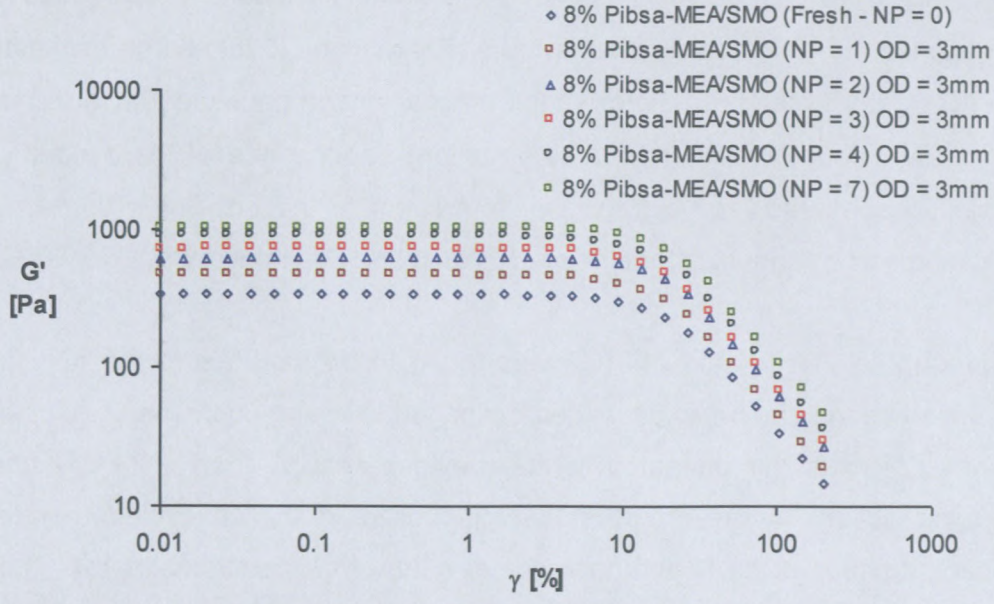

Figure 4.12: Amplitude sweep for sheared emulsion sample (8% PIBSA-MEA/SMO)

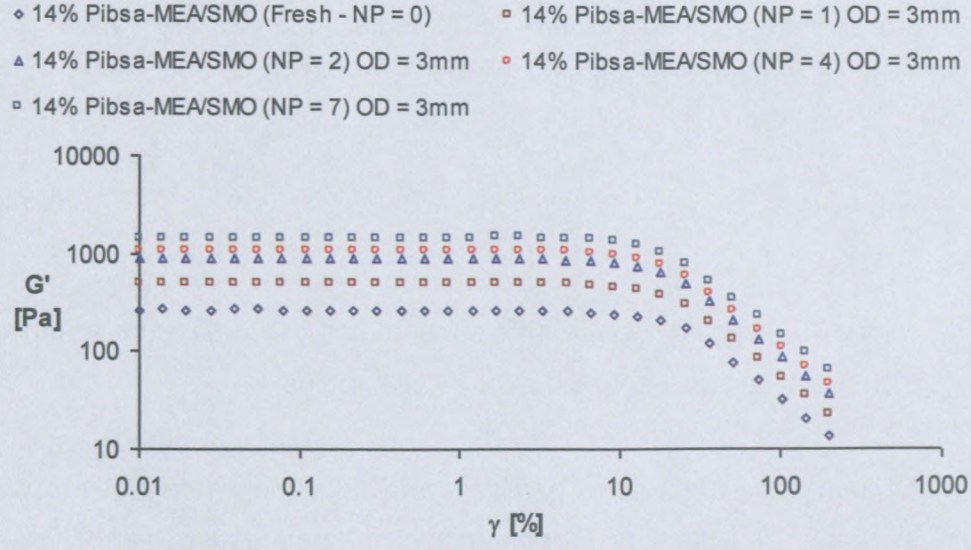

Figure 4.13: Amplitude sweep for sheared emulsion sample (14% PIBSA-MEA/SMO)

Figures 4.12 and 4.13 show a constantly high plateau region for all sheared samples with the strain increased; this indicates the linear viscoelastic range: the elastic domain. According to some authors and studies (Thomas, 2002; Kharatiyan, 2005), this plateau region that results with increased strain can be explained by means of the samples' structure, which was undisturbed by the shear at this level of strain. However, Masalova and Malkin (2007a), in

their publication dedicated to the peculiarities of rheological properties and flow, demonstrated "the rolling mechanism of larger droplets over smaller ones" to explain this constant plateau region when the strain increased. On the other hand, G' decreased as strain increased further, indicating that the sample's elasticity decreased and emulsions approached more viscous fluid behaviours (Kharatiyan, 2005) and predominated when $\gamma_{limiting}$ [7 – 10%] was exceeded. Therefore the mechanical properties of these samples were linear up to $\gamma_{limiting}$, above which (higher deformation) dependence of the dynamic moduli on the amplitude appeared, and a transition from linear to the non-linear domain was observed, indicating some serious distortions of droplet shape (Masalova & Malkin, 2007a).

Although, the elastic modulus (G') was found to be sensitive to the pumping condition; it increased as the sample experienced prolonged shearing (increase of number of pumpings). However, it was demonstrated in the previous section (Part A of this chapter) that the shearing action on the emulsion samples used in this study led to refinement of the dispersed phase droplets and decrease of width of their distribution, too. Thus, the possible reason for this increase in elastic modulus upon reduction of droplet size could be due to:

- Firstly, the internal pressure (Laplace pressure) of droplets where this increases as the size of the droplet decreases (McClements, 1999:127,159; Kharatiyan, 2005) – See the *Laplace Equation* (Equation 4.9) (Atkins, 1994):

$$\Delta P_L = \frac{2\sigma}{r}, \qquad \textbf{(Equation 4.9)}$$

  where ΔP_L is the pressure difference across the surface of an emulsion droplet σ is the interfacial tension, and r is the droplet radius.

- Secondly, the width of the particle size distribution where it was found that it decreased as droplet size decreased during pumping (shearing process). This latter has also been observed previously, by Barnes (1994).

4.3.2 FLOW PROPERTIES

Figures 4.14 and 4.16, below, illustrate the flow curve of the fresh and sheared samples where they exhibit strong non-Newtonian behaviour which was characterised by shear thinning and elastic effect and the existence of a yielding behaviour: yield-pseudoplastic behaviour. Kharatiyan (2005) stressed the closely packed configuration of the droplets and the profound hydrodynamic interaction between neighbouring droplets within the highly concentrated emulsion system as the source of such behaviour. These flow curves (Figures 4.14 to 4.16) indeed displayed the inflection point which was considered to be the bridge linking the two suggested mechanisms of flow of emulsions at low and high shear rates (Masalova & Malkin, 2007a). Thus, this mechanism was understood from the analysis of the photographic observations, where it was clearly seen that the movement of an emulsion at low shear rate presented the rolling of large droplets over smaller ones without any noticeable distortions of their shape; meanwhile, at high shear rates, serious distortions of the droplet shape took place (Masalova & Malkin, 2007a). The authors stressed that it was necessary to bear mind that during such movement of droplets, droplets do not mount over each other with an increase in the shear rate of a droplet (and therefore the effect of Reynolds' dilatancy does not appear), but slide between other droplets.

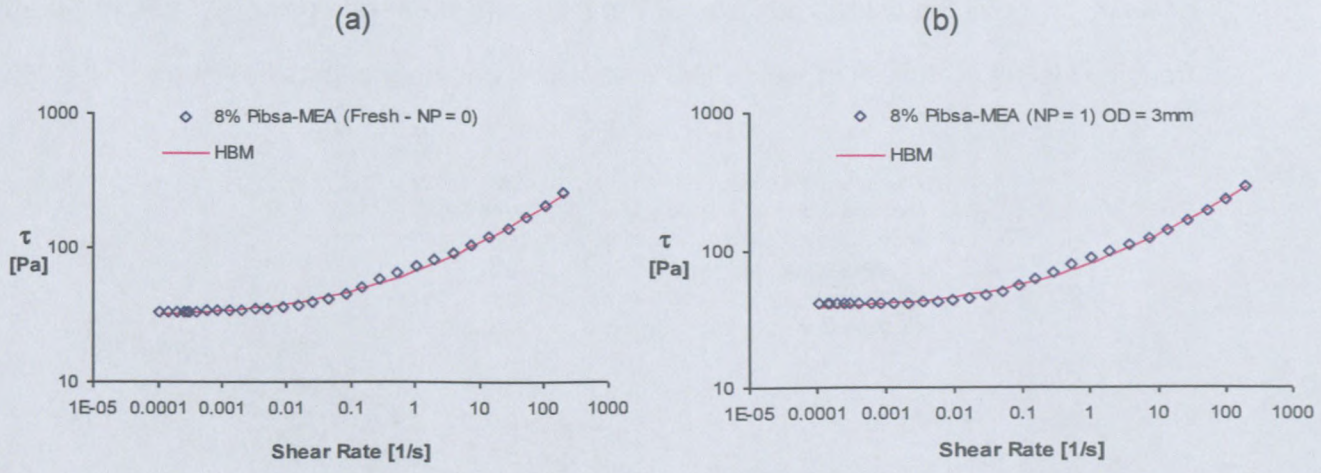

Figure 4.14: Approximation of flow curve by HBM – (a) fresh sample, (b) sheared sample

The appearance of yield stress, τ_y (parameter related to the strength of inter-particular interactions in the physical structure of a multi-phase system), where the downward sweeping shear rate mode was chosen as the measuring mode, was previously mentioned in the publications devoted to super-concentrated emulsions (Masalova *et al.*, 2003, 2005) which demonstrated the rheopectic behaviour in shear flow of such types of emulsion

material. The flow curves (Figures 4.14 and 4.15) were approximated using the Herschel-Bulkley model (HBM), whereas this was used to determine the yield stress of the samples by extrapolation of the flow curve to the zero shear rate. It is defined as follows:

$$\tau = \tau_y + K\dot{\gamma}^n, \qquad \textbf{(Equation 4.10)}$$

where $\dot{\gamma}$ is the shear rate (s^{-1}), τ is the shear stress (Pa), τ_y is the yield stress (Pa), n is the flow behaviour index and K is the consistency index.

And the calculation of average error, E, used in the approximation was determined by the following equation:

$$E = \frac{1}{N}\sqrt{\sum_{n=1}^{N}\left(\frac{\tau_{\exp,n} - \tau_{cal,n}}{\tau_{\exp,n}}\right)^2}, \qquad \textbf{(Equation 4.11)}$$

where $\tau_{cal,n}(\dot{\gamma})$ is the experimental value of τ at several points, $\dot{\gamma}_n$, along the shear rate scale $\tau_{cal,n}(\dot{\gamma})$, is the calculated value of τ at the same shear rate point, $\dot{\gamma}_n$, which is derived from the Herschel-Bulkley model (HBM), and N is the number of measurements.

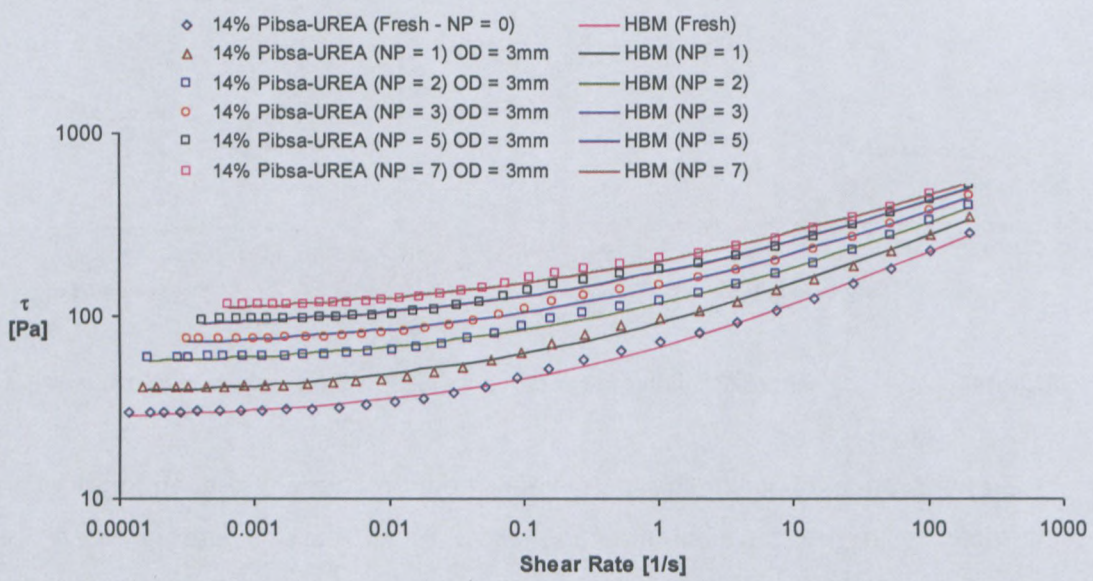

Figure 4.15: Approximation of flow curves of sheared samples by means of the HBM

Figures 4.14 and 4.15, above, show the "Good" approximation of the flow curves of the sheared emulsion using the Herschel-Bulkley model (HBM). It is clear from these figures that the behaviour of the flow (yield pseudoplastic) was not affected by the shearing process, but that, with prolonged shearing, the flow curves shifted to the higher shear stresses over the whole range of shear rates (see Appendix F for the rest of the sample formulations). Thus the yield stress was also sensitive to the pumping condition, therefore to the structure of the emulsion. Here, again, this observation can be explained by the reduction of droplet size when the emulsion samples were exposed to high shearing during pumping (see Part A, above).

Table 4.7: Summary of fitting parameters for the Herschel-Bulkley equation – Equation 4.10

8% PIBSA-MEA (OD = 3 mm)				
NP	**τ_y**	**K**	**N**	**E_{ave}, Error**
0	31	38	0.34	0.007
1	37	44	0.33	0.007
2	40	47	0.33	0.008
3	47	52	0.32	0.007
4	50	57	0.32	0.008
5	59	61	0.32	0.007
6	59	62	0.31	0.007
7	63	63	0.31	0.007

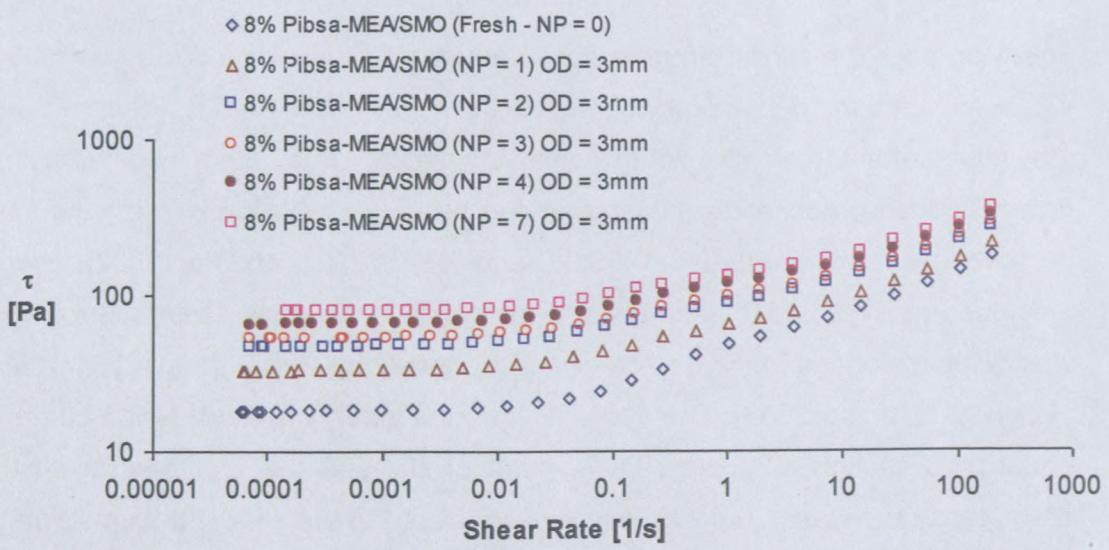

Figure 4.16: Effect of pumping conditions on flow behaviour (8% PIBSA-MEA/SMO)

4.3.3 DEPENDENCE OF ELASTIC PROPERTIES ON DROPLET SIZE

The following figure, Figure 4.17, illustrates the dependency of elastic modulus G'_0 on the droplet size. The experimental data for the elastic modulus was successfully approximated by the following empirical power-law equation:

$$G = K_G D^{-n}, \qquad \textbf{(Equation 4.12)}$$

where K_G is a measure of elasticity (higher K_G means higher elasticity). When the exponent n = 1, it means that the rheological properties follow Princen's model (Princen & Kiss, 1986a).

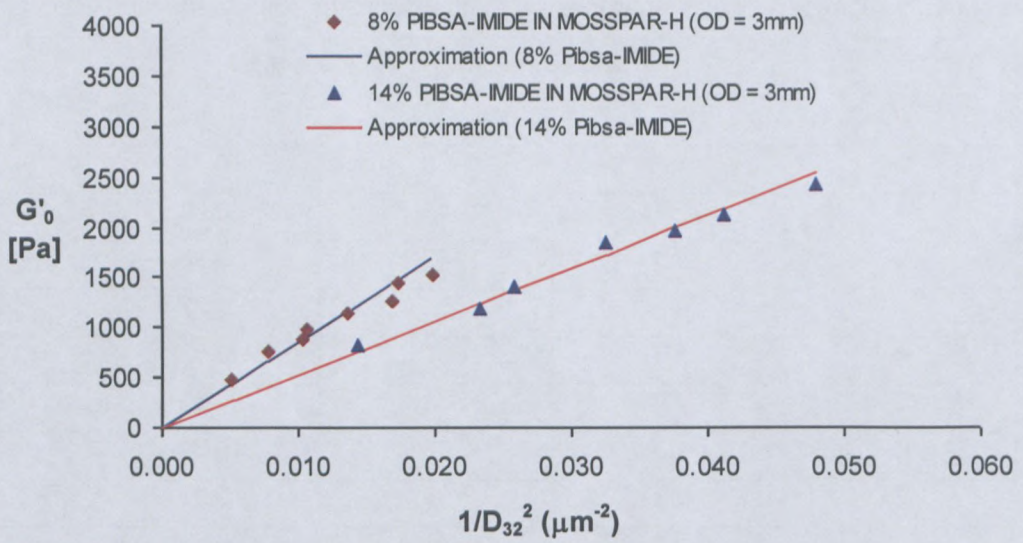

Figure 4.17: Dependency of elasticity on droplet size.

Following approximation using the above equations, it was found (as summarised in Table 4.8, below) that the dependency of the elastic modulus was on D^{-2}, with $n \approx 2$, instead of D^{-1}. This means that the elasticity of this emulsion material was determined by the surface of the droplets. Such an observation was found to be in contradiction with the theoretical models proposed by Princen and Kiss (1986a), Babak *et al.* (2001) and Pal (2002), where the elastic modulus was expected to depend on reciprocal diameter. Nevertheless, such an observation was quite analogous to the one observed previously by Malkin *et al.* (2004a); Masalova and Malkin (2007a and 2008), The publication by the latter was to verify the correctness of this equation (Equation 4.2) using D_{32} instead of D_{50} and the argument given there for the discrepancy in the experimental results was related to the type of the emulsion used (highly concentrated emulsion), as well to differences in the averaging procedure for polydispersed samples, which was indeed similar than the samples for this current study (see Appendix G

for the rest of the fittings). However, it is worth mentioning the Princen theory of elasticity and fluidity of high concentrations (see Equation 4.13) which adequately described the concentration dependence of the elastic modulus in several studies, particularly those similar in emulsion type and composition to these studies (Masalova & Malkin, 2007a, 2007b, 2008) as:

$$G = A\frac{\Gamma}{R_{SV}}\varphi^{1/3}\left(\varphi - \varphi^{*}\right), \qquad \textbf{(Equation 4.13)}$$

where R_{SV} is the mean (by the volume-to-surface ratio) characteristic size of dispersed droplets and A is the coefficient, φ^{*} represents the "limiting" degree of the filling of system volume with dispersed particles, φ is the volume concentration of dispersed particles (irrespective of their sizes), G is elastic modulus and Γ is the surface tension.

The numerical value of the coefficient (K_G) is of the order 10^4 to 10^5 (Pa*μm^2) (Malkin *et al.*, 2004a) and its variation from sample to sample holds and explains some effects connected with the structural rearrangement as one's changing emulsion composition with regard to surfactant concentration and surfactant type.

It was also so evident that the linear dependence of G_0 vs. D^{-2} passing through the zero point was obtained for all formulation samples under study, with the unusual effect of a decrease of elasticity with the increase of surfactant concentration (14% concentration yielded lower elasticity compared to 8% concentration). Table 4.8 clearly illustrates the effect of surfactant type and surfactant concentration on the elasticity properties of the emulsion. The following trends were observed when either diameter (3 mm or 4 mm) of the orifice was used to shear the samples:

- Emulsion material with higher surfactant concentration showed lower elasticity, while interfacial tension did not change.

- For effect of surfactant type, the following trend was observed:

  PIBSA-MEA > PIBSA-IMIDE > PIBSA-UREA > PIBSA-MEA/SMO

Table 4. 8: Fitting parameter for dependence of elasticity on drop size (Equation 4.12)

Orifice Diameter	Surfactant Concentration	Emulsion Materials	K_G (Pa*μm^n)	n	Average Error, E
3 mm	8%	PIBSA MEA	8.90×10^4	2	0.002
		PIBSA IMIDE	8.51×10^4	2	0.003
		PIBSA UREA	8.03×10^4	2	0.02
		PIBSA MEA/SMO	5.41×10^4	2	0.05
	14%	PIBSA MEA	6.95×10^4	2	0.04
		PIBSA IMIDE	6.43×10^4	2	0.05
		PIBSA UREA	5.45×10^4	2	0.04
		PIBSA MEA/SMO	3.82×10^4	2	0.07
4 mm	8%	PIBSA MEA	9.22×10^4	2	0.02
		PIBSA IMIDE	9.30×10^4	2	0.01
		PIBSA UREA	8.06×10^4	2	0.01
		PIBSA MEA/SMO	6.28×10^4	2	0.02
	14%	PIBSA MEA	7.37×10^4	2	0.02
		PIBSA IMIDE	7.19×10^4	2	0.03
		PIBSA UREA	6.49×10^4	2	0.04
		PIBSA MEA/SMO	4.45×10^4	2	0.04

Therefore, the observed effect of surfactant concentration on elastic properties of emulsions revealed that where the higher surfactant concentration emulsion possessed low elasticity compare to the lower, it could be due to the following:

Previous experiments on highly concentrated water-in-oil emulsions (Reynolds *et al.*, 2000, 2001; Zank *et al.*, 2006) consisting of 90% by volume supersaturated ammonium nitrate solution as the dispersed phase and stabilised by PIBSA-based surfactants revealed that the micron-scale aqueous droplets within the emulsion were stabilised by a monolayer of surfactant at the aqueous-oil interface; whereas the majority of surfactants were in the form of reverse micelles in the oil phase. The tail group of PIBSA-based surfactants was highly branched polymers (see Chapter 3 under Materials) and provided stability to the emulsion by steric forces, whereas an addition of the Van der Waals interaction dominated as the droplets in highly concentrated systems were compressed (Rudnick, 2003). However, an electrostatic interaction between the head groups in the presence of salt could also have influenced the packing of acyl chains by affecting the spacing and the corresponding Van der Waals interactions between the chains (Papke & Robinson, 1994). Thus, a repulsive

interaction between interfaces and reverse micelles in the oil phase was expected to take place as a result of a failure of the closer manner of packing of the carbon chains which repulse each other. Therefore the increasing concentration of reverse micelles (resulting from the increase of the surfactant concentration) strengthened the interaction between them and led to a decrease in rheological properties during applied stress.

On the other hand, the high rheological properties of emulsions stabilised by IMIDE surfactants might be explained by the size of micelles, which was described to be one of the factors influencing rheology (McClements, 1999:83-125). An interesting experiment (Reynolds *et al.*, 2001) performed on emulsions stabilised by PIBSA-MEA compared the size of micelles at the presence and absence of ammonium nitrate salt respectively. It was found that, in the presence of salt, the micelles were getting smaller. Meanwhile one could expect that the bigger micelles increased rheology by resisting/opposing the rolling mechanism of droplet movement. Thus, the determination of the volume of the head group of PIBSA surfactants (needs to be confirmed) might reveal the IMIDE head group to be bigger, which, in turn, might form bigger sized micelles, therefore affecting rheology by increasing its properties. Thus, this might illustrate the high rheological properties of emulsions stabilised by PIBSA-IMIDE.

4.3.4 ESTIMATION TO LIMITING STRAIN DEFORMATION

This section of the thesis presents the observation related to the stability of the emulsion in shearing concerns the yield stress, τ_y. This parameter characterises the limit of quasi-solid behaviour of an emulsion under applied stresses. After this threshold, an emulsion begins to flow, which becomes possible due to the rupture of its static structure. The value of τ_y should be correlated with elastic modules, and the ratio of these parameters:

$$\gamma^* = \frac{\tau_y}{G}, \qquad \textbf{(Equation 4. 14)}$$

This gives the limiting deformation characterising the transition from the solid-like state of an emulsion to its flow state. In Figure 4.18 all the experimental points for all recipe studied in this part of research project are collected. One can see that the points all lie inside a rather narrow band. The average value of γ^* is approximated to 0.07, and at any rate does not exceed 0.11.

This level of the γ^* values had been already met in previous publications (Masalova & Malkin, 2007a), where the threshold of the transition was estimated as approximately 0.1. So, it is so evidence that this value has real physical sense.

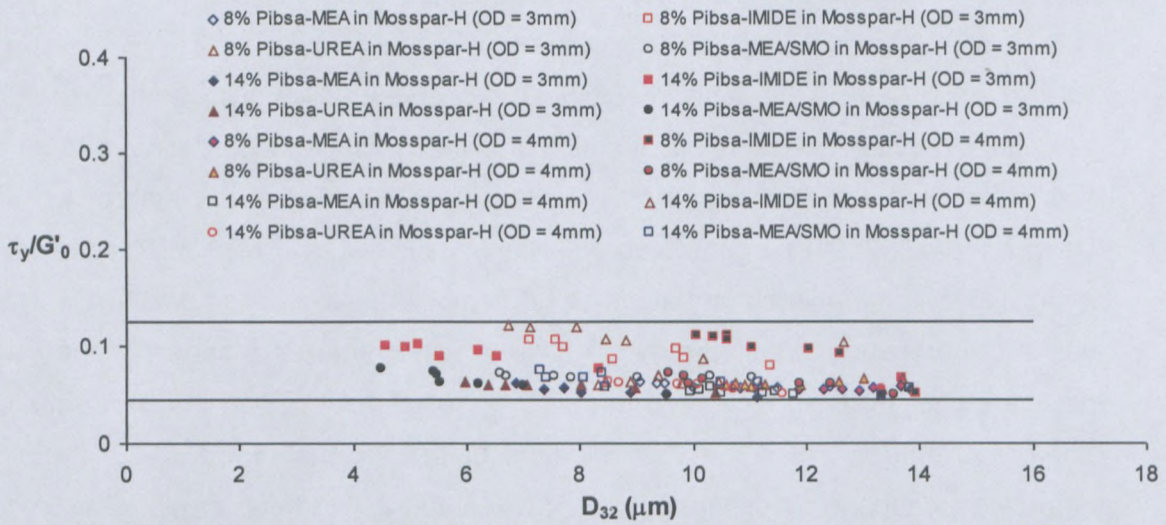

Figure 4.18: Estimation of limiting strain deformation and/or the transition point between the two mechanisms – "inflection point"

4.3.5 SUMMARY

The elastic modulus in the amplitude sweep can be summarised as constant over a wide range of strain deformations regardless of the formulation content of the fresh and sheared emulsions. This plateau zone might be treated as the elastic domain where the sample's structure was undisturbed by the shear at this level of strain and its particles were crowded and could not move freely. Some previous studies using similar types of emulsion and formulation revealed the peculiarities of rheological properties and flow where "the rolling mechanism of larger droplets over smaller ones" was proposed to explain this constant plateau region when the strain increased. Above a certain deformation (particularly between 7 and 10%) referred to as the limiting strain ($\gamma_{limiting}$), the sample's elasticity decreased and emulsions approached more viscous fluid behaviours in what is known as the non-linear domain, and indicating some serious distortions of droplet shape as strain increased further.

However, the elastic modulus (G') was found to be sensitive to the pumping condition: it increased with the number of pumpings. This sensitivity of elastic modulus might be related to the reduction of droplet size (indicating the Laplace pressure which increases as the size

of the droplet decreases) and the width of their distribution that narrows with prolonged shearing.

Highly concentrated emulsions used in this study behaved like non-Newtonian fluids, and have been characterised by shear thinning and elastic effect and the existence of yielding behaviour: It displayed an inflection point which was considered to be the bridge linking the two suggested mechanisms of flow of emulsions at low and high shear rates: the rolling mechanism of large droplets over smaller ones without any noticeable distortions of their shape, and the serious distortions of the droplet shape respectively. The Herschel-Bulkley model (HBM) was used to fit the flow curve of fresh and sheared samples from which the yield stress was determined. However, the behaviour of the flow (yield pseudoplastic) was not affected by the shearing process, but with prolonged shearing the flow curves shifted to the higher shear stresses over the whole range of shear rates. Thus the yield stress was also sensitive to the pumping condition; therefore the above argument on reduction of drop size and width of distribution supported such behaviour.

The elastic modulus was found to be dependent on square reciprocal droplet size (D^{-2}), instead of reciprocal diameter (D^{-1}), as predicted by the Princen theory. Such a contraction with regard to the Princen-Kiss theory has been reported previously in numerous experiments where such a discrepancy was related to the type of emulsion used (highly concentrated emulsions) as well to differences in the averaging procedure for polydispersed samples.

The decrease of elasticity with increased surfactant and its dependence on type of surfactant were explained by the possible interaction forces that exist between the monolayer surfactant at the aqueous-oil interface and the reverse micelles in the oil phase, as well as the size of micelles (dependent to the volume of the head group of PIBSA surfactants) respectively.

The ratio $(\tau_y/G)_{average}$ as function of D_{32} for all the sheared emulsion samples demonstrated the informative meaning of the transition from the solid-like state of an emulsion to its flow state. This value for all samples under investigation on average equalled 0.07.

4.4 PART C – THE EFFECT OF AMMONIUM NITRATE CONCENTRATION ON THE TRANSFORMATION OF THE MATERIAL STRUCTURE UNDER PUMPING CONDITIONS

This section of this chapter illustrates the effect of ammonium nitrate concentration on the shearing process of highly concentrated emulsions. To investigate this, three emulsion samples with different droplet sizes were prepared, as stipulated in the previous chapter (Chapter 3 – Materials and experimental procedure) with their dispersed phase consisting of 65% ammonium nitrate by mass of this phase. The remainder was water. The fudge point (crystallisation temperature) of the salt solution decreased from that in which the salt was beyond 80% by mass (material composition of Parts A and B above) to approximately to be 18°C. The surfactant used was PIBSA-UREA for all three samples, but the difference lay in the droplet size (as illustrated in Figure 4.19, below), which was achieved by the technology of emulsion preparation by which the size of droplets depended on the conditions of mixing in a vessel (Malkin *et al.*, 2004a); in this study, the mixing time was 2, 4 and 10 minutes respectively. Figure 4.20 presents a microscopic image of the fresh emulsion.

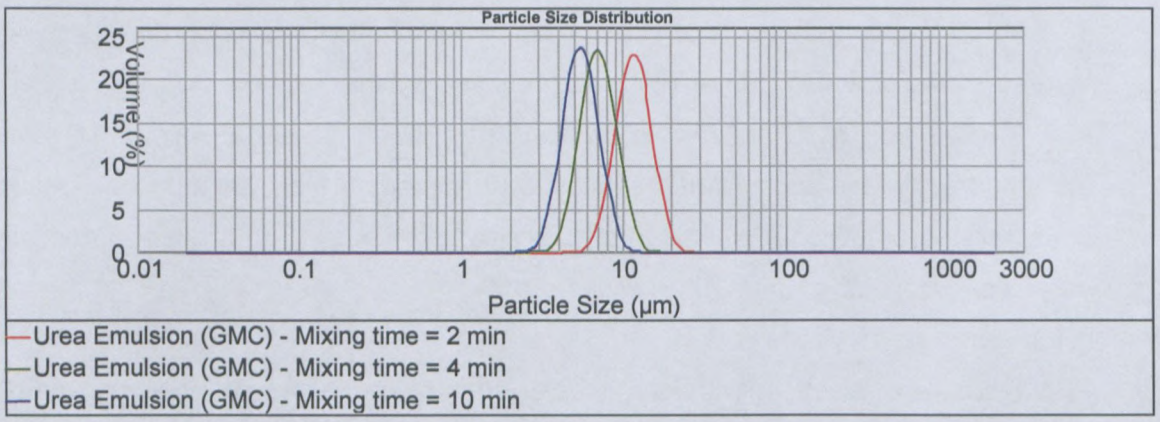

Figure 4.19: Histogram of drop size distribution of fresh emulsion (65% AN) with three different droplet sizes (different mixing time).

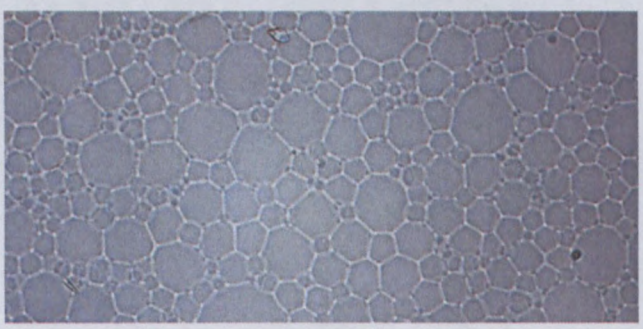

Figure 4.20: Microscopic picture of the fresh emulsion (65% AN)

4.4.1 DROPLET SIZES AND THEIR DISTRIBUTIONS FOR SHEARED SAMPLES

To shear these fresh samples, the same technique was used. Figure 4.21 illustrates the droplet size distribution profiles for sheared emulsion samples using the 3 mm diameter orifice. All the other formulations followed similar trends and are presented in Appendix A. In all cases, an evolution toward smaller droplets was observed as the number of pumpings increased and/or energy increased (see Table 4.9, below).

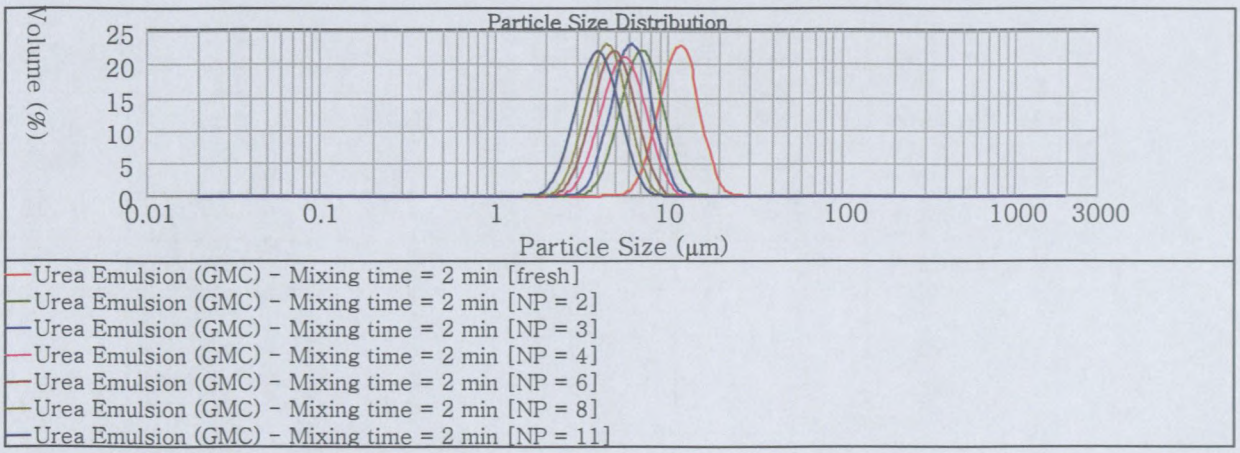

Figure 4.21: Histogram of drop size distribution of sheared urea emulsion (65% AN) (GMC) – t_{mix} = 2 min.

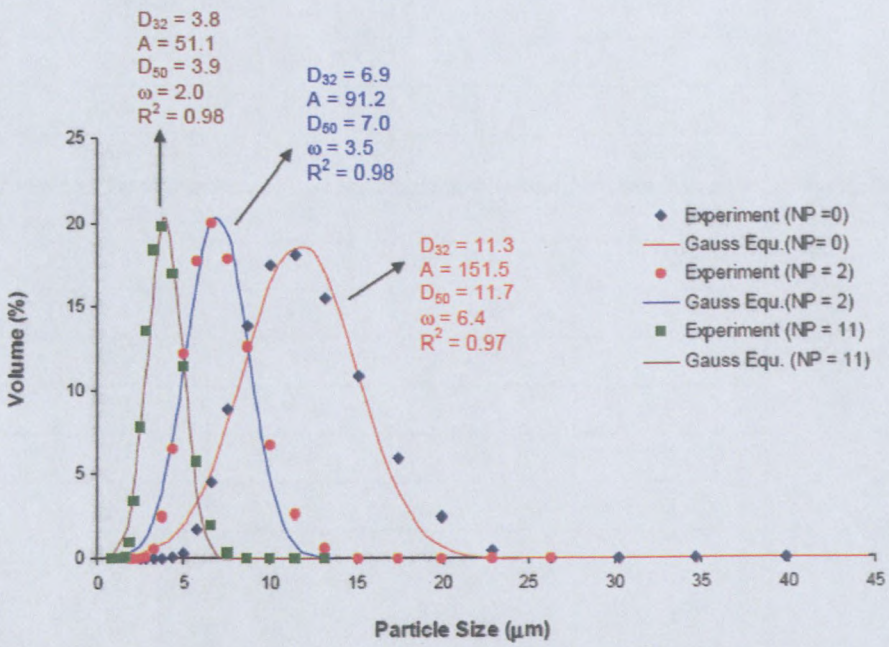

Figure 4.22: Characterisation of DSD of sheared emulsion (65% AN) using the standard Gauss equation

Figure 4.22 shows the fitting of the size distribution of droplets of sheared emulsion samples using the Gauss equation (Equation 4.2). They were of Gaussian type and had a wider distribution. All the sheared samples of different droplet sizes showed similar trends. The fitting characteristics of distribution for all samples are summarized in Table 4.9. They indicate that the width of the distribution, the D_{50} and/or D_{32}, decreased with the increased number of pumpings (NP) and/or energy, and had a tendency to approach a constant value as the number of pumpings increased.

Table 4.9: Summary of the characterisation of the width of DSD of sheared emulsions (65% AN)

Mixing Time	NP	D_{32}	D_{50}	ω	A
2 minutes	0	11.3	11.7	6.4	152
	2	6.9	7.0	3.5	91
	3	6.0	6.1	2.9	80
	4	5.3	5.5	2.9	72
	6	4.7	4.8	2.5	63
	8	4.3	4.4	2.2	58
	11	3.8	3.9	2.0	51
4 minutes	0	7.2	7.1	3.8	93
	2	5.4	5.5	2.7	72
	3	4.9	5.0	2.4	65
	4	5.0	5.1	2.4	67
	6	4.4	4.5	2.1	59
	8	4.0	4.0	2.0	53
	11	3.7	3.7	1.8	49
10 minutes	0	5.3	5.4	2.5	70
	2	4.6	4.7	2.2	61
	3	4.1	4.2	2.0	55
	4	4.1	4.1	2.0	54
	6	3.9	3.9	1.8	51
	8	3.8	3.9	1.8	51
	11	3.4	3.4	1.6	45

4.4.2 CHARACTERISATION OF CRITICAL DROPLET DIAMETER AND ENERGY DENSITY

Using the proposed models (see Equations 4.3 and 4.4, above), the evolution of droplet refinement and the width of distribution are illustrated. Figures 4.23 and 4.24 show the evolution of these parameters as function of the number of pumpings. The curves show an exponential decrease of the average droplet size and the width of the distribution as the number of pumpings increased and approached a constant value ($w_{critical}$, $D_{crit.}$).

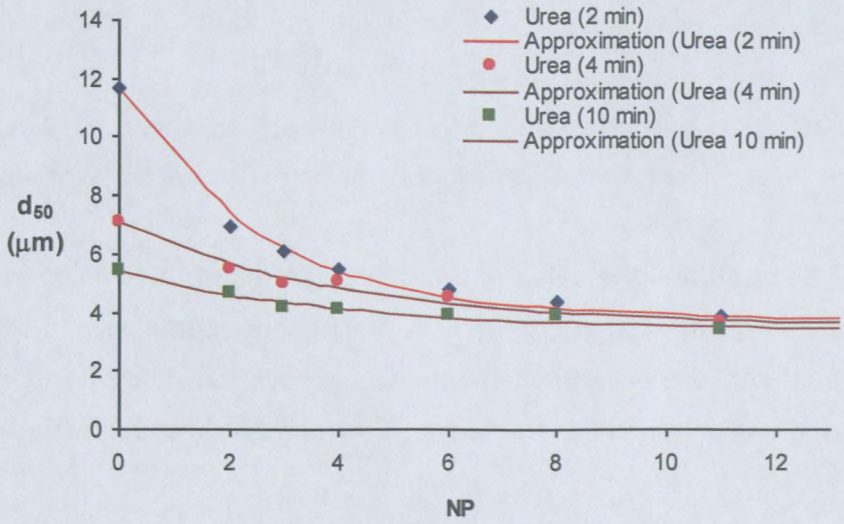

Figure 4.23: Evolution of the volume median diameter (D_{50}) as a function of the number of pumpings for the three urea emulsion samples (65% AN).

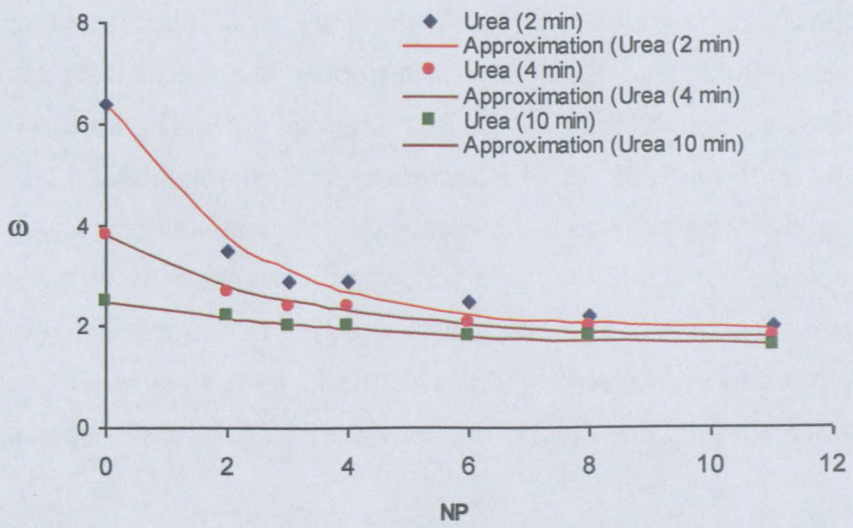

Figure 4.24: Evolution of the width of DSD as a function of the number of pumpings – for the three urea emulsion samples (65% AN).

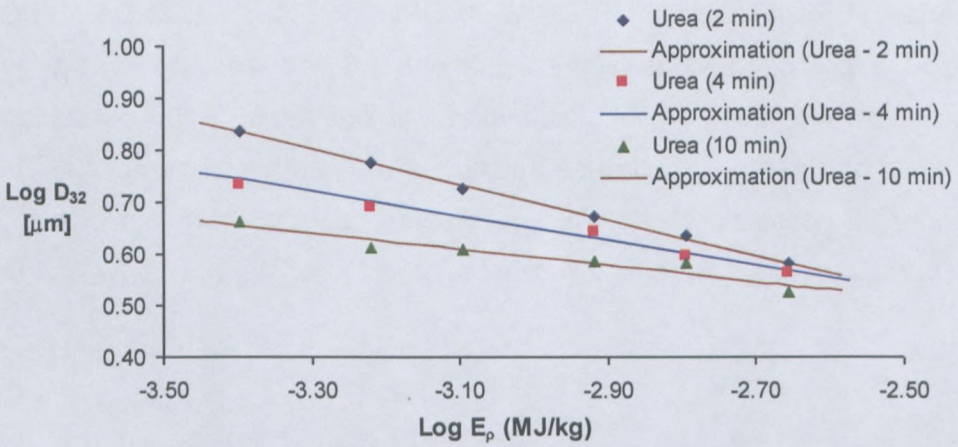

Figure 4.25: Dependencies of the Sauter average diameter of droplets against energy density for the three urea emulsion samples (65% AN) with different mixing times

Figure 4.25 illustrates the value of the dependencies of the Sauter average diameter of the emulsion sample against energy density for the three samples with different droplet sizes. It can be seen that the experimental data was successfully fitted using log-scale of the power-law equation as mentioned in the previous section of this chapter (Equation 4.8).

Figures 4.23 to 4.25 demonstrate the effect of the dependency of droplet refinement on the initial fresh emulsion's droplet sizes, where it can be seen that the fresh emulsion with an initial bigger droplet size refined more easily in the initial shearing process before approaching a constant value which was the critical point in the process where no further disruption of droplets was possible. Such behaviour can be described by the Laplace theory concerning interfacial forces during the disruption of emulsion droplets (Equation 4.9 above – Atkins, 1994), according to which the internal pressure (Laplace pressure) of droplets increases as the size of droplets decrease (McClements, 1999:127,159; Kharatiyan, 2005), while the interfacial tension was constant for all three samples (due to being manufactured with the same surfactant type and surfactant concentration). Higher resistance to reduction of droplet size during shearing was expected with fresh emulsion of smaller droplets. Therefore the following tables (Tables 4.10 and 4.11) summarise the characteristic pumping parameters whereby the effect of droplet size of fresh emulsions can be clearly estimated.

Table 4.10: Summary of the characterisation of critical droplet diameter of urea emulsion sample (65% AN) during the shearing process (OD = 3mm)

Mixing time of fresh	$D_{critical}$	θ_D	Error	$\omega_{critical}$	θ_ω	Error
2 min	2.56	3.80	0.01	1.95	2.24	0.02
4 min	4.03	3.53	0.01	1.73	3.17	0.01
10 min	4.13	3.38	0.01	1.52	5.17	0.009

Table 4.11: Coefficient C and b values for the three emulsions (65% AN) with different starting points of refinement

Mixing time of fresh	C	B	Average Error, E
2 min	0.48	0.34	0.002
4 min	0.88	0.24	0.006
10 min	1.33	0.16	0.008

4.4.3 RHEOLOGICAL PROPERTIES

The following figures (Figures 4.26 to 4.29) illustrate the amplitude sweep test and flow curves for the sheared and fresh emulsions prepared with the same surfactant type and concentration but with 65% by mass of ammonium nitrate of the dispersed phase. The measurements were performed by rotational rheometer (MCR 300). With regard to the viscoelastic properties, all three samples showed a constantly high plateau region as the strain increased, which indicated the linear viscoelastic range. G' decreased as strain increased, indicating that the sample's elasticity decreased and emulsions approached more viscous fluid behaviours and predominated when $\gamma_{limiting}$ was exceeded. In the case of flow curves, the materials showed non-Newtonian fluid behaviour with the existence of a yield point. They also displayed an inflection point. The mechanism of large droplets "rolling over smaller" and "serious distortion of shape of droplets" at low and high shear rate respectively, as reported in previous studies, held and these observations were described. However in both cases, the rheological properties increased with the decrease of emulsion droplets. This was also observed in the sheared emulsion samples where the rheology was sensitive to the shearing process: the elastic modulus and yield stress increased with droplet refinement. The Laplace pressure theory can still be used to explain this trend, accompanied by the decrease of width of distribution as pumping increased.

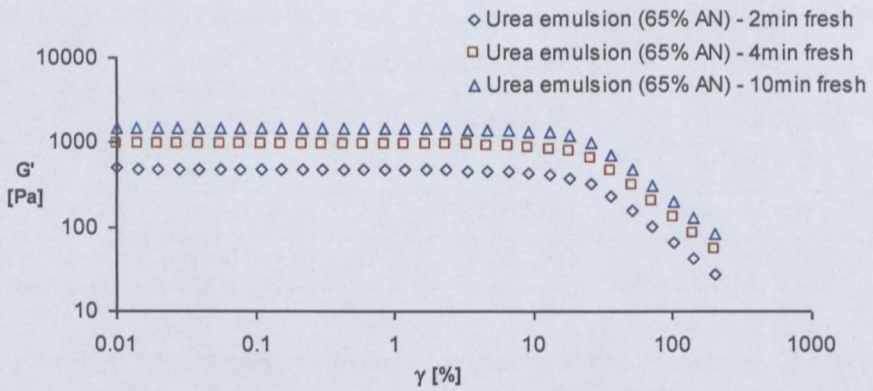

Figure 4.26: Variation of the storage modulus (G') from the oscillatory measurement for the three fresh emulsion samples of three different droplet sizes

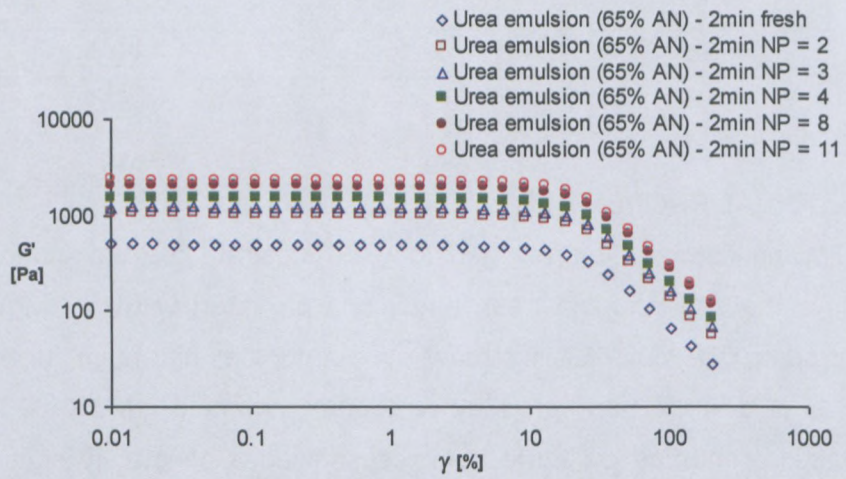

Figure 4.27: Variation of the storage modulus (G') from the oscillatory measurement for the fresh and sheared emulsion sample (t_{mix} = 2 min)

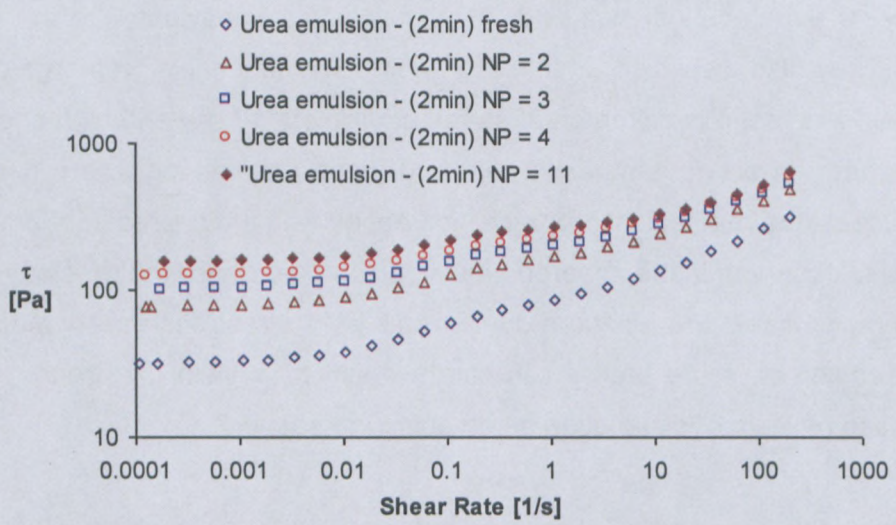

Figure 4.28: Flow curve for the sheared emulsion samples

4.4.4 CHARACTERISATION OF FLOW CURVES AND THEIR FLOW PREDICTION

It was again of huge interest to characterise the flow curve with the use of the Herschel-Bulkley model (HBM) for the determination of flow characteristics that might be used for pipeline design. Following this, Equation 4.10 (part B – Section 4.3.2) was used to fit all the fresh and pumped emulsions. Figure 4.29, below, shows the "Good fit" of flow curves using the HBM equation and Table 4.12 summarises the coefficients of fitting parameters (see Appendix F for the rest of the fitting graphs and tables).

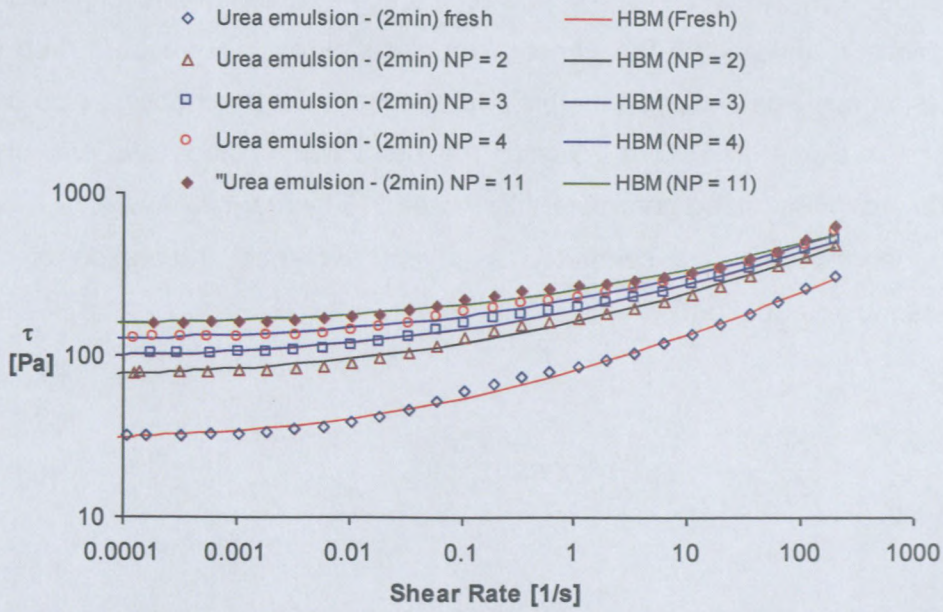

Figure 4.29: Characterisation of flow using the Herschel-Bulkley equation

Table 4.12: Summary of fitting parameter for the Herschel-Bulkley equation

Urea emulsion (GMC) : t_{mix} = 2 min				
NP	τ_y	**K**	**N**	**Error**
0	28	54	0.31	0.009
2	69	94	0.27	0.008
3	91	101	0.27	0.007
4	117	107	0.27	0.006
6	136	109	0.27	0.006
8	141	113	0.26	0.007
11	146	126	0.25	0.008

For any flow process taking place in industry, it was always prototypical to design and predict its flow characteristics in order to control and maximise operations to give reasonable cost and less energy loss. However, previous studies on the prediction of pumping characteristics of highly concentrated water-in-oil emulsions (Malkin *et al.*, 2004b; Nkomo, 2005) demonstrated the close prediction of ΔP dependence of some data obtained directly from industrial flow conditions with those calculated through the rheological parameters (such as the above coefficients of the HBM mode) in a quantitative manner. This prediction was achieved through the computed numerical integration of the Rabinowitsch-Weissenberg equation (see Equation 4.14). It was expected to be interesting to use this empirical technique to investigate the effect of droplet size on the pressure drop (ΔP) for the fresh emulsion samples discussed in this part of this thesis. By choosing pipe boundaries of L = 1 m and a diameter of D = 76 mm, the prediction of flow rate and pressure drop from rheometry (HBM fitting parameter) illustrated in Figures 4.30 and 4.31 was achieved. The Q (ΔP) dependence was computed by direct numerical integration of the Rabinowitsch-Weissenberg equation:

$$\dot{\gamma} = \frac{8\dot{V}}{D} = \frac{8Q}{\pi D^3} = \frac{4}{\tau_w^3}\int_0^{\tau_w} \tau^2 \dot{\gamma} d\tau \qquad \textbf{(Equation 4.15)}$$

with

$$\tau_w = \frac{\Delta P D}{4L} \qquad \textbf{(Equation 4.16)}$$

where ΔP is the pressure drop, V is the average velocity, Q is the volume flow rate, D and L denote pipe diameter and length, respectively, τ_w is the shear stress at the pipe wall and $\dot{\gamma}_{av}$ is the relationship between shear rate and shear stress.

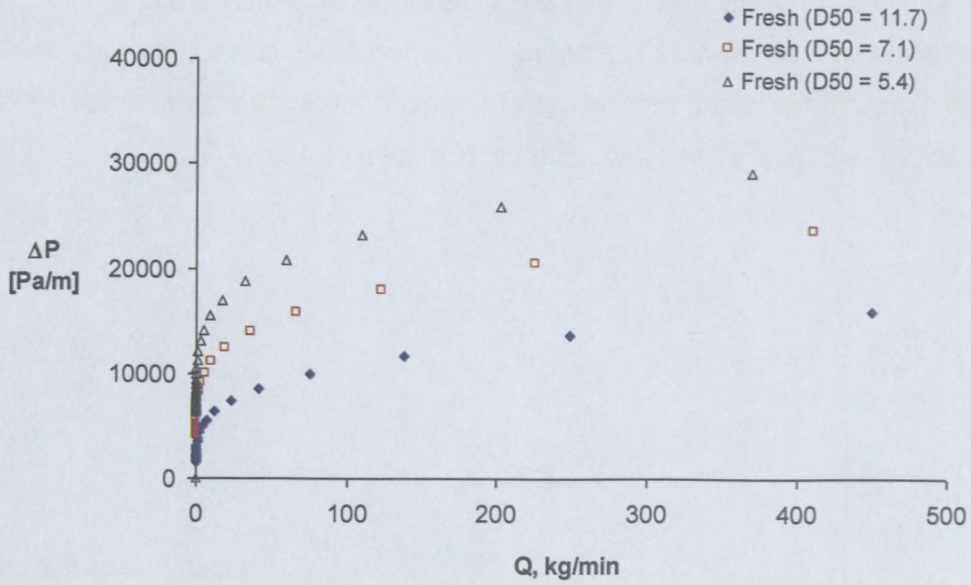

Figure 4.30: Effect of droplet size on pressure drop (ΔP)

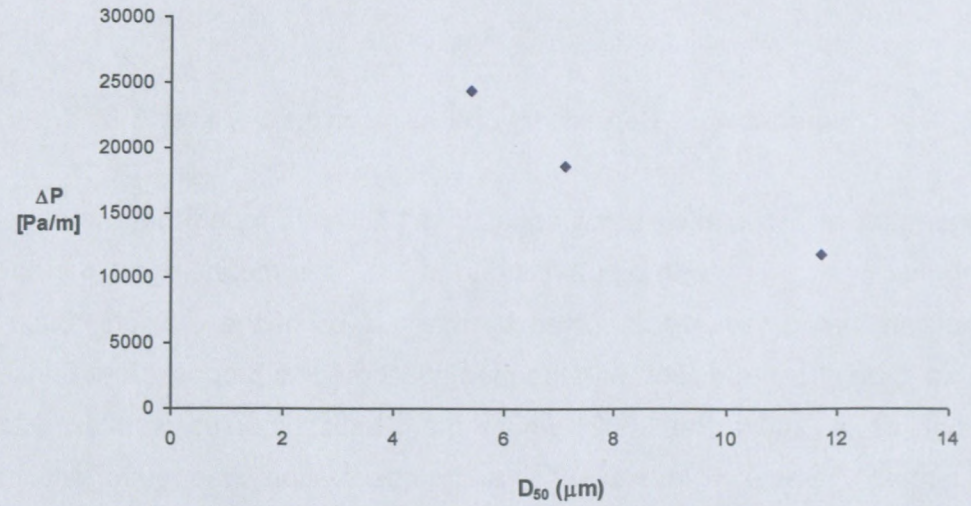

Figure 4.31: Increase of pressure drop as function of drop sizes

It can be seen that the pumping characteristic depended on the droplet size: increase of mixing time led to decrease of droplets size within the emulsion and the pressure drop also increased. Thus, from the emulsion with droplet size D_{50} = 11.7 μm to emulsion D_{50} = 7.1 μm, ΔP increased by approximately 6500 Pa/m (for Q = 150 kg/min). And from D_{50} = 11.7 μm to D_{50} = 5.4 μm, ΔP increased about 5500 Pa/m (for Q=150kg/min). Therefore, it is possible to hypothesise that reducing droplet size below a certain value led to an increase of rheological properties which, in turn, increased energy and/or pressure during pumping.

4.4.5 DEPENDENCE OF ELASTIC PROPERTIES ON DROPLET SIZE

The following Figures 4.32 illustrated the dependency of elastic modulus G'_0 on the droplet size. Although the experimental data for elastic modulus was successfully approximated by the above empirical power-law equation (Equation 4.12)

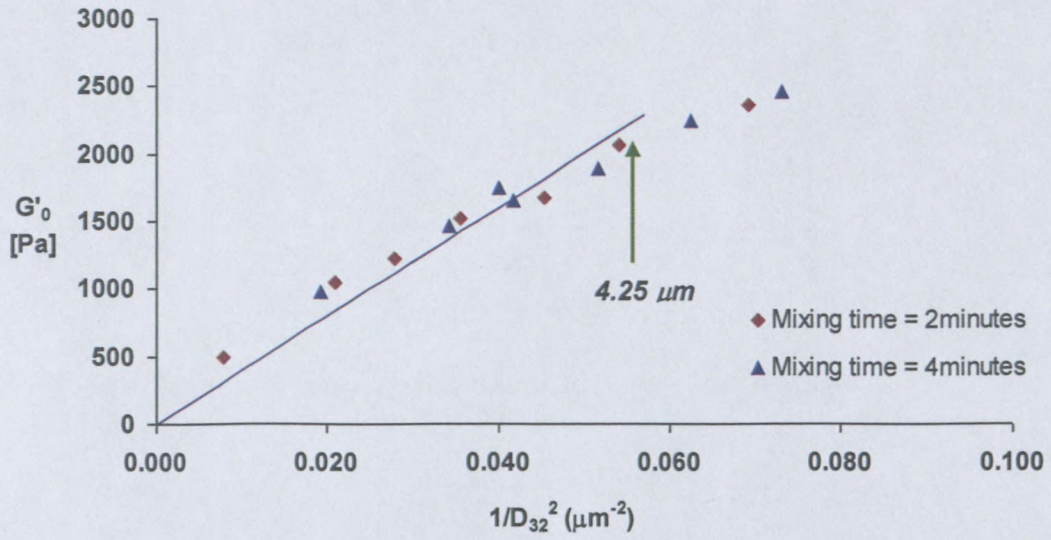

Figure 4.32: Dependency of elasticity on the droplet size.

Thus, after approximation using equation 4.12, it was found that the dependency of elastic modulus was on D^{-2}, with $n \approx 2$, instead of D^{-1}. This means again that the elasticity of this emulsion material was determined by the surface of the droplets. Such observation was found to be in contradiction with the theoretical models proposed by (Princen and Kiss 1986; Babak *et al.* 2001; Pal 2002) where the elastic modulus was expected to depend on reciprocal diameter. Nevertheless, such observation was quite analogous to the one observed previously by (Malkin *et al.* 2004a; Masalova and Malkin, 2007a) and (Masalova and Malkin, 2008). And the argument given there for such discrepancy of the experimental results was related to the type of the emulsion used (high concentrated emulsion) as well to difference in the averaging procedure for polydisperse samples, which was indeed similar to the samples for this current study.

It was also so evident that the linear dependence of G_0 vs. D^{-2} passing through the zero point was been obtained for these emulsion samples under study. However the $G(D)$ dependence can be treated up to some critical value of D. Thus this reciprocal squared dependence is valid in the range of relatively large droplets (> 4.25μm), while at smaller sizes, the $G_0(D)$ dependence becomes different.

4.4.6 ESTIMATION TO LIMITING STRAIN DEFORMATION

The last remark related to stability of emulsion in shearing concerns the yield stress, τ_y. This parameter characterizes the limit of quasi-solid behavior of an emulsion under applied stresses as described above in (section 4.3.4). After this threshold an emulsion begins to flow that becomes possible due the rupture of its static structure. The value of τ_y should be correlated with elastic modules, and the ratio of these parameters (Equation 4.14) gives the limiting deformation characterizing the transition from solid-like state of an emulsions to its flow state. Figure 4.33 collects all the experimental points of the three samples with different droplet size (see section 4.4) . One can see that all of them lie inside a rather narrow band. The average value of γ^* is approximated to 0.07, and at any rate it does not exceed 0.1.

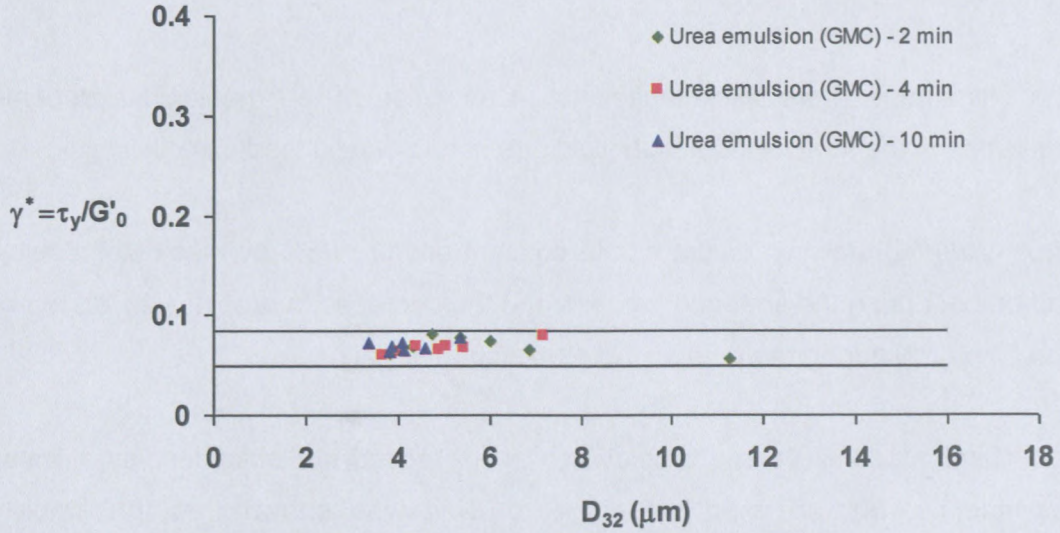

Figure 4. 33: Estimation to limiting strain deformation and/or the transition point between the two mechanism – "inflection point".

4.4.7 SUMMARY

All three samples with the same formulation content and lower ammonium nitrate concentration (65% m/m of dispersed phase) but different droplet sizes were stable under pumping conditions in terms of crystallisation and coalescence.

The refinement of droplets took place during pumping. The resistance to reduction of droplet size depended on the starting point of drop size of the fresh sample – a bigger droplet size was refined more easily during the initial shearing process before approaching critical point as suggested in the Laplace theory on interfacial forces during the disruption of emulsion droplets where the internal pressure (Laplace pressure) of droplets increased as the size of the droplets decreased.

The pumping process or shearing process narrowed the droplet size distribution, which was found to be of Gaussian type.

The refinement of droplets resulted to an evolution of the rheological properties of these emulsions in the form of increased yield stress and elastic modulus.

Thus, lowering the ammonium nitrate concentration to 65% by mass still resulted in droplet refinement during the shearing process and the decrease in droplet size led to an increase in pressure drop during the pumping of emulsion material.

The shear modulus versus droplet size is expressed not obligatory by a linear reciprocal dependence, but an exponent equal to 2. It was shown that the stability of highly concentrated emulsions in shearing is determined by some critical value of deformation with reference to the yielding conditions. This value on average equalled 0.07 for all samples under investigation.

CHAPTER 5
SUMMARY AND CONCLUSION

The emulsions investigated in this research are classified as highly concentrated water-in-oil emulsions. They are commonly used as a re-pumpable material. The problem of droplet size and rheological properties of such highly concentrated emulsions was studied and their stability under shearing was investigated experimentally. The results present the effect of high shearing caused by transportation conditions (such as pumping) on the rheological and structural properties of these materials. The effect of surfactant concentration and surfactant type, effect of ammonium nitrate salt concentration in the dispersed phase, and the effect of orifice diameter during the shearing process were considered.

The fresh emulsion samples were sheared using a newly designed piston-pumping instrument. High pressure was applied into the piston-shaft to force the emulsion material out of the chamber of the piston through the outlet, an orifice with a small diameter.

The high shearing resulting from the pumping process played an important role in determining whether the droplets of such (highly concentrated) emulsions crystallised, coalesced or were just refined when they were pushed through the small orifice.

A Leica optical microscope with high magnification and equipped with a digital camera was used for qualitative examination of the sheared emulsion. The droplet size and droplet distribution and the rheological measurements were carried out using a Malvern Mastersizer 2000 and a rotational dynamic MCR 300 rheometer (Paar Physica) respectively. Samples with different surfactant concentrations (8% and 14%), different PIBSA surfactant head groups (MEA, UREA, IMIDE and MEA/SMO), and different salt concentrations in the dispersed phase (>80% & 65% by mass) were investigated.

The measurement of the droplet size distribution involved the distribution of droplets in fresh and sheared emulsions and an approach considering some arguments on process parameter was proposed. These arguments involved the average size of droplets and width of distribution with regard to pumping conditions.

The rheological measurement involved an amplitude sweep test, where the elastic domain was determined, and flow curves where the yield stress was approximated. The dependence of elasticity properties and the estimation to limiting strain deformation were demonstrated.

Neither crystallisation nor other destabilisation phenomena such as coalescence, partial coalescence, or phase inversion occurred during the shearing process of these emulsions, regardless of their formulation content. It was found that the high shearing action within this experimental window induced droplet refinement, which was confirmed by the qualitative microscopic analysis. The droplet size distributions for the fresh and sheared emulsions were wider and of Gaussian type and their width narrowed with prolonged shearing. Two models were proposed and used to fit the refinement evolution of these prepared and "cooled to room temperature" emulsions:

$$D_{cal} = D_{crit.} + e^{-(N/\theta_D)}\left(D_0 - D_{crit.}\right) \qquad \textbf{(Equation 4.17)}$$

and

$$\omega_{cal} = \omega_{crit.} + e^{-(N/\theta_\omega)}\left(\omega_0 - \omega_{crit.}\right) \qquad \textbf{(Equation 4.18)}$$

The models showed an exponential decrease of the average droplet size and the width of the distribution as the number of pumpings increased, and approached a constant value referred to here as the critical width ($\omega_{critical}$) and critical diameter ($D_{crit.}$). The effect of surfactant type and surfactant concentration and the effect of orifice diameter were determined with the use of these characteristic pumping parameters ((θ_D and θ_ω): The higher the value of these parameters, the lower the efficiency of droplet refinement.

An engineering illustration of the work done on the material during the pumping process was derived in terms of energy density (the ratio of applied pressure to the density of the material) and used to illustrate the dependencies of the Sauter average diameter of the emulsion sample against energy in the power law equation. This illustration (power law equation) was mentioned previously in many studies where a coefficient C was found to be the efficiency of droplet disruption which, in turn, could be used to estimate the effect of surfactant concentration and surfactant type during the shearing process. According to this, a lower value of coefficient C indicated higher efficiency of droplet refinement.

All parameters ((θ_D, θ_ω, D_{crit}, $\omega_{critical}$ and C) gave a clear estimation of the factors that influence droplet refinement during high shearing within the experimental window of this study. Therefore the following observations are recorded:

- Higher surfactant concentration induced faster refinement.

- The droplet disruption efficiency in terms of surfactant type followed this trend, with PIBSA-MEA revealing the greatest resistance to droplet disruption:

PIBSA-MEA > PIBSA-IMIDE > PIBSA-UREA > PIBSA-MEA/SMO

The interpretation of these findings can be summarised as follows: the quicker the surfactant adsorbed to the surface of the droplets during the process of disruption, the smaller the droplets produced; and the greater the amount or concentration of surfactant accumulated at the surface, the easier the droplets disrupted or, in other words, the less energy was required for the reduction of droplet size.

Besides these two factors, the orifice geometry also influenced the refinement efficiency of droplets, with the smaller diameter providing higher droplet reduction. Therefore shrinking the orifice edge caused the material to be exposed to higher shearing, which led to greater droplet disruption.

From the rheological approach, an elastic domain was observed during the amplitude sweep test for all formulations of the emulsion, regardless of whether sheared or fresh. This was characterised by a constant plateau zone at a wide range of strain deformation. Above certain values of strain [7 to 10%] (referred to here as the limiting strain – $\gamma_{limiting}$), the sample's elasticity decreased and the emulsions approached more viscous fluid behaviours. However, some previous studies involving similar types of emulsions and formulations revealed peculiarities of rheological properties and flow by identifying "the rolling mechanism of larger droplets over smaller ones" to explain the elastic domain, and "serious distortions of droplet shape" to explain the non-linear domain where the strain was high.

The sensitivity of the elastic domain to pumping conditions was related to the reduction of droplet size (governed by the Laplace pressure which increases as the size of the droplet decreases) and the width of their distribution, which became narrower with prolonged shearing.

The flow behaviour of these emulsions was found to be non-Newtonian, and characterised by shear thinning and elastic effect and the existence of a yielding point (yield-pseudoplastic behaviour). This flow behaviour was independent of the shearing process. It displayed an inflection point which was considered to be the bridge linking the two suggested mechanisms of flow of emulsions at low and high shear rates: the rolling mechanism of large droplets over smaller ones without any noticeable distortion of their shape, and the serious distortions of the droplet shape respectively. The yield stress was also sensitive to the pumping conditions and the above argument on reduction of drop size and width of distribution supported such behaviour.

Shear stability of highly concentrated emulsions is determined by some critical value of deformation referring to the yielding conditions and expressed as the ratio ($\tau_y/G = \gamma^*$) as function of D_{32} for all the sheared emulsion samples. It demonstrated the informative meaning of the limiting deformation characterising the transition from the solid-like state of an emulsion to its flow state. All the experimental points for all recipe studies in this research project lie inside a rather narrow band. The average value of $\gamma^*_{average}$ is approximated to 0.07, and at any rate does not exceed 0.11.
This level of the γ^* values had been already met in previous publications, where the threshold of the transition was estimated as approximately 0.1. So, it is so evidence that this value has real physical sense.

The research indicated that the droplet size dependence on the elastic modulus can not be described by the Princen-Kiss model. It was found to be dependent on the square reciprocal droplet size (D^{-2}). The discrepancy with regard to the Princen-Kiss theory was related to the type of emulsion used (highly concentrated), as well as to differences in the averaging procedure for polydispersed samples, as reported in some previous studies.

The decrease of elasticity with increased surfactant and its dependence on surfactant type were among the trickiest observations to be elucidated in this experimental work. However, possible arguments put forward in support of these observations follow:

- Concerning the effect of surfactant concentration, the possible interaction forces that existed between the monolayer surfactant in the aqueous-oil interface and the reverse micelles in the oil phase might apply in this study. Thus, the Van der Waals attraction between the droplets, steric forces provided by the surfactant tail group and the electrostatic interaction with the head group together resulted in net repulsive interaction between interfaces and reverse micelles in the oil phase. Therefore the increasing concentration of reverse micelles (increase of surfactant concentration) strengthened the interaction between them and led to a decrease in rheological properties during applied stress.

- On the other hand, the size of micelles, which was dependent on the volume of head group of PIBSA surfactants, has been proposed to describe the effect of surfactant type on rheology. Thus, bigger surfactant head groups provided micelles of a larger size which, in turn, affected the rheology by increasing the emulsion's rheological properties.

Lowering the ammonium nitrate concentration to 65% by mass of the dispersed phase still resulted in droplet refinement and the narrowing of width of distribution during the shearing process. The disruption of droplets was associated with the main mechanism for the evolution of the emulsion's rheological properties. And the pressure drop during the pumping of fresh emulsions, as predicted with the use of the computerised numerical integration of the Rabinowitsch-Weissenberg equation: it (pressure drop) increased significantly with a decrease of droplet size.

As a recommendation and with an eye to continuing this work, the methodology used in the research supporting this thesis could be applied directly to different techniques of shearing, and could also be used when extrapolating the process to bigger scale pipeline transportation.

In terms of future research, the following should be investigated:

- The effect of high shearing on the evolution of rheological properties of this emulsion (highly concentrated emulsion explosives) with ageing.

- The effect of oil type on the rheological and structural properties of the highly concentrated emulsion under high shearing.

- The effect of variation of temperature during the high shearing process of the emulsion.

And, finally, the empirical approach followed for the work presented in this dissertation can be regarded as a valuable technique to mimic the manufacturing process conditions on a small scale in the laboratory, where the relationship between rheology, pumping and droplet refinement could be studied. However, further experimental work will always present further challenges concerning more quantitative analysis of the stability of such highly-concentrated emulsion types during the shearing process caused by transportation conditions.

REFERENCES

Acrivos, A., Lo, T.S. 1978. Deformation and break up of single slender drop in an extensional flow. *Journal of fluid Mechanics*, 86(4):641-672.

Adamson, A.W. 1997. *Physical chemistry of surfaces*. 6th ed. New York: Wiley-Interscience.

Aronson, M.P., and Princen, H.M. 1980. Contact angles associated with thin liquid films in emulsions. *Nature*, 286:370-372.

Aronson, M.P., and Princen, H.M. 1982. Contact angles in oil-in-water emulsions stabilized by ionic surfactant. *Colloids and surfaces*, 4:173-184.

Aronson, M.P., and Petko, F.M. 1993. Highly concentrated water-in-oil emulsions: Influence of electrolyte on their properties and stability. *Journal of colloid and interface science,* 159(1):134-149.

Atkins, P.W. 1994. *Physical chemistry*. 5th ed., Oxford, UK: Oxford university press

Babak, V.G., Langfield, A., Fa, N., Stebe, M.J. 2001. Rheological properties of highly concentrated fluorinated emulsions. *Progress in colloid & polymer science*, 118:216-220

Balian, R. 2007. *From microphysics to macrophysics*. Methods and applications of statistical physics. Ter Haar, D., Gregg, J.F (Translators), vol 1. New York: Springer.

Bampfield, H.A. 1984. Water-in-wax emulsion blasting agents. *United stated patent*, Patent number: 4470855.

Barnes, H.A. 1994. Rheology of emulsions – A review. *Colloids and surfaces A: physicochemical and engineering Aspects*, 91:89-95.

Barry, B.W. 1975. Viscoelastic properties of concentrated emulsions. *Advances in Colloid and Interface Science*, 5:37-75.

Barthes-Biesel, D., Acrivos, A. 1973. The rheology of suspensions and its relations on phenomenological theories for non-Newtonian fluids. International journal of multiphase flow, 1.

Bashir, A., Odell, J.A., and Keller, A. 1984. High modulus filaments of polyethylene with lamellar structure by melt processing; the role of high molecular weight component. *Journal of materials science*, 19(11):3713-3725.

Bazhlekov, I.B., Anderson, P.D. 2006. Meijer H. E.H. Numerical investigation of the effect of insoluble surfactants on drop deformation and breakup in simple shear flow. *Journal of colloid and Interface Science*, 298(1):369-394.

Becher, P. 1988. *Encyclopedia of emulsion technology*, Vol. 3. New York: Marcel Dekker.

Benali, L. 1993. Rheological and granulometrical studies of a cutting oil emulsion. I. The effect of oil concentration. *Journal of colloid and interface science*, 156(2):454-461.

Bergenstahl, G. 1997. Physiochemical aspects of an emulsifier functionality, Hasenhuettl, G.L., Hartel, R.W. (Eds), Chap. 6. *Food emulsifiers and their applications.* New York: Chapman & Hall.

Bibette, J. 1992. Stability of thin film in concentrated emulsions. *Langmuir*, 8(12):3178-3182.

Bikerman, J.J. 1973. *Foams.* New York: Springer.

Binks, B.P. 1998. Emulsions: recent advances in understanding, Binks, B.P. (Ed.). *Modern aspects of emulsion science.* Cambridge – UK: The royal society of chemistry.

Bird, R.B., Armstrong, R.C., Hassager, O. 1987. *Dynamic Liquids.* New York:Willey.

Bluhm, H.F. 1969. Ammonium nitrate emulsion blasting agent and method of preparing same. *United stated patent*, Patent number: 3447978.

Boer, W.G. 2003. Composition and emulsifier. *United stated patent*, Patent number: 6630596 B2.

Boode, K., Bisperink, C., Walstra, P. 1991. Destabilisation of w/o emulsions containing fat crystals by temperature cycling. *Colloids and surfaces.* 61:55-74.

Boode, K., Walstra, P. 1993. Partial Coalescence in oil-in-water emulsions. 1. Nature of the aggregation. *Colloids and surfaces. A: physicochemical and engineering aspects,* 81:121-137.

Boode, K., Walstra, P., & deGroot-Mostert, A.E.A. 1993. Partial coalescence of oil-in-water emulsions. 2. Influence of the properties of the fat. *Colloids and surfaces. A, physicochemical and engineering aspects*, 81:139-151.

Bourne, N.K., Field, J.E. 1991. Bubble collapse and the initiation of explosion. *Proceedings of the royal society of London, Series* A 435:423-435.

Bourne, N.K., Milne, A.M. 2003. The temperature of a shock-collapsed cavity. *Proceedings of the royal Society of London, Series* A 459:1851-1861.

Boxer, G. 1987. *Work out engineering thermodynamics.* London: MacMillan education LTD.

Braginsky, L.M., and Belevitskaya, M.A. 1996. Kinetics of droplets breakup in agitated vessels. Kulov, N.N. (Ed). *Liquid-liquid systems.* Chap. 1. New York: Nova science, Commack.

Brockington, J.W. 1980. Water-in-oil NCN emulsion blasting agent. *United stated patent*, Patent number: 4218272.

Campbell, I., Norton, I., and Morley, W. 1996. Factors controlling the phase inversion of oil-in-water emulsions. *Netherlands milk and dairy journal*, 50(2):167-182.

Chattopadhyay, A.K. 1996. Emulsion explosive. *United state patent*, patent number: 5500062.

Coppola, S., Grizzuti, N., and Maffettone, P.L. 2001. Microrheological modeling of flow-induced crystallization. *Macromolecules*, 34(14):5030-5036.

Cumming, I.W., Holdich, R.G., Smith, I.D. 2000. The rejection of oil by microfiltration of a stabilized kerosene/water emulsion. *Journal of membrane science*, 169(1):147-155.

Curle, N., and Davies, H.J. 1968. *Modern fluid dynamics*. Vol.1. London: D. van Nostrand.

Da Silva, G., Dlugogorski, B.Z., and Kennedy, E.M. 2006. An experimental and theoretical study of the nitrosation of ammonia and thiourea. *Chemical engineering science*, 61(10):3186-3197.

Darling, D.F., Birkett, R.J. 1987. Food colloids in practice. Dickinson, E. (ed). *Food emulsions and foams.* London: Royal society of chemistry (RSC).

Davis, H.T. 1994. Factors determining emulsion type: Hydrophile-lipophile balance and beyond. *Colloids and surfaces A: physicochemical and engineering aspects*, 91:9-24.

Defay, R., Petre, G. 1979. Surface and colloid Science. Matijevie, E. (Ed). *Dynamic surface tension*. New York - USA: Willey.

Dickinson, E. 1989. Food colloids – an overview. *Colloids Surfaces*, 42:191-204

Dickinson, E. 1992. *Introduction to food colloids*. Oxford: Oxford University Press.

Dickinson, E., Stainsby, G. 1982. *Colloids in foods*. London: Applied science publishers.

Dickinson, E., Euston, S.R., and Woskett, C.M. 1990. Progress in colloid and polymer science. Kilian, H.-G., Lagaly, G. (Ed.). *Competitive adsorption of food macromolecules and surfactants at the oil-water interface*. Lindman, B., Rosenholm, J.B., Stenius, P. (Guest Editors). Vol.82, pp. 65-75. Germany: Springer berlin / Heidelberg.

Dickinson, E., McClements, D.J. 1995. *Advances in Food Colloids*. Chapman & Hall, London.

Edwards, D.A., and Wasan, D.T. 1988. Surface rheology. I.The planar fluid surface. *Journal of rheology*, 32(5):429-455.

Edwards, D.A., Brenner, H., Wasan, D.T. 1991. *Interfacial Transport Process and Rheology*. UK: Butterworth-Heinemann.

Elmoumni, A., Winter, H.H., Waddon, A.J., and Fruitwala, H. 2003. Correlation of material and processing time scales with structure development in isotactic polypropylene crystallization. *Macromolecules*, 36(17):6453-6461.

Evans, D.F., and Wennerstrom, H. 1994. *The colloidal domain: where physics, chemistry, biology and technology meet*. New York: VCH Publishers.

Evison, J., Dickinson, E., Apenden, O.R.K., Williams, A. 1995. Formulation and properties of protein stabilized water-in-oil-in-water multiple emulsions. Dickinson, E. and Lorient, D. (Eds). *Food Macromolecules and colloids*. Cambridge 235 – UK: Royal society of chemistry.

Fischer, P., Eugster, A., Windhab, E.J., Schuleit, M. 2007. Predictive stress tests to study the influence of processing procedures on long term stability of supersaturated pharmaceutical o/w creams. *International journal of pharmaceutics,* 339(1-2):189-196.

Forgiarini, A., Esquena, J., Gonzalez, C., and Solans, C. 2001. Formation of nano-emulsions by low-energy emulsification methods at constant temperature. *Langmuir*, 17(7):2076-2083.

Fradette, L., Brocart, B., & Tanguy, P.A. 2007. Comparison of mixing technologies for the production of concentrated emulsions. *Chemical engineering research and design*, 85(11):1553-1560.

Franco, J.M., Guerrero, A., Gallegos, C. 1995. Rheology and processing of salad dressing emulsions. *Rheologica acta*, 34(6):513-524.

Fredrickson, A.G. 1964. *Principles and Applications of Rheology*. New Jersey: Prentice-Hall.

Friberg, S.E. 1997. Emulsion stability, Friberg, S.E., Larsson, K. (Eds.). *Food emulsions*. 3rd ed. New York: Marcel Dekker.

Gopal, E.S.R. 1968. Principles of emulsion formation. Sherman, P. (Ed). *Emulsion science*. chap.1. London: Academic press.

Grace. H.P. 1982. Dispersion phenomena in high viscosity immiscible fluid systems and application of static mixers as dispersion device in such systems. *Chemical engineering communications*, 14():225-277.

Greene, M.R., Hammer, P.A., Olbricht, W.L. 1994. The Effect of Hydrodynamic Flow Field on Colloidal Stability. *Journal of colloid and interface science*, 167(2):227-470.

Guerrero, A., Partal, P., Gallegos, C. 1998. Linear viscoelastic properties of sucrose ester-stabilized oil-in-water emulsions. *Journal of rheology*, 42(6):1375-1388.

Guido, S., and Simeone, M. 1998. Binary collision of drops in simple shear flow by computer-assisted video optical microscopy. *Journal of fluid mechanics,* 357:1-20.

Hales, R.H., Cranney, D.H., Hurley, E.K., Preston, S.B. 2004. Emulsion phase having improved stability. *United stated patent*, patent number: 6808573 B2.

Harkins, W.D. 1952. *The physical chemistry of surface films*. New York: Reinhold Publishing Corporation.

Hartley, G.S. 1936. *Aqueous solutions of paraffin chain salts*. Paris: Hermann et cie.

Hetzel, F., Nielsen, J., Wiesner, S., Brummer, R. 2000. Dynamic mechanical freezing points of cosmetic o/w emulsions and their stability at low temperatures. *Applied rheology*, 10(3):114-118.

Hiemenz, P.C. 1986. *Principles of colloid and surface chemistry*. New York: Marcel Dekker.

Hong, A., Fane, A.G., Burford, R. 2003. Factors affecting membrane coalescence of stable oil-in-water emulsions. *Journal of membrane science*, 222 (1-2):19-39

Hu, Y.T., Pine, D.J., and Leal, L.G. 2000. Drop deformation, breakup, and coalescence with compatibilizer. *Physics of fluids*, 12(3):484-489.

Israelachvili, J. N. 1992. *Intermolecular and surface forces*. London – UK: Academic Press.

Israelachvili, J.N. 1994. The science and applications of emulsions – an overview. *Colloids and surfaces. A, Physicochemical and engineering aspects*, 91:1-8.

Jafari, S. M., He, Y., & Bhandari, B. 2007. Production of sub-micron emulsions by ultrasound and microfluidization techniques. *Journal of food engineering*, 82(4):478-488.

Jager-Lézer, N., Tranchant, J.F., Alard, V., Vu, C., Tchoreloff, P.C., and Grossiord, J.L. 1998. Rheological analysis of highly concentrated w/o emulsions. *Rheologica acta*, 37(2):129-138.

Janssen, J.J.M., Boon, A., Agterof, W.G.M. 1994. Influence of dynamic interfacial properties on droplet breakup in simple shear flocs. *Fluid mechanics and transport phenomena - AIChE*, 40(12):1929-1939.

Jeelani, S.A.K., Hartland, S. 1993. Effect of velocity fields on binary and interfacial coalescence. *Journal of colloid and interface scienc*e, 156(2):467-477.

Kabalnov, A., and Wennerstrom, H. 1996. Macroemulsion Stability: the orientated wedge theory revisited. *Langmuir*, 12(2):276-292.

Karbstein, H., Schubert, H. 1995. Developments in the continuous mechanical production of oilin-water macro-emulsions. *Chemical engineering and processing*, 34(3):205-211.

Kawakami, D., Hsiao, B.S., Ran, S., Burger, C., Fu, B., Sics, I., Chu, B., and Kikutani, T. 2004. Structural formation of amorphous poly(ethylene terephthalate) during uniaxial deformation above glass temperature. *Polymer*, 45(3):905-918.

Kawakami, D., Ran, S., Burger, C., Avila-orta, C., Sics, I., Chu, B., Benjamin, S.H., and Kikutani, T. 2006. Superstructure Evolution in Poly(ethyleneterephthalate) during Uniaxial Deformation above Glass Transition Temperature. *Macromolecules*, 39(8):2909-2920.

Keller, A., and Kolnaar, H.W.H. 1997. Flow-induced orientation and structure formation. Meijer, H.E.H. (ed). *Materials science and technology: A comprehensive treatment*. Vol. 18, Processing of polymers. New York: VCH.

Kertes, A.S., and Gutmann, H. 1976. *Surface and colloid science*. Vol.8., pp.193-295. Matijevic, E. (Ed.). New York: Wiley-Interscience.

Khan, S.A., Armstrong, R.G. 1987. Rheology of foam. II. Effect of polydispersity and liquid viscosity for foams having gas fraction approaching unity. *Journal of non Newtonian fluid mechanics*, 25(1):61-92.

Kharatiyan, E. 2005. *Time effects in evolution of structure and rheology of highly concentrated emulsion*. Doctoral thesis, Cape Peninsula University of Technology, South Africa.

Kim, Y-H., Koczo, K., Wasan, D.T. 1997. Dynamic film and interfacial tensions in emulsion and foam systems. *Journal of colloid and interface science*. 187(1):29-44.

Kitchener, J.A., and Mussellwhite, P.R. 1968. The theory of stability of emulsions. Sherman, P. (Ed.). *Emulsion science*. Chap.2. London: Academic press.

Kruss. 2005. *Instruction manual* V2-05, K100 Tensiometer.

Kumaraswamy, G. 2005. Crystallization of polymers from stressed melts. *Journal of macromolecular science, part C: Polymer reviews*, 45(4):375-397.

Lacroix, C., Bousmina, M., Carreau, P.J., Favis, B.D., and Michel A. 1997. Properties of PETG/EVA blends: Viscoelastic, morphological and interfacial properties, part I. *Polymer*, 37(14):2939-2947.

Larson, R.G. 1999. *The structure and rheology of complex fluids*. New York: Oxford University Press.

Lissant, K.J. 1966. The geometry of high-internal-phase-ratio emulsions. *Journal of colloid and interface science*, 22(5):462-468.

Lissant, K.J. 1974. *Emulsion and Emulsion Technology*. Part 1, p. 103. New York: Marcel Dekker

Lissant, K.J., Mayhan, K.G. 1973. A study of medium and high internal phase ratio water/polymer emulsions. *Journal of colloid and interface science,* 42(1):201-208.

Lissant, K.J., Peace, B.W., Wu, S.H., Mayhan, K.G. 1974. Structure of high-internal-phase-ratio emulsions. *Journal of colloid and interface science,* 47(2):416-423.

Lizarraga, M.S., Pan, L.G., Anon, M.C., Santiago, L.G. 2008. Stability of concentrated emulsions measured by optical and rheological methods. Effect of processing conditions – I. Whey protein concentrate. *Food hydrocolloids*, 22(5):868-878.

Loewenberg, M., and Hinch, E. 1997. Collision of two deformable drops in shear flow. *Journal of fluid mechanics*, 338:299-315.

Loncin, M., Merson, R.L. 1979. *Food engineering: principles and selected applications*. New York – USA: Academic Press.

Lucassen-Reynders, E.H., Kuijpers, K.A. 1992. The role of interfacial properties in emulsification. *Colloids and surfaces*, 65(2-3):175-184.

Mader, C.L. 1965. Initiation of detonation by the interaction of shocks with density discontinuities. *Physics of fluids,* 8:1811-1816.

Malkin, A.Y. 1994. *Rheology Fundamentals*. Canada: ChemTec Publishing.

Malkin, A. Ya., Masalova, I., Slatter, P., & Wilson, K. 2004a. Effect of droplet size on the rheological properties of highly-concentrated w/o emulsions. *Rheologica acta*, 43(6):584-591.

Malkin, A. Ya., Masalova, I., Pavlovski, D., and Slatter, P. 2004b. Is the choice of flow curve fitting equation crucial for the estimation of pumping characteristics? *Applied rheology*, 14(2):89-95.

Mandelkern, L. 1964. *Crystallization of Polymers.* New York: McGraw-Hill.

Manka, J.S. 2004. Factors that affect the chemical gassing of emulsion explosives. *Proceedings of the 30th annual conference on explosives and blasting technique.*

Masalova, I., Malkin, A. Ya., Slatter, P., Wilson, K. 2003. The rheological characterization and pipeline flow of high concentration water-in-oil emulsions. *Journal of Non-Newtonian fluid mechanics,* 112(2-3):101-114.

Masalova, I., Taylor, M., Kharatiyan, E., & Malkin, A. Ya. 2005. Rheopexy in highly concentrated emulsions. *Journal of rheology,* 49(4):839-849.

Masalova, I., Malkin, A.Ya., Ferg, E., Kharatiyan, E., Taylor, M., and Haldenwang, R. 2006. Evolution of rheological properties of highly concentrated emulsions with aging—Emulsion-to-suspension transition. *Journal of Rheology*, 50(4):435-451.

Masalova, I., Malkin, A. Ya. 2007a. Peculiarities of rheological properties and flow of highly concentrated emulsions: the role of concentration and droplet size. *Colloid journal,* 69(2):185-197.

Masalova, I., Malkin, A. Ya. 2007b. Rheology of highly concentrated emulsions – concentration and droplet size dependencies. *Applied rheology,* 17(4):42250-1 – 42250-9.

Masalova, I., Malkin, A. Ya. 2008. Master curves for elastic and plastic properties of highly concentrated emulsions. *Colloid journal,* 70(3):327-336.

Mason, T.G., Bibette, J., and Weitz, D.A. 1996. Yielding and flow of monodisperse emulsions. *Journal of colloid and interface science*, 179(2):439-448.

Mazzanti, G., Guthrie, S.E., Sirota, E.B., Marangoni, A.G., & Idziak, S.H.J. 2004. Novel shear-induced phases in cocoa butter. *Crystal growth & design*, 4(3):409-411.

McBain, J.L., Collie, B., and Black, W. 1961. *Surface activity: the physical chemistry, technical applications and chemical constitution of surface active agents.* 2nd ed. UK: Spon.

McClements, D.J. 1999. *Food Emulsions. Principles, Practice, and Technology*. Boca Raton, USA: CRC Press.

McClements, D.J. 2005. *Food Emulsions. Principles, Practice, and Technology*. 2nd ed. Boca Raton, USA: CRC Press.

McKenzie, L.F., and Lawrence, D.L. 1990. Emulsion explosives containing a polymeric emulsifier. *United states patent*, Patent number: 4931110.

Mitchell, K.A.W. 1984. Emulsion explosive composition. *United stated patent*, Patent number: 4448619.

Mittal, K.L.(Ed.) 1975. *Colloidal dispersions and micellar behaviour*. Washington: American chemical society.

Monks, A.W., White, H.M., and Bassett, D.C. 1996. On shish-kebab morphologies in crystalline polymers. *Polymer*, 37(26):5933-5936.

Mulder, H., and Walstra, P. 1974. *The milk fat globule – Emulsion science as applied to milk products and comparable foods.* England: Commonwealth Agricultural Bureaux.

Mutaftschiev, B. 1993. Nucleation theory. Hurle, D. T. J. (ed). *Handbook of crystal growth, Vol.1. Fundamentals, Part A: thermodynamics and kinetics*. North Holland:Amsterdam.

Myers, D. 1988. *Surfactant science technology*. Weinheim, Germany: VCH.

Myers, D. 1992. *Surfactant science and technology*. 2nd ed. New York: VCH.

Narine, S.S., Marangoni, A. G. 1999. Relating structure of fat crystal network to mechanical properties: a review. *Food research international*, 32(4):227-248.

Nie, S. 1997. Pressure desensitization of a gassed emulsion explosive in comparison with micro-balloon sensitized emulsion explosives. *Proceedings of the annual symposium on explosives and blasting Research*:161-172.

Nkomo, S.E. 2005. *Using rheometry for predicting the pumping characteristics of highly concentrated w/o explosive emulsions*. Master thesis, Cape Peninsula University of Technology, South Africa.

Olson, D.W., White, C.H., and Richter, R.L. 2004. Effect of Pressure and Fat Content on Particle Sizes in Microfluidized Milk. *Journal of dairy science*, 87(10):3217-3223.

Orr, C. 1988. Determination of particle size. Becher, P. (ed). *Encyclopedia of emulsion technology*. Vol. 3. New York: Marcel Dekker: chap. 3.

Otsubo, Y., Prud'homme, R.K. 1994a. Rheology of oil-in-water emulsions. *Rheologica Acta*, 33(1):29-37.

Otsubo, Y., Prud'homme, R.K. 1994b. Effect of drop size distribution on the flow behaviour of oil-in-water emulsions. *Rheologica Acta*, 33(4):303-306.

Pal, R. 1996a. Rheology of emulsions containing polymeric liquids. Becher, P. (Ed.). *Encyclopedia of Emulsion Technology*. pp.93-293. New York – USA: Marcel Dekker, New York.

Pal, R. 1996b. Effect of droplet size on the rheology of emulsions. *AIChe journal,* 42(11):3181-3190.

Pal, R. 1997. Scaling of relative viscosity of emulsions. *Journal of rheology*, 41(1):141-150.

Pal, R. 1999. Anomalous wall effects in parallel plate torsional flow of highly concentrated emulsions. *American society of mechanical engineers*, 249:137-150.

Pal, R. 2002. Novel shear modulus equations for concentrated emulsions of two immiscible elastic liquids with interfacial tension. *Journal of non-Newtonian fluid mechanics*, 105(1):21-33

Papke, B.L., Robinson, L.M. 1994. Factors affecting poly(isobutenyl)succinimide dispersant adsorption onto surfactant-coated colloidal particles in nonaqueous media. *Langmuir*, 10(6):1635-2034.

Pare, J.R.J. 1981. Kinetics and mechanism of reaction of thiourea nitrite in a highly ionic medium. *Indian journal of chemistry* 20A:1116-1119.

Park, S.H., Yamaguchi, T., Nakao, S. 2001. Transport mechanism of deformable droplets in micro&ltration of emulsions. *Chemical engineering science*, 56(11):3539–3548

Partal, P., Guerrero, A., Berjano, M., and Gallegos, C. 1997. Influence of concentration and temperature on the flow behaviour of oil-in-water emulsions stabilized by sucrose palmitate. *Journal of the american oil chemists' society*, 74(10):1203-1212.

Phipps, L.W. 1985. *The high pressure dairy homogenizer*. England: Reading – the national institute for research in dairying, reading.

Pons, R., Solans, C., and Tadros, T.F. 1995. Rheological behaviour of highly concentrated oil-in-water o/w emulsions. *Langmuir*, 11(6):1966-1971.

Ponton, A., Clement, P., Grossiord, J.L. 2001. Collaboration of Princen's theory to cosmetic concentrated water-in-oil emulsion. *Journal of rheology*, 45(2):521-526.

Princen, H.M. 1979. Highly Concentrated Emulsions: I. Cylindrical Systems. *Journal of colloid and interface science,* 71:55-66.

Princen, H.M. 1983. Rheology of foams and highly concentrated emulsions. I. Elastic properties and yield stress of a cylindrical modes system. *Journal of colloid and interface science,* 91(1):160-175.

Princen, H.M. 1985. Rheology of foams and highly concentrated emulsions. II. Experimental study of the yield stress and wall effects for concentrated oil-in-water emulsions. *Journal of colloid and interface science*, 105(1):150-171.

Princen, H.M. 1988. Pressure/volume/surface area relationships in foams and highly concentrated emulsions: Role of volume fraction. *Langmuir*, 4(1):164-169.

Princen, H.M., Aronson, M.P., Moser, J.C. 1980. Highly Concentrated Emulsions: II. Real Systems. The Effect of Film Thickness and Contact Angle on the Volume Fraction in Creamed emulsions. *Journal of colloid and interface science*, 75:246-271.

Princen, H.M., Kiss, A.D. 1986. Rheology of foams and highly concentrated emulsions. III. Static shear modulus. *Journal of colloid and interface science*, 112(2):427-437

Princen, H.M., Kiss, A.D. 1989. Rheology of foams and highly concentrated emulsions. IV. An experimental study of the shear viscosity and yield stress of concentrated emulsions. *Journal of colloid and interface science*, 128(1):176-187.

Rallison, J.M. 1980. Note on the time-dependent deformation of a viscous drop which is almost spherical. *Journal of fluid Mechanics*, 98(3):625-633.

Reinelt, D.A., Kraynik, A.M. 1993. Large elastic deformations of three-dimensional foams and highly concentrated water-in-oil emulsions (gel emulsions). *Journal of colloid and interface science*, 159(2):460-470.

Reynolds, P.A., Gilbert, E.P., and White, J.W. 2000. High internal phase water-in-oil emulsions studied by small-angle neutron scattering. *The journal of physical chemistry B*, 104(30):7012-7022.

Robin, O., Blanchot, V., Vuillemard, J.C., Paquin, P. 1992. Microfluidization of dairy model emulsions. I. Preparation of emulsions and influence of processing and formulation on the size distribution of milk fat globules. *Lait*, 72(6):511-531.

Robin, O., Kalab, M., Britten, M., Paquin, P. 1996. Microfluidization of model dairy emulsions. II. Influence of composition and process factors on the protein surface concentration. *Lait*, 76(6):551-570.

Romero, A., Cordobes, F., Puppo, M. C., Guerrero, A., & Bengoechea, C. 2008. Rheology and droplet size distribution of emulsions stabilized by crayfish flour. *Food hydrocolloids*, 22(6):1033-1043.

Rother, M.A., Zinchenko, A.Z., and Davis, R.H. 1997. Buoyancy-driven coalescence of slightly deformable drops. *Journal of fluid mechanics*, 346:117-148.

Rudnick, L.R. (ed.). 2003. *Lubricant Additives: Chemistry and Applications*. USA: CRC Press.

Rumscheidt, F.D., Mason, S.G. 1961. Particle motions in sheared suspensions. XII. Deformation and burst of fluid drops in shear and hyperbolic flow. *Journal of colloid and interface Science*, 16:238-261.

Saboni, A., Gourdon, C., Chesters, A.K. 1995. Drainage and Rupture of Partially Mobile Films during Coalescence in Liquid-Liquid Systems under a Constant Interaction Force. *Journal of colloid and interface science*, 175(1):27-35.

Salager, J.-L., Forgiarini, A., Marquez, L., Pena, A., Pizzino, A., Rodriguez, M.P., Gonzalez, M.R. 2004. Using emulsion inversion in industrial process. *Advances in colloid and interface science*, 108-109:259-272.

Sato, K. 2001. Crystallization behaviour of fats and lipids – a review. *Chemical engineering science,* 56(7):2255-2265.

Schubert, H., and Engel, R. 2004. Production and formulation engineering of emulsions. *Trans IchemE, Part A. chemical engineering research and design*, 82(9):1137-1143.

Shaw, D.J. 1970. *Introduction to colloid and surface chemistry*. 2nd ed. London: Butterworths.

Sherman, P. 1968. *Emulsion Science. (*Ed.). London – UK: Academic press.

Shinoda, K., and Friberg, S. 1986. *Emulsions and solubilization*. New York: John Wiley & son.

Slatter, P.T. 1999. The role of rheology in the pipelining of mineral slurries. *Mineral processing and extractive Metallurgy review*, 20(1):281-300.

Slatter, P.T. 2002. Non-Newtonian Laminar Pipe Flow – A place in the sun at last; invited keynote address – *11th International Conference on transport and sedimentation of solid Particles* – Ghent, 33-40.

Slatter, P.T., Chhabra, R.P. 2002. Lecture notes: the flow of non-Newtonian slurries and sludges. *Cape Town: Cape peninsula university of technology (former Cape Technikon)*:16 July – 19 July.

Slatter, P.T., Wasp, E.J. 2002. Yield stress – How low can you go? *11th International Conference on transport and sedimentation of solid Particles* – Ghent, 173-182.

Somani, R.H., Yang, L., Benjamin, S.H., Sun, T., Pogodina, N.V., and Lustiger, A. 2005. A shear-induced molecular orientation and crystallization in isotactic polypropene: Effects of the deformation rate and strain. *Macromolecules*, 38(4):1244-1255.

Somani, R.H., Yang, L., Zhu, L., Benjamin, S.H. 2005. Flow-induced shish-kebab precursor structures in entangled polymer melts. *Polymer*, 46(20):8587-8623.

St. Angelo, A.J. 1989. A brief introdution to food emulsions and emulsifiers, Charalambous, G., Doxastakis, G. (Eds). *Food emulsifiers: chemistry, technology, functional properties and applications*. Amsterdam: Elsevier.

Stone, H.A. 1994. Dynamics of drop deformation and breakup in viscous fluids. *Annual review of fluid mechanics*, 26:65-102.

Sudweeks, W.B., Jessop, H.A. 1980a. Emulsion blasting composition. *United stated patent*, Patent number: 4216040.

Sudweeks, W.B, Lawrence, L.D. 1980b. Emulsion blasting agent sensitized with perlite. *United stated patent*, Patent number: 4231821.

Sumiya, F., Hirosaki,Y., Kato,Y. 2002. Detonation velocity of precompressed emulsion explosives. *Proceedings of the annual conference on explosives and blasting technique*:253-263.

Swayambunathan, V., Mukesh, D., Krishnan, S., Chikale, S.V., Ghosh, P.K. 1993. Concentrated emulsions. 4. Freeze fracture SEM studies of chemically generated voids. *Journal of colloid and interface science,* 156(1):66-71.

Sychev, A.I. 1985. Shock-wave ignition of liquid-gas bubble systems. *Combustion, explosion, and shock waves*, 21:250-254.

Sychev, A.I. 1995. The effect of bubble size on the detonation wave characteristics. *Combustion, explosion and shock waves*, 31:577-584.

Sychev, A.I. 1997. Bubble detonation in polydisperse media. *Combustion, explosion and shock waves*, 33:339-343.

Tanford, C. 1980. *The Hydrophobic Effect*. New York: John Wiley & Sons.

Tanner, R. 2000. *Engineering rheology*, 2nd Ed., New York: Oxford University press.

Taylor, G.I. 1932. The Viscosity of a fluid containing small drops of another fluid. *Proceedings of the royal society of london. series A*, 138(834):41-48.

Taylor, G.I. 1934. The Formation of Emulsions in Definable Fields of Flow. *Proceedings of the royal society of london. series A*, 146(857):501-523.

Taylor, G.I. 1964. Static conical drop shape model. *Processing of the International Congress on Applied Mechanics*, (11):790-796.

The physics classroom. (1996 – 2009) *Definition and mathematics of work*, http://www.physicsclassroom.com/Class/energy/U5L1a.ht).

Thomas, G.M. 2002. *The rheology handbook: For users of rotational and oscillatory rheometers*. Hannover, Germany: Vincentz Verlag

Torza, S., Cox, R.G., Mason, S.G. 1972. Particle motions in sheared suspensions. XXVII. Trancient and steady deformations and bust of liquid drops. *Journal of colloid and interface science*, 38(2):395-411.

Tunon, I., Silla, E., and Pascual-Ahuir, J.L. 1992. Molecular surface area and hydrophobic effect. *Protein engineering design and selection*, 5(8):715-716.

Turner, D., Dlugogorski, B., Palmer, T. 1999. Factors affecting the stability of foamed concentrated emulsions. *Colloids and surfaces A: physicochemical and engineering aspects*, 150(1-3):171-184.

Van Boekel, M.A.J.S., Walstra, P. 1981a. Stability of oil-in-water emulsion with crystals in the disperse phase. *Colloids and Surfaces*, 3:109-118

Van Boekel, M.A.J.S., Walstra, P. 1981b. Effect of coquette flow on stability of oil-in-water emulsions. *Colloids and surfaces*, 3:99-107.

Vanapalli, S.A., Coupland, J.N. 2001. Emulsions under shear – the formation and properties of partially coalesced lipid structure. *Food hydrocolloids*, 15(4-6):507-512.

Vanapalli, S.A., Palanuwech, J., Coupland, J.N. 2002. Stability of emulsions to dispersed phase crystallization: effect of oil type, dispersed phase volume fraction, and cooling rate. *Colloids and surfaces A: Physicochemical and engineering aspects*, 204(1-3):227-237.

Varga, J., Karger-Kocsis, J. 1996. Rules of supermolecular structure formation in sheared isotactic polypropylene melts. *Journal of polymer science: Part B: Polymer physics*, 34(4):657-670.

Vleeshouwers, S., Meijer, H.E.H. 1996. A rheological study of shear induced crystallization. *Rheologica Acta*, 35(5):391-399.

Wade, C.G. 1978. Water-in-oil emulsion explosive composition. *United stated patent*, Patent number: 4110134.

Wade, C.G. 1979a. Cap sensitive emulsions containing perchlorates and occluded air and method. *United stated patent*, Patent number: 4149916.

Wade, C.G. 1979b. Cap sensitive emulsions without any sensitizer other than occluded air. *United stated patent*, Patent number: 4149917.

Walstra, P. 1983. Formation of emulsions, Becher, P. (Ed). *Encyclopedia of emulsion technology*. Vol. 1. New York: Marcel Dekker.

Walstra, P. 1993a. Introduction to aggregation phenomenon in food colloids. Dickinson, E., Walstra, P. (Eds). *Food colloids and polymers: stability and mechanical properties*. Cambridge – UK: Royal society of chemistry.

Walstra, P. 1993b. Principles of emulsion formation. *Chemical engineering science,* 48:333-349.

Walstra, P. 1996a. Emulsion stability. Becher, P. (Ed). *Encyclopedia of emulsion technology.* Vol. 4. New York: Marcel Dekker.

Walstra, P. 1996b. Disperse systems: Basic considerations. Fennema, O.R. (Ed). *Food chemistry*. 3rd edition, chapter 3. New York: Marcel Dekker.

Walstra, P., Oortwijn, H. 1982. The membranes of recombined fat globules. 3. Mode of formation. *Netherlands milk and dairy journal*, 36:103-133.

Webber, R.M. 1999. Relation between Laplace pressure and the rheology of high internal phase emulsions. American institute of chemical engineers–AIChE,:226-232.

Walstra, P., Wouters, J.T.M., & Geurts, T.J. 2005. *Dairy science technology.* U.S.A: CRC Boca Raton.

White, H.M., Bassett, D.C. 1997. On variable nucleation geometry and segregation in isotactic polypropylene. *Polymer*, 38(22):5515-5520.

Williams, D.L.H. 1977. *S*-nitrosation of thiourea and thiocyanate ion. Nitrosyl thiocyanate and the *S*-nitroso-adduct of thiourea as nitrosating agents. *Journal of the chemical society, Perkin transactions,* 2:128-132.

Williams, A., Janssen, J.J.M., Prins, A. 1997. Behaviour of droplets in simple shear flow in the presence of a protein emulsifier. *Colloids and surfaces A: physicochemical and engineering aspects*, 125(2-3):189-200.

Windhab, E.J., Dressler, M., Feigl, K., Fischer, P., & Megias-Alguacil, D. 2005. Emulsion processing – from single-drop deformation to design of complex processes and products. *Chemical engineering science*, 60(8-9):2101-2113.

Wolkowicz, M.D. 1978. Nucleation and crystal growth in sheared poly-(1-butene) melts. *Journal of polymer science: polymer symposia,* 63(1):365-382.

Xuguang, W. 1994. *Emulsion explosives*. Beijing – China: Metallurgical industry press.

Yan, L., Thompson, K.E., Valsaraj, K.T. 2006. A numerical study on the coalescence of emulsion droplets in a constricted capillary tube. *Journal of colloid and interface science*, 298(2):832-844.

Yiantsios, S.G., Davis, R.H. 1991. Close approach and deformation of two viscous drops due to gravity and van der waals forces. *Journal of colloid and interface science*, 144(2):412-433.

Yorke, W.J., Binet, R., Lee, M.C., Bampfield, H.A. 1983. Water-in-oil emulsion blasting agents containing unrefined or partly refined petroleum product as fuel component. *United stated patent*, Patent number: 4404050.

Yu, W., Bousmina, M. 2003. Ellipsoidal model for droplet deformation in emulsions. *Journal of rheology*, 47(4):1011-1039.

Zank, J., Reynolds, P.A., Jackson, A.J., Baranyai, K.J., Perriman, A.W., Barkerb, J.G., Kim,M.-H., White, J.W. 2006. Aggregation in a high internal phase emulsion observed by SANS and USANS. *Physica B*, 385–386(Part 1):776-779.

Zhang, R., Min, M., Gao, Y., Lu, A., Yu, X., Huang, Y., & Lu, Z. 2008. Row nucleation phenomenon of poly(phenylene sulfide) under shear condition. *Materials letters*, 62(8-9):1414-1417.

Zhou, C., Yue, P., Feng, J.J. 2008. Deformation of a compound drop through a contraction in a pressure-driven pipe flow. *International journal of multiphase flow*, 34(1):102-109.

Ziegleder, G. 1985. Improved crystallization behaviour of cocoa butter under shearing. *International zeitschrift fur lebensmittel technologie und verffarenstechnik,* 36:412-416.

APPENDICES

Appendix A

Droplet size distribution of the sheared emulsion samples

a) ***PIBSA – MEA***

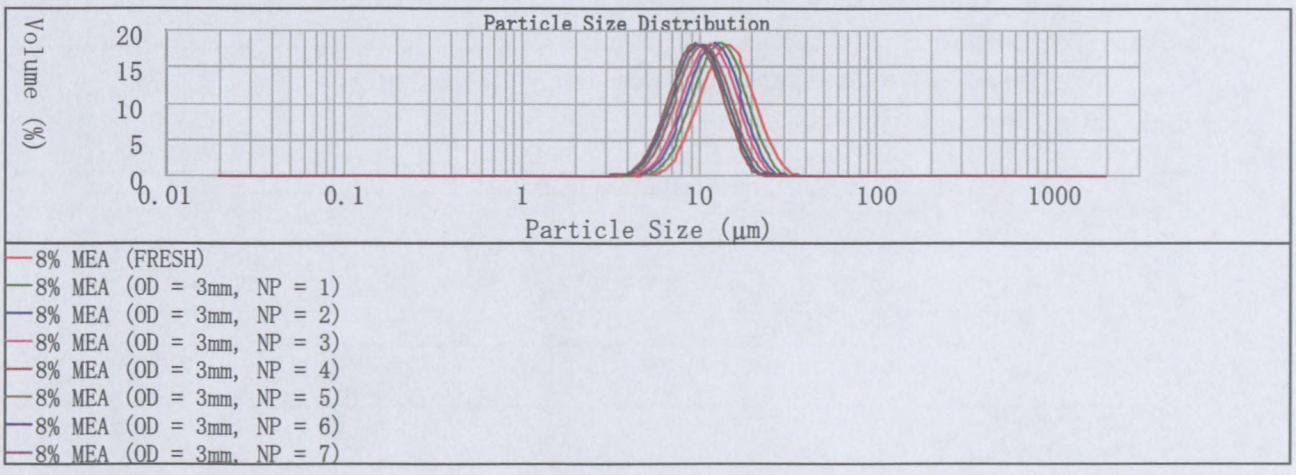

8% Pibsa-MEA in Mosspar-H (sheared using OD = 3mm)

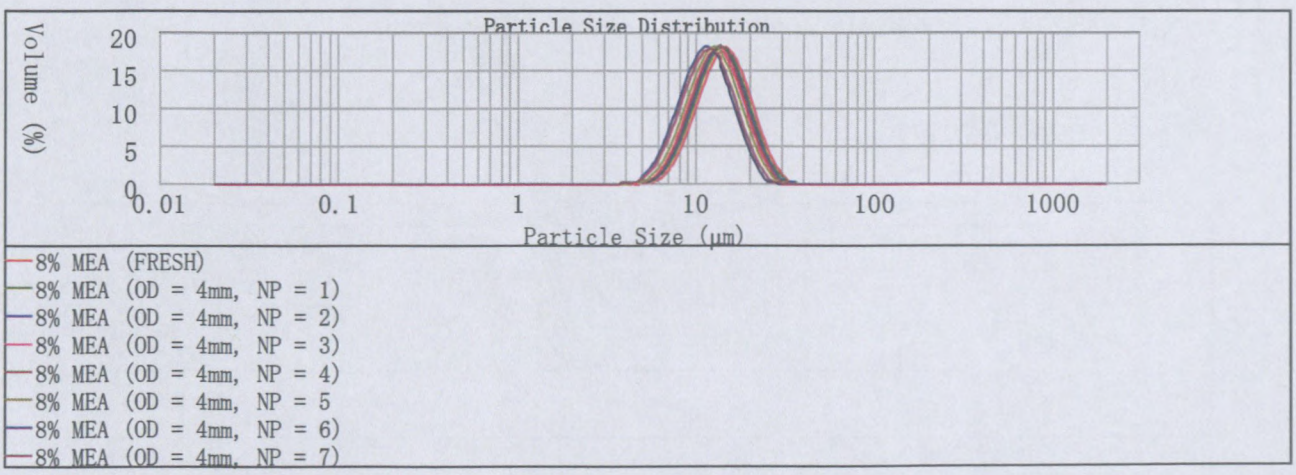

8% Pibsa-MEA in Mosspar-H (sheared using OD = 4mm)

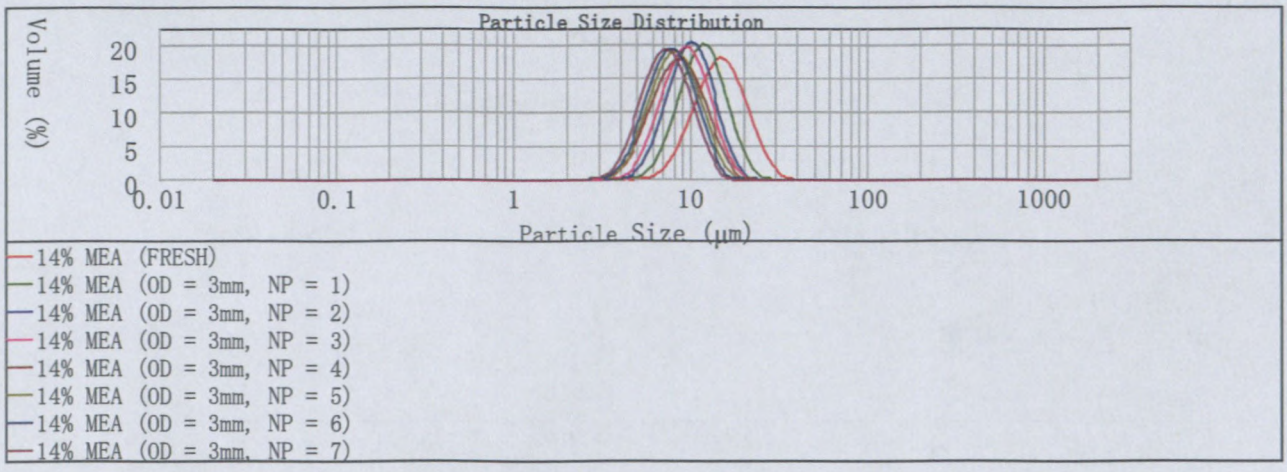

14% Pibsa-MEA in Mosspar-H (sheared using OD = 3mm)

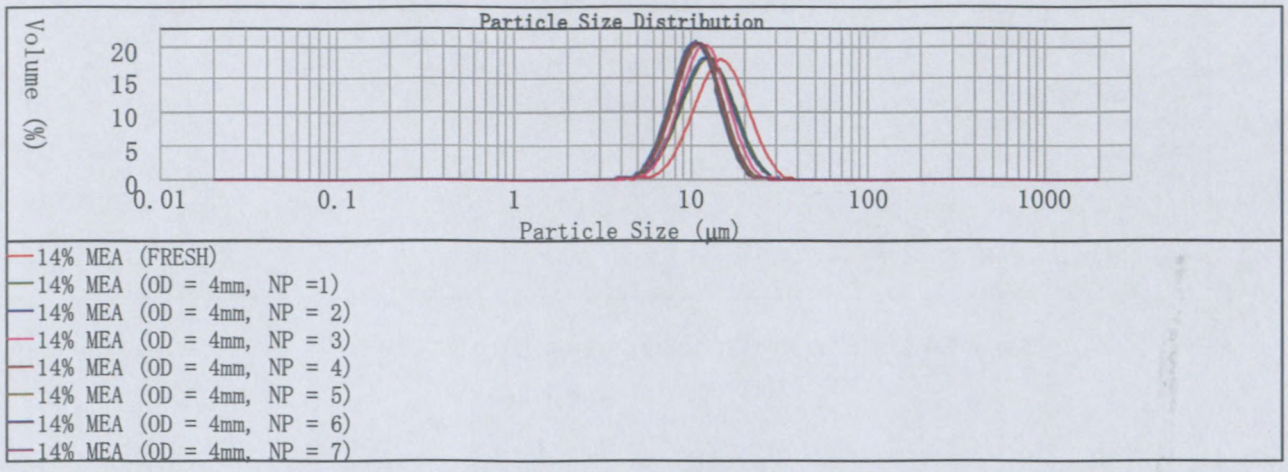

14% Pibsa-MEA in Mosspar-H (sheared using OD = 4mm)

b) PIBSA – IMIDE

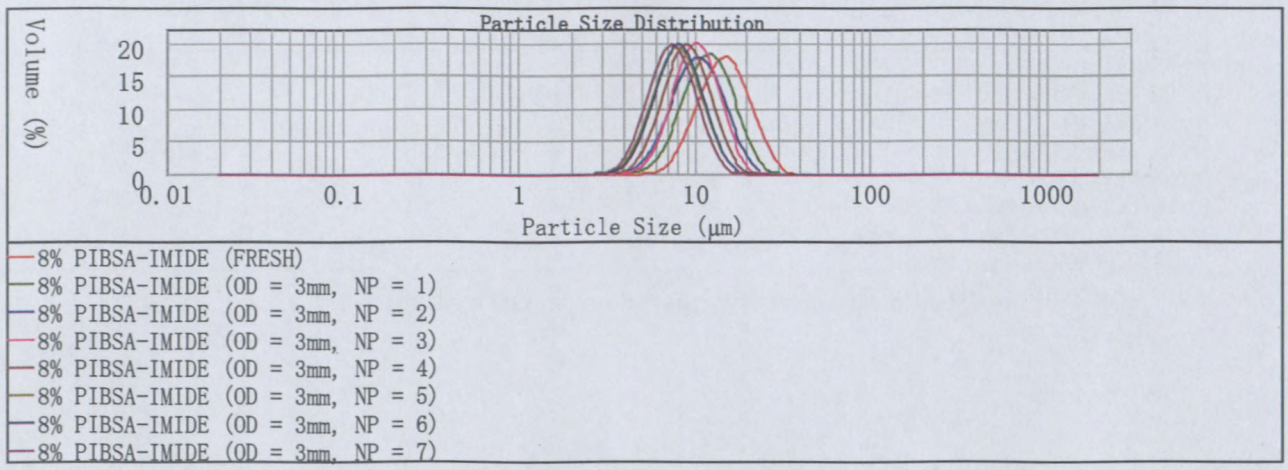

8% Pibsa-IMIDE in Mosspar-H (sheared using OD = 3mm)

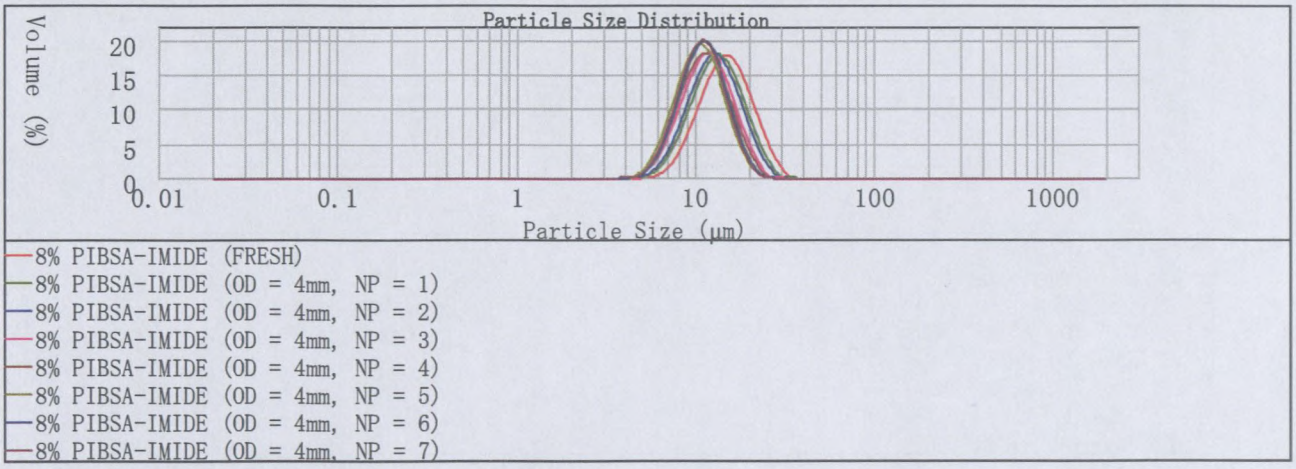

8% Pibsa-IMIDE in Mosspar-H (sheared using OD = 4mm)

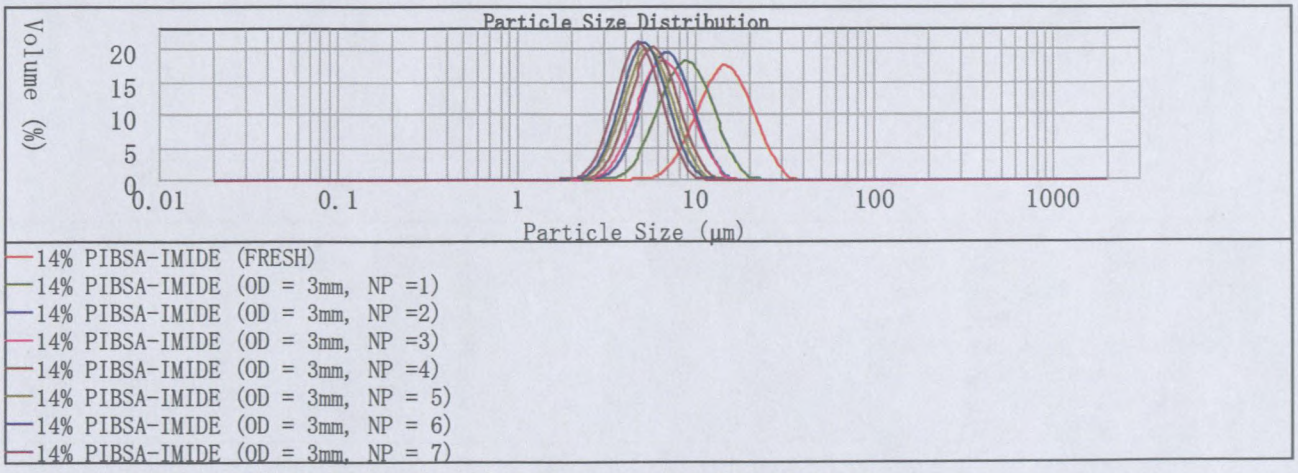

14% Pibsa-IMIDE in Mosspar-H (sheared using OD = 3mm)

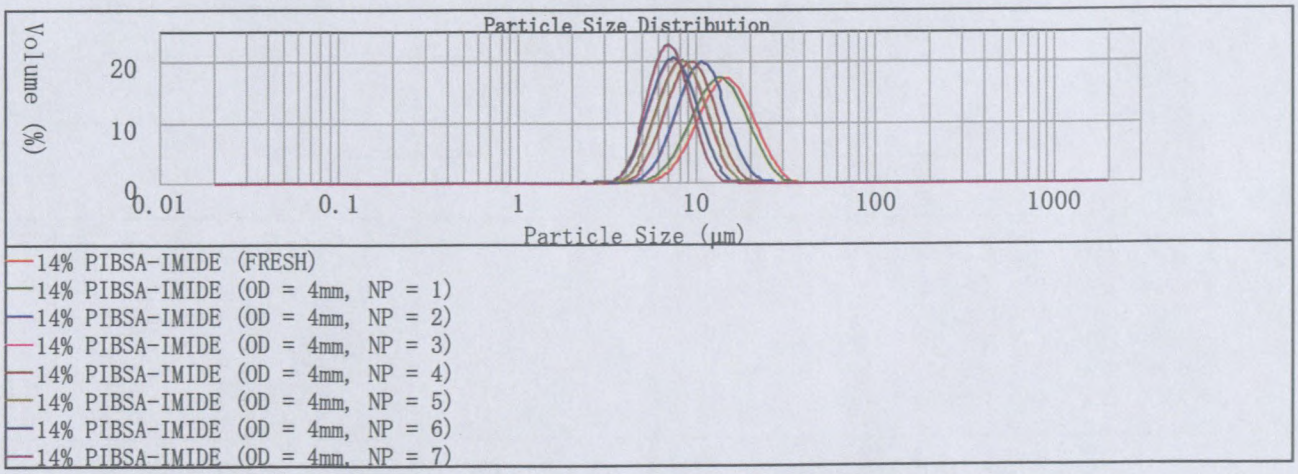

14% Pibsa-IMIDE in Mosspar-H (sheared using OD = 4mm)

c) ***PIBSA – UREA***

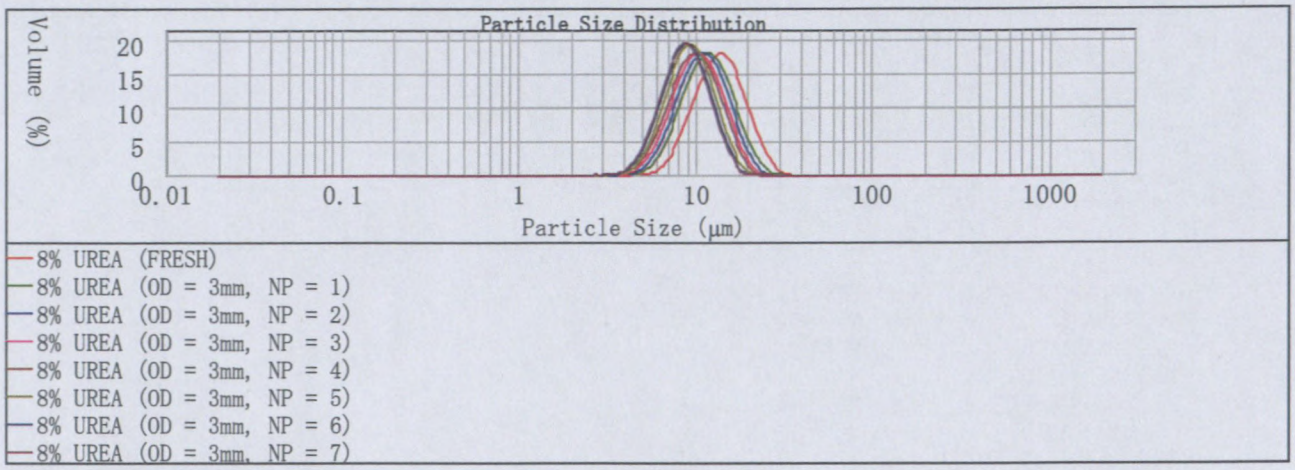

8% Pibsa-UREA in Mosspar-H (sheared using OD = 3mm)

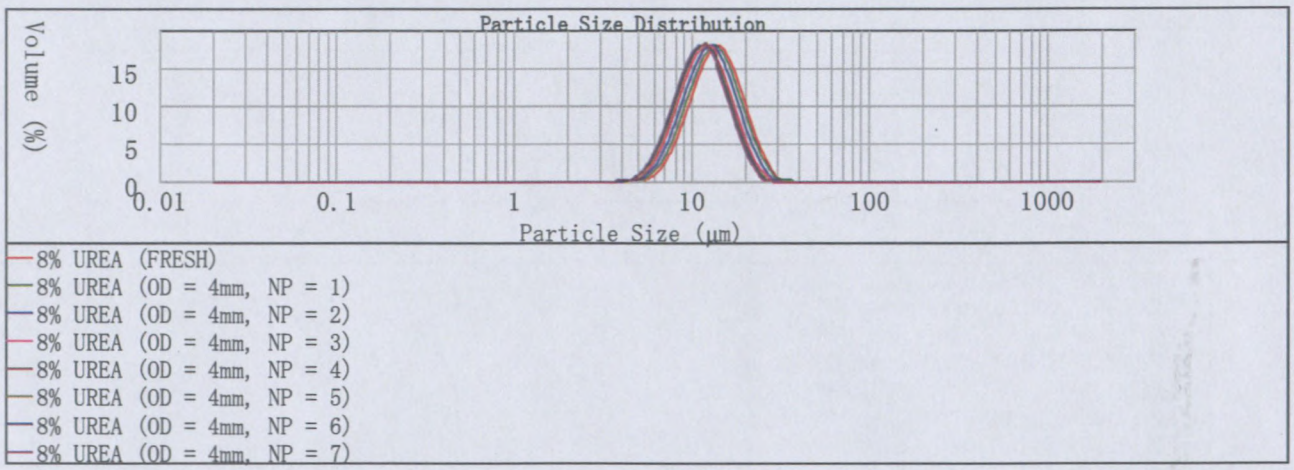

8% Pibsa-UREA in Mosspar-H (sheared using OD = 4mm)

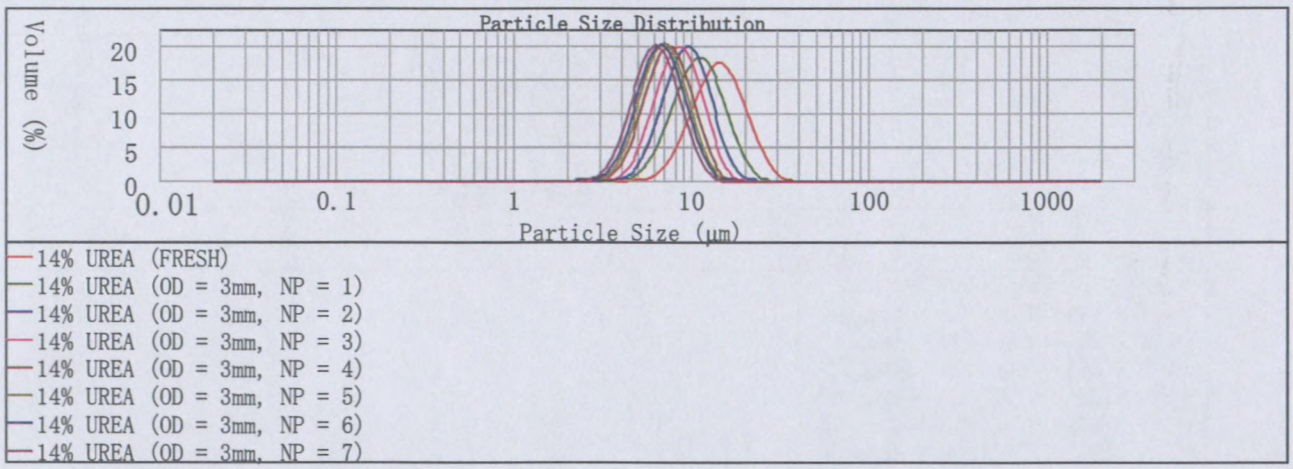

14% Pibsa-UREA in Mosspar-H (sheared using OD = 3mm)

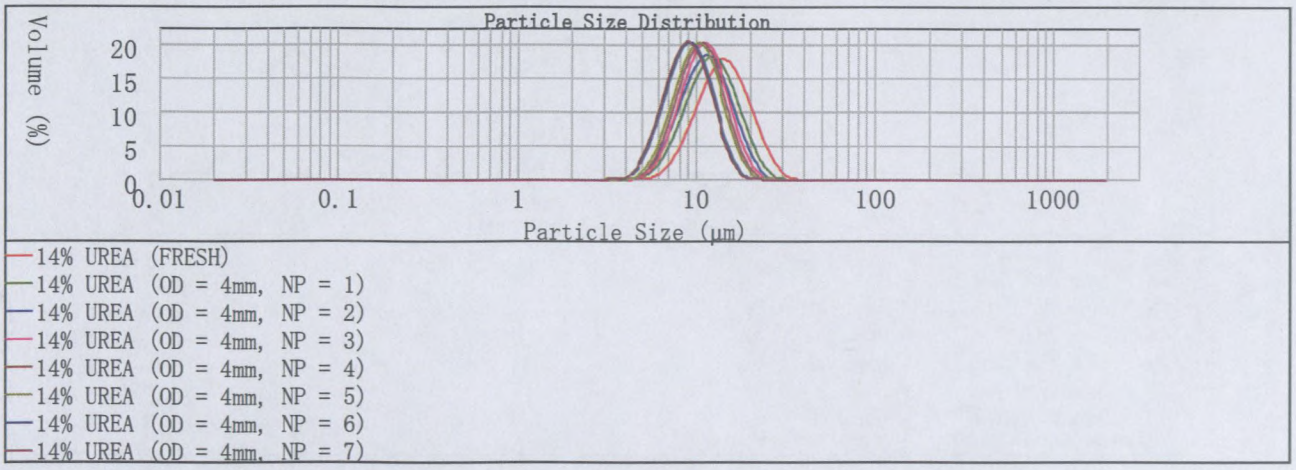

14% Pibsa-UREA in Mosspar-H (sheared using OD = 4mm)

d) PIBSA – MEA/SMO

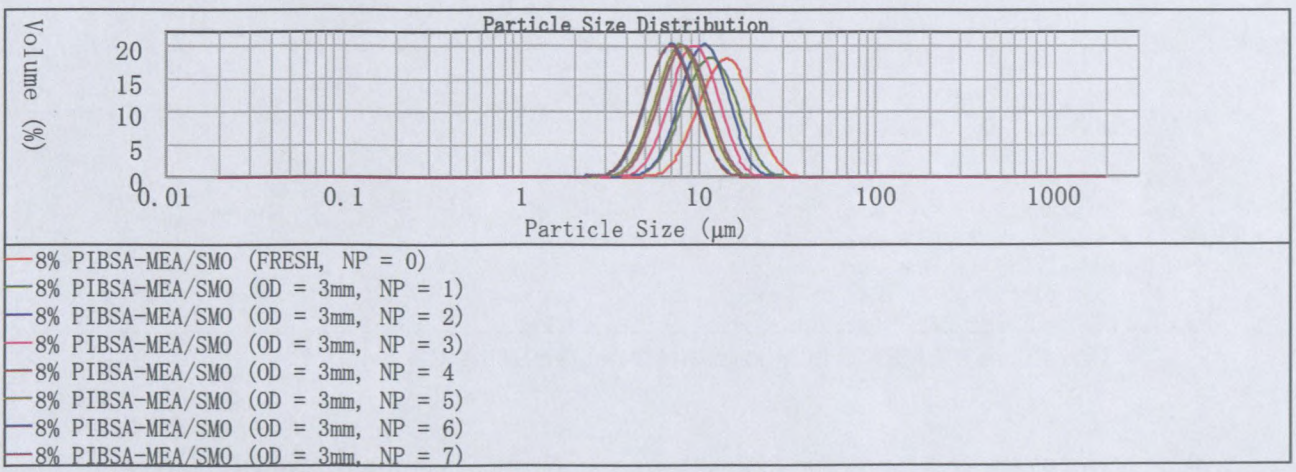

8% Pibsa-MEA/SMO in Mosspar-H (sheared using OD = 3mm)

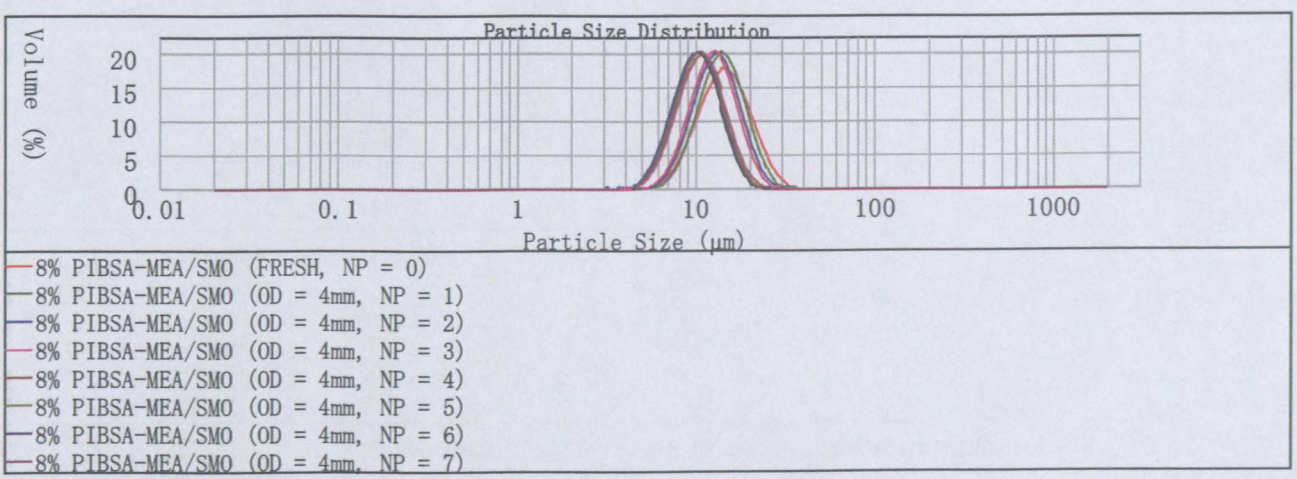

8% Pibsa-MEA/SMO in Mosspar-H (sheared using OD = 4mm)

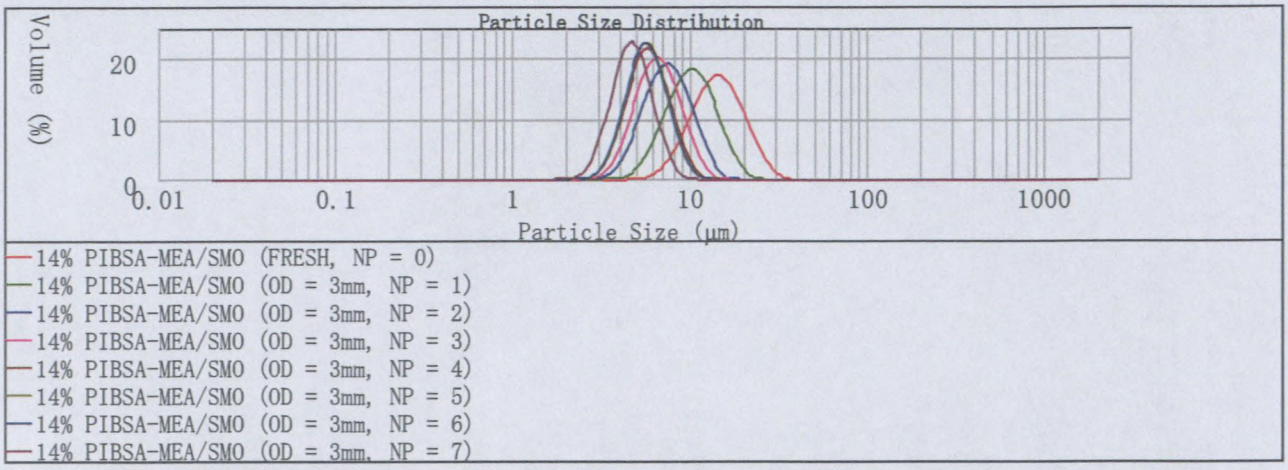

14% Pibsa-MEA/SMO in Mosspar-H (sheared using OD = 3mm)

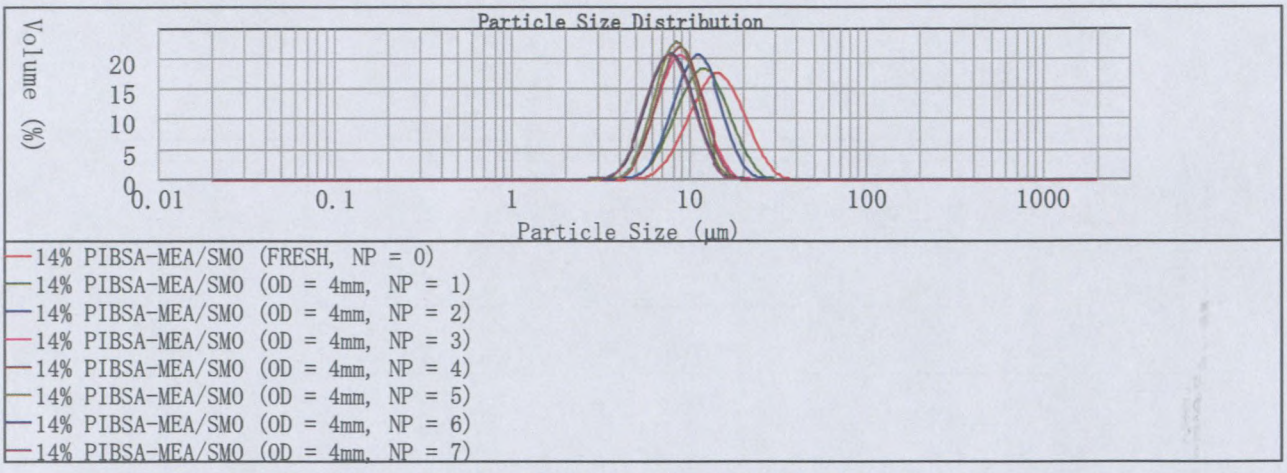

14% Pibsa-MEA/SMO in Mosspar-H (sheared using OD = 4mm)

e) The effect of Ammonium nitrate concentration (65% in the Dispersed phase)

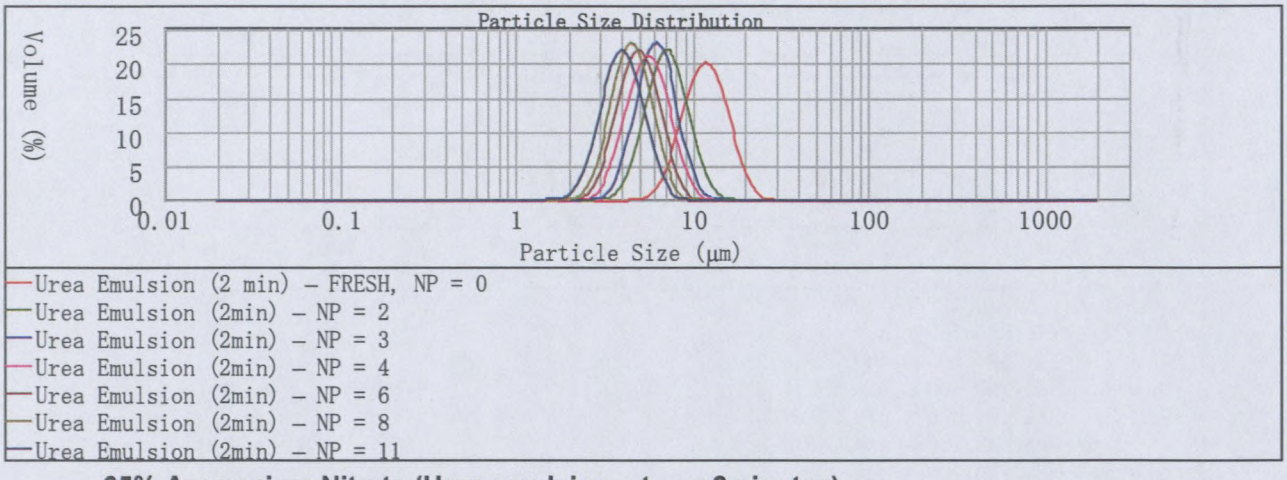

65% Ammonium Nitrate (Urea emulsion – t_{mix} = 2minutes)

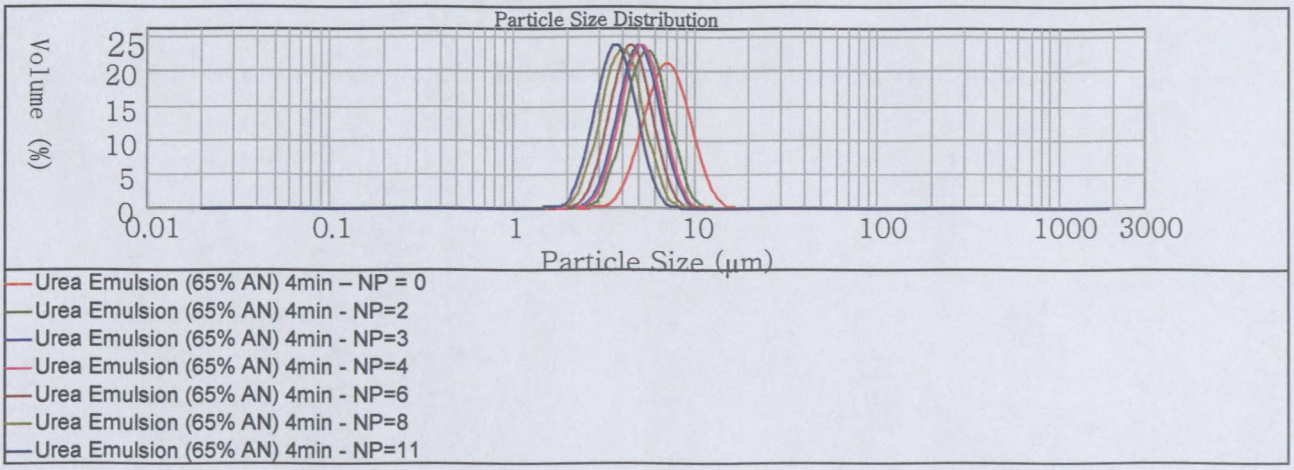

65% Ammonium Nitrate (Urea emulsion – t_{mix} = 4min)

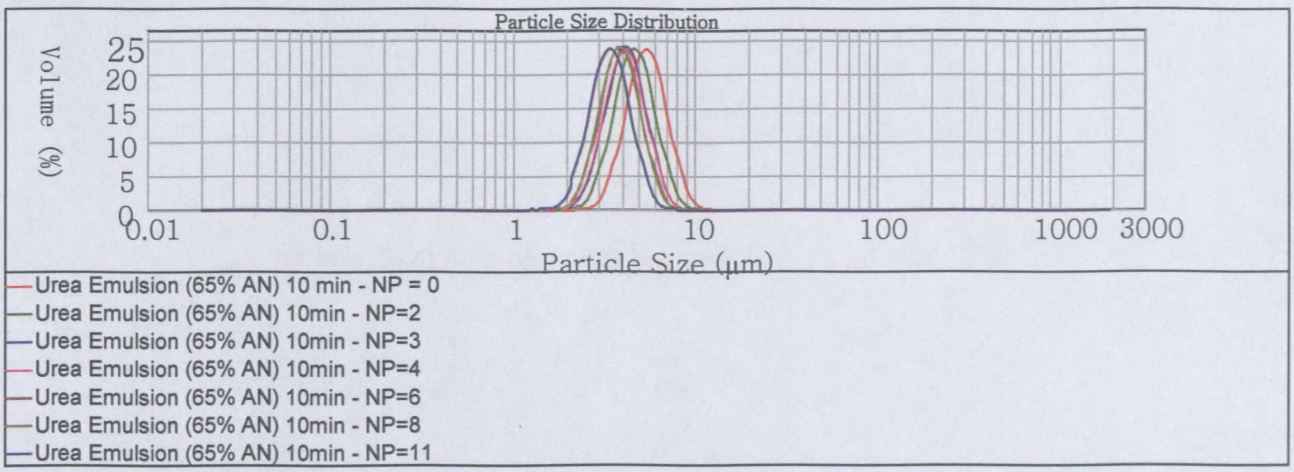

65% Ammonium Nitrate (Urea emulsion – t_{mix} = 10min)

Appendix B

Gauss fittings of size distribution of fresh and sheared emulsion samples

a) *PIBSA – MEA*

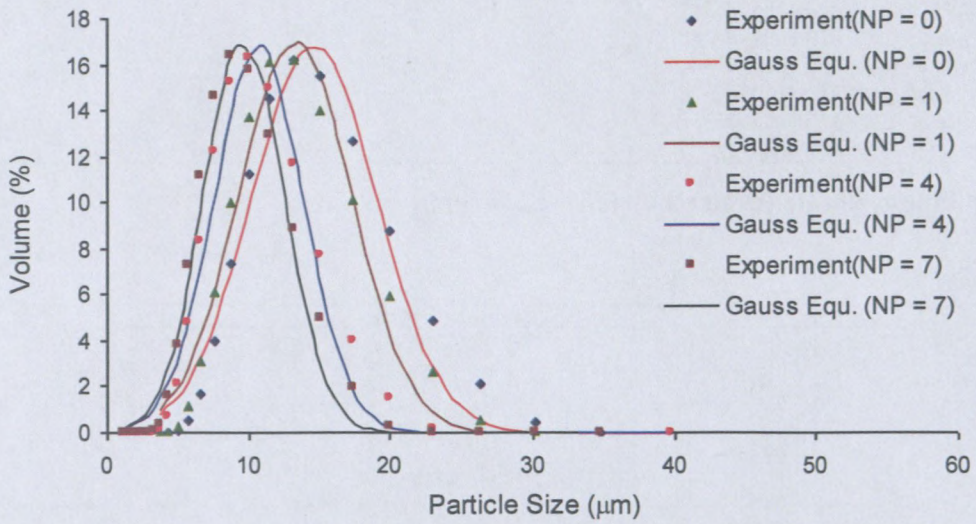

8% Pibsa-MEA in Mosspar-H (sheared using OD = 3mm)

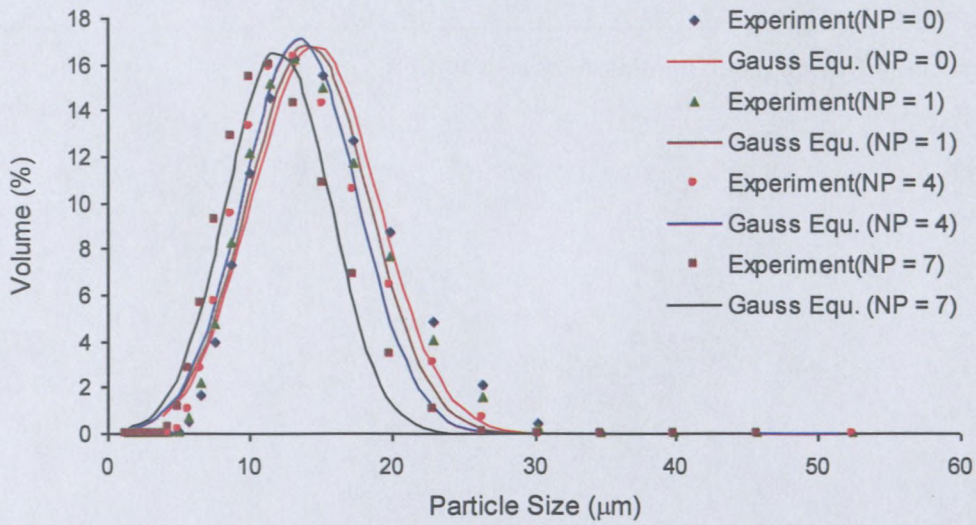

8% Pibsa-MEA in Mosspar-H (sheared using OD = 4mm)

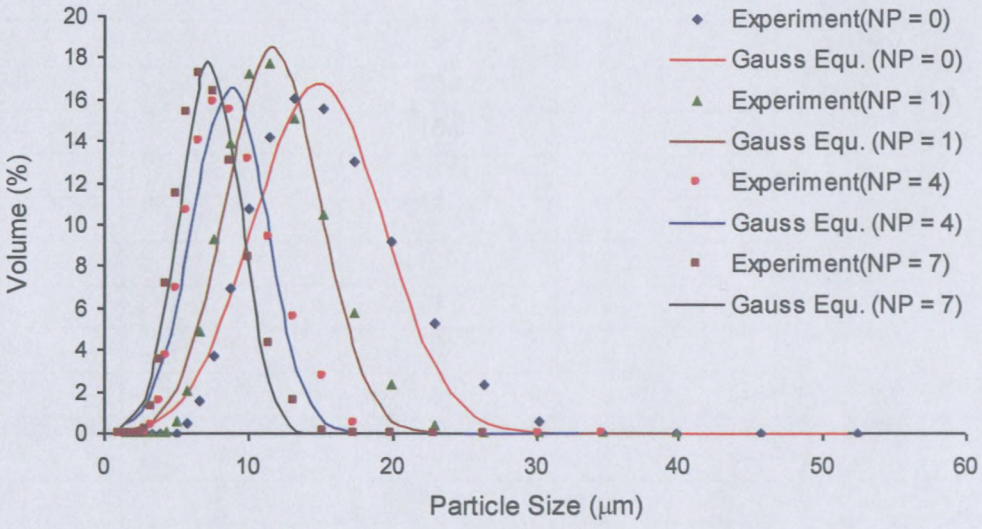

14% Pibsa-MEA in Mosspar-H (sheared using OD = 3mm)

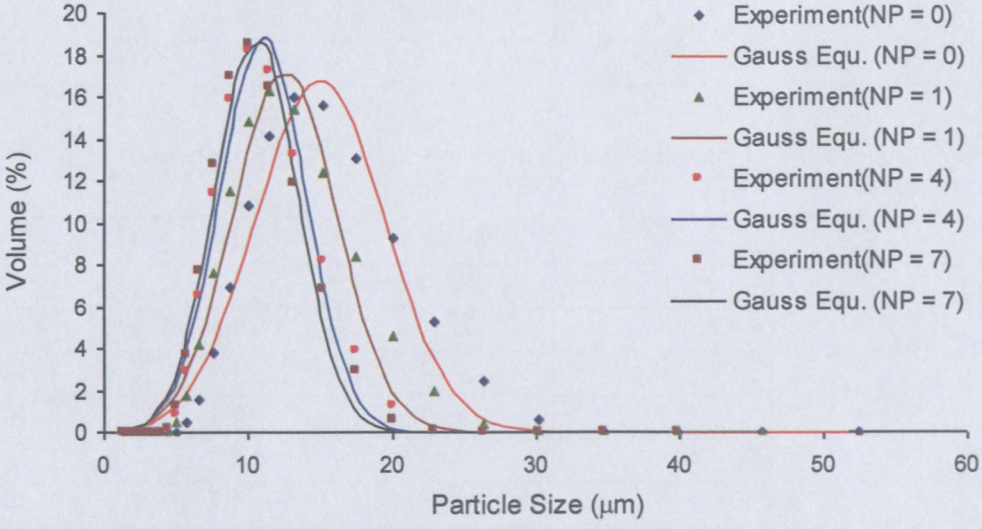

14% Pibsa-MEA in Mosspar-H (sheared using OD = 4mm)

Summary of table of the characterization of the width of DSD of sheared emulsion of formulation – 8% PIBSA-MEA in MOSSPAR-H

OD	NP	D_{50}	ω	A
3mm	0	14.63	8.8	186
	1	13.31	7.9	170
	2	12.3	7.3	157
	3	11.63	6.9	148
	4	10.7	6.4	136
	5	10.18	6	129
	6	10.07	6	128
	7	9.7	5.7	123
4mm	0	14.63	8.8	186
	1	14.12	8.4	179
	2	13.87	8.3	176
	3	13.53	8	172
	4	13.22	7.9	168
	5	12.72	7.6	161
	6	11.95	7.2	151
	7	11.51	6.9	146

Summary of table of the characterization of the width of DSD of sheared emulsion of formulation – 14% PIBSA-MEA in MOSSPAR-H

OD	NP	D_{50}	ω	A
3mm	0	14.89	7.2	159
	1	11.65	6.4	150
	2	9.96	5.4	129
	3	9.35	5.2	120
	4	8.63	5.2	109
	5	8.17	4.7	104
	6	7.77	4.4	100
	7	7.26	4.1	93
4mm	0	14.89	7.2	159
	1	12.5	7.2	157
	2	12.24	7.2	155
	3	11.73	6.4	151
	4	10.95	5.9	141
	5	10.72	5.8	138
	6	10.52	5.7	136
	7	10.35	5.6	134

b) PIBSA – IMIDE

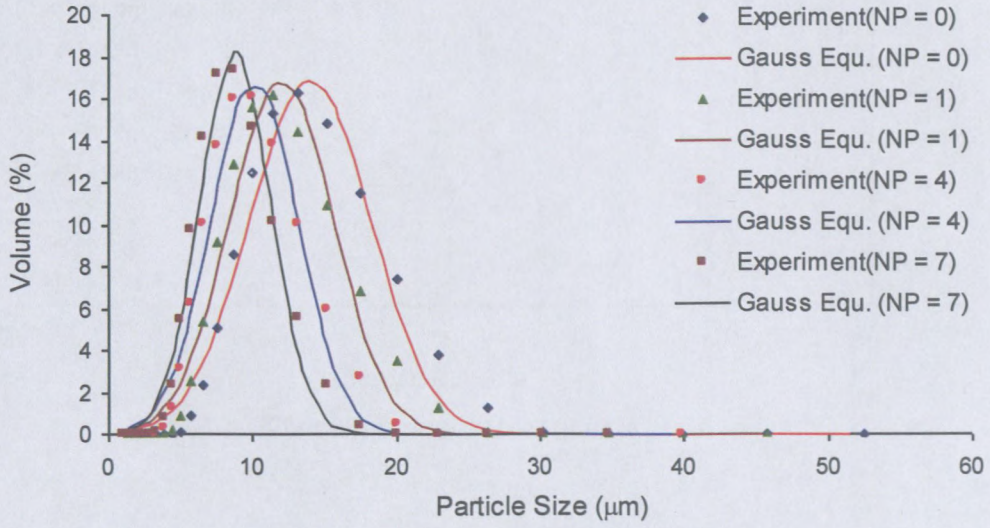

8% Pibsa-IMIDE in Mosspar-H (sheared using OD = 3mm)

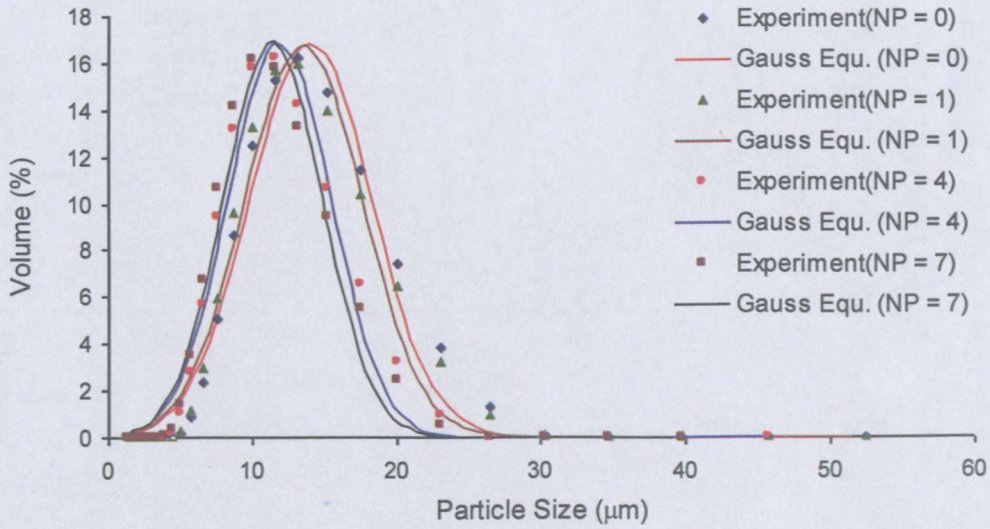

8% Pibsa-IMIDE in Mosspar-H (sheared using OD = 4mm)

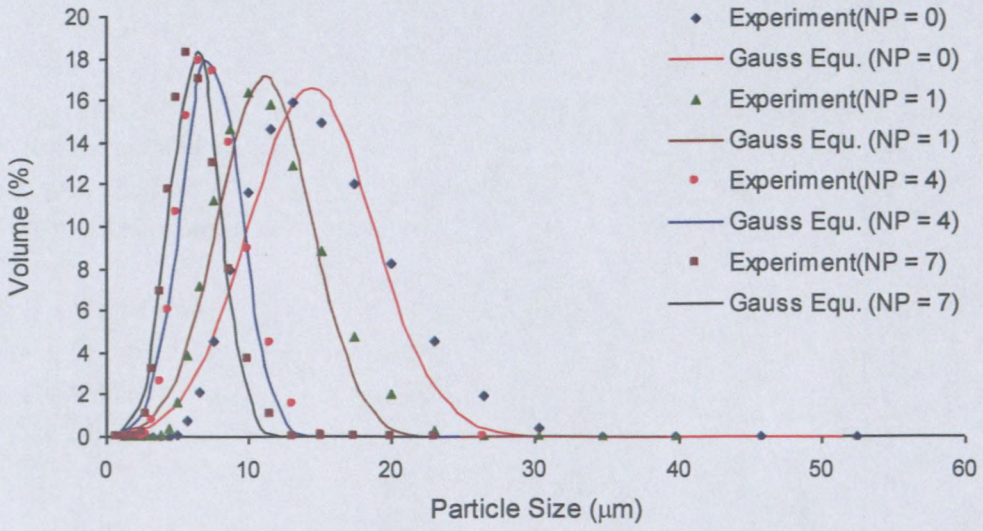

14% Pibsa-IMIDE in Mosspar-H (sheared using OD = 3mm)

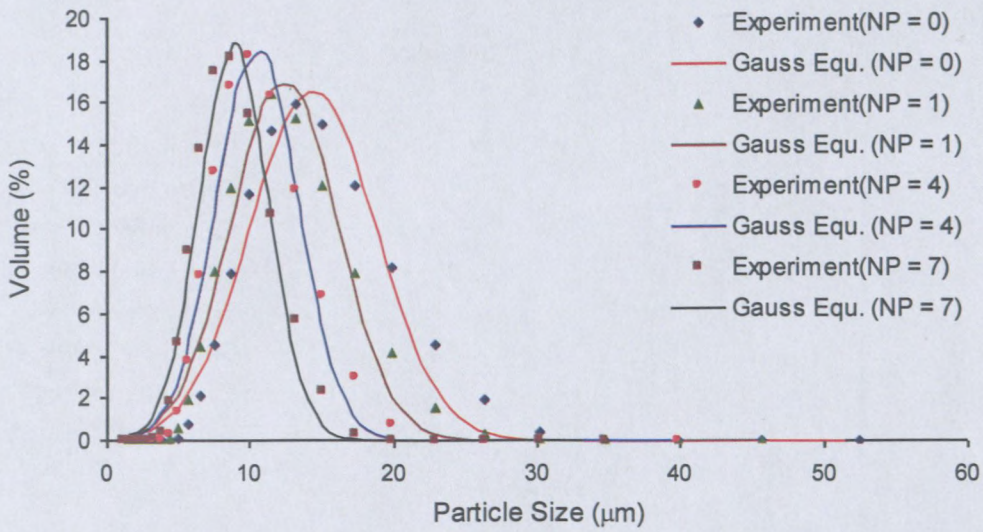

14% Pibsa-IMIDE in Mosspar-H (sheared using OD = 4mm)

Summary of table of the characterization of the width of DSD of sheared emulsion of formulation – 8% PIBSA-IMIDE in MOSSPAR-H

OD	NP	D_{50}	ω	A
3mm	0	13.99	8.4	177
	1	11.97	7.1	151
	2	11.22	6.7	142
	3	10.51	6.2	133
	4	10.08	6	128
	5	9.35	5.3	120
	6	8.9	5	114
	7	8.76	4.9	112
4mm	0	13.99	8.4	177
	1	13.5	8.1	171
	2	12.78	7.6	162
	3	12.07	7.2	153
	4	11.82	7	150
	5	11.73	7	149
	6	11.55	6.9	146
	7	11.36	6.8	144

Summary of table of the characterization of the width of DSD of sheared emulsion of formulation – 14% PIBSA-IMIDE in MOSSPAR-H

OD	NP	D_{50}	ω	A
3mm	0	14.39	8.7	182
	1	11.11	6.6	141
	2	9.4	5.2	121
	3	8.41	4.6	108
	4	7.38	4.1	95
	5	6.93	3.7	90
	6	6.67	3.6	86
	7	6.24	3.4	81
4mm	0	14.39	8.7	182
	1	12.41	7.3	158
	2	11.5	6.8	146
	3	11.02	6	142
	4	10.53	5.7	136
	5	10.15	5.5	131
	6	9.09	5	117
	7	8.88	4.8	115

c) *PIBSA – UREA*

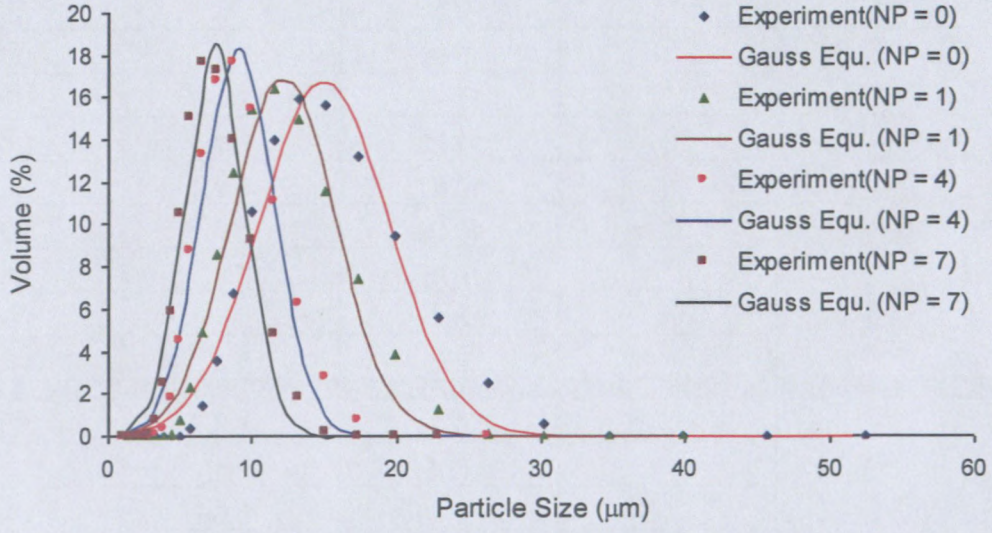

8% Pibsa-UREA in Mosspar-H (sheared using OD = 3mm)

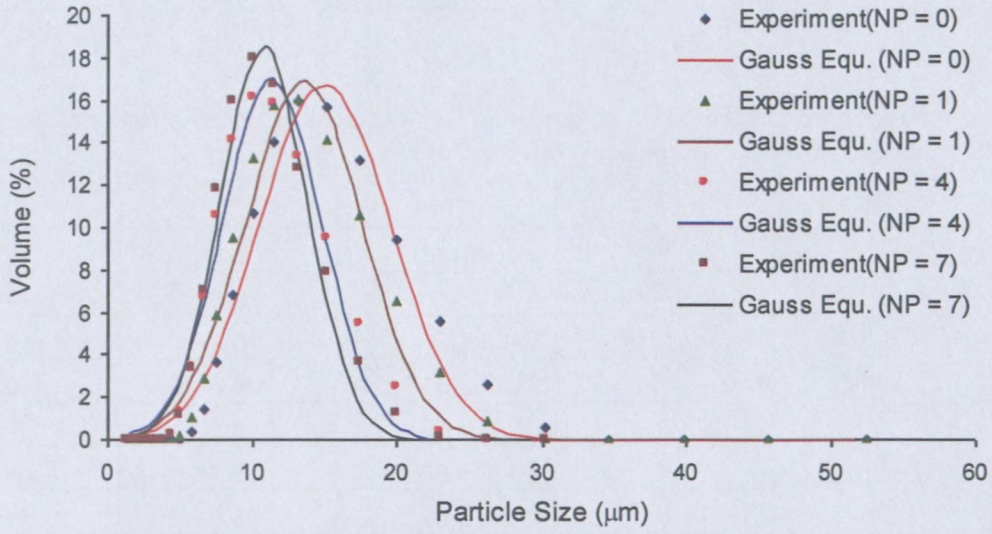

8% Pibsa-UREA in Mosspar-H (sheared using OD = 4mm)

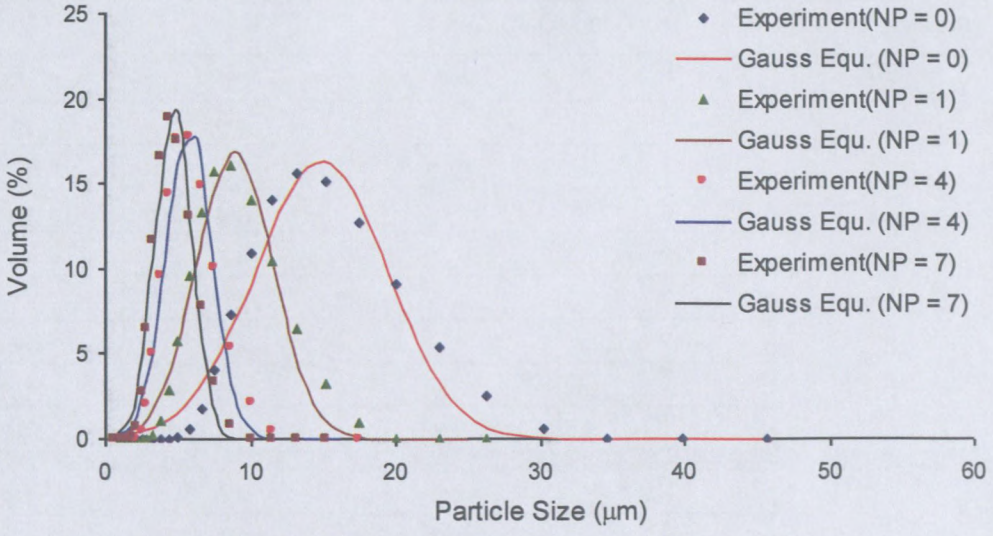

14% Pibsa-UREA in Mosspar-H (sheared using OD = 3mm)

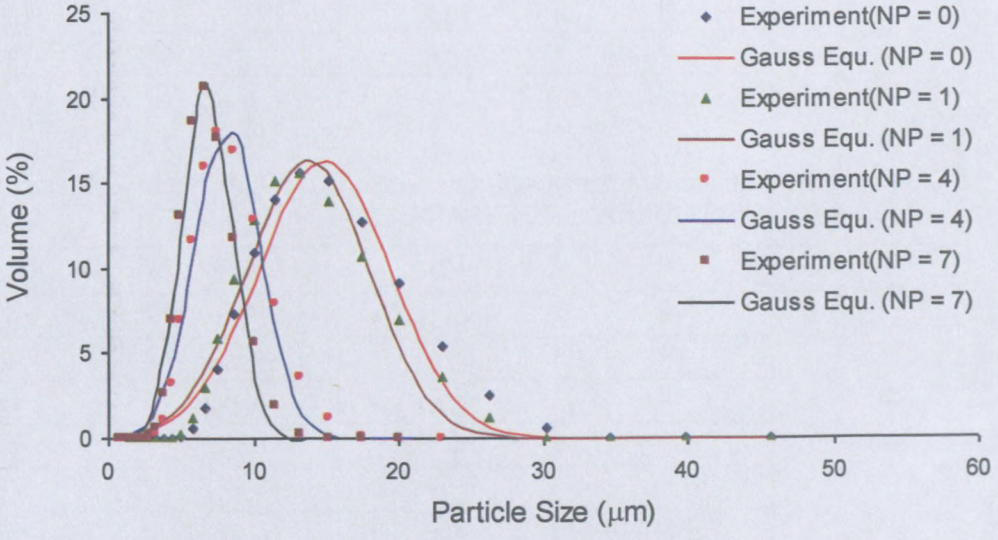

14% Pibsa-UREA in Mosspar-H (sheared using OD = 4mm)

Summary of table of the characterization of the width of DSD of sheared emulsion of formulation – 8% PIBSA-UREA in MOSSPAR-H

OD	NP	D_{50}	ω	A
3mm	0	15	9.2	190
	1	12.2	7.2	155
	2	10.6	6.4	134
	3	10.2	5.6	131
	4	9.0	5.0	115
	5	8.1	4.5	104
	6	8.0	4.5	102
	7	7.4	4.1	96
4mm	0	15	9.0	190
	1	13.5	8.1	172
	2	12.9	7.7	164
	3	11.8	7.0	150
	4	11.4	6.8	145
	5	11.1	6.2	143
	6	10.8	6.0	139
	7	10.6	5.9	135

Summary of table of the characterization of the width of DSD of sheared emulsion of formulation – 14% PIBSA-UREA in MOSSPAR-H

OD	NP	D_{50}	ω	A
3mm	0	14.9	9.1	187
	1	8.9	5.3	113
	2	6.9	3.9	88
	3	6.6	3.9	84
	4	5.8	3.2	74
	5	5.4	3.0	70
	6	5.1	2.7	66
	7	4.7	2.5	61
4mm	0	14.9	9.1	187
	1	13.7	8.4	173
	2	10.6	5.9	137
	3	8.3	4.5	107
	4	8.2	4.5	106
	5	8.0	4.5	102
	6	7.4	4.0	96
	7	6.9	3.4	90

d) PIBSA – MEA/SMO

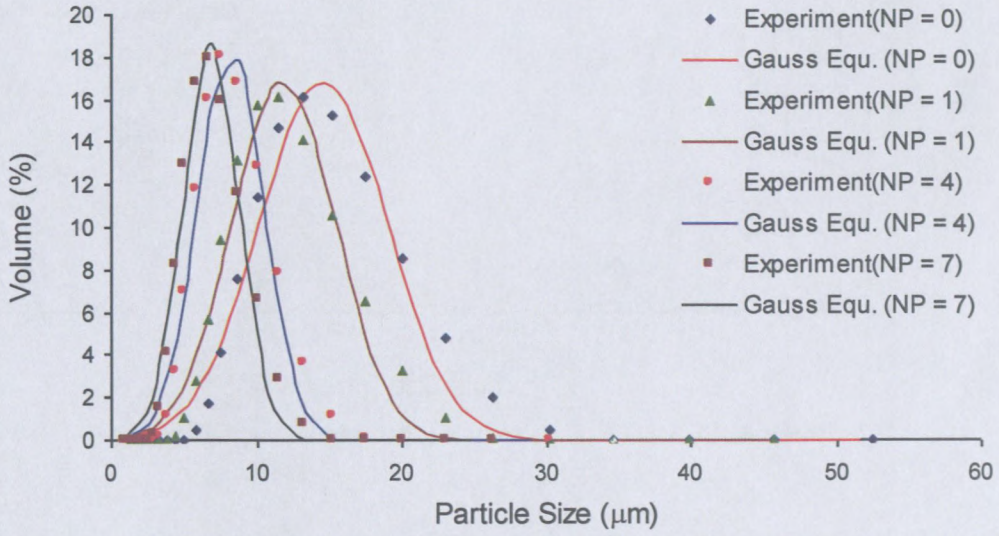

8% Pibsa-MEA/SMO in Mosspar-H (sheared using OD = 3mm)

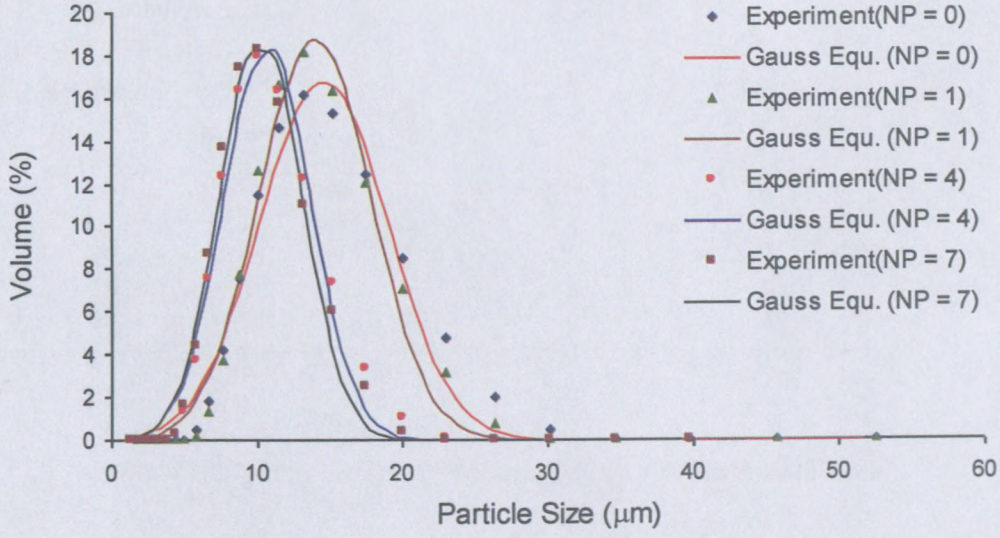

8% Pibsa-MEA/SMO in Mosspar-H (sheared using OD = 4mm)

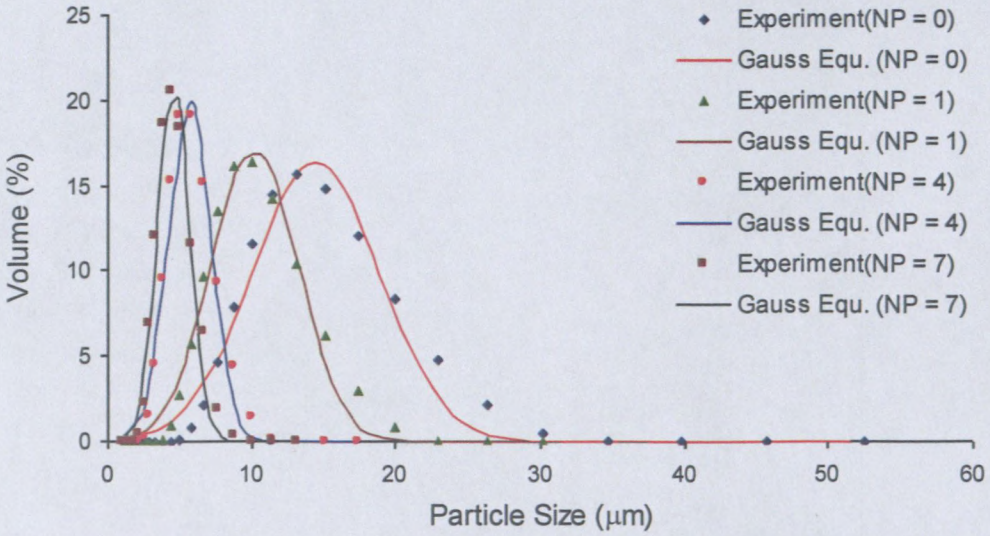

14% Pibsa-MEA/SMO in Mosspar-H (sheared using OD = 3mm)

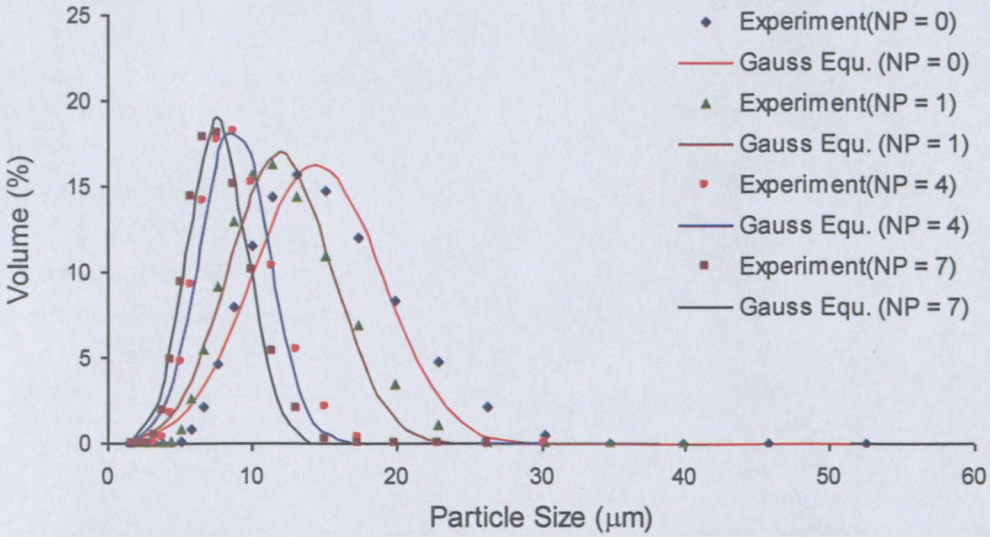

14% Pibsa-MEA/SMO in Mosspar-H (sheared using OD = 4mm)

Summary of table of the characterization of the width of DSD of sheared emulsion of formulation – 8% PIBSA-UREA in MOSSPAR-H

OD	NP	D_{50}	ω	A
3mm	0	14.5	8.7	184
	1	11.8	7.1	150
	2	10.8	5.9	139
	3	9.4	5.2	121
	4	8.2	4.5	106
	5	7.9	4.3	101
	6	7.0	3.8	90
	7	6.9	3.8	89
4mm	0	14.5	8.7	184
	1	13.9	7.6	180
	2	13.0	7.1	167
	3	12.4	6.7	160
	4	10.7	5.9	137
	5	10.4	5.7	134
	6	10.3	5.6	133
	7	10.0	5.5	129

Summary of table of the characterization of the width of DSD of sheared emulsion of formulation – 14% PIBSA-UREA in MOSSPAR-H

OD	NP	D_{50}	ω	A
3mm	0	14.5	8.9	182
	1	10.2	6.0	130
	2	7.4	4.2	95
	3	6.5	3.5	84
	4	5.7	2.9	74
	5	5.6	2.8	73
	6	5.5	2.7	72
	7	4.6	2.2	60
4mm	0	14.5	8.9	182
	1	12.0	7.1	152
	2	10.9	5.9	141
	3	8.8	4.8	114
	4	8.6	4.5	113
	5	8.2	4.1	108
	6	7.7	4.1	100
	7	7.6	4.1	98

e) *The effect of Ammonium nitrate concentration (65% in the Dispersed phase)*

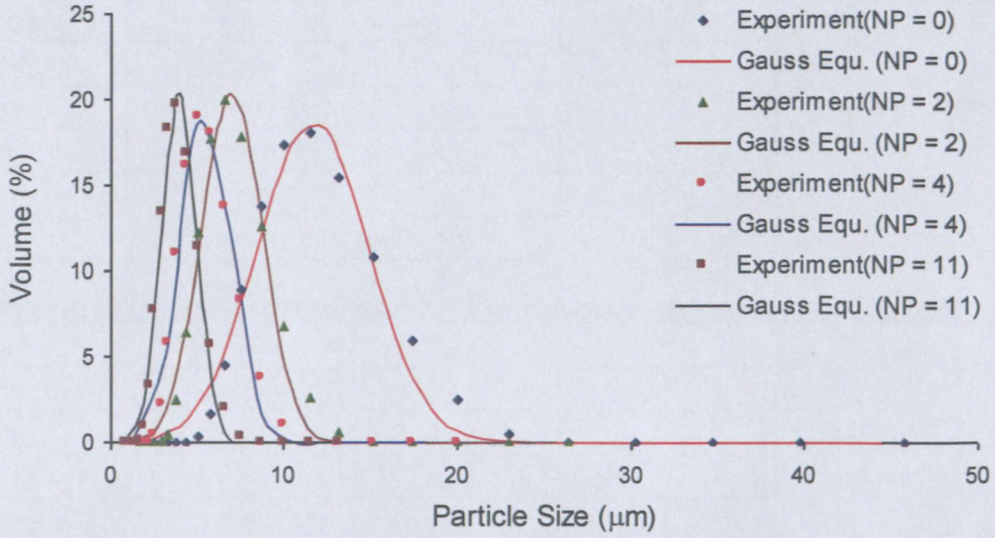

65% Ammonium Nitrate (Urea emulsion – tmix = 2min)

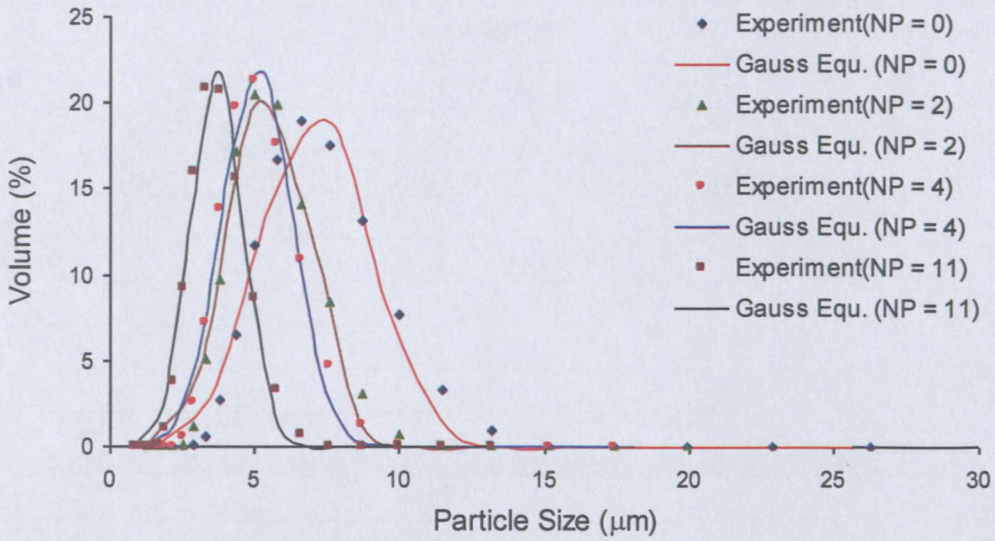

65% Ammonium Nitrate (Urea emulsion – t_{mix} = 4min)

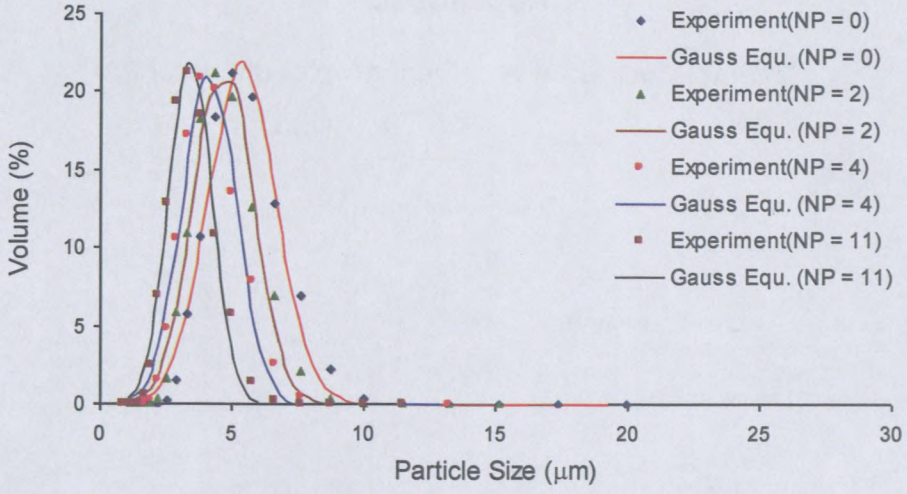

65% Ammonium Nitrate (Urea emulsion – t_{mix} = 4min)

Summary of the characterization of the width of DSD of sheared emulsions (65% AN)

Mixing Time	NP	D_{32}	D_{50}	ω	A
2 minutes	0	11.3	11.7	6.4	152
	2	6.9	7.0	3.5	91
	3	6.0	6.1	2.9	80
	4	5.3	5.5	2.9	72
	6	4.7	4.8	2.5	63
	8	4.3	4.4	2.2	58
	11	3.8	3.9	2.0	51
4 minutes	0	7.2	7.1	3.8	93
	2	5.4	5.5	2.7	72
	3	4.9	5.0	2.4	65
	4	5.0	5.1	2.4	67
	6	4.4	4.5	2.1	59
	8	4.0	4.0	2.0	53
	11	3.7	3.7	1.8	49
10 minutes	0	5.3	5.4	2.5	70
	2	4.6	4.7	2.2	61
	3	4.1	4.2	2.0	55
	4	4.1	4.1	2.0	54
	6	3.9	3.9	1.8	51
	8	3.8	3.9	1.8	51
	11	3.4	3.4	1.6	45

Appendix C

Characterization of critical droplet diameter

a) *Pibsa-MEA*

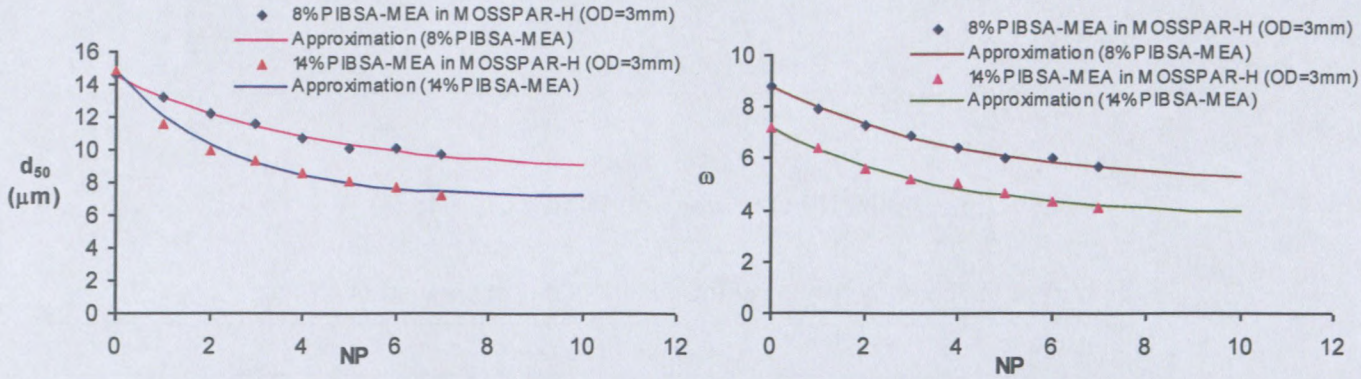

Evolution of the Sauter mean droplets diameter: (a) and the width of DSD (b) as function of the number of pumping – Effect of Surfactant concentration (OD = 3mm).

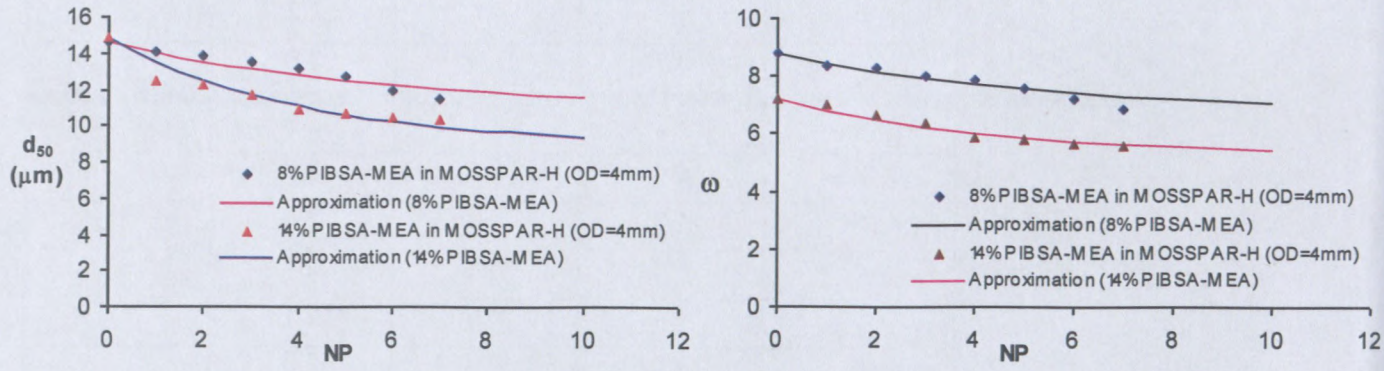

Evolution of the Sauter mean droplets diameter: (a) and the width of DSD (b) as function of the number of pumping – Effect of Surfactant concentration (OD = 4mm)

b) ***Pibsa-IMIDE***

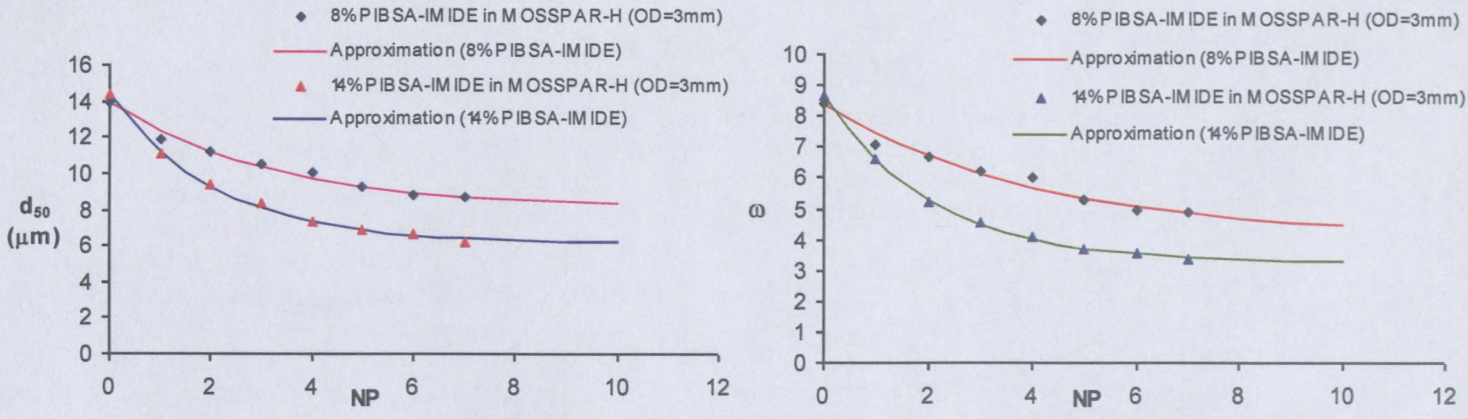

Evolution of the Sauter mean droplets diameter: (a) and the width of DSD (b) as function of the number of pumping – Effect of Surfactant concentration (OD = 3mm)

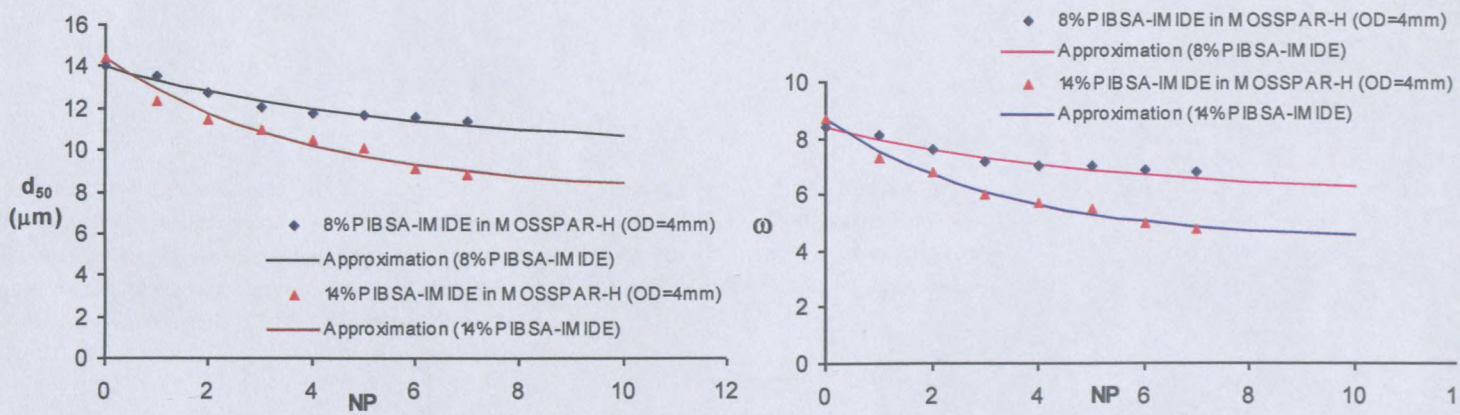

Evolution of the Sauter mean droplets diameter: (a) and the width of DSD (b) as function of the number of pumping – Effect of Surfactant concentration (OD = 4mm)

c) *Pibsa-UREA*

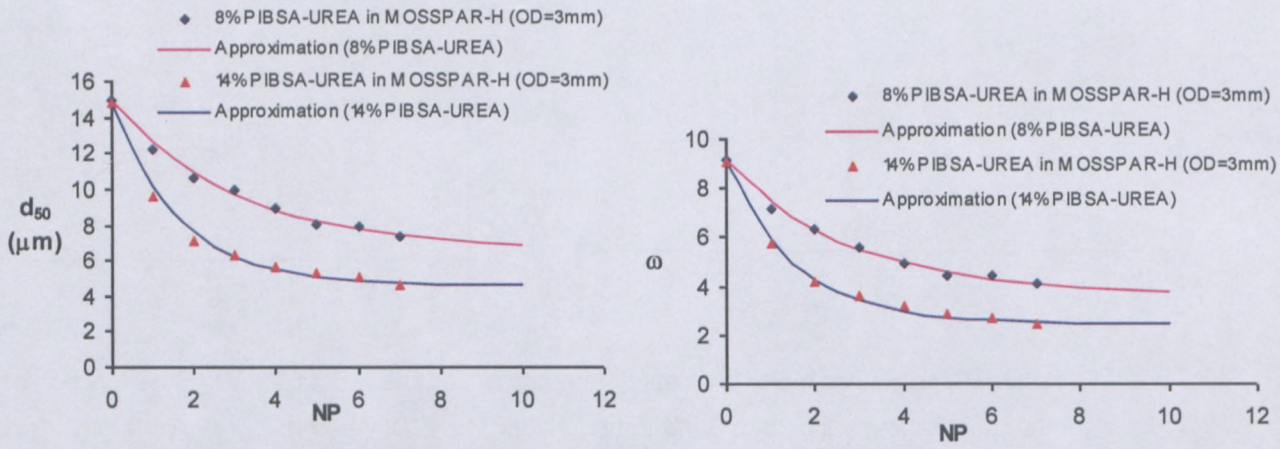

Evolution of the Sauter mean droplets diameter: (a) and the width of DSD (b) as function of the number of pumping – Effect of Surfactant concentration (OD = 3mm)

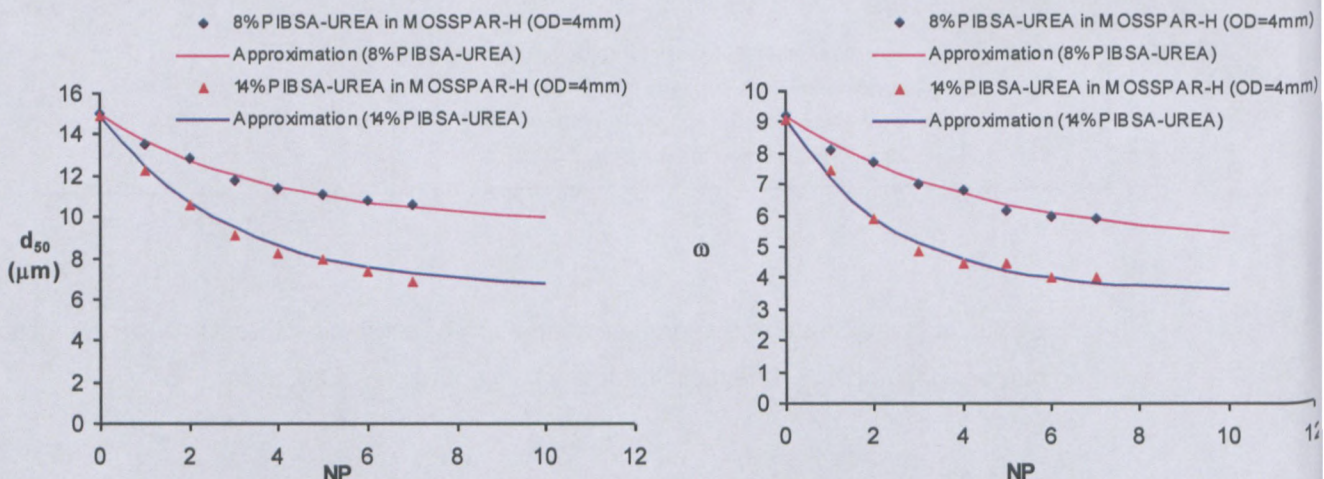

Evolution of the Sauter mean droplets diameter: (a) and the width of DSD (b) as function of the number of pumping – Effect of Surfactant concentration (OD = 4mm)

d) Pibsa - MEA/SMO

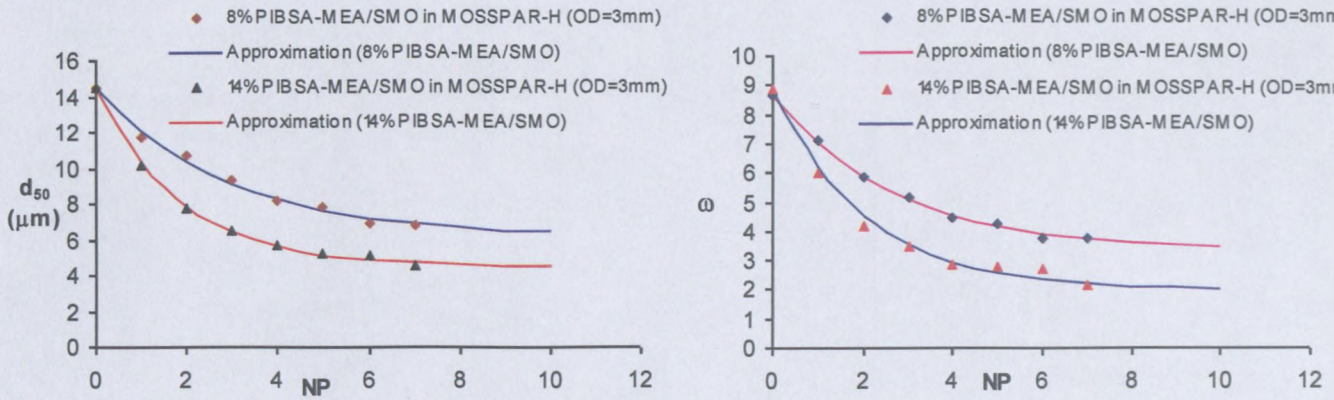

Evolution of the Sauter mean droplets diameter: (a) and the width of DSD (b) as function of the number of pumping – Effect of Surfactant concentration (OD = 3mm)

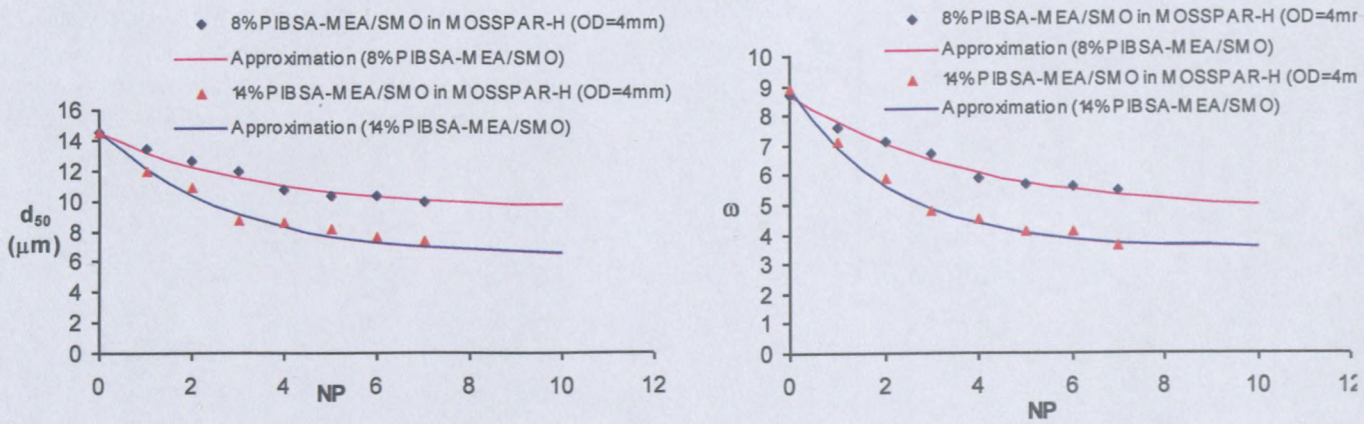

Evolution of the Sauter mean droplets diameter: (a) and the width of DSD (b) as function of the number of pumping – Effect of Surfactant concentration (OD = 4mm)

Appendix D

Energy density characterization

a) *PIBSA – MEA*

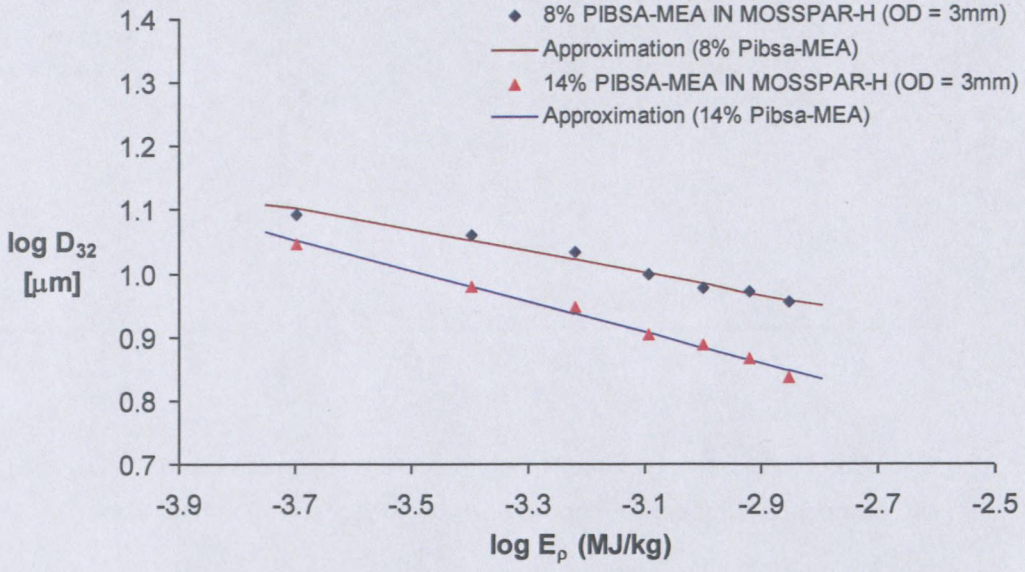

8% & 14% Pibsa-MEA in Mosspar-H (sheared using OD = 3mm)

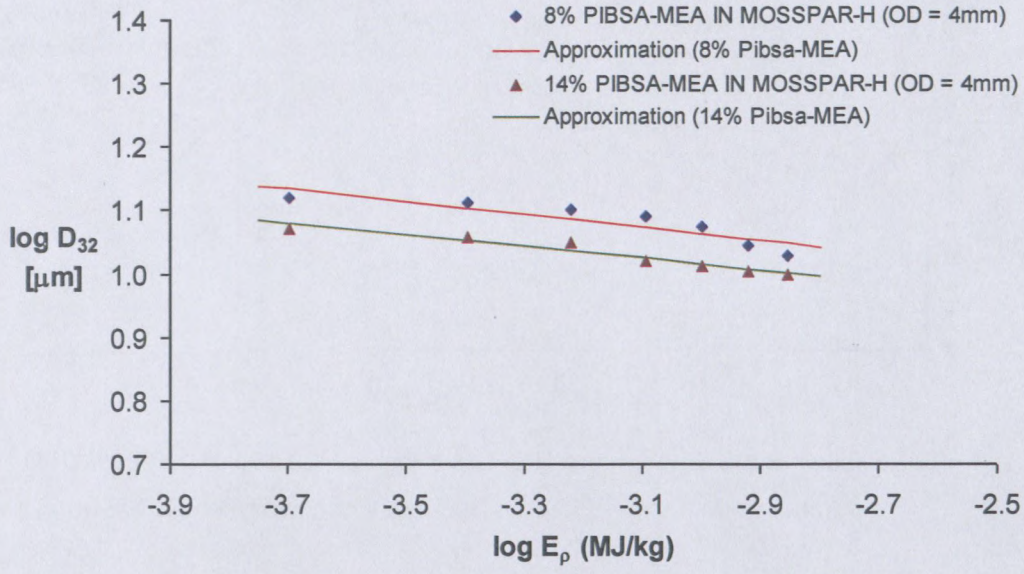

8% & 14% Pibsa-MEA in Mosspar-H (sheared using OD = 4mm)

b) PIBSA – IMIDE

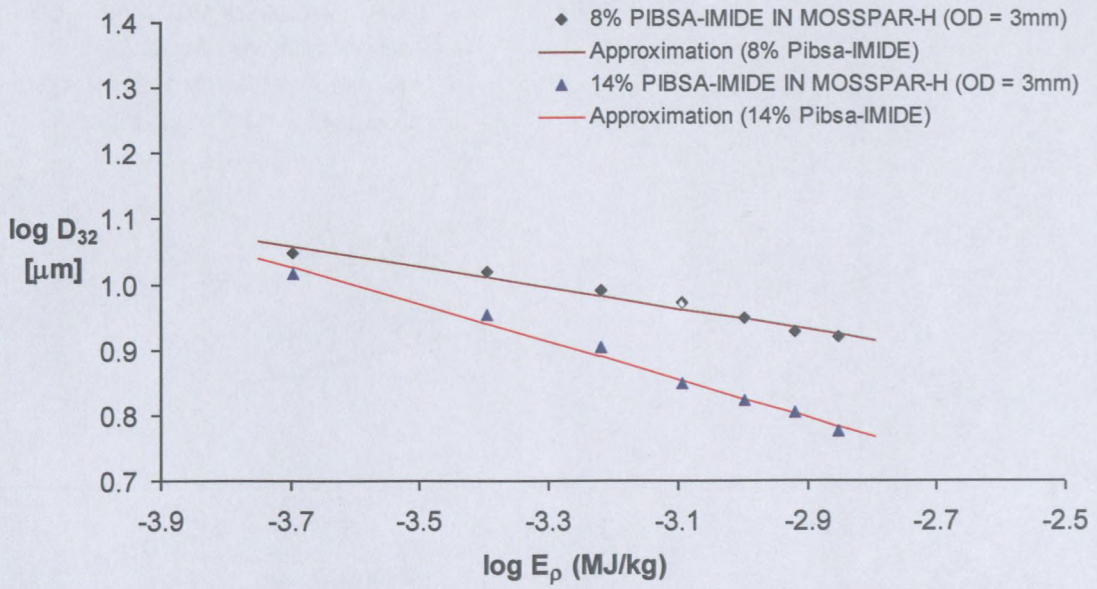

8% & 14% Pibsa-IMIDE in Mosspar-H (sheared using OD = 3mm)

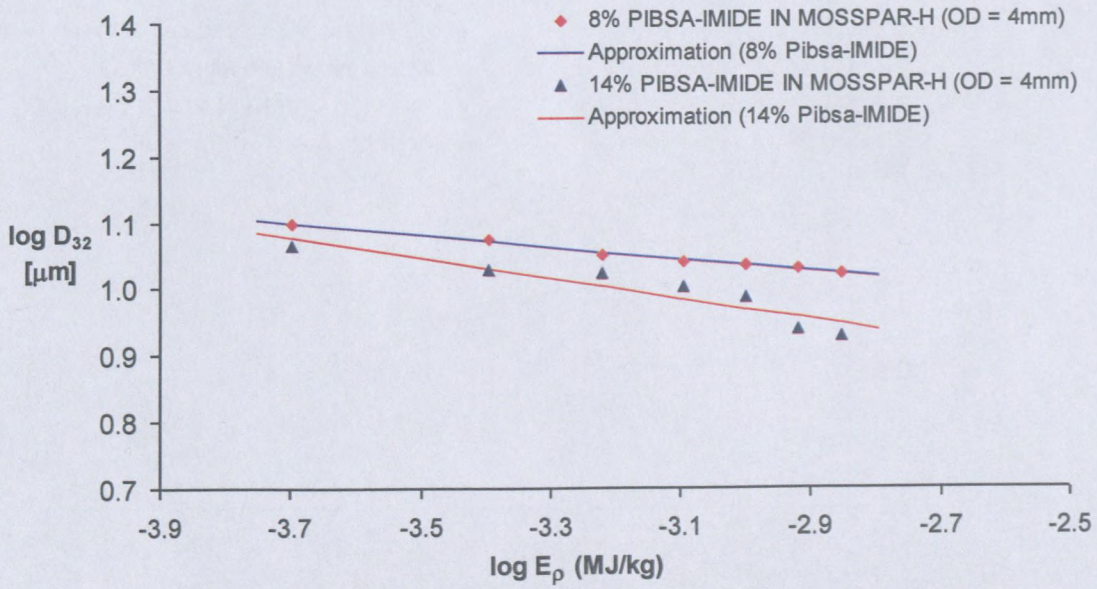

8% & 14% Pibsa-IMIDE in Mosspar-H (sheared using OD = 4mm)

c) *PIBSA – UREA*

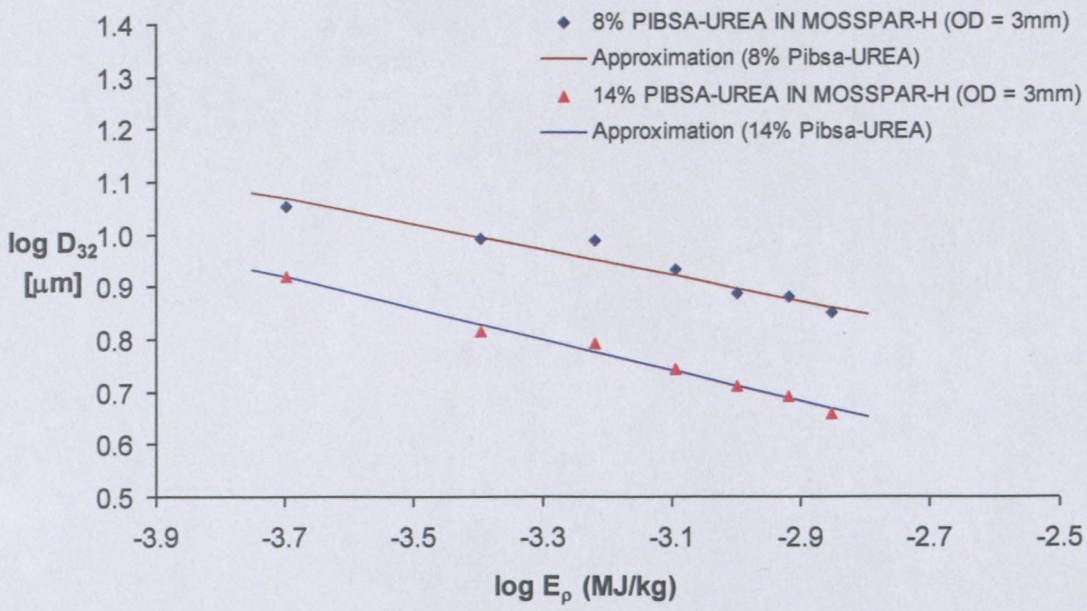

8% & 14% Pibsa-UREA in Mosspar-H (sheared using OD = 3mm)

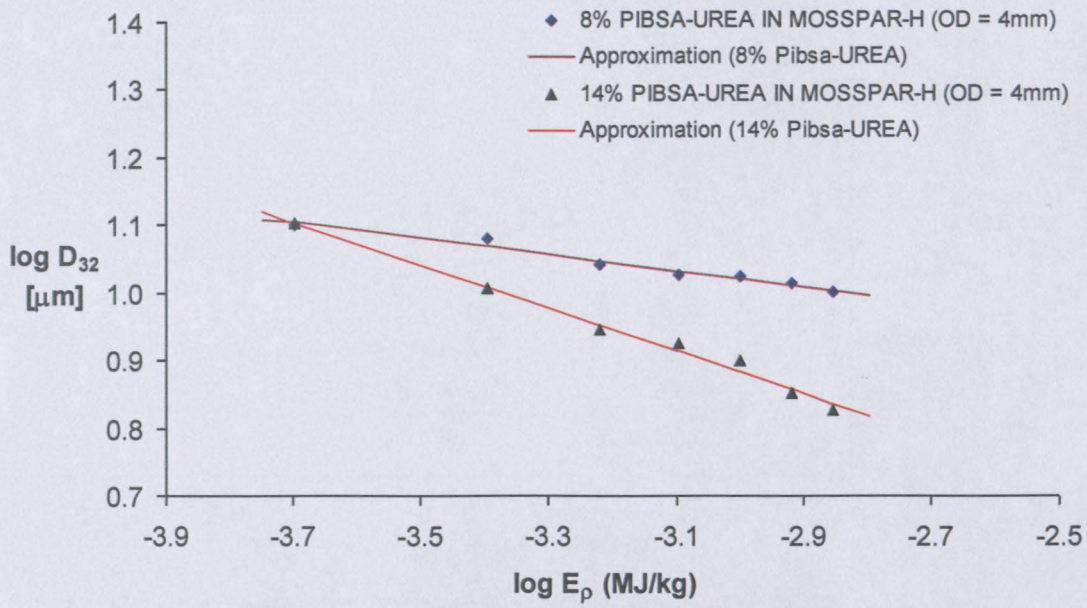

8% & 14% Pibsa-UREA in Mosspar-H (sheared using OD = 4mm)

d) *PIBSA – MEA/SMO*

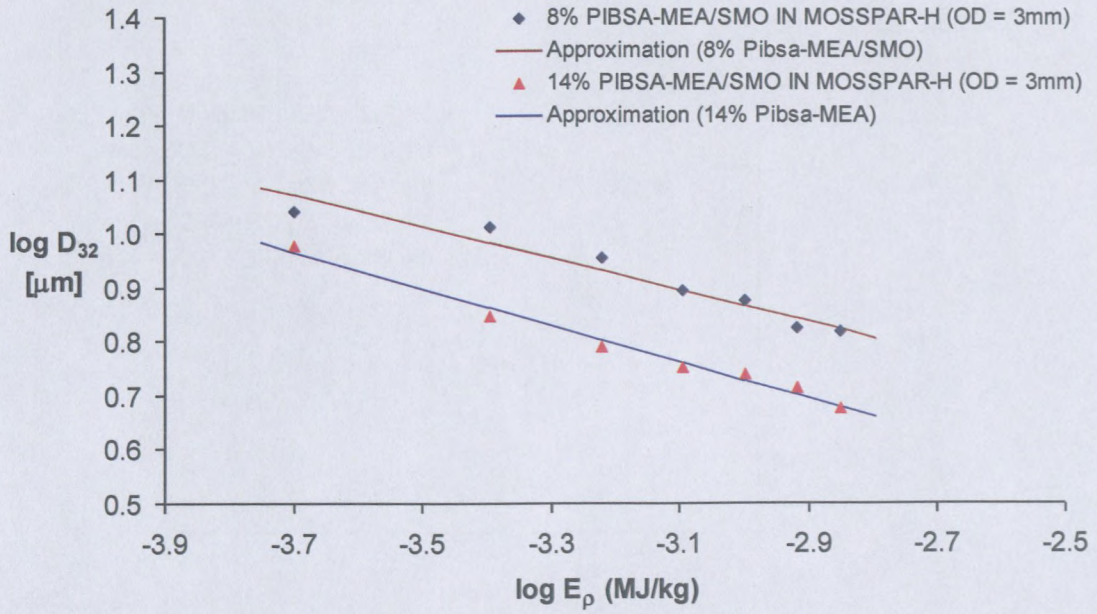

8% & 14% Pibsa-MEA/SMO in Mosspar-H (sheared using OD = 3mm)

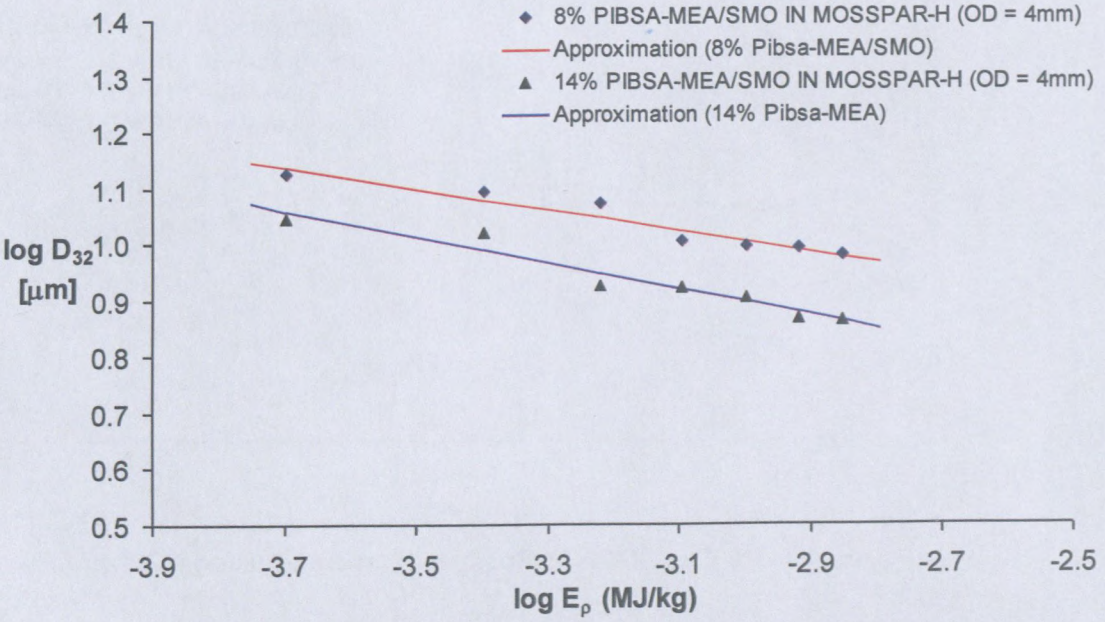

8% & 14% Pibsa-MEA/SMO in Mosspar-H (sheared using OD = 4mm)

Appendix E

Rheology – Viscoelastic properties

a) *PIBSA – MEA*

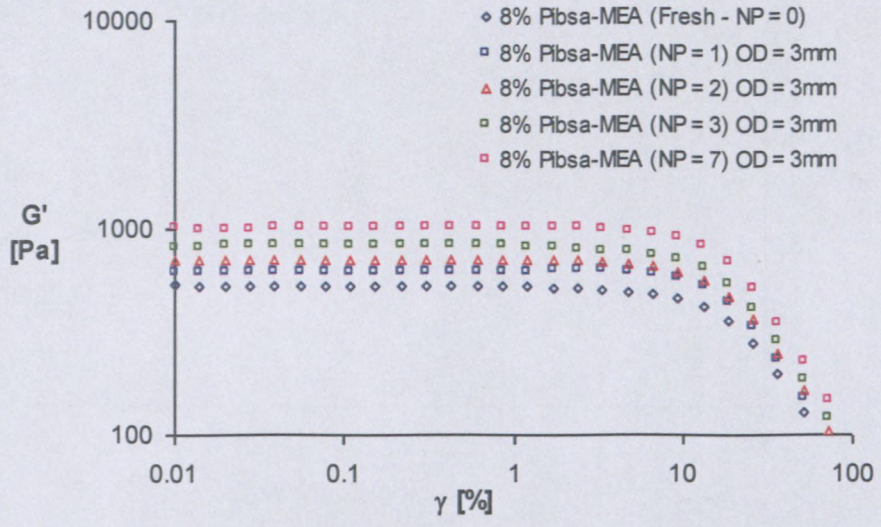

8% Pibsa-MEA in Mosspar-H (sheared using OD = 3mm)

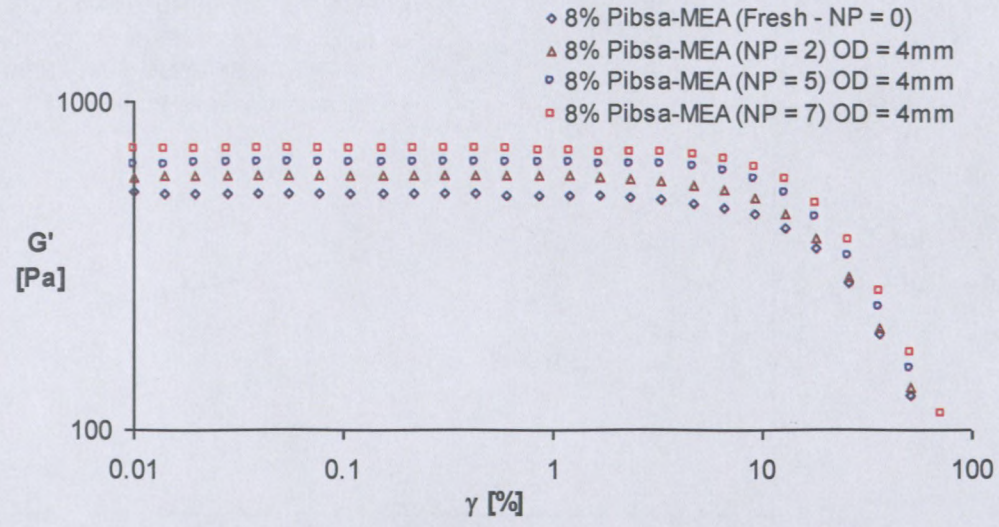

8% Pibsa-MEA in Mosspar-H (sheared using OD = 4mm)

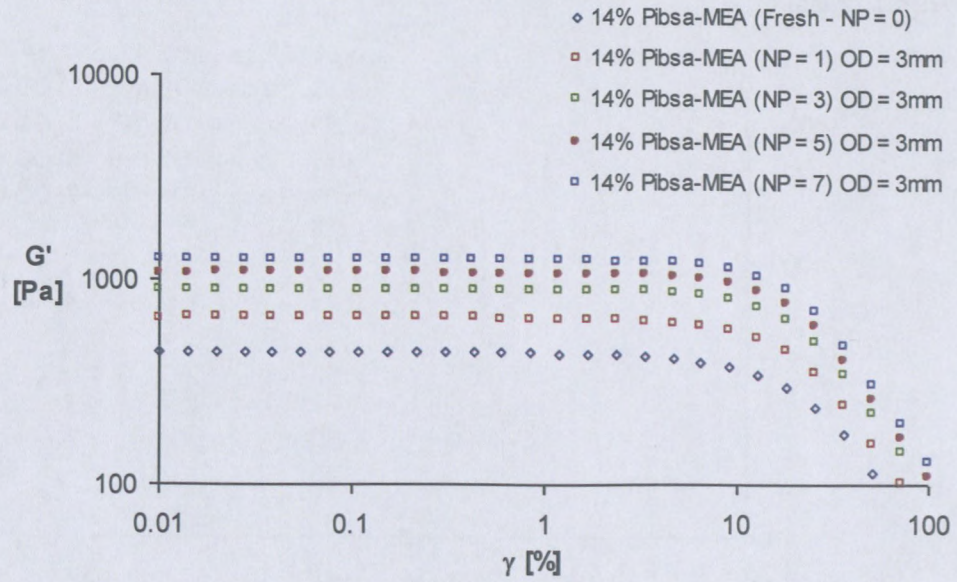

14% Pibsa-MEA in Mosspar-H (sheared using OD = 3mm)

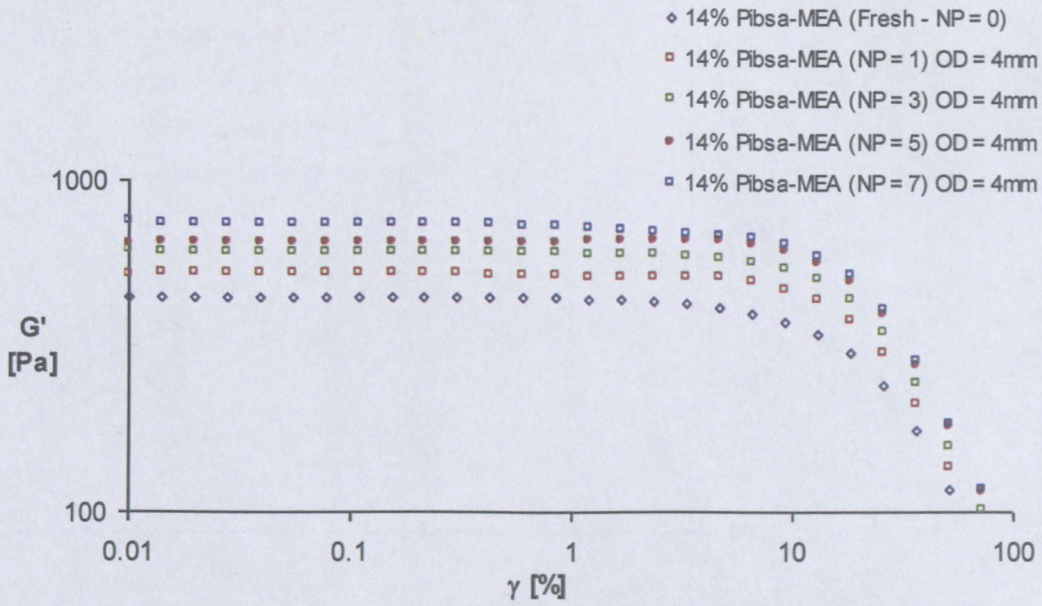

14% Pibsa-MEA in Mosspar-H (sheared using OD = 4mm)

b) PIBSA – IMIDE

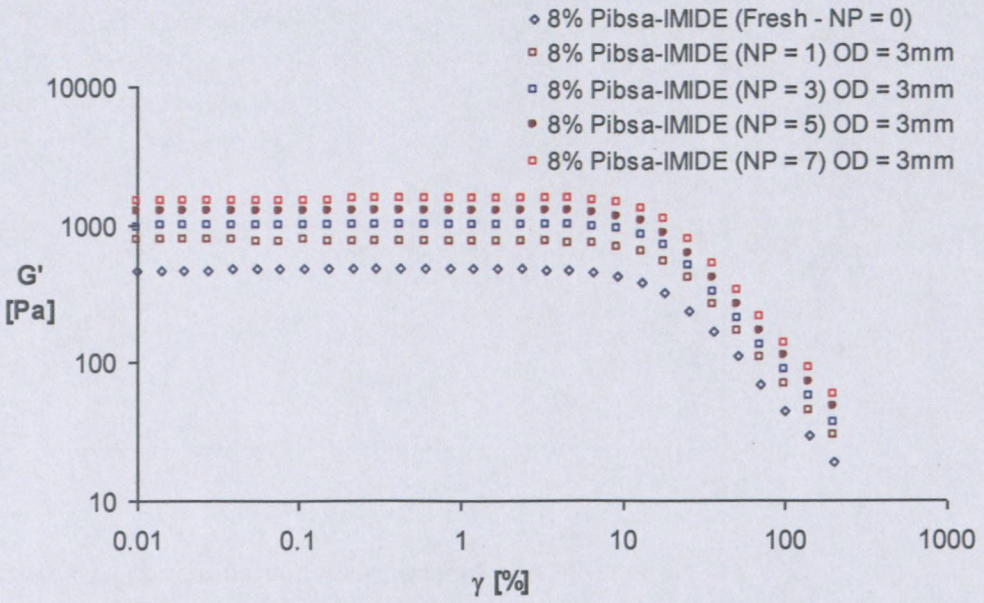

8% Pibsa-IMIDE in Mosspar-H (sheared using OD = 3mm)

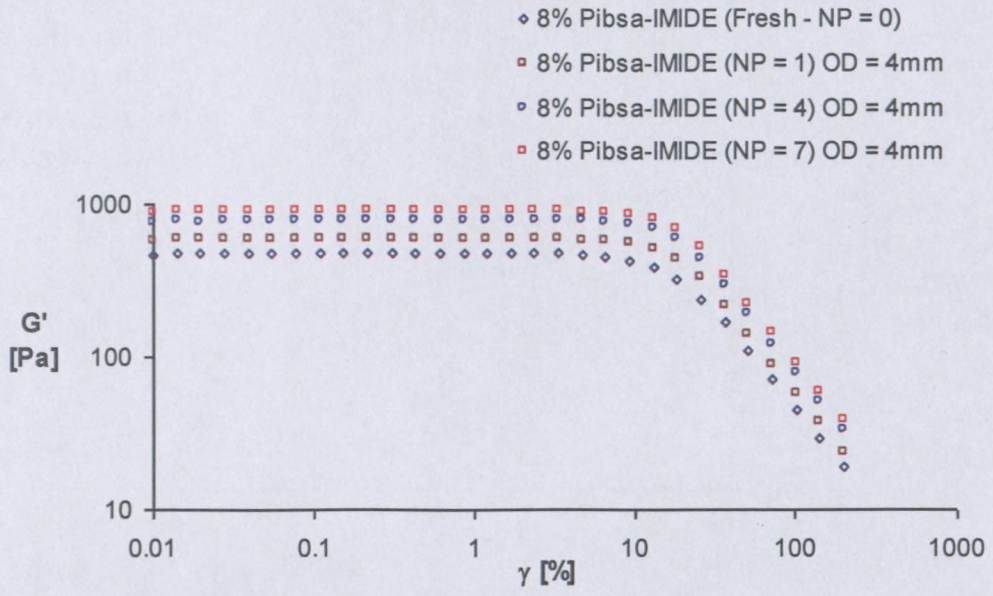

8% Pibsa-IMIDE in Mosspar-H (sheared using OD = 4mm)

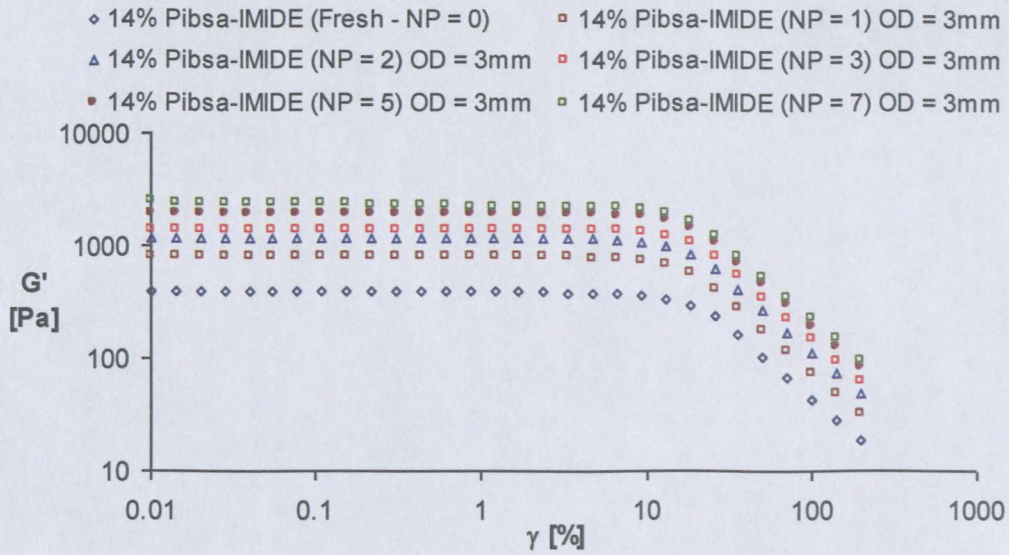

14% Pibsa-IMIDE in Mosspar-H (sheared using OD = 3mm)

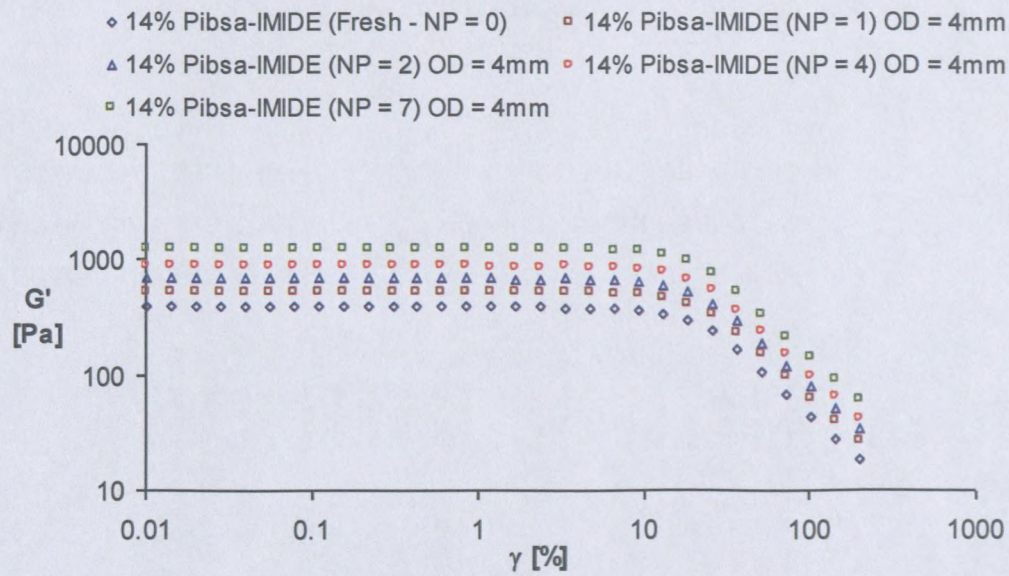

14% Pibsa-IMIDE in Mosspar-H (sheared using OD = 4mm)

c) *PIBSA – UREA*

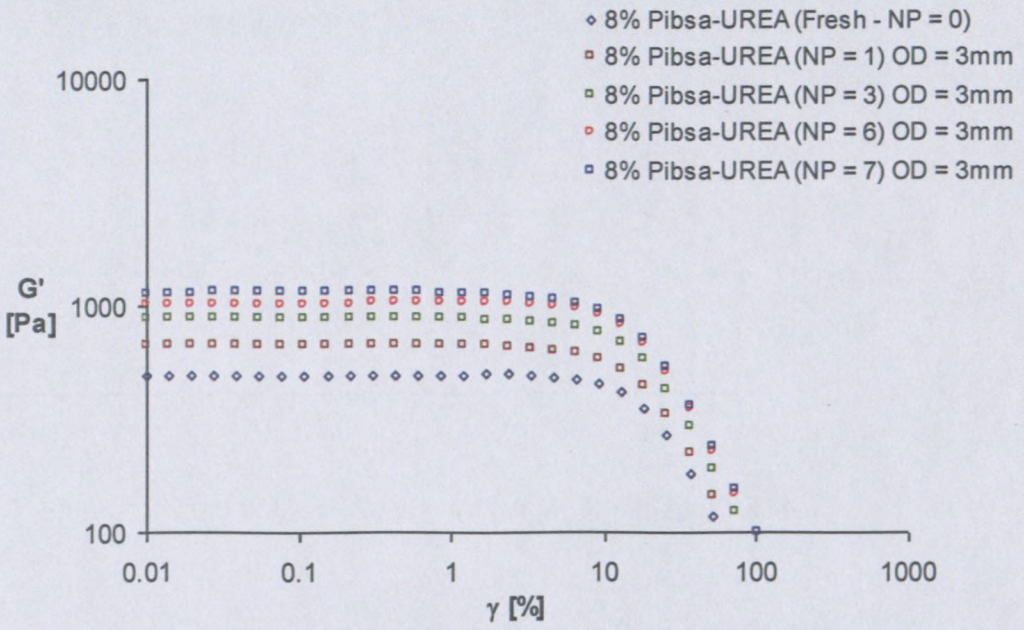

8% Pibsa-UREA in Mosspar-H (sheared using OD = 3mm)

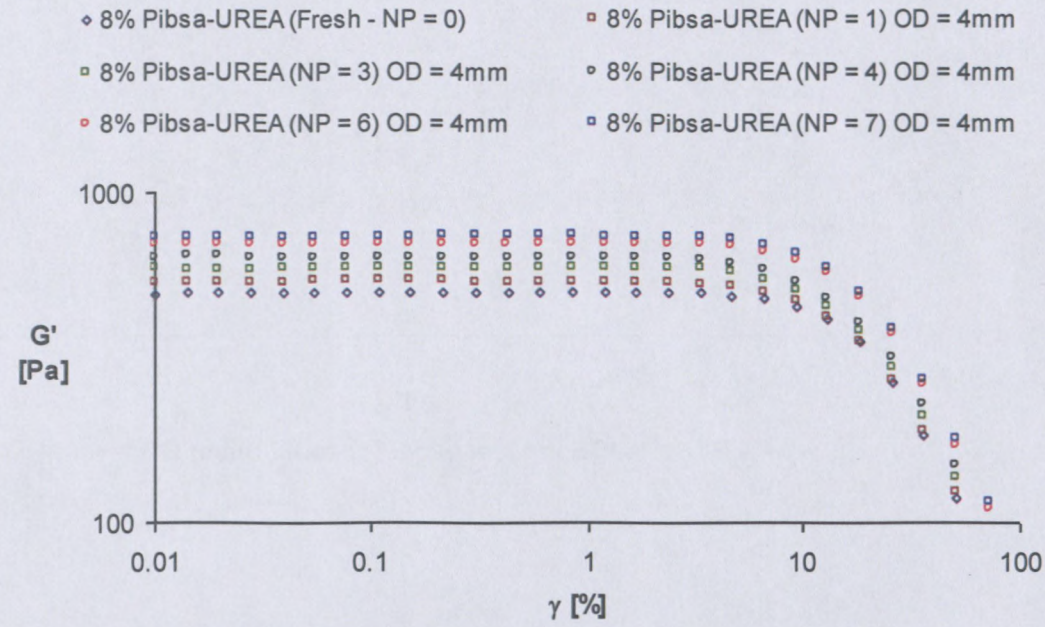

8% Pibsa-UREA in Mosspar-H (sheared using OD = 4mm)

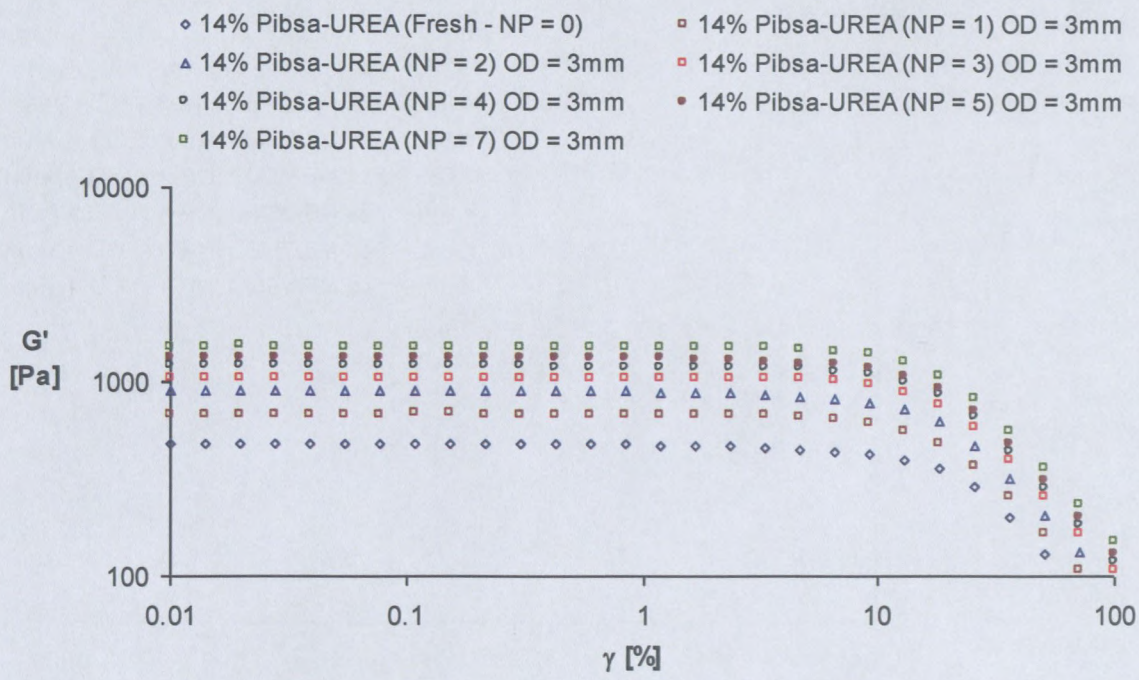

14% Pibsa-UREA in Mosspar-H (sheared using OD = 3mm)

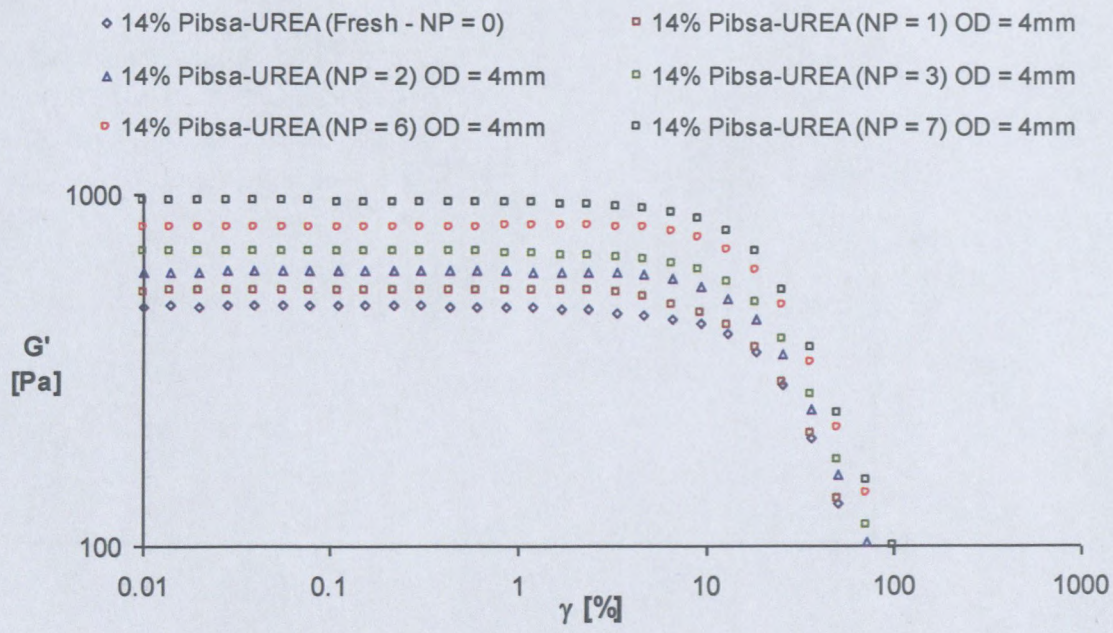

14% Pibsa-UREA in Mosspar-H (sheared using OD = 4mm)

d) *PIBSA – MEA/SMO*

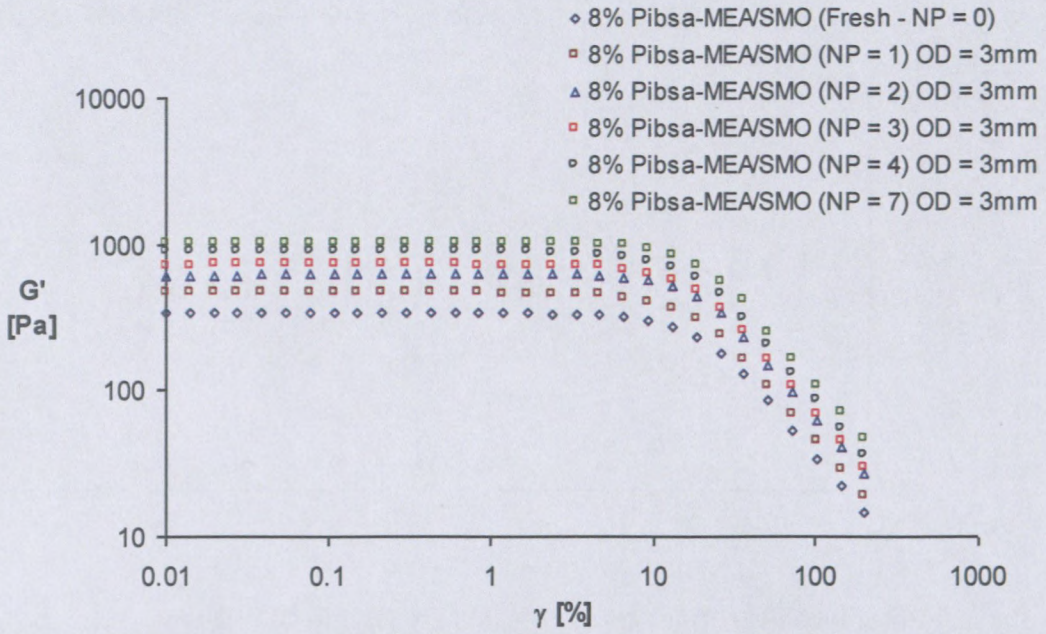

8% Pibsa-MEA/SMO in Mosspar-H (sheared using OD = 3mm)

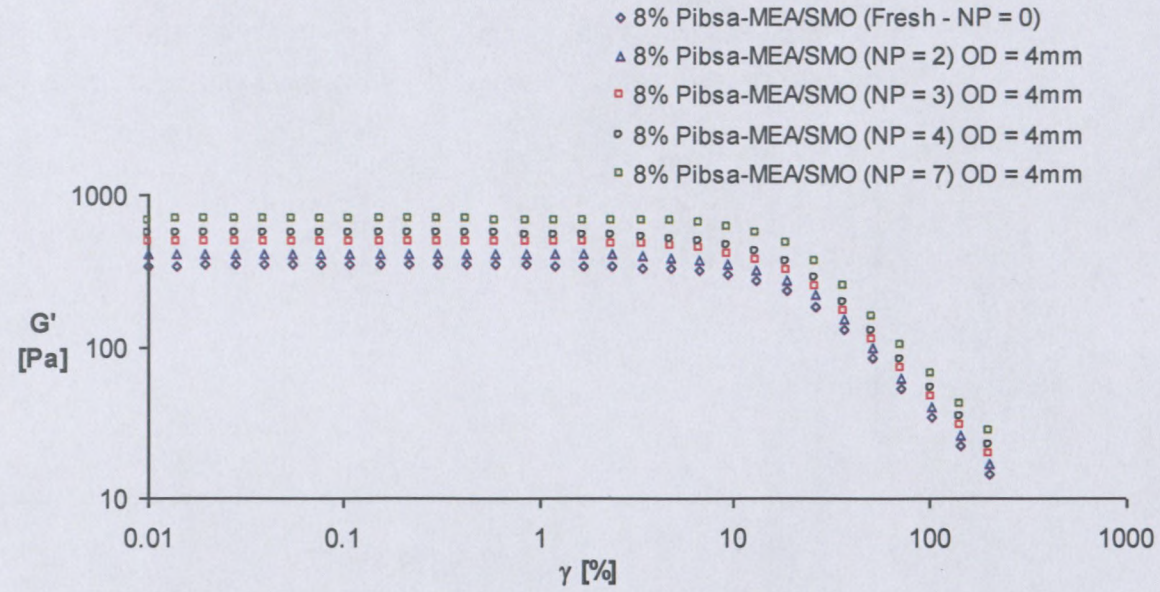

8% Pibsa-MEA/SMO in Mosspar-H (sheared using OD = 4mm)

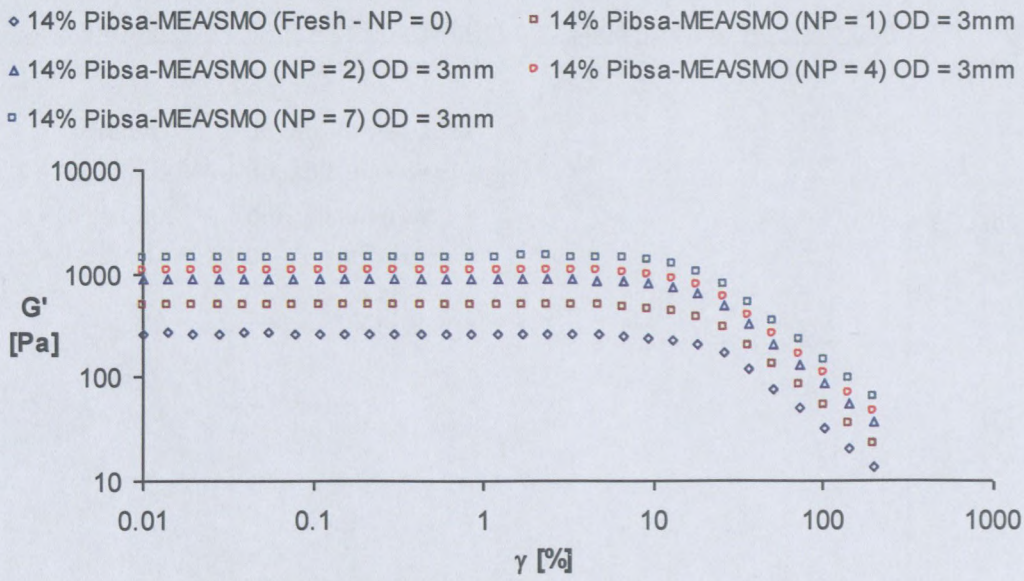

14% Pibsa-MEA/SMO in Mosspar-H (sheared using OD = 3mm)

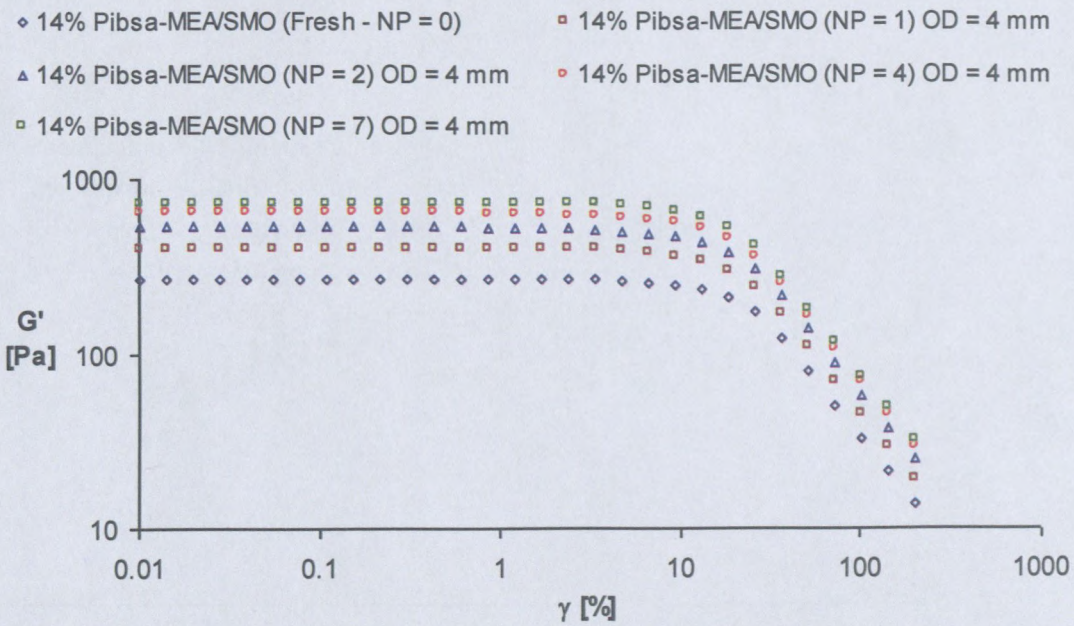

14% Pibsa-MEA/SMO in Mosspar-H (sheared using OD = 4mm)

e) *The effect of Ammonium nitrate concentration (65% in the Dispersed phase)*

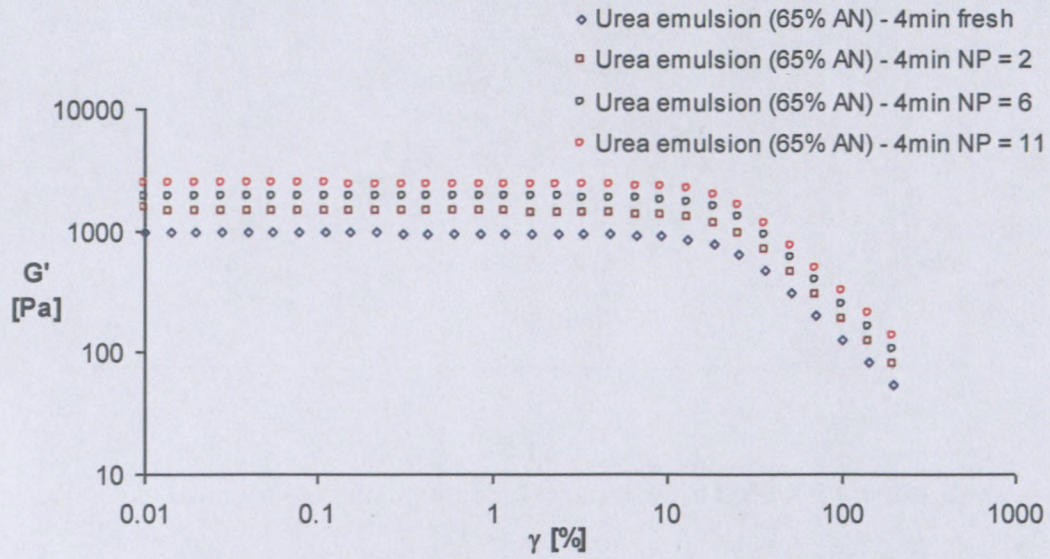

65% Ammonium Nitrate (Urea emulsion – t_{mix} = 4min)

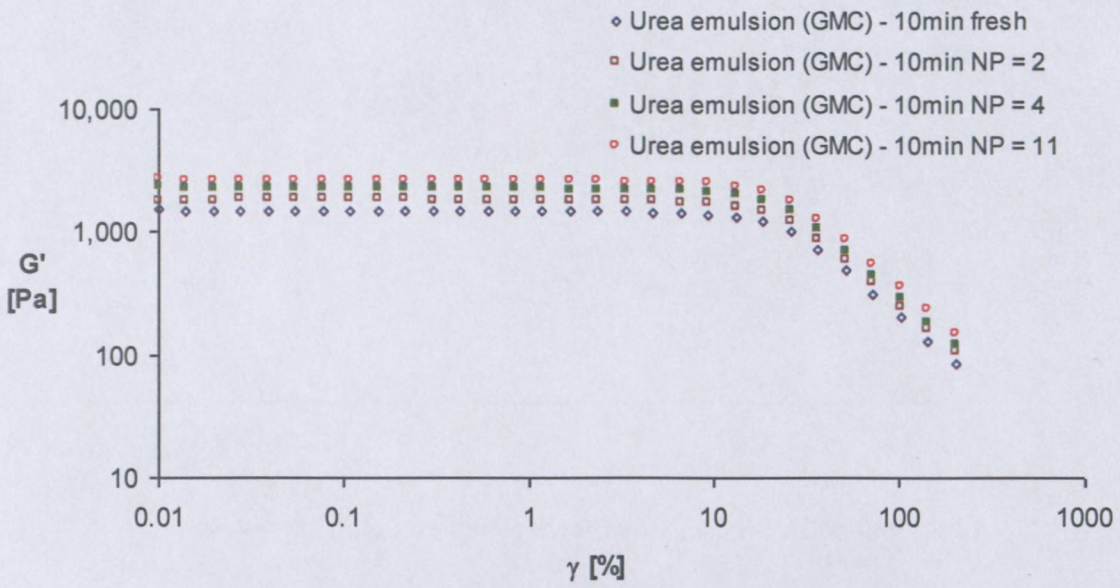

65% Ammonium Nitrate (Urea emulsion – t_{mix} = 10min)

Appendix F

Rheology – Flow properties

a) *PIBSA – MEA*

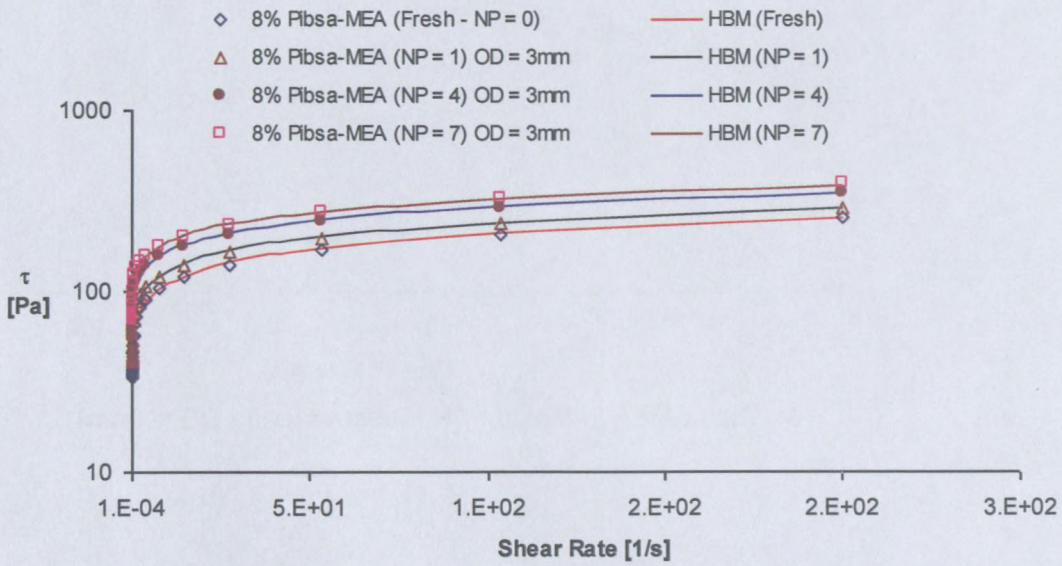

8% Pibsa-MEA in Mosspar-H (sheared using OD = 3mm)

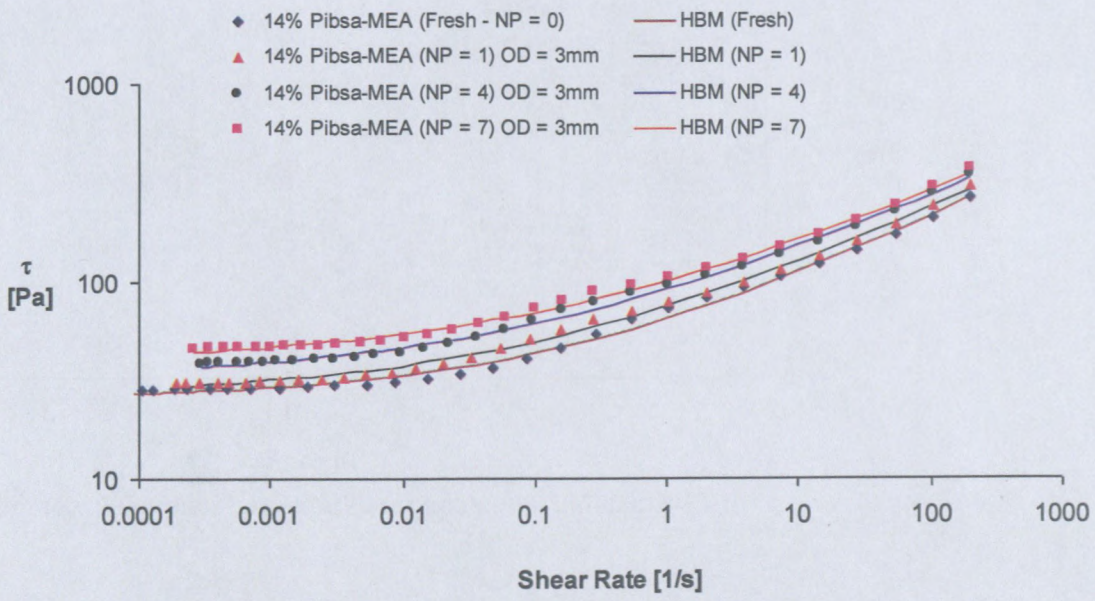

14% Pibsa-MEA in Mosspar-H (sheared using OD = 3mm)

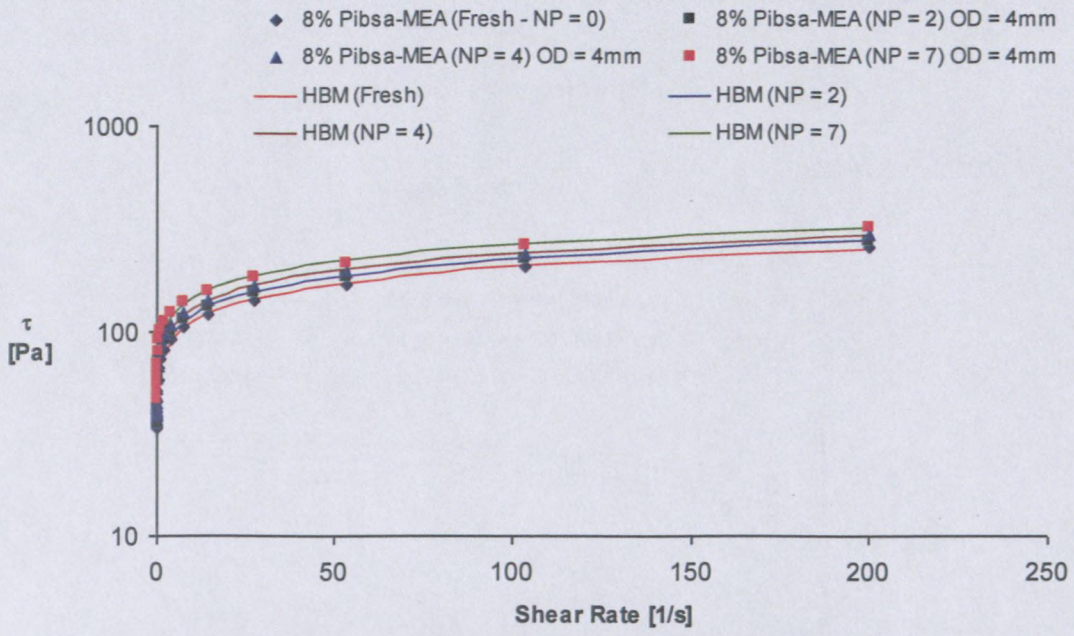

8% Pibsa-MEA in Mosspar-H (sheared using OD = 4mm)

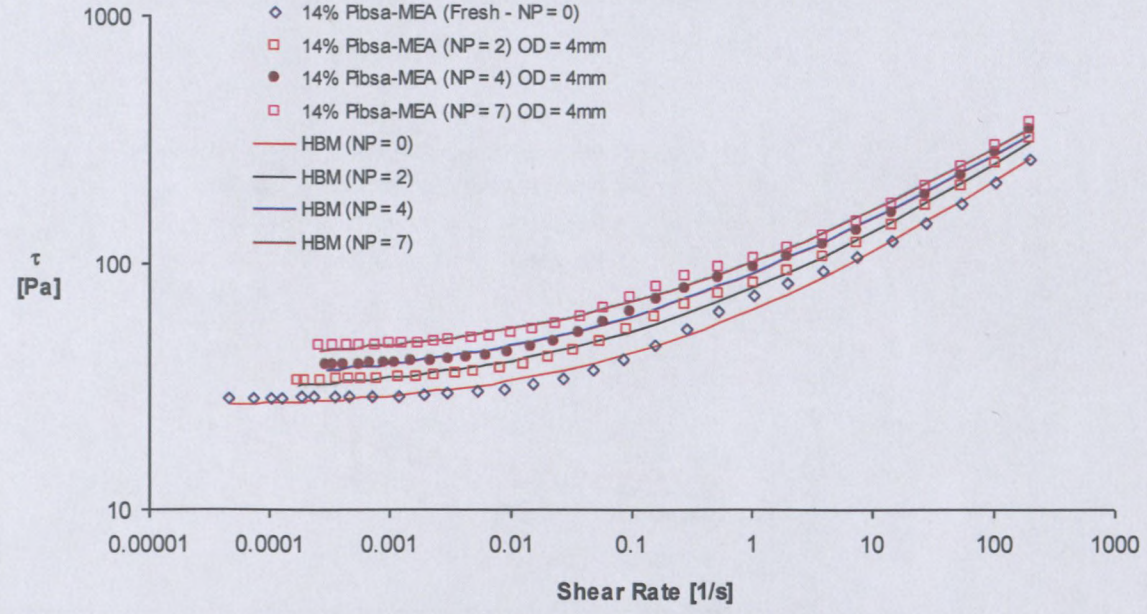

14% Pibsa-MEA in Mosspar-H (sheared using OD = 4mm)

b) PIBSA – IMIDE

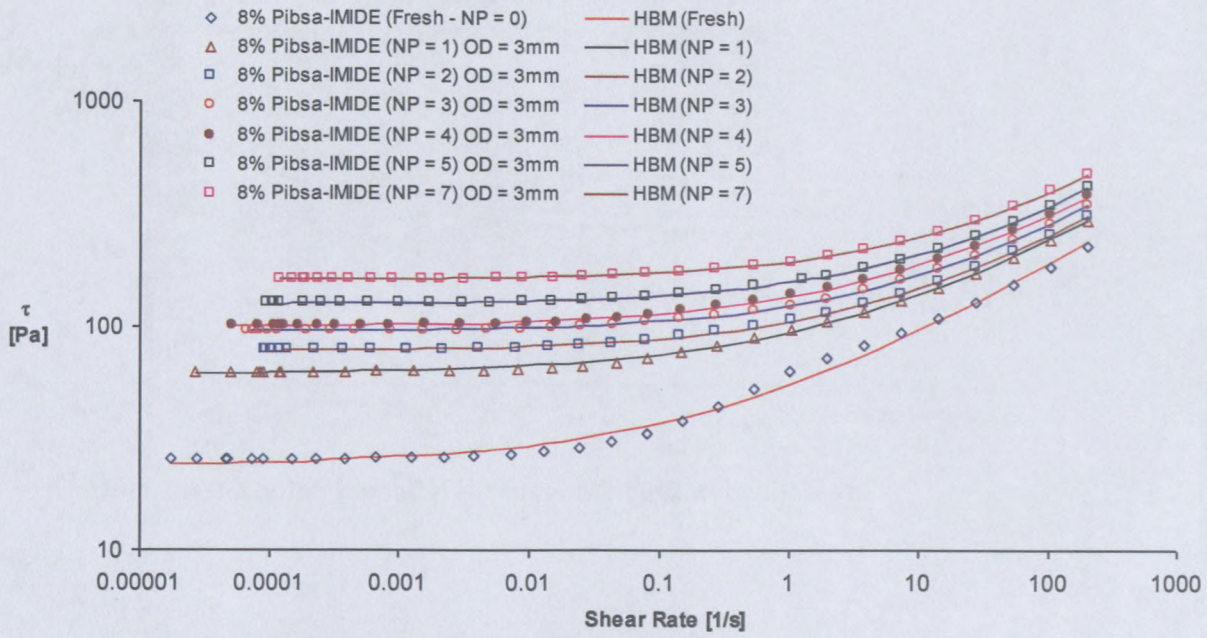

8% Pibsa-IMIDE in Mosspar-H (sheared using OD = 3mm)

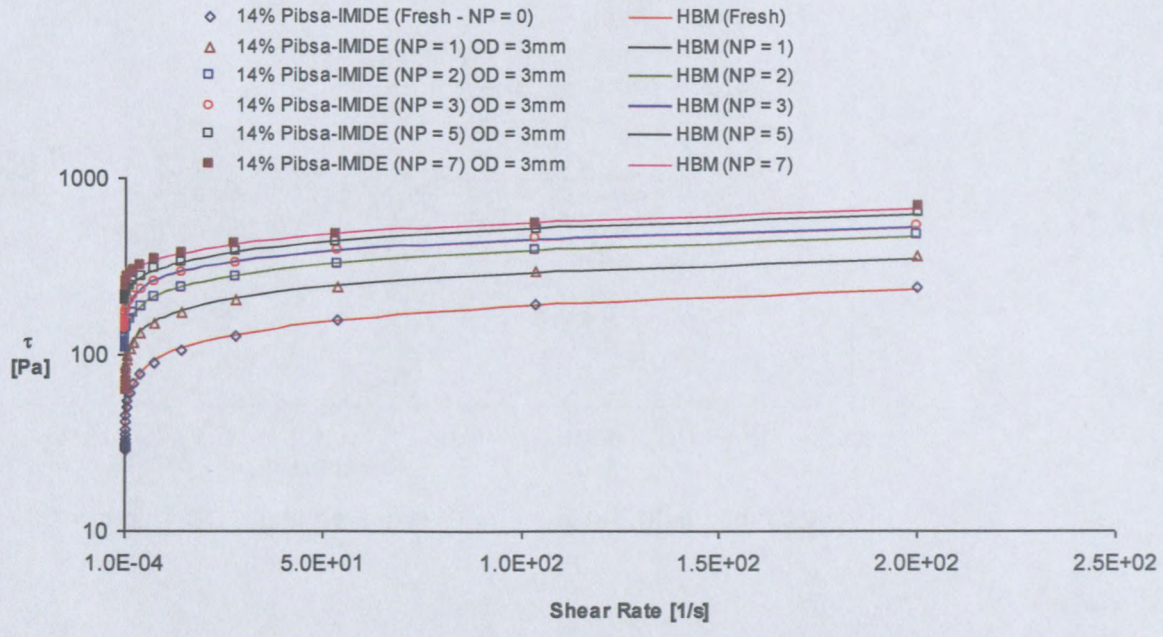

8% Pibsa-IMIDE in Mosspar-H (sheared using OD = 4mm)

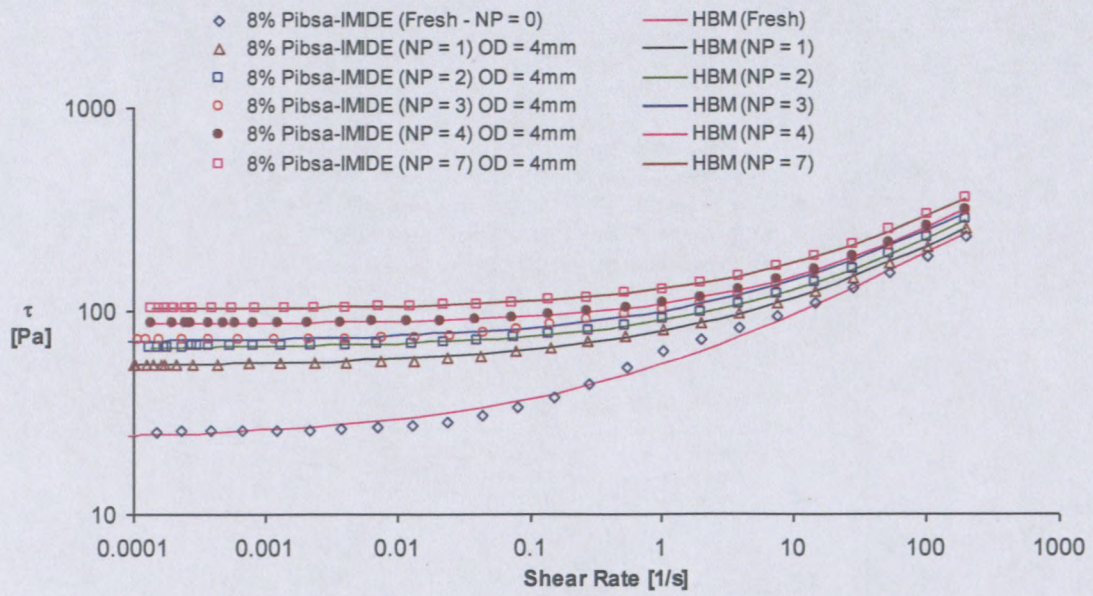

14% Pibsa-IMIDE in Mosspar-H (sheared using OD = 3mm)

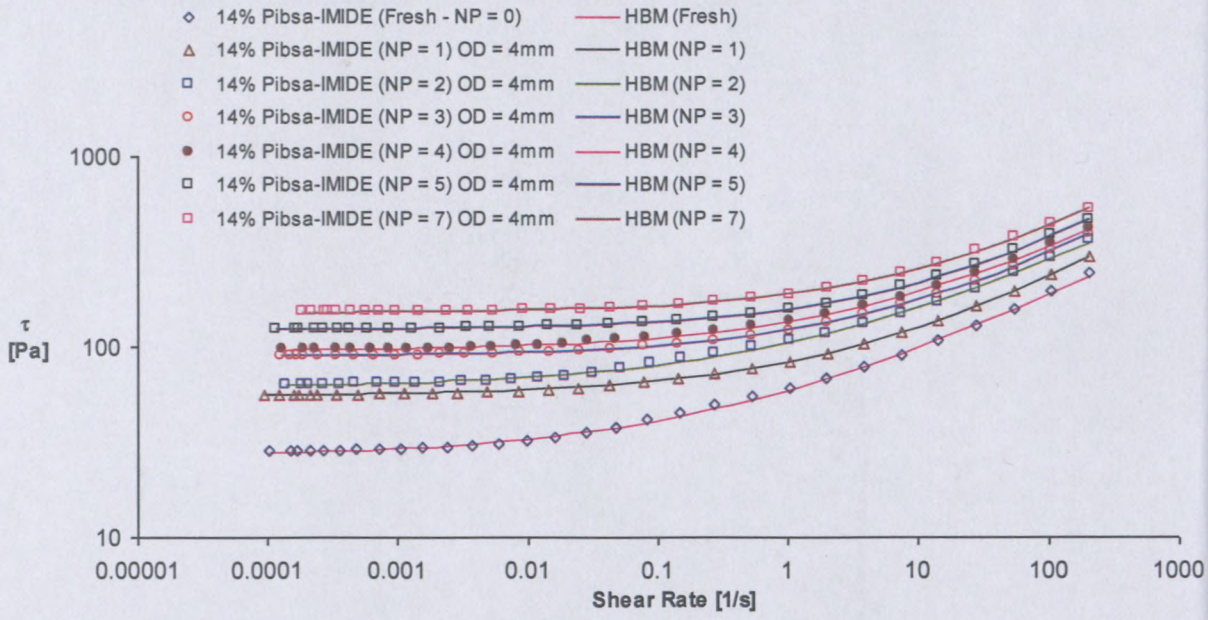

14% Pibsa-IMIDE in Mosspar-H (sheared using OD = 4mm)

c) *PIBSA – UREA*

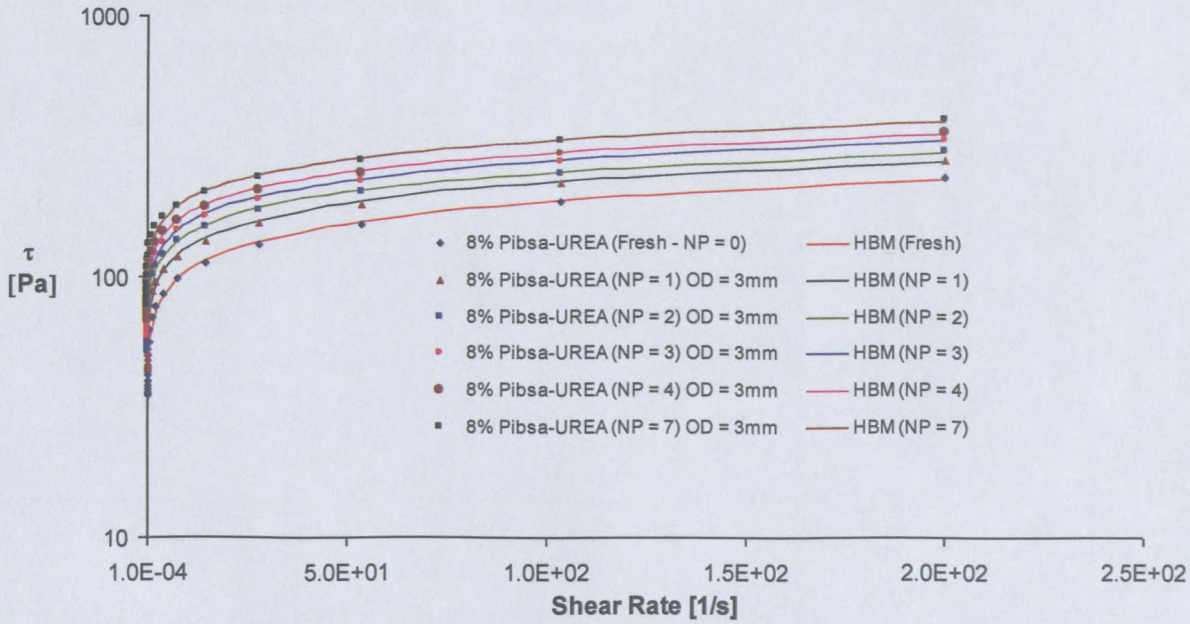

8% Pibsa-UREA in Mosspar-H (sheared using OD = 3mm)

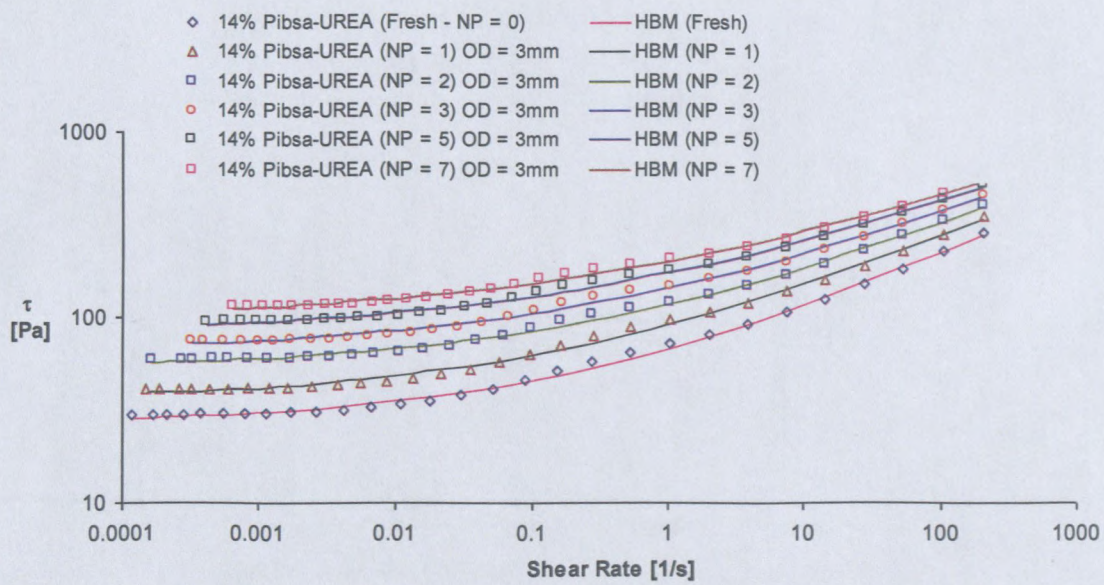

14% Pibsa-UREA in Mosspar-H (sheared using OD = 3mm)

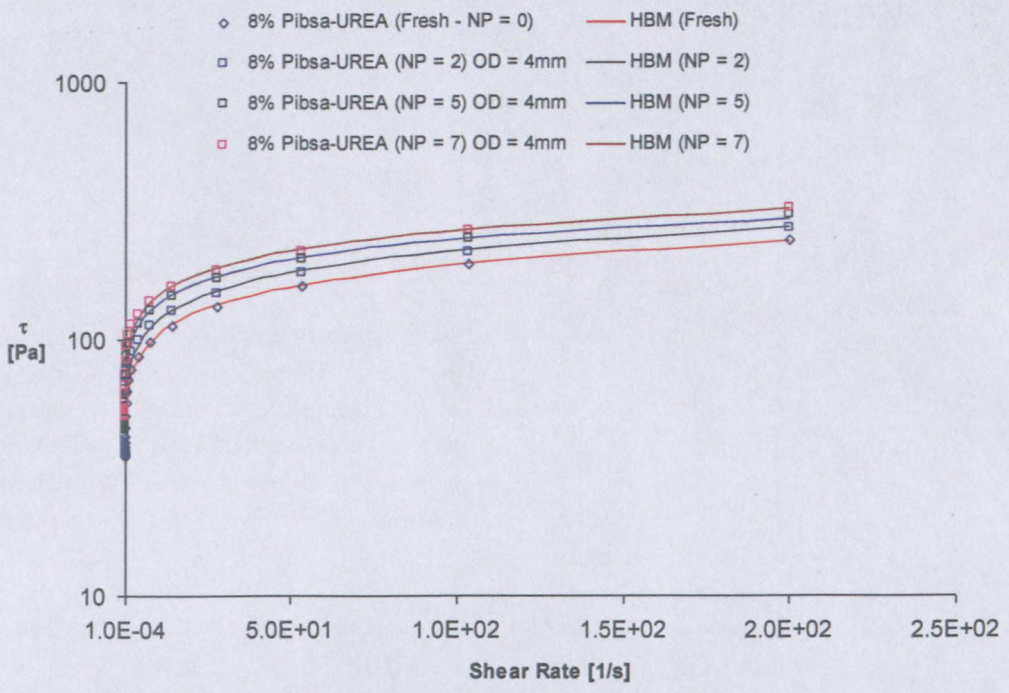

8% Pibsa-UREA in Mosspar-H (sheared using OD = 4mm)

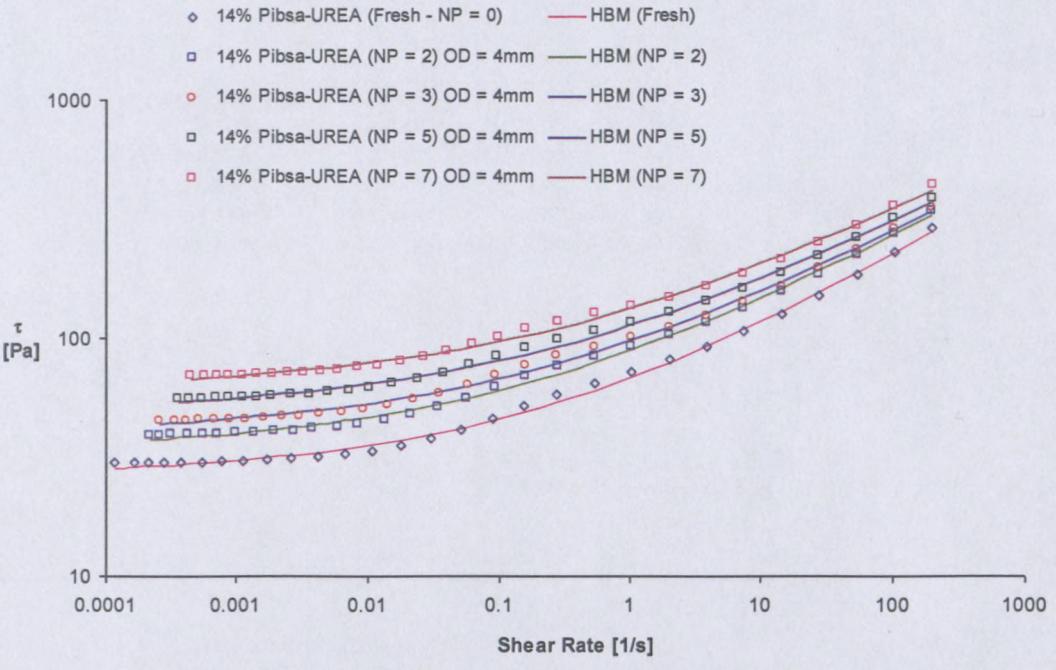

14% Pibsa-UREA in Mosspar-H (sheared using OD = 4mm)

d) *PIBSA – MEA/SMO*

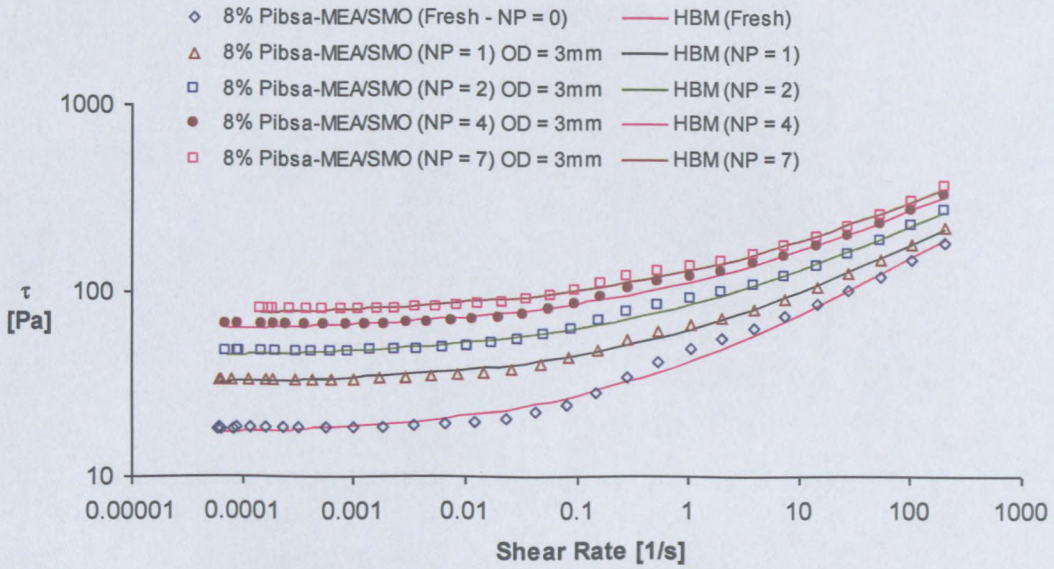

8% Pibsa-MEA/SMO in Mosspar-H (sheared using OD = 3mm)

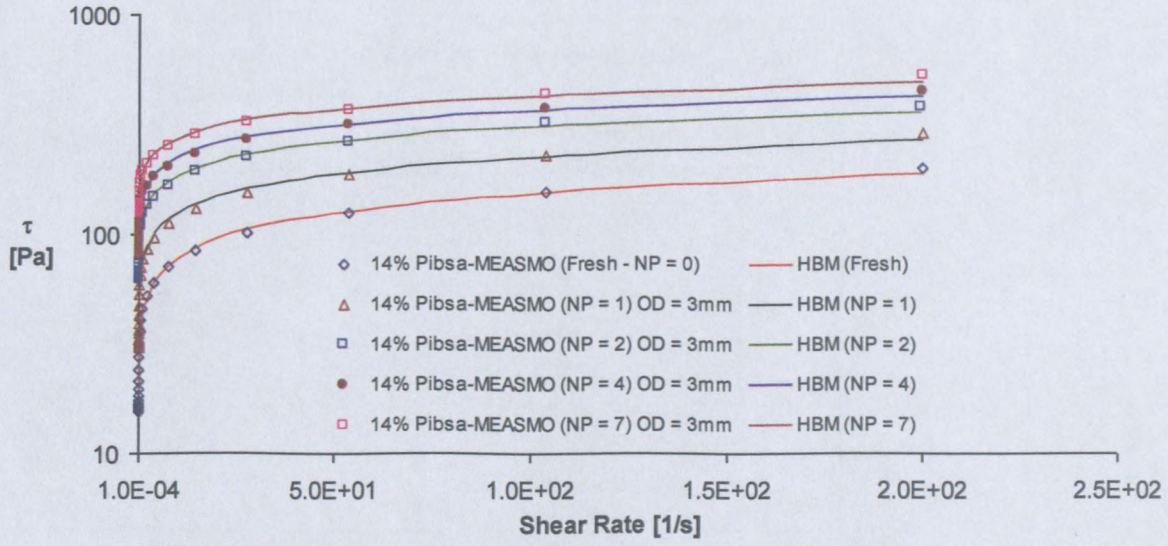

14% Pibsa-MEA/SMO in Mosspar-H (sheared using OD = 3mm)

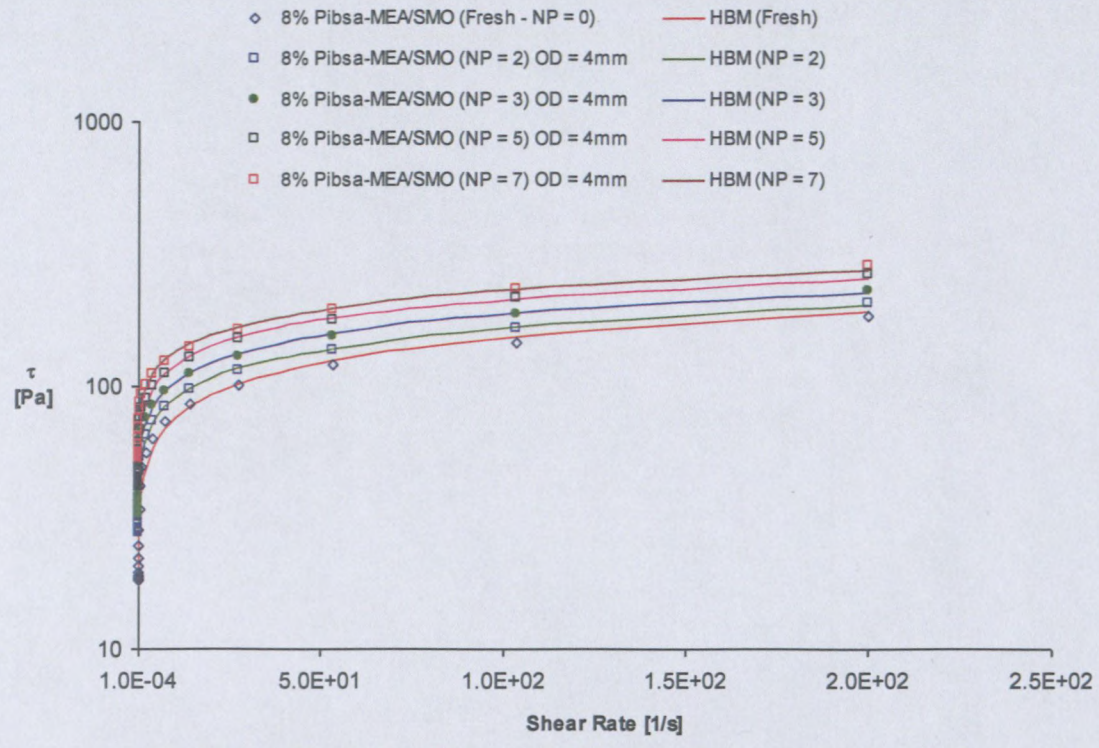

8% Pibsa-MEA/SMO in Mosspar-H (sheared using OD = 4mm)

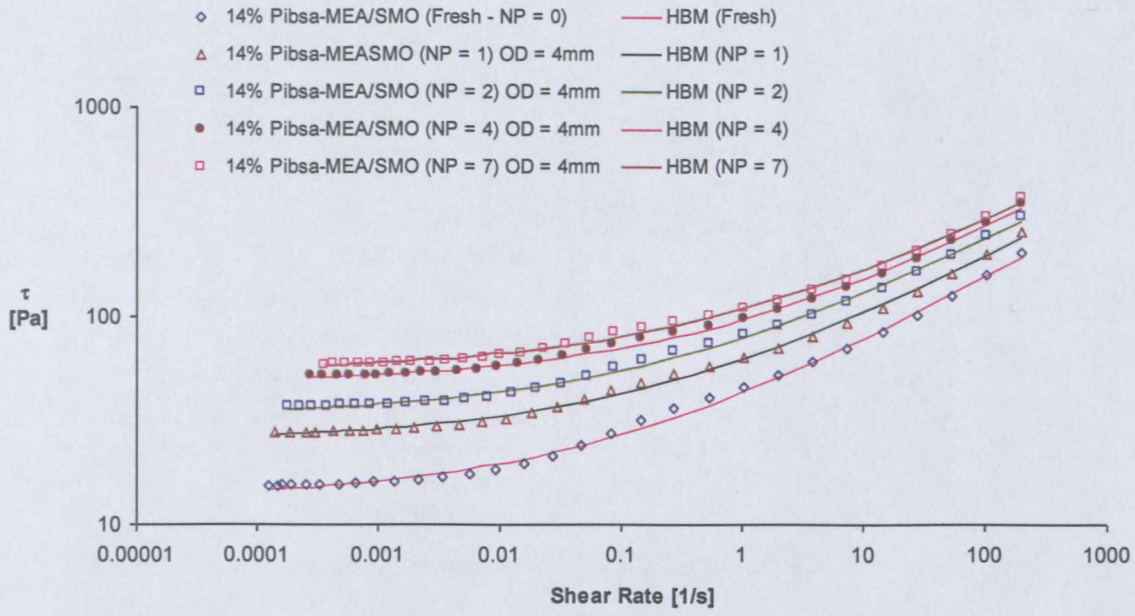

14% Pibsa-MEA/SMO in Mosspar-H (sheared using OD = 4mm)

Appendix G

Elasticity properties

a) *PIBSA – MEA*

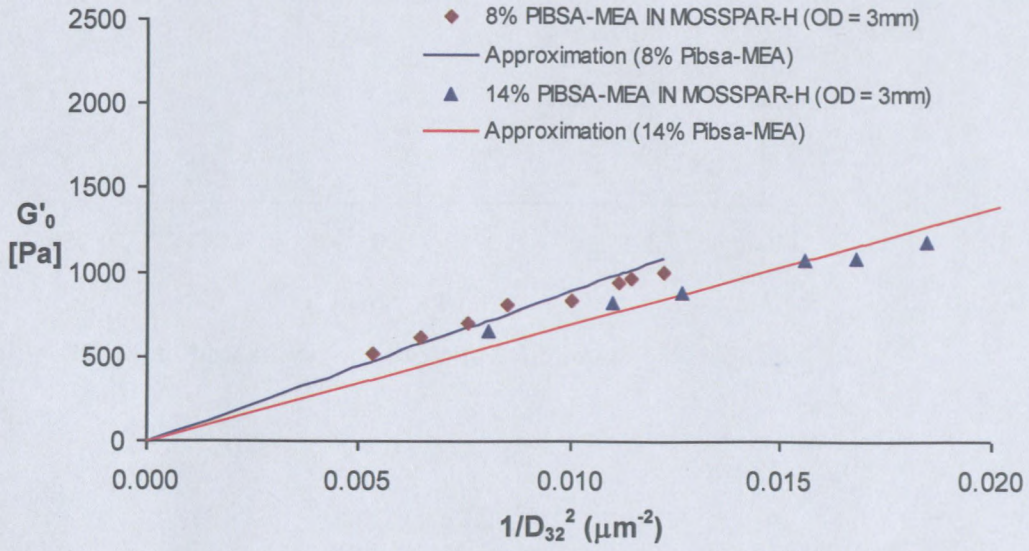

8% & 14% Pibsa-MEA in Mosspar-H (sheared using OD = 3mm)

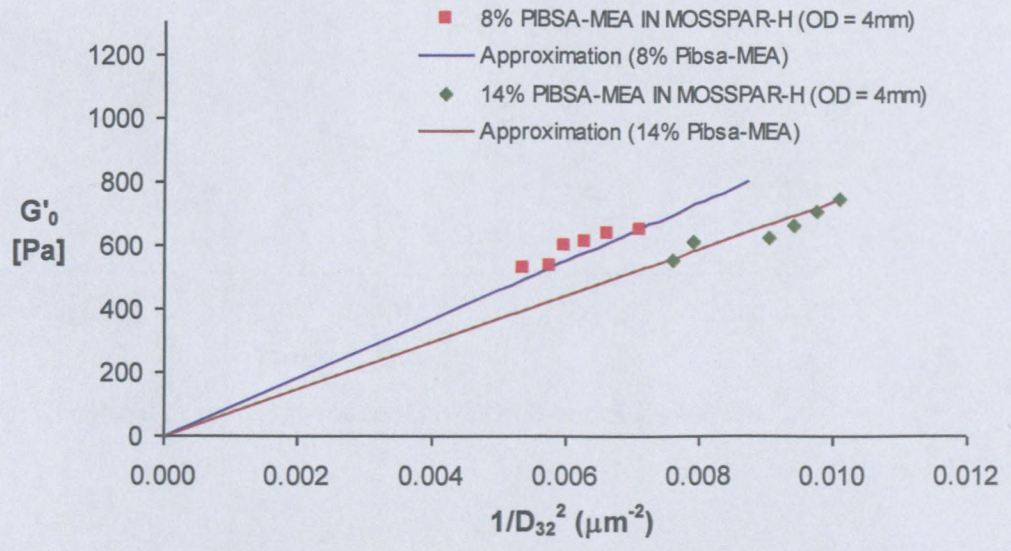

8% & 14% Pibsa-MEA in Mosspar-H (sheared using OD = 4mm)

b) *PIBSA – IMIDE*

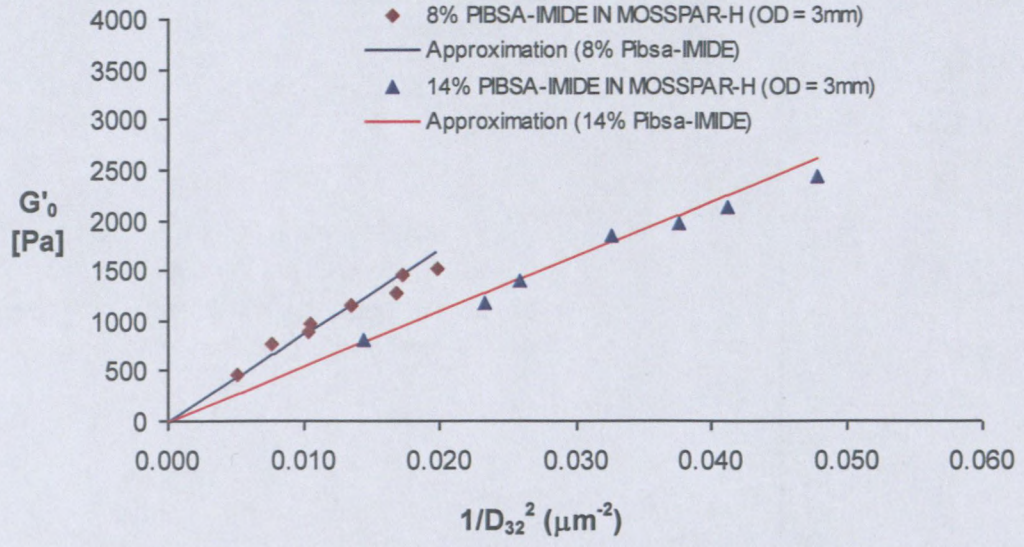

8% & 14% Pibsa-IMIDE in Mosspar-H (sheared using OD = 3mm)

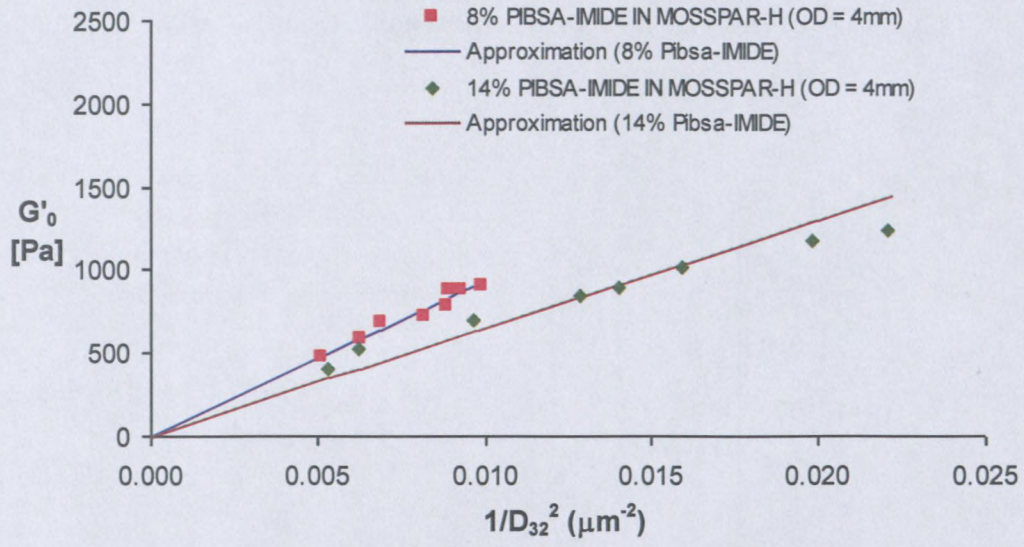

8% & 14% Pibsa-IMIDE in Mosspar-H (sheared using OD = 4mm)

c) *PIBSA – UREA*

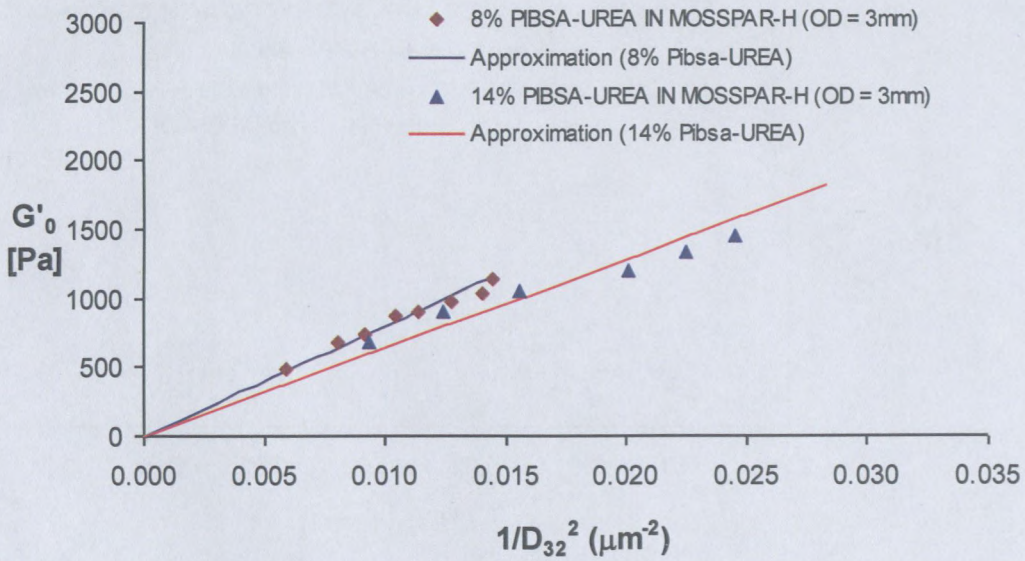

8% & 14% Pibsa-UREA in Mosspar-H (sheared using OD = 3mm)

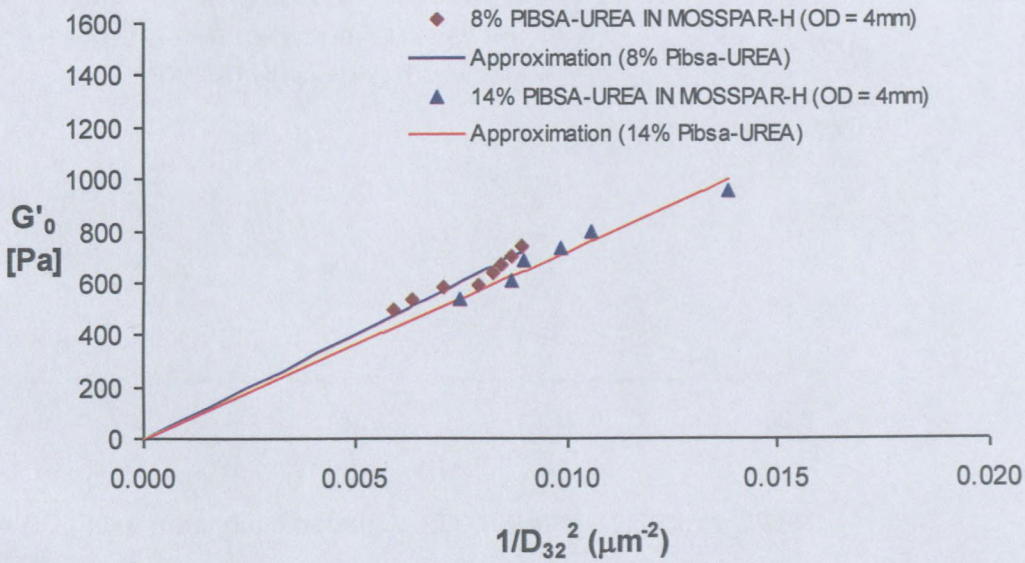

8% & 14% Pibsa-UREA in Mosspar-H (sheared using OD = 4mm)

d) PIBSA – MEA/SMO

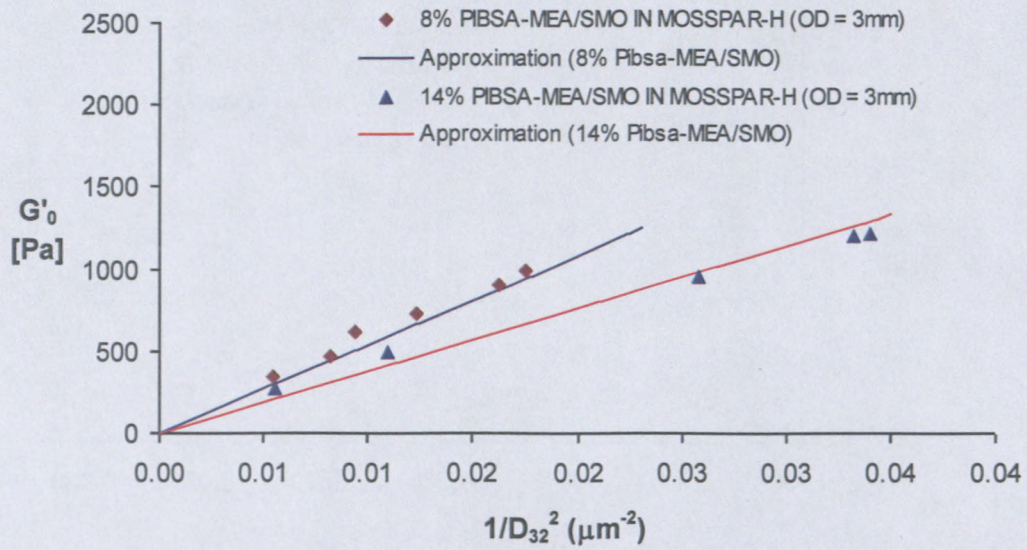

8% & 14% Pibsa-MEA/SMO in Mosspar-H (sheared using OD = 3mm)

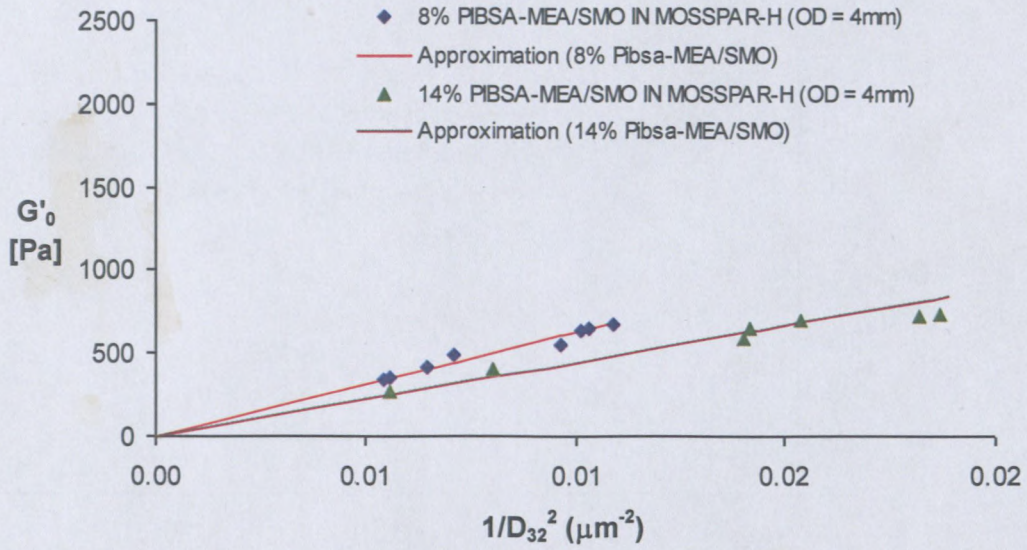

8% & 14% Pibsa-MEA/SMO in Mosspar-H (sheared using OD = 4mm)